

# ADVENTS

Assessment and Discovery of Venus' past Evolution  
and Near-Term climatic and geophysical State

Mission Concept Study Report to the NRC Planetary  
Science and Astrobiology Decadal Survey 2023-2032

**Science Champion:**

Joseph O'Rourke, Arizona State University

**Science Team:**

Kandis-Lea Jessup, Southwest Research Institute

James Kasting, Pennsylvania State University

Bernard Marty, Université de Lorraine / CRPG-CNRS

Thomas Navarro, UCLA / McGill University

**Study Point of Contact:**

Michael Amato, Goddard Space Flight Center

## EXECUTIVE SUMMARY

Scientists can tell **two stories** about the divergent evolution of Venus and Earth. In the first story, Venus and Earth were dichotomous from the start—unlike Earth, Venus was never cold enough for liquid water to exist on the surface, and the thick, CO<sub>2</sub>-rich atmosphere that we see today was formed immediately after accretion. But in the second story, Venus resembled Earth for billions of years. Both worlds started with similar internal reservoirs of volatiles such as water and initially degassed similar atmospheres. Venus may have sustained oceans and perhaps life for most of the Solar System's history—before a climatic catastrophe caused by the evolution of the Sun and massive amounts of volcanic activity. In the maximalist version of this story, life migrated from the early oceans into the last habitable niche on Venus: the cloud layers with Earth-like temperature and pressure conditions. Currently, **no one knows which story is true**—but the **ADVENTS** (Assessment and Discovery of Venus' past Evolution and Near-Term climatic and geophysical State) Mission will tackle this question head on—complementing the new VERITAS, EnVision, and DAVINCI+ missions.

ADVENTS will aim to study Venus' present state and its planetary and climatic evolution, including the habitability of Venus now and through time, helping to place the origin and evolution of Venus in context among rocky planets in our Solar System and beyond. Specifically, ADVENTS has three science goals: Understand (1) how Venus formed and evolved for comparison to other rocky (exo)planets; (2) the potential past habitability of the Venus surface; and (3) the composition, dynamics, and potential habitability of the present-day atmosphere of Venus. With many launch opportunities for a **Falcon Heavy**, ADVENTS will deliver an **Orbiter** and a **variable-altitude Aerobot** to Venus. Synergistic instruments on both platforms collect *in situ* and remote measurements of the atmosphere, along with remote sensing of the surface, for **at least 60 Earth-days**. A single **Dropsonde** is also deployed to sample the chemistry of the atmosphere from the clouds to the surface. ADVENTS will reveal if Earth and Venus formed with similar volatile inventories and how volatiles are cycled through the clouds—as well as if broad, ancient terrains formed in the presence of water oceans, whether Venus is seismically and volcanically active, and if the crust records evidence of an early magnetic field.

No single mission can fully answer all the outstanding science questions about Venus. Although this report was nearly finalized before any selections were announced, ADVENTS has **minimal overlap with the two missions recently chosen for the NASA Discovery Program, VERITAS and DAVINCI+, or with EnVision**, the Venus-targeting M5 mission in the ESA Cosmic Visions Program. ADVENTS provides unique scientific benefits—chiefly enabled by the aerobot dwelling in the cloud layers and collecting data at multiple locations and all local times—tied to many priority questions for planetary science and astrobiology. Several elements of ADVENTS are included in the five-platform **Venus Flagship Mission** (VFM) concept study. Relative to VFM, ADVENTS features a more mature engineering design of the aerobot. Overall, ADVENTS was developed as a stand-alone mission.

The cost of the baseline ADVENTS concept is between the New Frontiers (NF) and small Flagship classes. Specifically, the **Phase A–D costs with reserves are ~\$1.5B** (2025 \$s), with the technology development costs prior to PDR totaling ~\$29M. We chose an ambitious baseline payload for ADVENTS to illustrate the range of science objectives that a NF-class mission to Venus could pursue, especially given the (at the time) uncertainty about other NASA and ESA missions. We identify possible ADVENTS descopes to meet the anticipated cost cap for NF; synergizing ADVENTS with the three new Venus missions is the best way to lower costs. In addition, we fully support giving actual proposal teams the freedom to make reasoned changes to the mission objectives and payload. The community has developed multiple Venus NF mission studies and proposals that are responsive to NF Venus mission science defined in previous NF calls that fit into the NF cap with margin. This study also considered additions to ADVENTS (*e.g.*, a towbody for sub-cloud imaging) that would raise the mission cost to a small Flagship, while providing a commensurate increase in science return. The top risks to the mission are (in order) critical separation events, overall mission complexity, the caustic Venus atmosphere, and required technology development. What we report here is a resource-limited study conducted over a few months. Ultimately, the ADVENTS mission is within the current state of the art of Venus spacecraft exploration. **Together with DAVINCI+, VERITAS, and EnVision, ADVENTS would essentially re-discover the enigmatic second planet.**

## TABLE OF CONTENTS

<b>EXECUTIVE SUMMARY</b> .....	<b>I</b>
<b>TEAM LIST</b> .....	<b>a</b>
<b>1 SCIENTIFIC OBJECTIVES</b> .....	<b>1</b>
1.1 Science Questions and Objectives .....	1
1.1.1 General Overview .....	1
1.1.2 Study Goals and Assumptions .....	2
1.2 Science Traceability Matrix .....	3
<i>FOLDOUT 1, Science Traceability Matrix</i> .....	4
1.3 Descope Strategies for ADVENTS .....	5
<b>2 HIGH-LEVEL MISSION CONCEPT</b> .....	<b>7</b>
2.1 Overview .....	7
2.2 Concept Maturity Level .....	9
2.3 Key Trades .....	10
2.3.1 Balloon Type .....	10
2.3.2 Dropsonde Mounting .....	11
2.3.3 Towbody .....	12
<b>3 TECHNICAL OVERVIEW</b> .....	<b>13</b>
3.1 Instrument Payload Description .....	13
3.2 Flight System .....	15
3.2.1 Orbiter .....	15
3.2.2 Aerobot .....	15
3.2.3 Concept of Operations and Mission Design .....	17
3.2.3.1 Operations .....	17
3.2.3.1.1 Launch and Cruise to Venus .....	18
3.2.3.1.2 Aerobot Operations .....	18
3.2.3.1.3 Nominal 60-day Mission .....	19
3.2.3.1.4 Venus Orbit Operations .....	21
<b>4 RISK LIST</b> .....	<b>22</b>
<b>5 DEVELOPMENT SCHEDULE AND SCHEDULE CONSTRAINTS</b> .....	<b>22</b>
5.1 High-Level Mission Schedule .....	22
<i>SCHEDULE FOLDOUT 1</i> .....	23
5.2 Technology Development Plan .....	24
5.3 Mission Life-Cycle Cost .....	25
5.3.1 Costing Methodology and Basis of Estimate .....	25
<b>APPENDIX A - DESIGN TEAM STUDY REPORT</b> .....	<b>A-1</b>
A.1 Science .....	A-1
A.1.1 Science Rationale for the ADVENTS Payload, Relative to the VFM Study .....	A-1
A.1.1.1 Scientific Rationale for the New IR Camera (NIR-C) .....	A-1
A.1.1.2 Scientific Rationale for the Dropsonde .....	A-4
A.1.1.3 Scientific Rationale for the Miniature Tunable Laser Spectrometer (TLS) .....	A-4
A.1.1.3.1 Noble Gases .....	A-4

A.1.1.3.2 Oxygen Isotopes . . . . .	A-5
A.1.1.3.3 Contextualizing the Claimed Detection of Phosphine . . . . .	A-6
A.1.1.3.4 Synergy between the TLS and AMS-N . . . . .	A-6
A.1.2 Potential Enhancements to the ADVENTS Payload . . . . .	A-7
A.1.2.1 Visible Cameras . . . . .	A-7
A.1.2.2 Atmospheric Composition and Dynamics from Orbital Measurements . . . . .	A-7
A.1.2.3 Sub-Cloud Imaging with a Towbody . . . . .	A-8
A.1.2.4 Multiple Descent Probes . . . . .	A-8
A.1.3 Traceability from ADVENTS to the 2019 NASA VEXAG GOI . . . . .	A-9
A.2 Mission Overview . . . . .	A-9
A.2.1 Key Architecture and Mission Trades . . . . .	A-11
A.2.1.1 Balloon Type . . . . .	A-11
A.2.1.2 Dropsonde Mounting. . . . .	A-13
A.2.1.3 Towbody . . . . .	A-14
A.2.2 Mission Requirements . . . . .	A-15
A.2.3 Mission Design . . . . .	A-16
A.2.3.1 ADVENTS Launch Vehicle Analysis . . . . .	A-17
A.2.3.2 Primary Launch Opportunity . . . . .	A-19
A.2.3.3 ADVENTS Design Point . . . . .	A-19
A.2.3.4 Aerobot Entry Analysis . . . . .	A-21
A.2.3.5 Science Orbit Operations Analysis . . . . .	A-22
A.2.4 Concept of Operations . . . . .	A-27
A.2.4.1 Launch and Cruise to Venus . . . . .	A-28
A.2.4.2 Aerobot Operations. . . . .	A-28
A.2.4.2.1 Five and a Half Day Cruise . . . . .	A-28
A.2.4.2.2 Entry and Descent . . . . .	A-28
A.2.4.2.3 Nominal 60-day Mission . . . . .	A-30
A.2.4.3 Venus Orbit Operations. . . . .	A-33
A.3 Flight System . . . . .	A-34
A.3.1 Aerobot. . . . .	A-35
A.3.1.1 Instruments . . . . .	A-37
A.3.1.1.1 Aerosol Mass Spectrometer with Nephelometer (AMS-N) . . . . .	A-37
A.3.1.1.2 Tunable Laser Spectrometer (TLS) . . . . .	A-39
A.3.1.1.3 Meteorological Suite and Infrasond Measurements (MET) . . . . .	A-39
A.3.1.1.4 Dropsonde (Dropsonde) . . . . .	A-40
A.3.1.1.5 Chemical Sensor Array Technology Maturity . . . . .	A-41
A.3.1.2 Entry Vehicle. . . . .	A-41
A.3.1.2.1 Summary of Performance Capability . . . . .	A-42
A.3.1.2.2 Challenges . . . . .	A-44
A.3.1.2.3 Technology Maturity . . . . .	A-44
A.3.1.2.3.1 Thermal Protection System . . . . .	A-44
A.3.1.2.3.2 Parachute . . . . .	A-44
A.3.1.2.3.3 EDL ConOPS Trigger(s) . . . . .	A-44
A.3.1.2.4 Key Trades. . . . .	A-45
A.3.1.2.4.1 EFPA . . . . .	A-45
A.3.1.2.4.2 Dropsonde descent time. . . . .	A-45
A.3.1.2.4.3 Aeroshell cg and mass properties . . . . .	A-45

- A.3.1.2.4.4 Narrow Entry Corridor . . . . . A-45
- A.3.1.3 Aerobot Subsystems . . . . . A-45
  - A.3.1.3.1 Avionics . . . . . A-45
  - A.3.1.3.2 Balloon . . . . . A-46
  - A.3.1.3.3 Communication . . . . . A-47
  - A.3.1.3.4 Power . . . . . A-47
    - A.3.1.3.4.1 Dropsonde Battery Sizing . . . . . A-49
  - A.3.1.3.5 Radiation . . . . . A-49
  - A.3.1.3.6 Structure . . . . . A-51
    - A.3.1.3.6.1 Parachute, Balloon, Tether System Stowage . . . . . A-51
    - A.3.1.3.6.2 Tether System . . . . . A-52
    - A.3.1.3.6.3 Balloon Fill & Tank Assembly Separation . . . . . A-52
    - A.3.1.3.6.4 Solar Panel Array . . . . . A-52
    - A.3.1.3.6.5 Deployable Structures . . . . . A-53
  - A.3.1.3.7 Thermal . . . . . A-54
- A.3.1.4 Dropsonde . . . . . A-56
- A.3.1.5 Towbody . . . . . A-58
  - A.3.1.5.1 Background . . . . . A-58
  - A.3.1.5.2 Motivation . . . . . A-58
  - A.3.1.5.3 Concept . . . . . A-58
  - A.3.1.5.4 Design and Accommodation . . . . . A-59
- A.3.2 Orbiter . . . . . A-60
  - A.3.2.1 Instruments . . . . . A-62
  - A.3.2.2 Attitude Control . . . . . A-63
  - A.3.2.3 Avionics . . . . . A-66
  - A.3.2.4 Communication . . . . . A-68
  - A.3.2.5 Power . . . . . A-70
  - A.3.2.6 Propulsion . . . . . A-71
  - A.3.2.7 Structure . . . . . A-74
    - A.3.2.7.1 Load Path and Mechanisms . . . . . A-75
  - A.3.2.8 Thermal . . . . . A-75
- APPENDIX B - ADVENTS COST BASIS OF ESTIMATE . . . . . B-1**
  - B.1 CEMA Cost Estimate for ADVENTS Orbiter Bus . . . . . B-2
  - B.2 CEMA Cost Estimate for ADVENTS Aerobot Bus . . . . . B-3
  - B.3 CEMA Cost Estimate for ADVENTS Dropsonde (Not including instrumentation). . . . . B-4
- APPENDIX C - REFERENCES . . . . . C-1**
- APPENDIX D - ACRONYMS & ABBREVIATIONS . . . . . D-1**

**TEAM LIST**

<b>Science Team (Venus Panel)</b>
Joseph O'Rourke
Kandis-Lea Jessup
James Kasting
Bernard Marty
Thomas Navarro

<b>Study Design and Management Team</b>
Naeem Ahmad
Michael Amato
Branimir Blagojevic
James Bufkin
Eric Cardif
Jaime Esper
Chris Evans
Amani Frazier
Eric Grob
Jeff Hall
Mae Huang
Kyle Hughes
Stephen Indyk
Andrew Jones
Richard Lynch
Stephen McKim
Suman Muppidi
Tony Nicoletti
Sean O'Brien
Adan Rodriguez-arroy
Miguel Benayas Penas
Eric Queen
Cabin Samuels
Bruno Sarli
Lauren Schlenker
Marcia Segura
Colin Sheldon
Terry Smith
Thomas Spitzer
Rob Thate
Sarah Wallerstedt

## 1 SCIENTIFIC OBJECTIVES

### 1.1 Science Questions and Objectives

#### 1.1.1 General Overview

The ADVENTS (Assessment and Discovery of Venus' past Evolution and Near-Term climatic and geophysical State) Mission has three scientific goals: Understand (1) how Venus formed and evolved for comparison to other rocky (exo)planets; (2) The potential past habitability of the Venus surface; and (3) The composition, dynamics, and potential habitability of the present-day atmosphere of Venus. Venus offers an abundance of scientific puzzles that have broad implications for all of planetary science and astrobiology (Glaze *et al.*, 2018). In particular, the idea that Venus could have been habitable—with water oceans on the surface (**Figure 1**)—for billions of years has remained tantalizing but unverified (Way *et al.*, 2016). In fact, we know so little about the atmospheric chemistry and dynamics of Venus that we cannot exclude the possibility that life exists today in the clouds (Greaves *et al.*, 2020; Limaye *et al.*, 2018). Even ignoring its astrobiological potential, Venus is a giant blind spot in our models of the evolution of the protoplanetary disk; for example, did Earth and Venus form from similar building blocks (Chassefière *et al.*, 2012)? Venus is also drawing more attention as "the exoplanet in our backyard" (Kane *et al.*, 2019). The most productive methods of characterizing exoplanets (the radial velocity and transit photometry methods) are biased towards planets that orbit close to their parent stars. If planet–star distance (and stellar evolution over time) controls the fate of planets, then we should expect to discover more exoplanetary Venus-analogues than Earth-twins (Kasting & Catling, 2003). Some Venus-sized planets are already being detected, and future observatories will characterize their atmospheric properties. Whether any of these planets are suitable for life depends on their volatile abundances, especially water, and on their climates. Our ignorance about when and why the evolution of Earth and Venus diverged is a huge hindrance to understanding rocky planets in general.

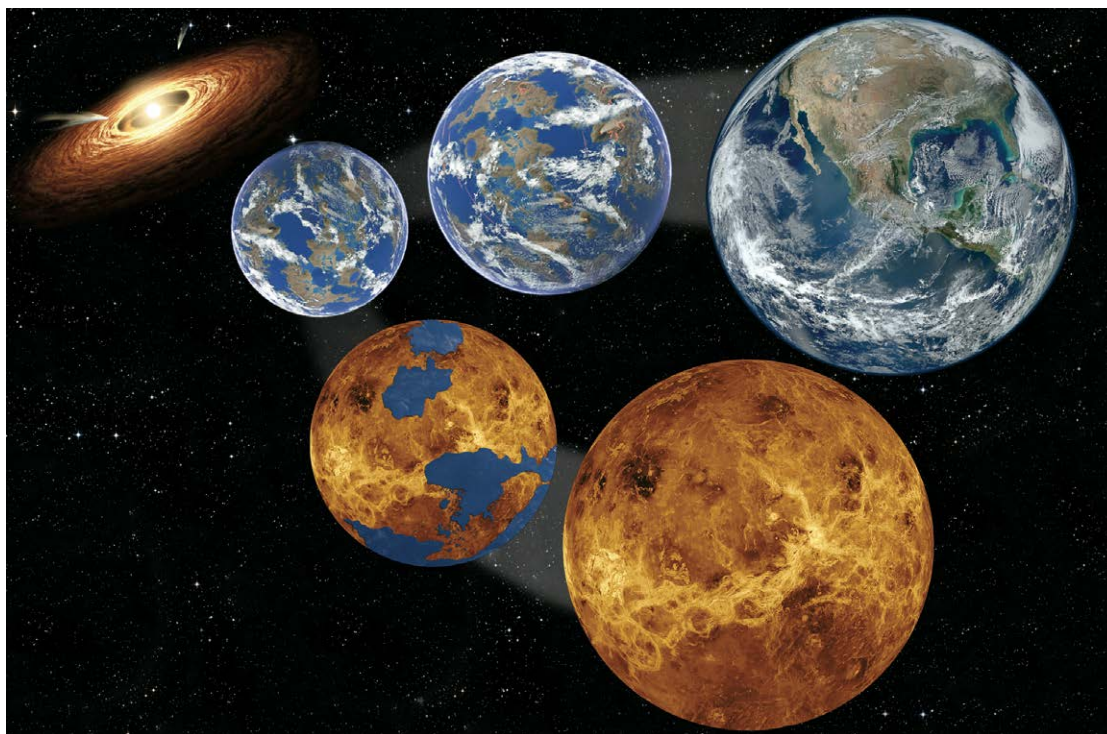


**Figure 1:** ADVENTS aims to determine when and why the evolution of Venus and Earth diverged, complementing the newly selected NASA VERITAS and DAVINCI+ missions and the ESA EnVision mission. Was Venus an Earth-like world with water oceans for billions of years (Way & Del Genio, 2020)? Alternatively, was Venus always different than Earth as a consequence of how their magma oceans solidified and degassed an atmosphere after accretion as a function of solar distance (Hamano *et al.*, 2013)?

Our mission architecture features three synergistic platforms that work together to achieve our science goals and objectives. Specifically, ADVENTS includes an orbiter, a variable-altitude aerobot, and one dropsonde (**Figure 2**). Our baseline instrument payload (**Table 1**) was selected to provide multiple, complementary datasets that would enable us to assess the habitability potential of Venus both in the past and today—and to collect key information to inform studies of comparative planetology in our Solar System and beyond. All but one of our instruments were assessed in detail during the Venus Flagship Mission (VFM) concept study—please consult their report for details not included here. Like the VFM team, we heavily favored instruments that collect data relevant to several priority questions. We do not divide our payload into non-overlapping magisteria of sub-domains such as atmospheric and surface science—ADVENTS science is all synergistic. For example, ADVENTS uses atmospheric probes to characterize geophysical activity on the surface and in the interior. We study the mineralogy of geologic units to learn when the atmosphere smothered the surface—and whether life may have migrated from a clement surface into the last habitable niche in the clouds.

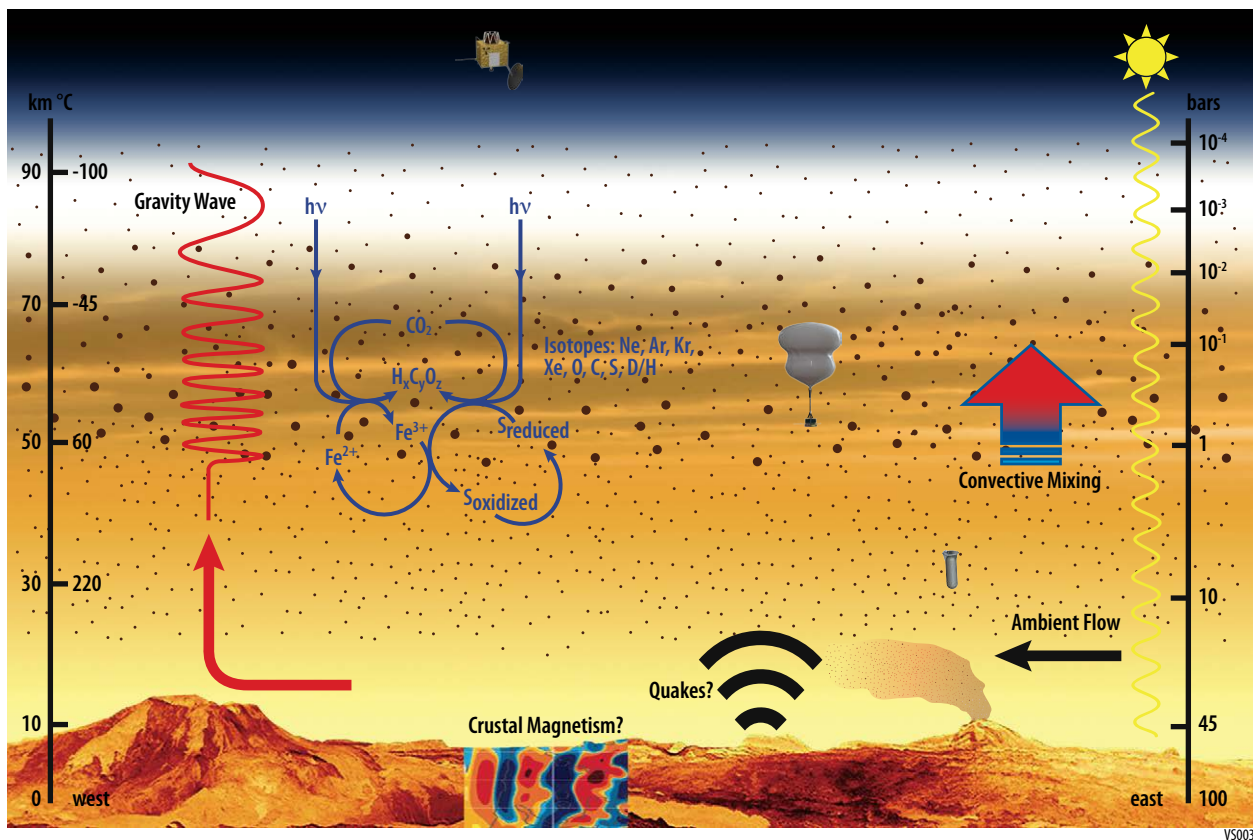


**Figure 2:** ADVENTS uses synergistic measurements from an orbiter, aerobot, and dropsonde to achieve its science objectives. In particular, the ADVENTS aerobot would dwell at cloud levels for 60 Earth-days to characterize the chemistry and astrobiological potential of this special region—potentially the last habitable niche in Venus—and how they vary with time and location. The aerobot also measures the key isotopes that reveal the origins of Venus in the protoplanetary disk—and searches for magnetized crust and volcanic and/or seismic activity. The dropsonde connects the chemistry of the clouds to that of the lower atmosphere. The orbiter provides regional context imaging and characterizes the forcing from the Sun and solar wind. Crucially, the orbiter also determines rock types at different geological regions, testing the hypothesis that tesserae are continent-analogues that were formed in a past period when Venus had oceans (Campbell & Taylor, 1983; Gilmore *et al.*, 2017).

### 1.1.2 Study Goals and Assumptions

ADVENTS was designed with the cost cap in mind for the New Frontiers (NF) program, which is anticipated to be ~\$1.1B for Phase A-D. The ADVENTS team decided to define a baseline concept with a higher cost (~\$1.5B for Phase A–D) for three reasons. First, the Steering Committee of the Planetary Science and Astrobiology Decadal Survey 2023-2032 provided guidance that a cost estimate



**Table 1:** ADVENTS instruments were also incorporated into the Venus Flagship Mission (VFM) concept study and/or have other spaceflight heritage. Nearly all of the performance requirements for our instruments were derived from the VFM STM as noted below (formatted as VFM Goal.Objective.Investigation). Please consult that study report for the detailed scientific rationale for each requirement. Our Appendix explains the few requirement changes that we made during the ADVENTS study—in particular, the additions of a mini-TLS to the aerobot and a second NIR imager to the orbiter.

Orbiter	Performance Requirement	Aerobot	Performance Requirement
Near IR Imager, Surface (NIR-S)	VFM I.1.A.	Aerosol Mass Spectrometer with Nephelometer (AMS-N)	VFM I.1.C, I.2.A., I.3.A., III.2.B.
Near IR Imager, Clouds (NIR-C)	Not in VFM — JAXA Akatsuki IR camera analogue	Tunable Laser Spectrometer (TLS)	VFM I.1.C. — Miniature version of TLS from VFM lander
Magnetometer, Orbiter (MAG-O)	VFM I.1.E., III.1.A.	Meteorological Suite (MET)	VFM I.2.B., I.3.A.
EUV Monitor (EUV)	VFM I.1.D., I.3.A.	Magnetometer, Gondola (MAG-G)	VFM I.1.E., III.1.A.
Radio Occultation (ROCC)	VFM I.1.D., I.2.A.	Dropsonde	VFM I.2.A., I.2.B. — Descopes of VFM lander

of ~\$1.5B (Phase A–D) was adequate to illustrate the scope and character of New Frontiers science. Second, our study was required to provide a conservative minimum of 50% cost reserves for Phase A–D (excluding launch vehicle), independent of the maturity of each architecture component, and 25% reserves for Phase E. Finally, our study was largely conducted when neither NASA nor ESA had selected any other Venus-targeting missions for flight. Selections of three Venus missions were announced one week (NASA) and hours (ESA) before this report was finalized.

The ADVENTS study team selected an ambitious instrument payload to ensure that the highest-priority science objectives would be achieved—and to present a broad range of possible investigations and measurement techniques. We fully support giving actual proposal teams the freedom to make reasoned changes to our baseline ADVENTS concept. Descopes to ADVENTS might become necessary to achieve the cost and risk profiles desired by proposal teams and/or NASA (see below). Proposers might also want to substitute certain science objectives and thus instruments for others. **Appendix A** provides a non-exhaustive list of the scientific benefits of instruments that were not included in our baseline concept but could enable high-priority science via multiple avenues (*e.g.*, via ride-along missions, architecture trades, and/or an upgrade to a Flagship-class mission).

The option to expand or “upscope” ADVENTS to a small Flagship mission would be well-justified because Venus is critical to answering most of the priority science questions for planetary science and astrobiology in the next decade. The VFM concept study report includes many architecture elements that could enhance the ADVENTS payload. For example, a “Flagship-lite”-class ADVENTS concept might also include additional UV and IR instruments on the orbiter to provide better, regional context for the chemical measurements made by the aerobot. Or, SmallSats designed to study atmospheric escape processes could enhance the scientific return of any version of ADVENTS. An alternative “upscope” element that was not included in the VFM concept is a towbody that would be deployed from the aerobot to conduct surface imaging below the cloud deck. This towbody is detailed in the Appendix. Ultimately, only a large Flagship (*e.g.*, VFM) can address the complete list of outstanding questions about Venus in a single mission. However, such a mission has many complexities that would be reflected in the total mission cost. A mission such as ADVENTS can make significant advancements in prioritized Venus science goals including: revealing the chemistry and dynamics of the cloud layers and how they change with time and location, and completing key geophysical investigations that can only be adequately achieved via an in-situ element such as an aerobot.

## 1.2 Science Traceability Matrix

**Foldout 1** shows the full ADVENTS Science Traceability Matrix (STM), which lists the science objectives and their associated measurement and instrument performance requirements. Nearly all of our performance requirements are extracted from the VFM study—please consult **Appendix A** for the detailed scientific justifications. **Table A-1** shows how the ADVENTS STM maps onto the VEXAG GOI. **Appendix A** explains the scientific rationale for choices we made that were different than in the VFM.

A		B		
Science Investigation Goals	Science Measurement Requirements Objectives	Instruments Physical Parameters	Observables	Instruments
<p><b>1.</b> Understand how Venus formed and evolved for comparison to other rocky (exo)planets. NASA VEXAG Goals I (Early Evolution) and III (Geologic History)</p>	<p><b>1A.</b> Determine if Venus and Earth accreted volatiles from similar reservoirs.</p>	Abundances and isotopic ratios of noble gases (Xe, Kr, Ar, and Ne) below the homopause	Mass spectra with sufficient range and resolution	AMS-N
		Abundances and isotopic ratios of stable gases below the homopause, including D/H in H <sub>2</sub> O, <sup>18</sup> O/ <sup>17</sup> O/ <sup>16</sup> O and <sup>13</sup> C/ <sup>12</sup> C in CO <sub>2</sub> , <sup>34</sup> S/ <sup>33</sup> S/ <sup>32</sup> S and <sup>13</sup> C/ <sup>12</sup> C in OCS, and <sup>13</sup> C/ <sup>12</sup> C in CO	Mass spectra and laser transmission spectra with sufficient range and resolution	AMS-N, TLS
	<p><b>1B.</b> Determine if there is active tectonic and volcanic activity on Venus today.</p>	Frequency and magnitude of seismic activity	Atmospheric pressure at infrasound frequencies	MET
		Thermal anomalies associated with volcanic activity	Spatially resolved emissivity of regions of the nightside surface in NIR channels	NIR-S
		Cloud layer aerosol and gas species properties, including changes in sulfuric acid cloud droplets, SO <sub>2</sub> and CO <sub>2</sub> gas variations and evidence of ash	Droplet sizes	AMS-N
			Non-liquid particles in cloud layer	IR spectral reflectance
<p><b>2.</b> Understand the potential past habitability of the Venus surface. NASA VEXAG Goal I (Early Evolution)</p>	<p><b>2A.</b> Determine if tesserae on Venus formed in the presence of water oceans.</p>	Bulk composition (mafic vs. felsic) of key surface terrains (e.g., plains, tesserae) from nightside surface emissivity	Spatially resolved IR emissivity of regions of the nightside surface in key channels	
	<p><b>2B.</b> Determine if the crust of Venus preserves a record of an early dynamo.</p>	Crustal remanent magnetism: Magnetization or its upper bound at multiple different surface terrains	B-fields measured continuously above and below the ionosphere.	MAG-G, MAG-O
<p><b>3.</b> Understand the composition, dynamics, and potential habitability of the present-day atmosphere of Venus. NASA VEXAG Goal II (Atmospheric Composition and Dynamics)</p>	<p><b>3A.</b> Assess the present-day habitability of the Venus cloud environment.</p>	Environmental conditions at multiple local times at cloud levels over multiple different surface terrains	Pressure, temperature, ionizing radiation levels	MET, NIR-C
		Availability and vertical distribution of biologically important elements (CHNOPS) in gaseous, liquid, and/or solid form at multiple local times at cloud levels	Particle size, refractive index, identify non-spherical particles, mass spectra	AMS-N
	<p><b>3B.</b> Determine what mechanisms control the composition, transport, and production of volatiles in the Venus cloud environment.</p>	Atmospheric composition and its spatial and temporal variability at cloud levels, including 1) in both cloud droplets and aerosols, SO <sub>2</sub> , SO <sub>3</sub> , HCl, CO, OCS, H <sub>2</sub> S—and H <sub>2</sub> SO <sub>4</sub> , H <sub>2</sub> O, FeCl <sub>3</sub> , and S <sub>x</sub> and 2) from the cloud layers to the surface in one location, H <sub>2</sub> , O <sub>2</sub> , CO, H <sub>2</sub> O, HCl, NO	Mass spectra with sufficient range and resolution	AMS-N
			Size distribution, shape and refractive indices of clouds and hazes. Identify non-spherical (non-liquid) particles. Intensity and polarization of scattered light	Dropsonde
		Chemical abundances	Dropsonde	
		Incoming UV radiation and solar wind	EUV, MAG-O	
		Vertical and horizontal wind speeds and turbulence	MET	
		P/T conditions	NIR-C	
		P/T, turbulence, up- and down-welling mass transport, cloud motions at 30–50 km altitude		
		Winds and convective stability, and their spatial and temporal variability in the cloud layers and 30–50 km at multiple local times, and from the cloud layers to the surface at one location	P/T profile from cloud layers to surface	Dropsonde
Incoming UV radiation and solar wind	EUV, MAG-O			
Vertical T profiles from 38–150 km altitude	ROCC			

Instrument Performance Requirements	Functional Requirements
<p><b>Orbiter:</b>                      NIR Imager, Surface (NIR-S) [1B, 2A, 3B]                      • ≥ 8-channel (6 petrology, 2 cloud bands) at 0.80–1.55 um with pixel scale &lt; 50 km.                      • SNR sufficient for emissivity to ±0.03 in processed data.                      • &gt; 25% surface coverage with a mix of major geomorphological terrains, 5-km elevation range, and at least 1 Venera site.</p> <p>NIR Imager, Clouds (NIR-C) [1B, 3A, 3B]                      • ≥ 5-channels at 0.8–2.4 um with pixel scale &lt; 50 km.                      • SNR sufficient to determine cloud dynamics and opacity.</p> <p>EUV Monitor (EUV) [3A]                      • Channel A: thin foil C/Al/Nb/C for 0.1–3 nm and 17–22 nm.                      • Channel B: thin foil C/Al/Ti/C for 0.1–7 nm.                      • Channel C: interference filter for 121–122 nm.</p> <p>Magnetometer, Orbiter (MAG-O) [2B]                      • 32 Hz sampling. Sensitivity: 0.7 nT. Accuracy: 0.7 nT. Precision: 0.1 nT @ ±1000 nT. Range: ±1000 nT.</p> <p>Radio Occultation (ROCC) [3B]                      • T profiles with vertical resolution &lt; 100 m and &lt; 1 K accuracy.</p> <p><b>Aerobot:</b>                      Aerosol Mass Spectrometer with Nephelometer (AMS-N) [1A, 1B, 3A, 3B]                      • Abundances and isotopic ratios of Xe, Kr, Ar and Ne to ±5 per mil.                      • Certain stable gas isotopes (<sup>15</sup>N/<sup>14</sup>N in N<sub>2</sub> to ±10 per mil).                      • CHNOPS, including SO<sub>2</sub>, SO<sub>3</sub>, HCl, CO, OCS, H<sub>2</sub>O, HDO, H<sub>2</sub>S, to 1 ppm.                      • H<sub>2</sub>SO<sub>4</sub>, H<sub>2</sub>O, FeCl<sub>3</sub>, and sulfur (S<sub>3</sub>, S<sub>4</sub>, S<sub>x</sub>) to 1%.                      • Nephelometer: Effective size of particles to 0.1 μm. Refractive index to &lt; 0.02. Identify non-spherical (non-liquid) particulates.</p> <p>Tunable Laser Spectrometer (TLS) [1A]                      • Channel 1: CO<sub>2</sub> and H<sub>2</sub>O for isotopic ratio of <sup>18</sup>O/<sup>17</sup>O/<sup>16</sup>O in CO<sub>2</sub> and H<sub>2</sub>O, D/H in H<sub>2</sub>O, and <sup>13</sup>C/<sup>12</sup>C in CO<sub>2</sub>, all to ±1 per mil precision.                      • Channel 2: CO and OCS for <sup>34</sup>S/<sup>33</sup>S/<sup>32</sup>S in OCS, <sup>13</sup>C/<sup>12</sup>C in CO and OCS to ±5 per mil precision.</p> <p>Meteorological Suite (MET) [1B, 3A, 3B]                      • Temperature, pressure, turbulence, wind speeds, and ionizing radiation levels.                      • Seismology: Infrasound at 0.01–80 Hz to ~0.001 Pa.</p> <p>Magnetometer, Aerobot (MAG-G) [2B]                      • Same as MAG-O</p> <p><b>Dropsonde:</b>                      P/T Sensors [3B]                      • T: Range 230–750 K. Accuracy/precision: &lt; 0.1 K                      • P: Range 20 mbar to 90 bar. Accuracy/precision &lt; 0.1 mbar</p> <p>Chemical Sensors [3B]                      • H<sub>2</sub>, O<sub>2</sub>, CO, H<sub>2</sub>O, HCl, NO to ppm level (ppb for H<sub>2</sub>, O<sub>2</sub>, NO)</p>	<p>1. Transport the flight system to Venus</p> <p>2. With the orbiter, achieve the required observing geometry for at least 60 Earth-days for                      • NIR-S &amp; NIR-C: IR images of Venus at the specified spatial coverages and resolutions                      • MAG-O: B-field data from the solar wind                      • EUV: Monitor the Sun                      • ROCC: Occultations of Earth by the Venus atmosphere</p> <p>3. With the aerial platform, dwell at altitudes from 52–62 km (“cloud levels”) for at least 60 Earth-days and operate the science instruments as follows                      • AMS-N: One set of measurements at &gt; 50 different local times during each circumnavigation                      • TLS: One set of measurements                      • MAG-G: Continuous B-field measurements                      • MET: Continuous P measurements at infrasound frequencies. T, windspeed, and ionizing radiation measurements at &gt;50 different local times, including at &lt;15 Earth-minute frequency for 14 Earth-hours centered on local noon.</p> <p>4. Deploy a dropsonde at &gt;52 km altitude for P/T and chemical sensor measurements with &lt;0.5 km vertical spacing down to the surface.</p> <p>5. Deliver all the required science data to Earth.</p>

### 1.3 Descope Strategies for ADVENTS

ADVENTS was designed to perform many of the highest-priority science investigations for Venus exploration with cross-cutting relevance to all of planetary science and astrobiology. In particular, the ADVENTS mission is designed to meet 8 of 12 essential objectives defined in the VEXAG GOI document. We did not define a separate threshold mission in this study, although we suggest four descope options below. Future teams may consider a few descopes for ADVENTS, which could reduce the total cost and technical risk of the mission without dramatically reducing the overall science return.

Shortly before this ADVENTS report was finalized, NASA committed to return to Venus with two highly capable missions. Out of four finalists for the Discovery Program, NASA selected DAVINCI+ (Deep Atmosphere Venus Investigation of Noble gases, Chemistry, and Imaging Plus) and VERITAS (Venus Emissivity, Radio Science, InSAR, Topography, and Spectroscopy). Additionally, a geophysical orbiter called EnVision, which is similar and complementary to VERITAS, was newly selected to become the fifth medium-class mission (M5) in the ESA Cosmic Vision Programme.

Given that the NASA and ESA selections were announced at the very end of the study process, this study could not include comprehensive modifications to the ADVENTS STM in response to these selections. As a result, two of the six science objectives for ADVENTS overlap in some way with the objectives identified by the selected NASA and ESA missions (**Table 2**). For example, DAVINCI+ will achieve Objective 1A (Origin of Volatiles). All the competed missions, including EnVision, target Objective 2A (Ancient Oceans) because this objective is supremely important to the goals of the Venus community and the overarching mandate of the NASA Planetary SMD. Regardless of these overlaps, this ADVENTS study shows that the synergistic ADVENTS orbiter and aerobot payloads can accomplish unique, high-priority science that extends beyond what is possible from mission architectures lacking long-lived, cloud dwelling, in-situ elements. As a result, we are confident that the ADVENTS concept has the potential to fill a key role in advancing Venus science priorities even with the newly defined programmatic landscape for Venus exploration. A robust strategy for planetary exploration should include multiple successive and/or overlapping missions to Venus with synergistic architectures and science goals. Future teams can and should update the ADVENTS concept to be responsive to lessons learned from recent and forthcoming NASA and ESA selections.

**Table 2:** ADVENTS has minimal science overlap with the two Venus-targeting missions that were recently selected for the NASA Discovery Program. In many cases, all three missions are complementary and would work together to unveil the mysteries of Venus. For the purpose of assessing overlap with ADVENTS, VERITAS and EnVision are functionally similar.

ADVENTS Science Objective	Addressed by NASA DAVINCI+?	Addressed by NASA VERITAS or ESA EnVision?
<b>1A.</b> Origin of volatiles.	Yes — However, ADVENTS would verify that key isotopic ratios are homogenous, as often assumed, below the homopause.	No
<b>1B.</b> Tectonic and volcanic activity.	Limited — DAVINCI+ does not constrain tectonic activity. ADVENTS would search for signatures of volcanism at many different locations.	Complementary — Radar mapping also provides unique constraints on tectonics and volcanism. ADVENTS alone conducts seismic investigations.
<b>2A.</b> Tesserae formed near water oceans.	Complementary — DAVINCI+ returns high-resolution data from one tessera. ADVENTS uses multi-spectral imaging to make global maps of rock types.	Yes — VERITAS & EnVision would also achieve ADVENTS Objective 2A using the same instrument.
<b>2B.</b> Crustal magnetism.		No
<b>3A.</b> Habitability of the cloud environment.	Limited — ADVENTS dwells in the clouds for at least 60 Earth-days, studying atmospheric chemistry and dynamics at all local times and many locations.	No
<b>3B.</b> Volatiles in the cloud environment.		No

The comparative advantage of ADVENTS is its ability to provide a comprehensive assessment of Venus current climatic state. The ADVENTS aerobot would dwell in the atmosphere and collect data for months at many local times (and altitudes), over multiple key surface regions—while the orbiter simultaneously obtains context on the cloud layers (relative to the underlying geology) from orbit.

VERITAS (and EnVision) will provide a generational leap in our understanding of the surface geology of Venus. Unlike ADVENTS, neither VERITAS nor EnVision will search for seismic activity or crustal remanent magnetism. The relatively late launch date for EnVision (~2030s) would potentially enable repeated radar imaging while ADVENTS characterizes, for example, the atmospheric signatures of on-going volcanic activity. DAVINCI+ will deliver superb measurements of atmospheric chemistry from the top of the atmosphere to the surface, along with human-scale geologic images and rock types—at one region (Alpha Regio). In contrast, ADVENTS would acquire the data that is needed to constrain aerosol formation and composition and the chemical, dynamical, and microphysical response of the cloud layer atmosphere to external/internal forcing such as incoming solar flux, seismic activity, volcanic activity, local solar time, underlying topography, and the altitude of solar deposition. Assessing the spatial and temporal variability of chemical and dynamical processes is essential to understanding is key region of the Venus atmosphere, and to interpreting the full gamut of spectral observations of the atmospheres of terrestrial exoplanets.

Trimming investigations from ADVENTS that are redundant with DAVINCI+ and VERITAS/EnVision is a natural descope strategy (**Table 3**)—but will inevitably lead to some science loss. **Table 4** suggests one possible version of more modest ADVENTS with a lower cost than the baseline version. The first descope would be the ADVENTS dropsonde. The single-trajectory DAVINCI+ probe has much more capability than the ADVENTS dropsonde, leading to an overall higher science return. The second descope would be the mini-TLS from the aerobot. Unlike the gas and aerosol chemistry measurements made with the aerobot AMS-N, the isotopes (*e.g.*, D/H and noble gases) measured with the TLS are not expected to vary much with time and space in the Venus atmosphere once below the region of photochemical activity. DAVINCI+ could thus provide these key measurements. However, including the TLS on ADVENTS would still support the gas measurements needed for ADVENTS Objective 3B and could corroborate certain time-variable detections, including potentially of phosphine gas, with very high-precision measurements of the abundances of species with similar masses. Furthermore, given the selection of VERITAS, teams should consider descoping NIR-S from the ADVENTS orbiter because it is a duplicate of the Venus Emissivity Mapper included on both VERITAS and EnVision. However, monitoring the surface IR emissivity with the ADVENTS orbiter would still support Objective 1B (characterizing active volcanism and its relationship to seismic activity) if neither VERITAS nor EnVision are operating at the same time as ADVENTS. Finally, ADVENTS Objectives 3A and 3B could be redefined if EUV were descoped from the orbiter. None of the other instruments on the orbiter or aerobot are appealing descope targets because they are all uniquely required to achieve one or more science objectives, even with the recent selections of DAVINCI+ and VERITAS.

**Table 3:** NASA’s late-breaking selections of VERITAS and DAVINCI+ motivate consideration of several descope options for ADVENTS. That said, proposal teams could make various arguments for retaining each instrument in the baseline payload.

Desclope Option	Reason(s) to Desclope	Reason(s) not to Desclope
NIR Imager, Surface (NIR-S)	VERITAS & EnVision carry an identical instrument.	If ADVENTS operates at a different time than other missions, NIR-S is useful for monitoring active volcanism and chemical weathering.
Tunable Laser Spectrometer (TLS)	DAVINCI+ will make precise measurements of the targeted isotopic ratios.	ADVENTS would verify that those isotopic ratios do not vary with location and/or local time, as is typically assumed.
Dropsonde (DROP)	DAVINCI+ will characterize atmospheric chemistry and dynamics from the clouds to the surface at one location.	ADVENTS could help assess the temporal and spatial variability of the sub-cloud atmosphere.

Overall, the four descope options in **Table 4** total \$116M (FY2025, including reserves) in direct savings for Phase A–D. Exercising these descope options would lead to even more savings because removing the Dropsonde and payload mass from the Aerobot (*i.e.*, the TLS) has a very long “lever arm” that would substantially reduce the mass and thus cost of the aerobot balloon and entry system. If all four descope options are exercised, then the total cost for Phase A–D with reserves is ~\$1.2B. Assuming realistic reserves (*i.e.*, < 50%) on high-heritage elements and reduced cost wraps to account for the descopes, this more modest version of ADVENTS should have a cost close to the cap anticipated for the New Frontiers program.

**Table 4:** Reducing the instrument payload for ADVENTS would substantially lower the total cost without dramatically reducing the science return. Additional savings would be realized via simplifications to the Aerobot and entry system designs and then from the decrease in cost wraps. Here, we estimate the total mission cost after implementing each descope option.

Desclope Order	Desclope Option	Direct Cost Savings (FY2025, including reserves)	Mission Cost (FY2025 Phase A–D, including reserves)
1	Dropsonde (DROP)	\$52.4M	\$1.5B
2	Tunable Laser Spectrometer (TLS)	\$30.0M	\$1.4B
3	NIR Imager, Surface (NIR-S)	\$6.0M	\$1.35B
4	Extreme UltraViolet Radiation Monitor (EUV)	\$27.6M	\$1.2B

## 2 HIGH-LEVEL MISSION CONCEPT

### 2.1 Overview

The ADVENTS flight system consists of an Orbiter and an Aerobot with a Dropsonde as shown in **Figure 3**. The Orbiter functions as a carrier for the Aerobot, a communication relay for the Aerobot and Dropsonde as well as a science platform. The Aerobot is contained within an entry system so that it can survive entry and descent through the Venus atmosphere. The Orbiter spins up to 5 rpm and then releases the Aerobot in its entry system for the entry and descent phase 5.5 days prior to the Orbiter inserting into its Operational Orbit about Venus. The Aerobot carries a dropsonde that is released during entry that carries pressure, temperature, and chemical sensors to measure the atmosphere down to the surface for up to an hour. During its nominal 60-day lifetime the Aerobot floats at a nominal altitude of 55 km with controlled altitude excursions in the band of 52-62 km allowing it to circumnavigate Venus every 7 days. Flight system characteristics are given in **Table 5**.

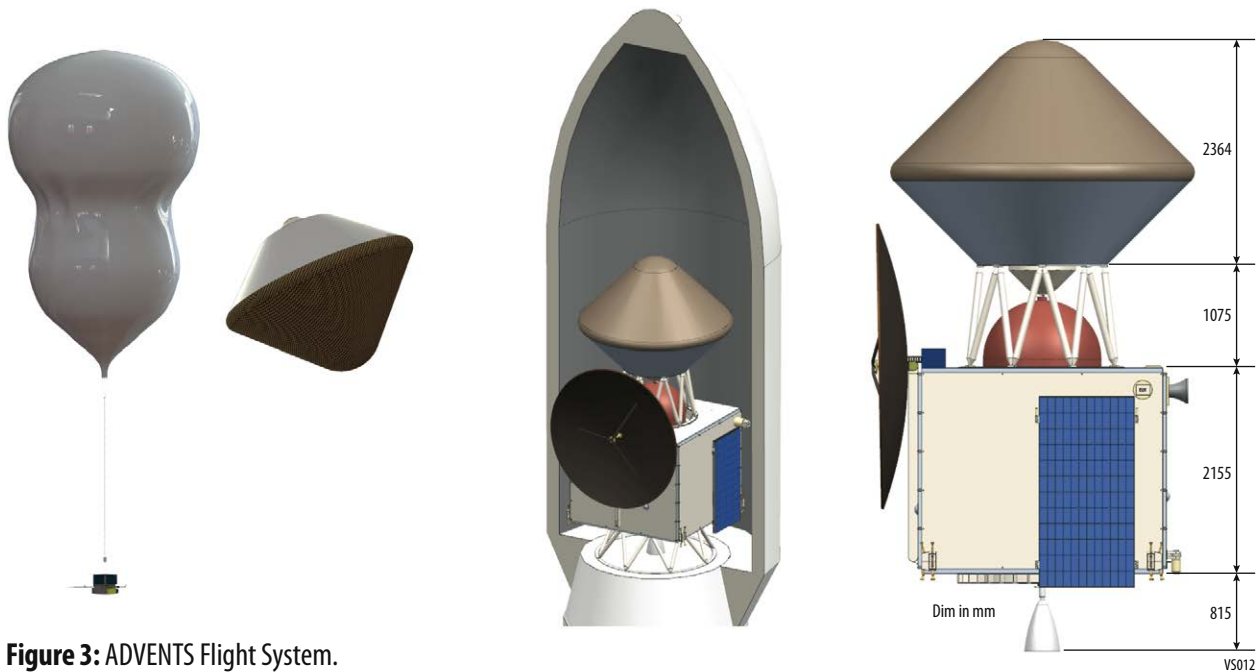


**Figure 3:** ADVENTS Flight System.

ADVENTS is launched from Cape Canaveral on a Falcon Heavy with a 5 m diameter fairing. The primary launch opportunity is June 4, 2039 with a backup launch opportunity of December 4, 2039. Both launch opportunities have a minimum of a 14-day launch window. The Orbiter releases the Aerobot days prior to the Venus Orbit Insertion (VOI) that places it in a low eccentricity, low-inclination, retrograde orbit with a ~12 hour period (24,856 km altitude) that enables frequent contacts with the Aerobot and the relay of all data back to Earth. **Table 6** shows the ADVENTS mission summary. The launch period for this study was defined by the requirement to launch within the next Planetary Decadal timeline window of 2036–2040 for New Frontiers 6. At the end of the study, the release of the New Frontiers 5 request for proposal was delayed. This delay provides an opportunity for

**Table 5:** Flight System Element Characteristics Table.

Flight System Element Parameters (as appropriate)	Aerobot	Orbiter
<b>General</b>		
Design Life, months	2	78
<b>Structure</b>		
Structures material (aluminum, exotic, composite, etc.)	Aluminum, honeycomb panels	Aluminum, honeycomb panels
Number of articulated structures	0	3 Solar Arrays, HGA, EUV spin table
Number of deployed structures	3 Mag Boom, Antenna boom, Wind sensor/Antenna boom	2 HGA and Mag boom
Aeroshell diameter, m	3.2	N/A
<b>Thermal Control</b>		
Type of thermal control used	Passive – convection and radiation off of white painted surfaces	MLI, radiator patches, heaters
<b>Propulsion</b>		
Estimated delta-V budget, m/s	N/A	2,380 m/s
Propulsion type(s) and associated propellant(s)/oxidizer(s)	N/A	Pressure Regulated, Bi-Propellant (MMH & MON-3)
Number of thrusters and tanks	N/A	1 Main Engine 20 ACS Thrusters (Pri+Red) 2 Propellant Tanks 4 COPV Helium Tanks
Specific impulse of each propulsion mode, seconds	N/A	Primary, ME Mode: 315s (299.7s at -3σ) Secondary, ACS Mode: 300s (285s at -3σ)
<b>Attitude Control</b>		
Control method (3-axis, spinner, grav-gradient, etc.)	N/A	3-axis, spinner
Control reference (solar, inertial, Earth-nadir, Earth-limb, etc.)	N/A	Inertial, Venus-Nadir, Solar
Attitude control capability, degrees	N/A	< 0.1 degrees
Attitude knowledge limit, degrees	N/A	< 30 arcsec
Agility requirements (maneuvers, scanning, etc.)	N/A	Spin S/C to 5 RPM. Slew rate during calibration not specified
Articulation/# – axes (solar arrays, antennas, gimbals, etc.)	N/A	Solar Array, HGA
Sensor and actuator information (precision/errors, torque, momentum storage capabilities, etc.)	N/A	CSS: stradian ST: 30 arcsec boresight IMU: ARW = 0.07°/root-hour, Bias: 1°/hr RCS: 5 lb Wheel: 0.2 Nm, 250 NMS
<b>Avionics</b>		
Flight Element housekeeping data rate, kbps	0.3	1
Data storage capacity, Mbits	600	20,000
Maximum storage record rate, kbps	20,000	20,000
Maximum storage playback rate, kbps	75,000	75,000
<b>Power</b>		
Type of array structure (rigid, flexible, body mounted, deployed, articulated)	Rigid, Body Mounted	Rigid, Deployed
Array size, meters x meters	2.1	8.3
Solar cell type (Si, GaAs, Multi-junction GaAs, concentrators)	TJGAS	TJGAS
Expected power generation at Beginning of Life (BOL) and End of Life (EOL), watts	510/432	3,658/2,989
On-orbit average power consumption, watts	Day 163.8 Night 100	1,442.4
Battery type (NiCd, NiH, Li-ion)	Li - Ion	Li-Ion
Battery storage capacity, amp-hours	260	210

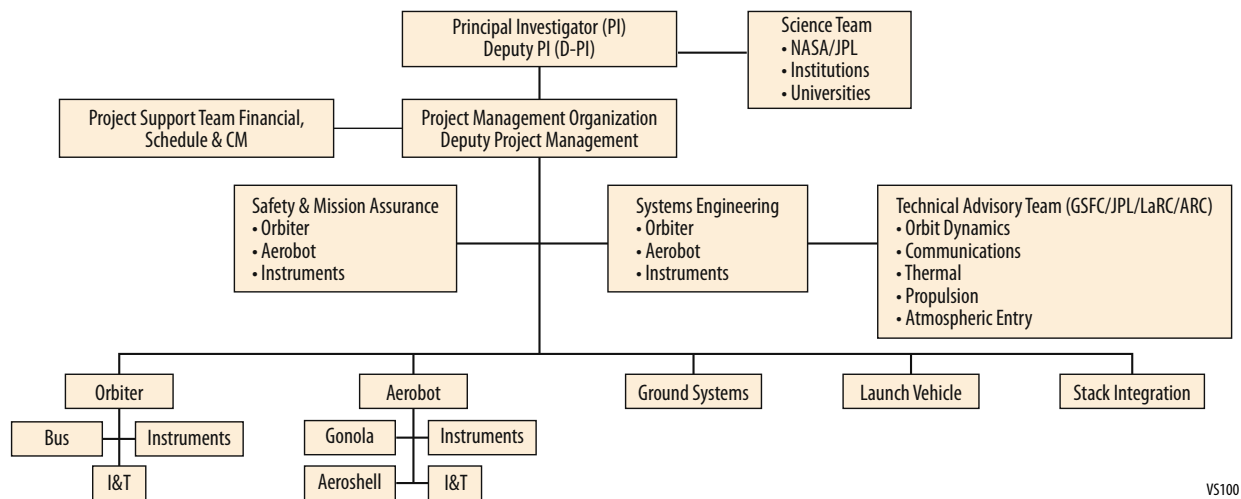
ADVENTS to be part of New Frontiers 5 with launch dates as early as 2030. **Figure 6** shows the full range of launch opportunities from 2030–2040. Launch dates with delta-V equivalent to the primary and backup launch dates are found on December 9, 2030 and June 5, 2031 respectively. The launch trajectories for 2030 and 2031 are expected to have similar eclipses and communication links, allowing

science operations for the earlier launch opportunity to be identical to the launch dates in 2039. The primary and backup launch dates discussed in the rest of the study report are for 2039.

## 2.2 Concept Maturity Level

This study was conducted with a goal of Concept Maturity Level (CML) 5. However, due to study duration limitations, the concept presented here is considered to be CML 4 (see **Table 7** for CML definitions). It presents an implementation concept at the subsystem level, as well as science traceability, mission requirements traceability, key technologies, heritage, risks and mitigations. Detailed cost models were developed. Further development is necessary to mature the final design architectures and approaches.

**Figure 4** illustrates a notional Organizational Chart assuming ADVENTS is implemented as a New Frontiers mission and would be PI-led with support from NASA centers, universities, and industry. As typical with PI-led missions the PI has overall authority and accountability for mission success and is supported by a deputy PI, a science team, and project management. Any organizational chart must show clear lines of responsibility and authority and this is especially crucial for a complex mission such as this. The ADVENTS concept as presented relies on no foreign instruments or contributions.



VS100

**Figure 4:** Notional ADVENTS Organizational Structure indicating key roles and responsibilities.

**Table 6:** ADVENTS Mission Summary.

Parameter	Value	Units
Orbit Parameters (apogee, perigee, inclination, etc.)	24,856.2 km circular 170° inclination	
Mission Lifetime	78	mos
Maximum Eclipse Period	58	min
Launch Site	Cape Canaveral	
Aerobot Entry Mass with contingency (includes instruments)	1,878.6	kg
Orbiter Mass with contingency (includes instruments)	1,494.7	kg
Propellant Mass without contingency	2,273.1	kg
Propellant contingency	10	%
Propellant Mass with contingency	2,500.4	kg
Launch Adapter Mass with contingency	71.0	kg
Total Launch Mass	5,944.7	kg
Launch Vehicle	Falcon heavy Expendable	Type
Launch Vehicle Lift Capability	11,694.0	kg
Launch Vehicle Mass Margin	5,749.3	kg
Launch Vehicle Mass Margin (%)	96.7	%

**Table 7:** Concept Maturity Level Definitions.

Concept Maturity Level	Definition	Attributes
CML 6	Final Implementation Concept	Requirements trace and schedule to subsystem level, grassroots cost, V&V approach for key areas
CML 5	Initial Implementation Concept	Detailed science traceability, defined relationships and dependencies: partnering, heritage, technology, key risks and mitigations, system make/buy
CML 4	Preferred Design Point	Point design to subsystem level mass, power, performance, cost, risk
CML 3	Trade Space	Architectures and objectives trade space evaluated for cost, risk, performance
CML 2	Initial Feasibility	Physics works, ballpark mass and cost
CML 1	Cocktail Napkin	Defined objectives and approaches, basic architecture concept

## 2.3 Key Trades

The primary mission trade was to determine the architecture elements for the mission. Options for a fixed balloon with a dropsonde vs variable-altitude balloon with dropsonde and a towbody were evaluated as shown in **Table 9**. A towbody that would deploy from the Aerobot to conduct surface imaging below the cloud deck was initially evaluated for inclusion on the fixed-altitude balloon, but the option was eliminated for further consideration on the fixed-altitude balloon due to the large length and mass of tether needed to deploy it from the 55 km fixed-altitude. It was evaluated for inclusion on the variable-altitude balloon. Details of the towbody are shown in **Appendix A.3.1.5**.

The result of the trade was an architecture composed of a variable-altitude balloon and a single dropsonde attached to the Aerobot that releases just prior to backshell separation and no towbody (**Table 10** highlighted column). The following paragraphs describe the trade in further detail. The dropsonde design concept is discussed in **Appendix A.3.1.4**. The towbody considered is discussed in **Appendix A.3.1.5**. Additional Aerobot (**Appendix A.3.1**) and Orbiter (**Appendix A.3.2**) subsystem and design trades are discussed in each of the subsystems.

### 2.3.1 Balloon Type

There are many different types of balloons possible for use at Venus and this study was asked to evaluate two of them:

- **A spherical superpressure balloon.** This type of balloon consists of a spherical structure that is inflated with enough gas to always be pressurized compared to the local atmosphere and therefore maintain its spherical shape throughout the flight. This constant volume feature provides passive altitude stability such that the balloon will always seek to fly at a constant density level in the atmosphere and will return to that point if displaced vertically by wind gusts. The 1985 Soviet VeGa balloons were of this type (**Figure 5**), though much smaller than the size considered for this study.
- **A variable-altitude balloon.** This type of long-duration balloon relies on gas pumping between chambers in a two-part balloon to change the net buoyancy and thereby effect altitude changes. This allows for exploration over a potentially wide altitude range, in contrast to the constant altitude superpressure balloon. Many different options exist for implementing such a variable-altitude balloon (see for example Hall *et al.*, “Altitude-Controlled Light Gas Balloons for Venus and Titan Exploration”, AIAA Paper 2019-3194) but this study adopted the same option as the 2020 Venus Flagship Study that consisted of a balloon-within-a-balloon architecture with helium gas pumping between the outer non-pressurized balloon (also known as a “zero pressure balloon”) and the inner pressurized balloon (a superpressure balloon itself). A recent Venus sub-scale prototype balloon of this type is shown in **Figure 6** with a diagram showing how this type of balloon works in **Figure 7**.

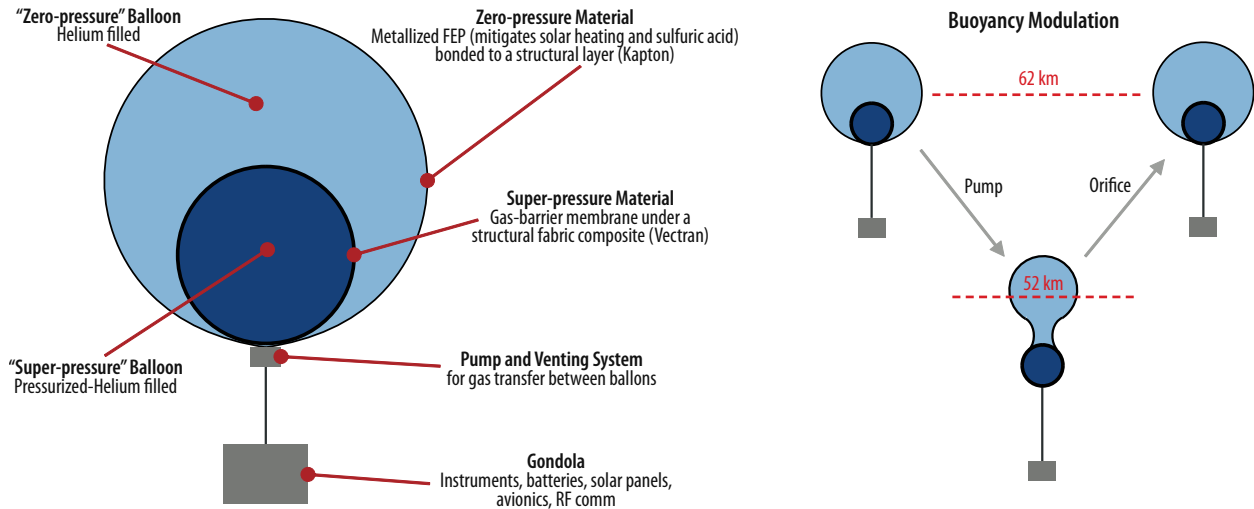


**Figure 5:** Soviet VeGa balloon (1985).



**Figure 6:** JPL/Near Space Corporation 4 m sub-scale variable altitude balloon (2020), illustrating the volume expansion required for changing altitude. [Izraelevitz, J., Pauken, M., Elder, T., Carlson, K., Lachenmeier, T.I.M., Baines, K., Cutts, J.A. and Hall, J.L.. “Pumped-Helium Aerobots for Venus: Technology Progress and Mission Concepts. 2020, December”. In AGU Fall Meeting 2020. AGU.]





VS015

**Figure 7:** Diagram summarizing the structure and operation of a balloon-in-a-balloon variable altitude concept.

The team conducted a trade study between these two options that quantified the mass penalty associated with using the more complicated, but more capable, variable-altitude balloon compared to the simpler constant altitude superpressure balloon. The results are summarized in **Table 8** for the scenario where the superpressure balloon is designed for a 55 km altitude and the variable-altitude balloon range is 52 to 62 km. The balloon materials used in these designs are shown in **Table 9**.

For both the inner and outer balloon, the Teflon provides sulfuric acid resistance to the aerosols in the Venus clouds, the metallization reflects most sunlight and limits solar heating, and the Vectran provides high strength to contain the pressurization loads.

**Table 8:** Mass Comparison Between Constant and Variable Altitude Balloon Options.

Gondola Mass (kg)	Fixed Altitude (55 km)			Variable Altitude (52-6 km)			Floating Mass Increase (%)
	Balloon Mass (kg)	Floating Mass (kg)	Gondola (% of Floating)	Balloon Mass (kg)	Floating Mass (kg)	Gondola (% of Floating)	Var. Alt. vs Fixed Alt.
140	78	218	64	126	266	53	22
180	98	276	65	149	329	55	19
200	105	305	66	156	356	56	17
230	117	347	66	170	400	58	15

**Table 9:** Inner and Outer Balloon Materials for the Variable Altitude Balloon.

Outer Balloon Material	Inner Balloon Material
1mil FEP – High Epsilon & Acid Barrier	Vectran Fabric – Superpressure Strength
150nm VD Silver/Inconel Layer - Low Alpha & Diffusion Barrier	
Thermoset Adhesive	
100nm VD Aluminum Layer - Diffusion Barrier	Urethane Bladder – Gas Barrier
1mil Kapton - Gas Barrier & Structure	

\*Adapted from Hall *et al.*, "Prototype design and testing of a Venus long duration, high altitude balloon", *Advances in Space Research*, Vol. 42, pp 1648-1655, 2008).

The data in **Table 8** shows that the constant altitude balloon provides a small mass advantage across a wide range of gondola masses. The team concluded that the significant science benefit provided by the variable-altitude capability was worth the additional mass required and therefore adopted it as the baseline.

### 2.3.2 Dropsonde Mounting

**Figure 8** shows the four mounting options that were considered for accommodating the dropsonde. To minimize float mass all options were required to release the dropsonde prior to Aerobot float.

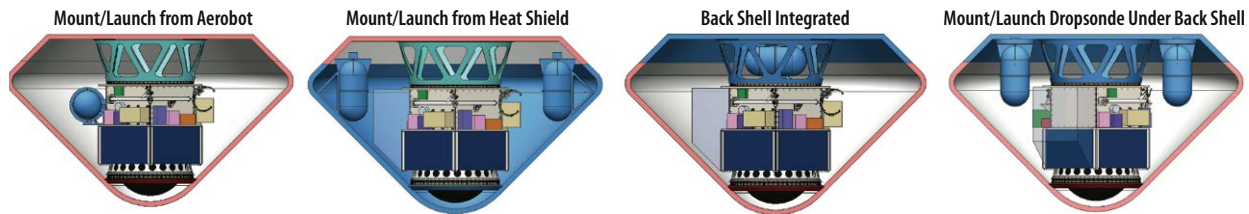


**Figure 8:** Dropsonde Accommodation Options.

The first option was to mount the dropsonde to the Aerobot and release it prior to the backshell separation. Due to packaging constraints only 1 dropsonde could be accommodated.

The second option allowed for mounting of multiple dropsondes to the back of the heat shield. **Figure 9** shows that the dropsondes would separate from the backshell after the backshell is jettisoned by the use of small parachutes.

The third option considered was to mount the dropsonde to the backshell as an integrated pressure vessel that would float away with the backshell as shown in **Figure 10**.

The four options were evaluated, and the team concluded that the significant entry mass required for options 2-4 would drive the size and cost of the entry system significantly more than option 1. Option 1 was selected as the baseline mounting design concept.

The final option considered was to mount dropsondes to the backshell and deploy them via lightband separation systems as shown in **Figure 11**.

Mounting the dropsonde to the Aerobot and releasing it prior to backshell separation was selected as the baseline concept since it minimized the mass of the entry system and allowed for the center of gravity to be lower during entry than the other options. A concern with this mounting is the c.g. offset that needs to be minimized due to the 5 rpm spin rate that the entry system has after release from the Orbiter and during entry and descent. Adjusting the mounting locations of electronic boxes and battery units was used to provide this offset.

### 2.3.3 Towbody

The evaluation of including a Towbody showed that in all cases a significant increase in cost and float mass occurred. For this reason, the Towbody was not selected for inclusion in the baseline concept.

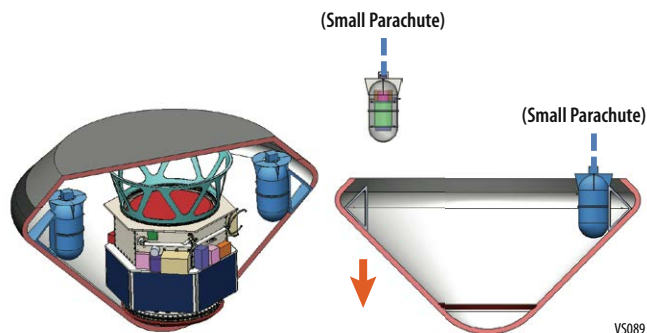


**Figure 9:** Dropsonde mounted to back of heat shield.

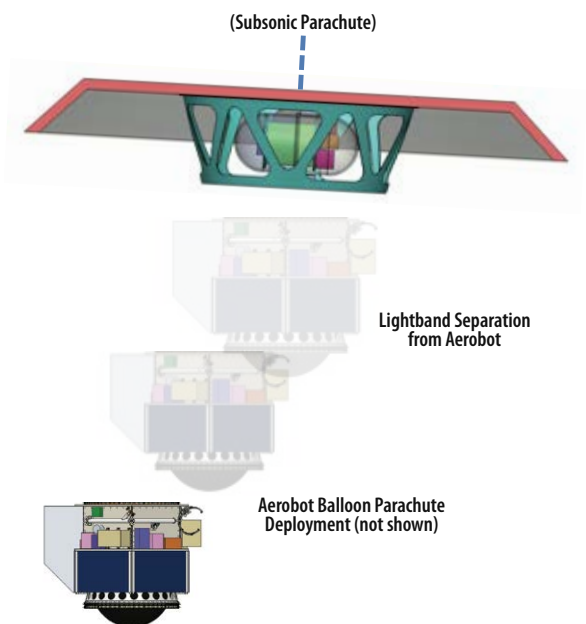


**Figure 10:** Backshell Integrated pressure vessel.

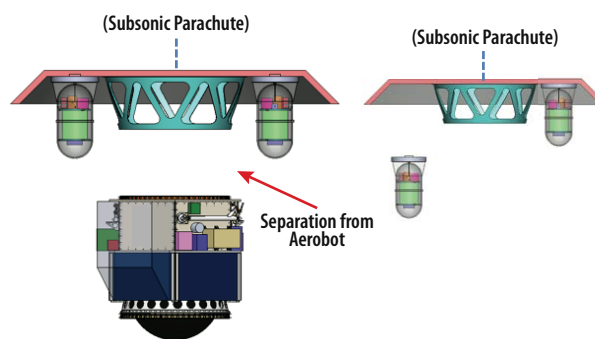


**Figure 11:** Backshell mounted dropsonde deployment.

**Table 10:** ADVENTS Configuration Trade.

	Fixed Altitude Balloon					Variable Altitude Balloon			
	Dropsonde Mounting Option 1	Dropsonde Mounting Option 2	Dropsonde Mounting Option 3	Dropsonde Mounting Option 4	Dropsonde Mounting Option 1	Towbody + Dropsonde Mounting Option 1	Towbody + Dropsonde Mounting Option 2	Towbody + Dropsonde Mounting Option 3	Towbody + Dropsonde Mounting Option 4
Cost	\$	\$\$	\$\$	\$\$	\$\$	\$\$\$	\$\$\$\$	\$\$\$\$	\$\$\$\$
Float Altitude Range (km)	55	55	55	55	52-62	52-62	52-62	52-62	52-62
Maintain Float Altitude	No	No	No	No	Yes	Yes	Yes	Yes	Yes
Adjust circumnavigation period	No	No	No	No	Yes	Yes	Yes	Yes	Yes
Number of Dropsondes	1	1+	1	1+	1	1	1+	1	1+
Dropsonde Support Mass on Gondola	Yes	No	No	No	Yes	Yes	No	No	No
Dropsonde Drop Time	1 hour	1-3 hours	1-3 hours	1-3 hours	1 hour	1 hour	1-3 hours	1-3 hours	1-3 hours
Dropsonde Parachute(s)	No	Yes	No	Yes	No	No	No	No	No
Dropsonde Release mechanism(s)	Yes	Yes	No	Yes	Yes	Yes	Yes	No	Yes
Dropsonde Parachute Required	No	Yes	No	No	No	No	Yes	No	No
1 Dropsonde mass (kg)	116.9	116.9	116.9	116.9	116.9	116.9	116.9	116.9	116.9
Dropsonde Accommodation on Gondola mass (kg)	6.5	0	0	0	6.5	6.5	0	0	0
Dropsonde accommodation Mass on Entry System (kg)	0.0	10	5	10	0.0	0.0	10	5	10
Towbody System mass (kg)	N/A	N/A	N/A	N/A	0.0	22.8	22.8	22.8	22.8
Towbody Accommodation on Gondola: Battery and SA Delta, Mounting Mass (kg)	0	0	0	0	0.0	12.0	12.0	12.0	12.0
Balloon Mass (kg)	136.5	130.7	130.7	130.7	214.3	233.1	234.7	232.4	234.7
He (kg)	38.8	37.2	37.2	37.2	38.8	44.8	45.3	44.5	45.3
He Tank (kg)	471.1	468.2	468.2	468.2	471.1	481.5	482.4	481.1	482.4
Entry System Mass (kg)	841.9	841.9	841.9	841.9	878.2	878.2	878.2	883.2	888.2
Entry Mass (kg)	1,800.8	1,800.5	1,795.5	1,800.5	1,878.6	1,913.8	1,930.2	1,916.0	1,930.2
Gondola Mass (kg)	198.0	191.5	191.5	191.5	198.0	239.3	242.8	237.8	242.8

### 3 TECHNICAL OVERVIEW

#### 3.1 Instrument Payload Description

The strawman payload on the ADVENTS Mission almost entirely consists of instruments that were also selected for the VFM study. It is comprised of these synergistic platforms: orbiter, variable-altitude aerobot, and a single dropsonde. The Orbiter carries (2) near infrared imagers (NIR-C for cloud layer dynamics and NIR-S for surface emissivity) and an Extreme Ultraviolet (EUV) monitor. The new addition is the NIR-C which draws heritage from JAXA Akatsuki IR2 instrument. The Aerobot instrument payload includes an aerosol mass spectrometer with nephelometer (AMS-N), mini tunable laser spectrometer (TLS), suite of meteorological (AMET) sensors to measure barometric pressure and temperature, wind speed, and ionizing radiation, and a dropsonde.

The Orbiter and Gondola each carry the NASA GSFC standard fluxgate magnetometer (MAG, MAG-O is full-sized and MAG-G is miniaturized) mounted on a deployable boom. The MAG draws heritage from MAVEN, Juno, and Parker Solar Probe and has been in Mars orbit since 2014.

The mass and power values are summarized in **Table 11**. The instrument characteristics are provided in **Table 12** and **Table 13**.

**Table 11:** Aerobot and Orbiter Instrument Summary.

Instrument Name	Flight Element(s)	Mass			Average Power		
		CBE (kg)	% Cont.	MEV (kg)	CBE (W)	% Cont.	MEV (W)
NIR-S	Orbiter	3.4	30	4.4	1.03	30	16.9
NIR-C	Orbiter	18.0	30	23.4	114.0	30	148.2
Magnetometer	Aerobot	1.5	30	1.3	1.0	30	0.7
	Orbiter		30	2.0			1.3
EUV	Orbiter	7.0	30	9.1	14.0	30	18.2
AMS-N	Aerobot	10.5	30	13.7	7.0	30	9.1
Mini-TLS	Aerobot	3.3	30	4.3	24.0	30	31.2
Meteorological sensors	Aerobot	4.0	30	5.2	5.0	30	6.5
Chemical Sensor Array	Dropsonde	0.1	30	0.13	3.0	30	3.9
Pressure and temperature sensors	Dropsonde	2.3	30	3.0	10.7	30	13.9
Total Payload Mass		51.6	30	67.2			

**Table 12:** Orbiter Instrument Characteristics.

Item	Near IR Imager, NIR-S	Near IR Imager, NIR-C	Extreme Ultraviolet Monitor, EUV	Magnetometer Orbiter, MAG-O
Type of instrument	Spectral imager	Spectral imager	EUV	Magnetometer
Number of channels	14	6	3	1
Size/dimensions (m x m x m)	0.6 x 0.22 x 0.21	0.25 x 0.25 x 0.20	0.97 x 1.5 x 1.1	0.08 x 0.10 x 0.12
Instrument mass without contingency (Kg, CBE*)	3.4	18	7	1.5
Instrument mass contingency (%)	30	30	30	30
Instrument mass with contingency (Kg, CBE+Reserve)	4.4	23.4	9.1	1.9
Instrument average payload power without contingency (W)	13	114	14	1
Instrument average payload power contingency (%)	30	30	30	30
Instrument average payload power with contingency (W)	16.9	148.2	18.2	1.3
Instrument average science data rate^ without contingency (kbps)	115.8	1,384.6	1.6	2
Instrument average science data^ rate contingency (%)	30	30	30	30
Instrument average science data^ rate with contingency (kbps)	150.5	1,800	2.1	2.6

**Table 13:** Aerobot Instrument Characteristics.

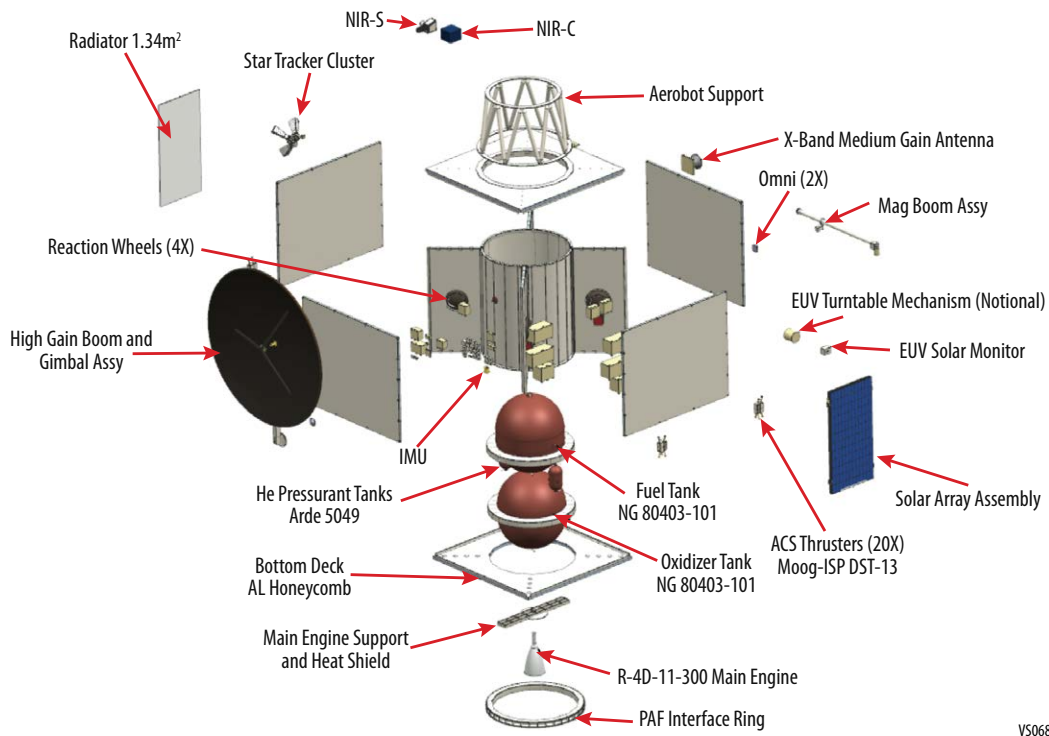
Item	Aerosol Mass Spectrometer with Nephelometer (AMS-N)	Mini Tunable Laser Spectrometer (TLS)	Meteorological Suite (MET)	Fluxgate Magnetometer Gondola MAG-G	Dropsonde Pressure and Temperature Sensors	Dropsonde Chemical Sensor Array
	Aerosol spectrometer	Laser Spectrometer	P, T, wind, radiation sensors, infrasound	Magnetometer	P, T sensors	Chemical sensors
Number of channels	6	2	3	1	2	8
Size/dimensions (m x m x m)	0.30 x 0.20 x 0.20	0.25 x 0.11 x 0.07	0.20 x 0.12 x 0.08	0.08 x 0.10 x 0.12	0.2 x 0.12 x 0.08	0.05 x 0.05 x 0.03
Instrument mass without contingency (Kg, CBE*)	10.5	3.3	4	1.5	2.3	0.1
Instrument mass contingency (%)	30	30	30	30	30	30
Instrument mass with contingency (Kg, CBE+Reserve)	13.7	4.3	5.2	1.9	2.9	1.03
Instrument average payload power without contingency (W)	7	24	5	0.5	10.7	3
Instrument average payload power contingency (%)	30	30	30	30	30	30

Item	Aerosol Mass Spectrometer with Nephelometer (AMS-N)	Mini Tunable Laser Spectrometer (TLS)	Meteorological Suite (MET)	Fluxgate Magnetometer Gondola MAG-G	Dropsonde Pressure and Temperature Sensors	Dropsonde Chemical Sensor Array
Instrument average payload power with contingency (W)	9.1	31.2	6.5	0.7	13.9	3.9
Instrument average science data rate without contingency (kbps)	0.4	37.6	0.9	2	0.4	0.4
Instrument average science data rate with contingency (kbps)	0.52	48.9	1.2	2.6	0.36	0.36

## 3.2 Flight System

### 3.2.1 Orbiter

The ADVENTS Orbiter (**Figure 12**) functions as a carrier for the Aerobot, a communication relay for the Aerobot and Dropsonde, and a science platform. **Table 14** shows the Orbiter subsystems masses and power as well as the total Orbiter mass.



VS068

**Figure 12:** Orbiter with Aerobot and with Aerobot released.

### 3.2.2 Aerobot

**Figure 13** shows the ADVENTS Aerobot (robotic balloon vehicle) that is a variable-altitude, floating platform for a broad range of scientific instruments. It is comprised of a helium-filled balloon attached by a tether to the gondola. The balloon generates the buoyancy lift force needed to float the gondola. The gondola (**Figure 14**) contains the science instruments and all supporting subsystems such as avionics, power, communications, structure, and thermal management.

The ADVENTS Aerobot uses a helium balloon system which enables the Aerobot to be flown at variable altitudes high above the Venusian surface. Throughout the (60) sixty-day mission, the balloon

system allows changes in the flight altitude by transferring helium between a large, low pressure chamber and a small, high-pressure chamber. Science instruments on the Aerobot will be able to gather data from different levels of the planet's atmosphere during one balloon mission. The operational range of the Aerobot is 52-62 km above the surface of Venus. Variations in temperature and pressure throughout this operational range will be a driving factor in the final package design of all instruments and systems on board Aerobot. The Aerobot is designed to survive down to 50 km and up to 64 km. **Table 15** shows the Aerobot flight system masses and power.

**Table 14: Orbiter Mass and Power Table.**

	Mass			Average Power		
	CBE (kg)	% Cont.	MEV (kg)	CBE (W)	% Cont.	MEV (W)
Structures & Mechanisms	568.7	30	739.3	N/A	N/A	N/A
Thermal Control	23.1	10	25.4	N/A	N/A	N/A
Propulsion (Dry Mass)	243.4	7.5*	261.6	N/A	N/A	N/A
Attitude Control	85.9	10	94.5	104.3	30	135.6
Avionics	59.6	10	65.6	166.5	30	216.5
Telecommunications	46.8	11.3	52.0	671.0	30	872.3
Power (includes harness)	197.6	10	217.4	0.3	30	0.4
<b>Total Spacecraft Bus Mass</b>	<b>1,225.1</b>	<b>18.8</b>	<b>1,455.8</b>	<b>942.1</b>	<b>30</b>	<b>1224.73</b>

\*Propulsion mass includes pressurant and residual propellant that have no contingency applied. Excluding these items results in the Propulsion subsystem having 10% contingency.

**Table 15: Aerobot Flight System Element Mass and Power Table.**

	Mass			Average Power		
	CBE (kg)	% Cont.	MEV (kg)	CBE (W)	% Cont.	MEV (W)
Payload	19.3	30.0	25.1	48.5	30.0	63.1
Gondola	147.6	17.2	173.0	86.1	11.6	96.1
Balloon System	173.8	23.3	214.3	77.0	30.0	100.1
<b>Subtotal Float Mass</b>	<b>321.4</b>	<b>21.0</b>	<b>412.3</b>			
Inflation System	370.4	27.2	471.1	N/A	N/A	N/A
Entry System	676.0	29.9	387.3	1.2	30.0	1.6
Dropsonde	89.9	30.0	116.9	21.2	30.0	27.6
<b>Total Entry Mass</b>	<b>1,477.0</b>	<b>27.2</b>	<b>1,878.6</b>			



**Figure 13: ADVENTS Aerobot.**

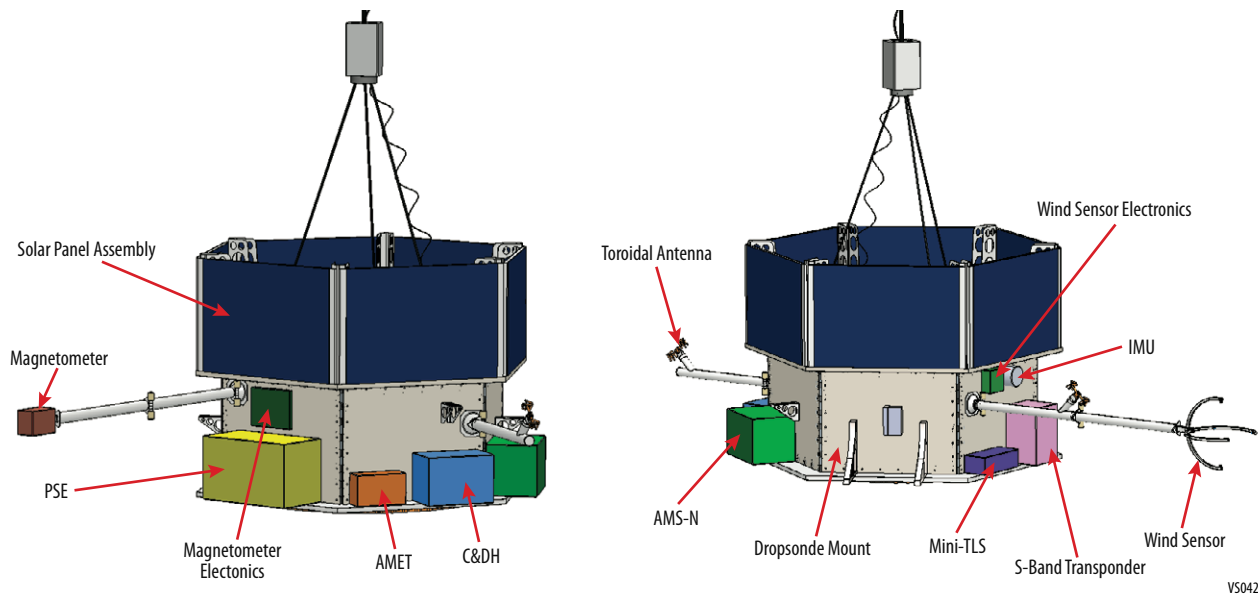


**Figure 14: Aerobot.**

### 3.2.3 Concept of Operations and Mission Design

The mission study began with an analysis to determine the heliocentric transfer trajectory and Venus orbit insertion. The results showed a variety of launch and arrival dates that have a required delta-V that meet mission requirements. The Falcon Heavy is selected as the primary launch vehicle for this study as it outperforms all other current commercial launch vehicles except for the SLS, which is not considered for the study. Solutions include a capture maneuver into a circular orbit around Venus. Direct captures into a circular orbit are not assumed to be the most efficient capture sequence but are suitable assumptions for the purpose of comparing the total delta-V of the various launch opportunities. The primary trajectory was selected from the trade results and a comprehensive capture analysis was performed to reduce the delta-V. The detailed mission design is provided in **Appendix A.2.3**. **Table 16** shows the Mission Operations and Ground Data systems summary.

The primary launch opportunity is June 4, 2039 and its associated trajectory is shown in **Figure 15**.

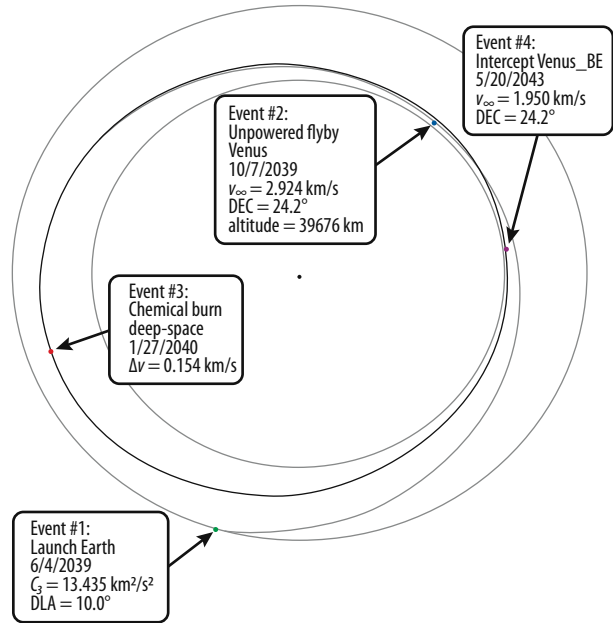


**Figure 15:** ADVENTS Primary Launch Opportunity Trajectory.

#### 3.2.3.1 Operations

ADVENTS operations are broken up into four phases (**Table 16**). The first is Launch and Cruise to Venus followed by Entry and Descent, Aerobot operations and Orbiter science operation. A summary of Aerobot and Orbiter operations is provided below. Additional operations detail are provided in **Appendix A.2.4**.

**Table 16:** Mission Operations and Ground Data Systems Summary.

Down link Information	Launch and Cruise to Earth	Dropsonde to Orbiter	Aerobot to Orbiter	Venus Orbiter to Earth
Number of Contacts per Week	1	1	7	7
Number of Weeks for Mission Phase, weeks	191	1 hour	8	113
Downlink Frequency Band, GHz	HGA 32 MGA LGA 2.1	2.1	2.1	HGA 32 LGA 2.1
Orbiter Antenna Telemetry Data Rate(s), kbps	HGA min 1,030 HGA max 42,700 MGA min 1.2 LGA min 0.04	MGA 0.01 HGA 2.23	LGA min 0.01 MGA min 0.033 HGA 8.9	HGA min 1,030 HGA max 42,700 MGA min 1.2 LGA min 0.04
Transmitting Antenna Type(s) and Gain(s), DBi	HGA 47.05 MGA 22.0 LGAs 7.4	MGA 5.0	Toroid 0 gain	HGA min 1,030 HGA max 42,700 MGA min 1.2 LGA min 0.04
Transmitter peak power, Watts	200	20	20	200
Downlink Receiving Antenna Gain, DBi	79.0	35.0	35.0	79.0
Transmitting Power Amplifier Output, Watts	100	10	10	100
Total Daily Data Volume, (MB/day)	1	24	128	14,400
Uplink Information				
Number of Uplinks per Week	1	1	7	7
Uplink Frequency Band, GHz	34.3	N/A	2.1	
Telecommand Data Rate, kbps	> 2,000	N/A	14.5	> 2,000
Receiving Antenna Type(s) and Gain(s), DBi	HGA 58.7	N/A	HGA 58.7	HGA 58.7

### 3.2.3.1.1 Launch and Cruise to Venus

ADVENTS launches from Cape Canaveral, Florida on a single Falcon Heavy vehicle with 5m fairing. The primary launch opportunity is June 4, 2039 with a backup launch opportunity of December 4, 2039. Both launch opportunities have a minimum of a 14 day launch window. The launch and cruise timeline is shown in **Table 17**. During cruise the Orbiter will primarily be in a low power mode with only essential systems on. The communication subsystem will be in receive mode, except for once a day to transmit health and status, perform ranging with DSN and receive any necessary updates from the ground. Just prior to the Venus flyby the Orbiter will enter a science mode for calibration of its instruments and to take measurements during the flyby. Ten days prior to Aerobot entry the Orbiter will perform the first Aerobot entry targeting trajectory correction maneuver (TCM1) to orient the Aerobot for its entry trajectory. Additional Aerobot entry targeting TCM's are planned as shown in **Table 17**. The Orbiter will spin up and release the Aerobot 5.5 days prior to the desired Aerobot entry. After Aerobot separation the Orbiter will maintain daily contact with the Aerobot communication beacon to monitor its trajectory.

**Table 17:** Mission Launch and Cruise timeline.

Date	Event
06/4/2039	Launch
10/7/2039	Venus Flyby
05/17/2043	Aerobot Entry Targeting TCM1
05/21/2043	Aerobot Entry Targeting TCM2
05/21/2043	Aerobot Separation
05/22/2043	Orbiter VOI Targeting TCM3
05/25/2043	Orbiter VOI Targeting TCM4
05/27/2043	Aerobot Entry
05/27/2043	VOI

### 3.2.3.1.2 Aerobot Operations

Aerobot operations are divided into three phases. The first is the 5.5-day cruise while inside the entry vehicle after separation from the Orbiter to the entry point in the Venus atmosphere. The second is the Entry and descent phase. The final phase is the 60-day float.

Five and a half days after release by the Orbiter the Aerobot enters the Venusian atmosphere on November 15, 2042 at 3:24pm Venus local time and begins the Entry, Descent, and Float (EDF) sequence shown in **Figure 16**.

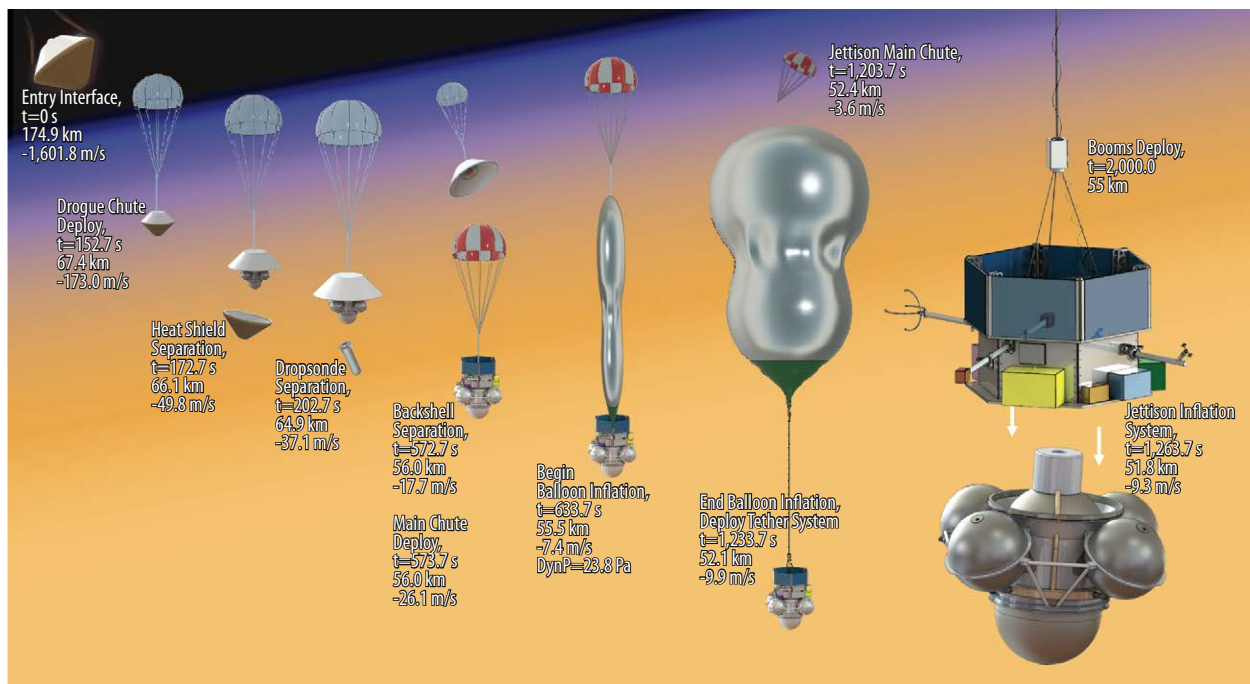


**Figure 16:** Aerobot Entry and Descent timeline.

VS036

The communication beacon remains active through backshell separation at entry plus 232.7 seconds. There is an expected gap in communication from backshell separation until the antennas are

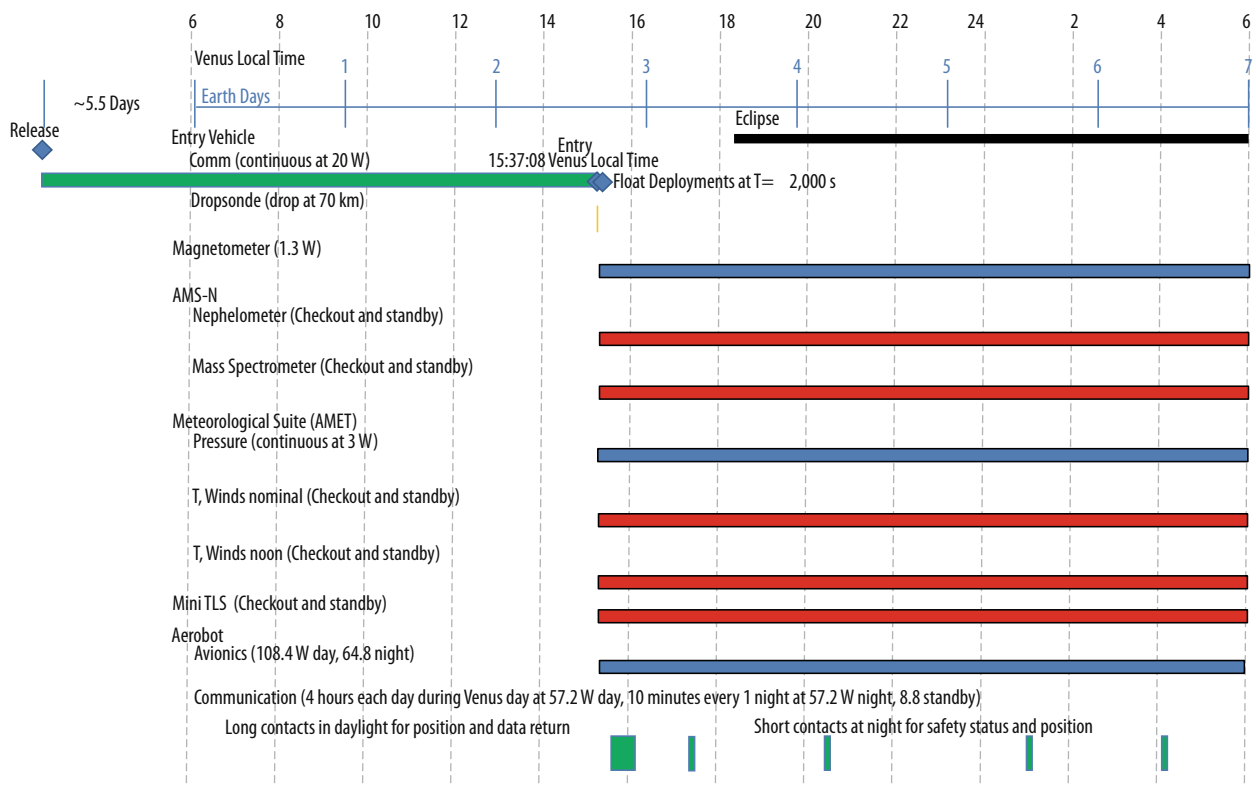


deployed at entry plus 2,000 seconds at the nominal float altitude of 55 km.

The Aerobot, like the Orbiter, is in view of Earth during its entry and descent. Due to the power of the Aerobot transmitter, it is not expected that the 34m DSN antennas will be able to obtain a communication link with the Aerobot. The Aerobot communicates directly with the Orbiter during its entry and descent and has 4 hours of contact (1 hour during entry and descent plus 3 hours during the initial float) during the first Earth day after its entry while in the Venusian sunlight (**Figure A-29**). Additional contacts are available with the Orbiter every 12 Earth-hours with one planned 10-minute opportunity (up to 4 hours are available as shown in **Figure A-29**) occurring 12 hours after initial float prior to the Venusian night. The dropsonde is released at 202.7 seconds and begins transmitting to the Orbiter. The dropsonde will take no longer than 1 hour to reach the surface.

Balloon inflation begins at 55.5 km and ends at 52.1 km altitude as shown in **Figure 16**.

Once the Aerobot is fully deployed after atmospheric descent, the Aerobot altitude will be set to a nominal 55 km altitude, where the temperature is about 20 °C. Carried by ambient winds, the Aerobot will circumnavigate Venus every 7 days, on average. The instruments will begin their checkout procedures as shown by the red bars in **Figure 17** and enter a standby state beginning at entry plus 2,000 seconds. Two instruments (blue bars in **Figure 17**), the magnetometer and the pressure sensors in the meteorological suite, will begin taking their continuous data. The Aerobot will have approximately 1 Earth day after entry to complete checkout before it enters the Venus night. During the Venus night the avionics will be in low power receive only mode with short 10-minute contacts each (green bars in **Figure 17**) Earth day while in the Venus night.



VS037

**Figure 17:** Aerobot Entry and initial float timeline.

### 3.2.3.1.3 Nominal 60-day Mission

Once the Aerobot exits the first Venusian night, all of the instruments will begin normal operations as shown in **Figure 18**. During the nominal mission, the Aerobot will communicate with the Orbiter daily during 1 of 2 planned communication opportunities during the Venusian daylight. During the Venusian night, one 10-minute communication opportunity is planned for every Earth day. Addition-

al night communication periods are available for mission operations within the limits of the battery. Should the Aerobot experience an anomaly, it will enter safe mode and broadcast an alert message to the Orbiter.

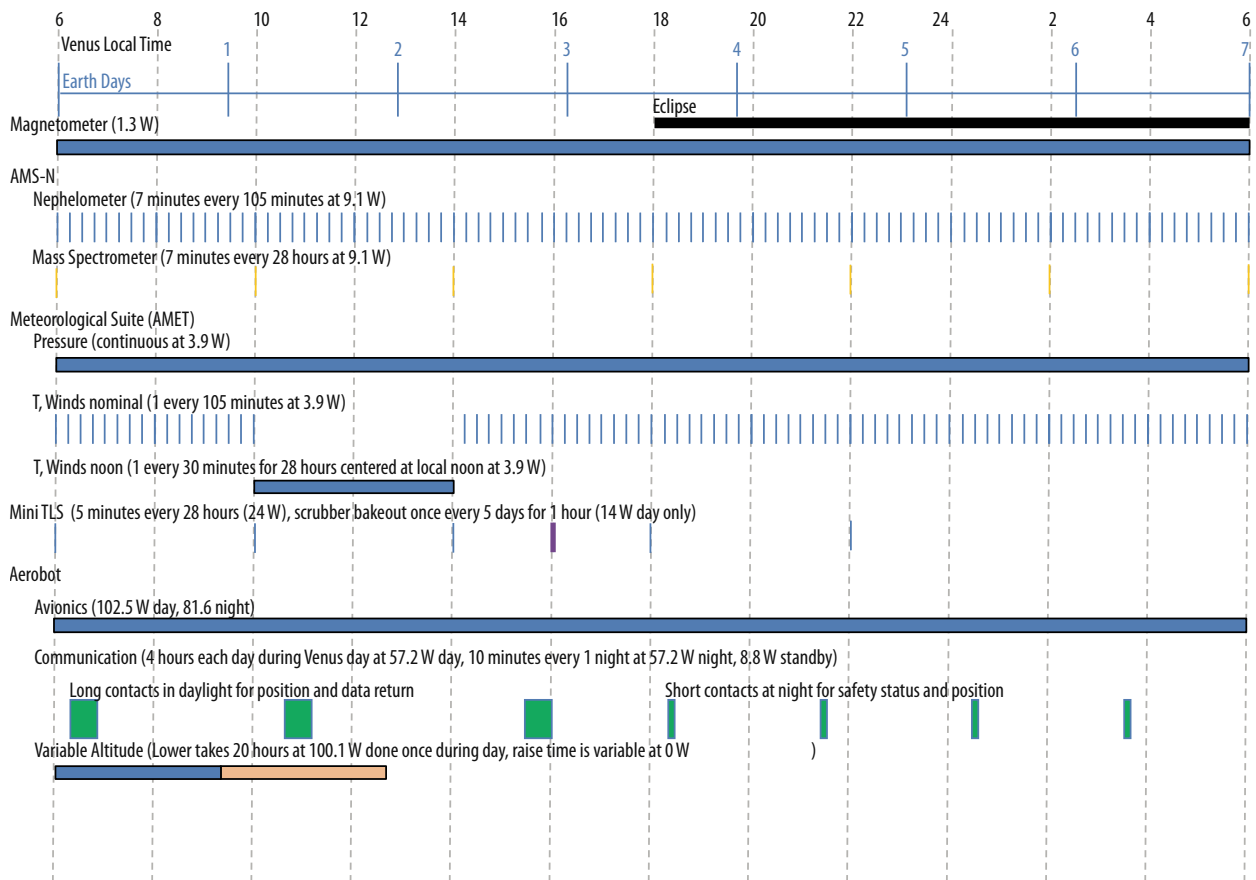


**Figure 18:** Typical 7-day circumnavigation timeline.

VS038

During the first circumnavigation, the balloon is passively altitude stable. The He pump can be used as the mission progresses to maintain a near-constant altitude by raising or lowering the balloon, and thus a near-constant temperature, for sensitive characterizations of atmospheric composition, including isotopic ratios of noble gases, if altitude dispersions are observed. In later circumnavigations, the Aerobot's altitude control will also be used to descend or ascend as needed to counter expected variations in the wind speed to maintain the 7-day circumnavigation period. For resource planning purposes, the variation in altitude is assumed to be done during the once each per circumnavigation in the Venusian daylight and Venusian night over the course of 20 hours as shown in **Figure 18**. Descents require the use of the He pump while Ascents do not require the use of the pump. This allows operational flexibility to plan descents just prior to Venusian night with ascents done at night.

The mission lifetime for the Aerobot is 60 Earth-days. During the nominal lifetime, the Aerobot will communicate with the Orbiter daily during 1 of 2 planned opportunities. Should the Aerobot experience an anomaly, it will enter safe mode and broadcast an alert message to the Orbiter.

The balloon's AMET pressure sensor will be powered on at all times, measuring continuously. Temperature will be taken every 1–5 minutes except around local noon when it will be taken every 30 minutes for 28 hours. Magnetometer data is taken continuously and down sampled to 0.5 Hz, which is sufficient for measurement of remnant magnetism, and occasional high-rate data for investigations such as Schumann resonances characterization and search for lightning.

The AMS-N is powered on for seven minutes, once every 105 minutes (or 1.75 hours). At each time, after a 2-minute warm up period, the mass spectrometer will measure composition of the atmosphere,

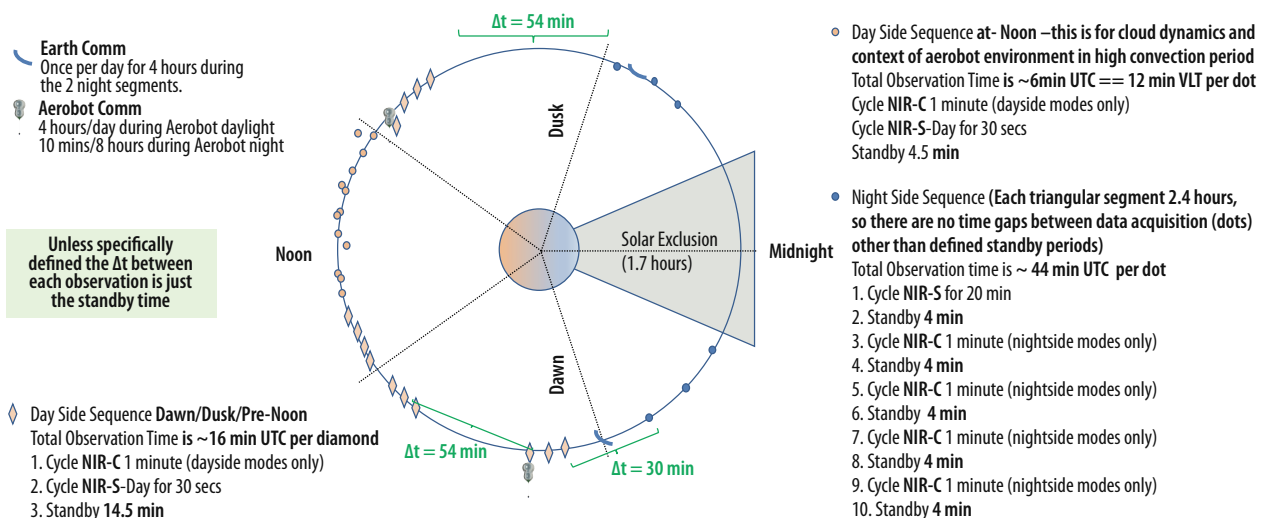
including isotopes, for five minutes, and then of cloud/aerosol particles which are separated from atmospheric gas using an aerodynamic aerosol separator. The incoming atmosphere passes through a nephelometer that optically interrogates cloud and aerosol particles entering the mass spectrometer to constrain their size, shape, composition. The mass spectrometer data are integrated over 10-second periods in order to reduce data rate. After each operational period, the instrument will remain in standby power until it is ready to ingest the next sample.

The mini-TLS operates for 5 minutes every 28 hours with a scrubber bakeout once every 5 days for one hour.

### 3.2.3.1.4 Venus Orbit Operations

The Orbiter is in a 12-hour orbit as shown in **Figure 19**. The Orbiter nominally communicates with the Aerobot once per day for 4 hours when the Aerobot is in the Venusian sunlight and for 10 mins/Earth day when the Aerobot is in the Venusian night throughout the Aerobots 60-day nominal life-time. There are two planned opportunities per day to communicate with the Aerobot. The primary opportunity is planned for the early dawn portion of the Orbiter orbit with backup opportunity in the late afternoon. The Orbiter is in listen mode on its low gain antennas at all times should the Aerobot enter safe mode and broadcast an alert. Communication with the Aerobot are constrained by the communications viewing angle constraints (as discussed in **Appendix A.2.3** and as shown in **Figure A-30**). Communication is not possible when the Orbiter is within 30 degrees of zenith with respect to the Aerobot or within 30 degrees of the horizon. As the Aerobot mission progresses the latitude of the Aerobot will change. To account for this the mission design analyzed four representative cases for daily maximum contact times as shown in **Figure A-29** thru **Figure A-33** for representative latitudes of 0, 15, -15, 45 and -45°.

Each of the 5 segments defined by the dashed lines in the figure is 2.4 hours. The Orbiter communicates 4 hours a day with Earth during the post dusk to early dawn segments. All EUV observations are sun pointed and continuous. All Orbiter NIR observations are nadir pointed looking at full Venus disk. The NIR observations shown in **Figure 19** are divided into three sequences: Day side sequence for Dawn/Dusk/Pre-noon, Day side sequence at noon, and the night sequence. The orbiter makes no NIR observations during the solar exclusion zone of 1.7 hours.



VS040

**Figure 19: Orbiter Operations.**

## 4 RISK LIST

Table 18 describes ADVENTS top mission, programmatic, and technical risks, with the associated Risk Matrix in Figure 20. These risks derive from the complexity of the mission, its multiple platforms, and critical separation events, the caustic Venus atmosphere, and the technology development associated with the mission. Each risk is significantly mitigated by implementing the associated strategy shown in Table 18.

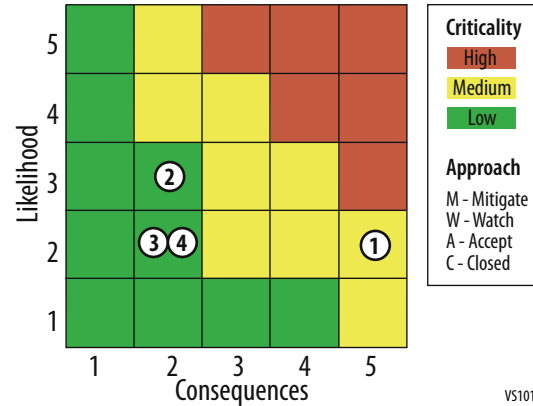


Figure 20: ADVENTS Risk Matrix.

Table 18: ADVENT risk list and associated mitigation strategy.

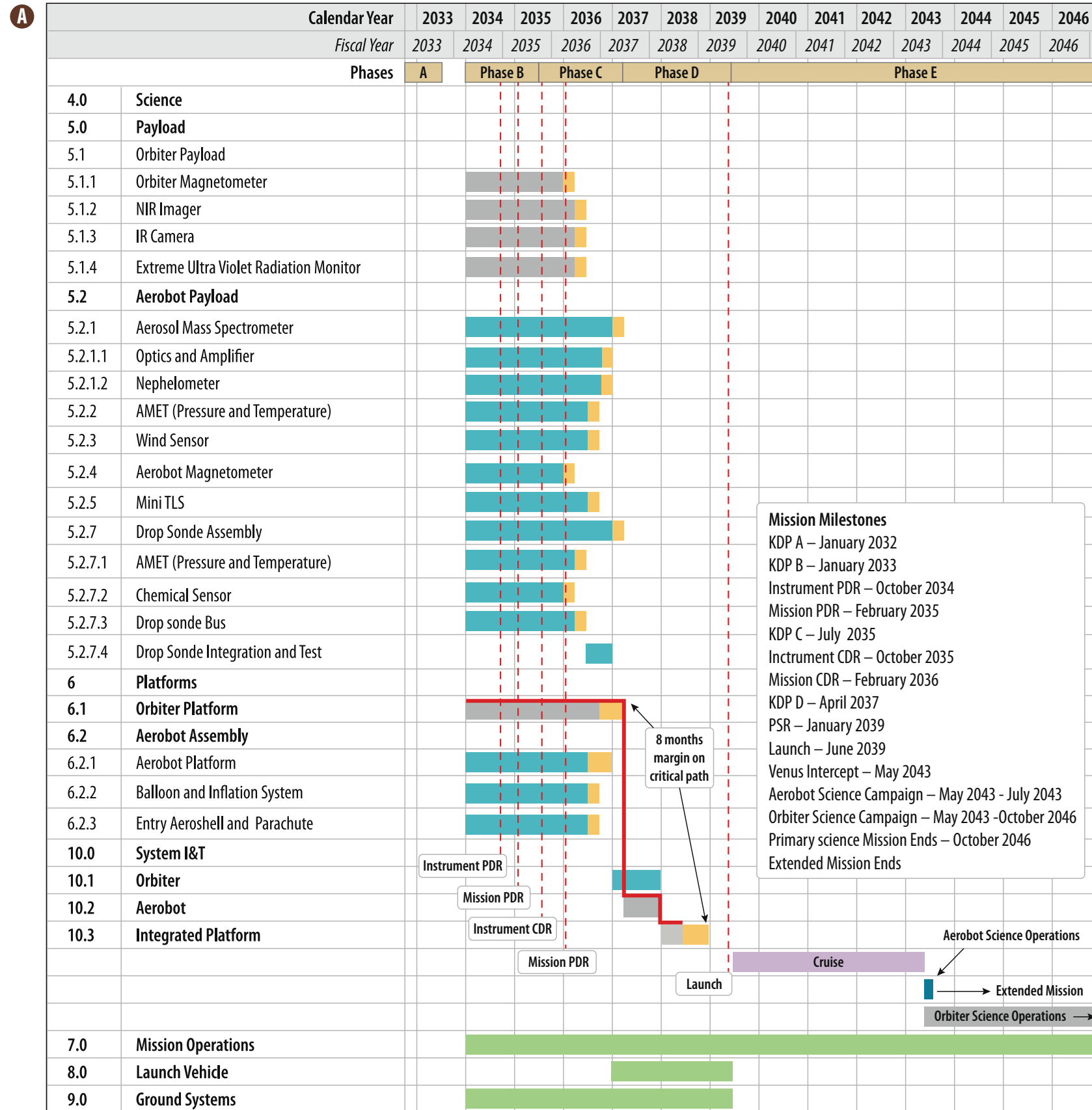
Rank (LXC)	Approach	ID	Risk Title	Risk Description	Mitigation Strategy
1 (2,5)	Mitigate	ADVENTS-001	Critical Separation Events	<b>Given that</b> the mission has multiple platforms with critical separation events <b>There is a possibility</b> one or more may not occur as designed <b>Resulting in</b> mission compromise and loss of science return	<ul style="list-style-type: none"> <li>Implement rigorous test programs for the hardware and software redundancy for critical subsystems</li> </ul>
2 (3,2)	Mitigate	ADVENTS-002	Mission Complexity	<b>Given that</b> the number of instruments and the multiple platforms associated with the mission <b>There is a possibility</b> mission development and integration will be complicated <b>Resulting in</b> cost increase and schedule delay	<ul style="list-style-type: none"> <li>Implement careful planning and resource scheduling in Phase A.</li> <li>Integrate appropriate reserves on cost and schedule</li> </ul>
3 (2,2)	Mitigate	ADVENTS-003	Venus Atmosphere	<b>Given that</b> the Venus atmosphere is caustic <b>There is a possibility</b> unexpected difficulties could be encountered adapting aerobot and instrument hardware to the atmosphere <b>Resulting in</b> cost increase and schedule delay	<ul style="list-style-type: none"> <li>Employ materials specialists early in Phase A to ensure part compatibility with Venus atmosphere.</li> <li>Develop and demonstrate necessary performance to achieve the Aerobot mission duration during Phase A.</li> </ul>
4 (2,2)	Mitigate	ADVENTS-004	Technology Development	<b>Given that</b> there are several instrument that require TRL development <b>There is a possibility</b> unexpected technology development difficulties could be encountered <b>Resulting in</b> cost increase and schedule delays	<ul style="list-style-type: none"> <li>Implement robust and comprehensive technology development plan</li> <li>Include appropriate cost and schedule reserve on hardware requiring technology development</li> <li>Invest in technology development prior to Phase A</li> </ul>

## 5 DEVELOPMENT SCHEDULE AND SCHEDULE CONSTRAINTS

### 5.1 High-Level Mission Schedule

The ADVENTS implementation schedule is assumed to follow a typical 2-step New Frontiers Announcement of Opportunity timeline beginning with a 9-month Phase in October 2032, which culminates in a Concept Study Report. A 6-month Bridge Phase leading to Phase B in January 2034 follows. Schedule is driven by the primary launch readiness date of June 4, 2039, and is consistent with commencement between 2023 and 2032 per study guidelines. The primary Launch window is 21 days wide and is followed by a second opportunity in December 2039. Launch opportunities occur at a regular cadence, as described in the mission design section.

This implementation schedule is largely consistent with historical New Frontiers missions though with a slightly longer Phase B–D at 67 months to reflect the multiple platforms and scope of the mission concept presented. The schedule is derived from analogous GSFC instrument and spacecraft development timelines with special cases, such as the Aerosol Mass Spectrometer and Dropsonde Chemical Sensors generated with input from instrument developers. **Schedule Foldout 1 (A)** shows the high-level schedule indicating key design reviews, the critical path, and the delivery time for each instrument and the major bus elements. **Schedule Foldout 1 (B)** summarizes schedule duration and delivery times.



**B ADVENTS Schedule Durations**

	Duration (Months)
Phase A – Conceptual Design	9
Phase B – Preliminary Design	18
Phase C – Detailed Design	21
Phase D – Integration & Test	25
Phase E – Primary Mission Operations	117
Phase F – Extended Mission Operations	As design allows
Start of Phase B to PDR	14
Start of Phase B to CDR	26
Start of Phase B to Delivery of Orbiter Magnetometer	24
Start of Phase B to Delivery of NIR Imager	30
Start of Phase B to Delivery of Extreme Ultra Violet Radiation Monitor	30
Start of Phase B to Delivery of Aerosol Mass Spectrometer	36
Start of Phase B to Delivery of AMET (P,T)	32
Start of Phase B to Delivery of Wind Sensor	32
Start of Phase B to Delivery of Gondola Magnetometer	24
Start of Phase B to Delivery of Mini TLS	34
Start of Phase B to Delivery of Dropsonde Assembly	35
Start of Phase B to Delivery of AMET (Pressure and Temperature)	30
Start of Phase B to Delivery of Chemical Sensor	24
Start of Phase B to Delivery of Orbiter Bus	32
Start of Phase B to Delivery of Aerobot Bus	30
Start of Phase B to Delivery of Balloon and Inflation System	28
Start of Phase B to Delivery of Entry Aeroshell and Parachute	28
Start of Phase B to System Level Integration & Test	36
Total Project Total Funded Schedule Reserve	8
Total Development Time Phase B - D	66

The Aerobot and Orbiter are built, integrated, and tested with their respective instrument suites in parallel. Then the integrated orbiter and aerobot are stacked and tested prior to launch. Cruise to Venus takes approximately 4 years with Venus Capture in May 2034, whereupon Orbiter and Aerobot science operations begin. The Aerobot baseline science campaign is 60 days and the Orbiter 3.5 years. The extent to which the mission operations can extend beyond the baseline line science operations is governed almost entirely by the Aerobot's extended exposure to the Venus atmosphere.

The schedule assumes Technology Development is completed as described in the Technology Development section with all hardware reaching TRL 6 prior to Mission PDR in February 2035. The schedule has approximately 8 months of funded schedule on the critical path which runs through Orbiter bus development and integration and test. This is consistent with GSFC GPR 7120.7B Funded Schedule Margin and Budget Margin for Flight Projects.

### 5.2 Technology Development Plan

The Meteorological Suite, Aerosol Mass Spectrometer with Nephelometer, Aerobot Balloon system, and the Chemical Sensor Array on the Dropsonde require technology development to reach TRL 6. **Table A-26** and **Table A-29** of the appendix show more details of the technology development plan for the AMS-N and chemical sensor array respectively. **Table 19** summarizes current TRL, actions to reach TRL 6 and associated timeline. Where there is not an approved technology development-funding plan in place, the cost is assumed borne by the ADVENTS mission. The total cost for technology development is \$19.3 million in \$FY25, not including the reserve costs. All technology development is complete prior to Mission PDR in February 2035.

**Table 19:** ADVENTS Technology Development Plan.

Item	Technology	Current TRL	TRL Develop Plan	Development Timeline to TRL 6	TRL 6 Milestone	Funding Source	Cost (\$M) FY 2025
Meteorological Suite	Pressure Sensor	4	Mature infrasound technology. Build and test high fidelity prototype	3.5 Years, Pre Phase A completion	Pre ADVENTS PHASE A	ADVENTS Mission	\$3.4
Aerosol Mass Spectrometer with Nephelometer	Quadrupole Ion Trap Mass Spectrometer Front End and Electronics	5	Conduct Thermal Vacuum Testing on high fidelity test model	Technology Development Effort in Progress	Prior to 2023	DALI 19	-
	Nephelometer	2	<ul style="list-style-type: none"> <li>• Build prototype and engineering model</li> <li>• Conduct Component Level thermal Analysis</li> <li>• Conduct Functional and life tests at expected operating pressure range</li> <li>• Perform Compatibility test in chemical environment of identified component</li> <li>• Conduct Vibration qualification testing</li> </ul>	Technology Development Effort in Progress	Prior to 2023	CNRS, CNES	-
	Aerosol Separator	2	<ul style="list-style-type: none"> <li>• Build prototype and engineering model</li> <li>• Conduct Component Level thermal Analysis</li> <li>• Conduct Functional and life tests at expected operating pressure range</li> <li>• Perform Compatibility test in chemical environment of identified component</li> <li>• Conduct Vibration qualification testing</li> </ul>	4-5 Years, Pre Phase A completion	Pre ADVENTS PHASE A	ADVENTS Mission	\$6.6
Aerobot	Balloon	4	Earth atmosphere flight tests with full scale prototype balloons	18 Months, spanning ADVENTS Phase A and B	October, 2034	ADVENTS Mission	\$9.1

Item	Technology	Current TRL	TRL Develop Plan	Development Timeline to TRL 6	TRL 6 Milestone	Funding Source	Cost (\$M) FY 2025
Chemical Sensors	Sensor Array	5	Simulated testing at various Venus altitudes	6 months Beginning ADVENTS Phase B	July, 2034	ADVENTS Mission	\$0.1
<b>Total Technology Development Cost (\$M)</b>							<b>\$19.3</b>

### 5.3 Mission Life-Cycle Cost

#### 5.3.1 Costing Methodology and Basis of Estimate

The Aerobot Bus, Orbiter Bus, and Dropsonde cost were estimated by the GSFC Cost Estimating, Modeling, & Analysis (CEMA) Office based on detailed Master Equipment Lists (MELs) generated by the engineering team. It was assumed a cost estimate at the 75% confidence level is equivalent to a grassroots cost with 50% reserve added. Refer to **Appendix B** for CEMA cost estimates. Costs of any identical instruments from the 2020 VFM study carry over into this study, with real year dollars updated to reflect the ADVENTS schedule. These instruments were largely costed through the GSFC Requirements Assessment (RAO) Office. Aerobot balloon and inflation system costs were carried over due to the similar designs. The magnetometer estimate is based on GSFC's many flight builds of similar hardware. Instruments unique to ADVENTS such as the mini-TLS and the IR camera (NIR-C) were costed through the GSFC RAO office as part of this study. As per study guidelines, 50% reserves, or equivalent, is added to all costs except for Phase E science operation, where reserves are 25%.

Project management, Systems engineering, Safety and Mission Assurance, and Integration and Test were estimated by percentage cost wraps developed by years of costing and building flight hardware at GSFC. TRL Development Cost were generated grass roots estimates from technology experts with the estimate for the balloon and Aerosol Mass Spectrometer (AMS-N) provided by JPL and the Chemical Sensor array (DROP) from NASA Glenn Research Center. **Schedule Foldout 1 (B)** shows Phase A-D real year and \$FY25 mission cost estimated. 50% reserve is added to Technology Development Costs for consistency with the conceptual nature of this study. For simplicity, the Technology Development Costs are separated from Phase A-D costs and not included in the real year breakdown. The total cost, including the Technology Development but excluding Phase E or Launch Vehicle services is \$1.47 Billion, including all reserves. This exceeds the expected New Frontiers cost cap and is reflective of multiple platforms each carrying capable instrument suites. With the margined Phase E and Launch Vehicle, the total is \$1.83B (\$FY25).

**Table 20:** ADVENTS Funding Profile in Real Year and \$FY25.

Item	Technology Development (\$FY25)	FY 2033	FY 2034	FY 2035	FY 2036	FY 2037	FY 2038	FY 2039	Total (RY)	Total (FY 2025)
Phase A Concept Study		\$9.2							\$9.2	\$7.5
<b>Phase A-D</b>										
Project Management		\$0.5	\$8.5	\$11.5	\$11.4	\$13.6	\$10.7	\$5.9	\$62.0	\$45.8
Systems Engineering		\$0.4	\$7.1	\$9.6	\$9.5	\$11.3	\$8.9	\$4.9	\$51.7	\$38.2
Safety and Mission Assurance		\$0.2	\$4.2	\$5.7	\$5.7	\$6.8	\$5.3	\$3.0	\$31.0	\$22.9
Pre-launch Science		\$0.4	\$7.4	\$10.0	\$9.9	\$11.8	\$9.3	\$5.1	\$53.8	\$39.8
Orbiter Magnetometer (MAG-0)		\$0.0	\$1.6	\$2.0	\$1.3	\$0.8	\$0.1	\$0.1	\$6.1	\$4.6
IR Camera (NIR-C)		\$0.1	\$2.1	\$2.6	\$1.8	\$1.1	\$0.2	\$0.1	\$7.9	\$6.0
NIR Imager (NIR-S)		\$0.6	\$22.7	\$27.9	\$19.0	\$11.8	\$2.0	\$1.1	\$85.2	\$64.7
Extreme Ultra Violet Radiation Monitor (EUV)		\$0.2	\$6.5	\$7.9	\$5.4	\$3.4	\$0.6	\$0.3	\$24.2	\$18.4
Aerosol Mass Spectrometer with Nephelometer (AMS-N)	\$6.6	\$0.6	\$19.8	\$24.4	\$16.6	\$10.3	\$1.8	\$1.0	\$74.5	\$56.6
Aerobot AMET (Pressure and Temperature)	\$3.4	\$0.1	\$4.5	\$5.5	\$3.7	\$2.3	\$0.4	\$0.2	\$16.7	\$12.7
Aerobot AMET (Wind Sensor)		\$0.0	\$1.6	\$2.0	\$1.3	\$0.8	\$0.1	\$0.1	\$6.1	\$4.6



Item	Technology Development (\$FY25)	FY 2033	FY 2034	FY 2035	FY 2036	FY 2037	FY 2038	FY 2039	Total (RY)	Total (FY 2025)
Gondola Magnetometer (MAG-G)		\$0.0	\$1.6	\$2.0	\$1.3	\$0.8	\$0.1	\$0.1	\$6.1	\$4.6
Mini TLS		\$0.2	\$7.0	\$8.6	\$5.9	\$3.6	\$0.6	\$0.3	\$26.3	\$20.0
Dropsonde Assembly	\$0.1	\$0.3	\$12.2	\$15.1	\$10.2	\$6.4	\$1.1	\$0.6	\$46.0	\$34.9
Orbiter Platform		\$2.5	\$72.0	\$92.7	\$77.0	\$58.9	\$24.2	\$13.4	\$340.7	\$256.3
Aerobot Platform	\$9.1	\$0.9	\$26.9	\$34.6	\$28.7	\$22.0	\$9.0	\$5.0	\$127.1	\$95.6
Ballon and Inflation System		\$0.3	\$11.7	\$14.4	\$9.8	\$6.1	\$1.0	\$0.6	\$43.9	\$33.4
Entry Aeroshell and Parachute		\$1.5	\$53.2	\$65.5	\$44.5	\$27.7	\$4.8	\$2.7	\$199.9	\$151.8
MSI&T		\$0.0	\$4.9	\$5.0	\$10.3	\$15.9	\$27.3	\$44.8	\$108.2	\$77.1
Mission Operations		\$0.2	\$4.1	\$5.5	\$5.5	\$6.5	\$2.1	\$2.8	\$26.7	\$22.0
Ground Data System Dev		\$0.0	\$1.6	\$1.6	\$3.4	\$5.2	\$8.8	\$14.5	\$35.1	\$25.0
Total Dev. w/o Reserves	\$19.3	\$9.2	\$281.1	\$354.1	\$282.3	\$227.1	\$118.4	\$106.8	\$1,379.1	\$1,034.9
Development Reserves	\$9.6	\$4.6	\$140.6	\$177.1	\$141.2	\$113.5	\$59.2	\$53.4	\$689.5	\$517.5
Total Development Cost (A-D)		\$14	\$422	\$531	\$423	\$341	\$178	\$160	\$2,069	\$1,552
Total Technology Development Cost	\$28.9									\$28.9
Total Including Technology Development										\$1,581
Launch services (\$FY25)		\$0.0	\$0.0	\$0.0	\$0.0	\$48.0	\$96.0	\$96.0		\$240.0
Phase E Science										\$49.5
Phase E Operations										\$40.5
Phase E Reserves										\$22.5
							<b>Total Mission Cost (\$FY25)</b>			<b>\$1,934</b>
<b>Scientist BY FY</b>	<b>2</b>	<b>5.1</b>	<b>5.2</b>	<b>6.0</b>	<b>8.5</b>	<b>9.0</b>	<b>7.2</b>	<b>6.1</b>	<b>10/yr Phase E</b>	



## APPENDIX A - DESIGN TEAM STUDY REPORT

### A.1 SCIENCE

#### A.1.1 Science Rationale for the ADVENTS Payload, Relative to the VFM Study

ADVENTS was designed to answer as many of the key science questions about Venus as possible with a total cost appropriate to the New Frontiers program. This study was not started from scratch—but was built on a foundation laid by the Venus Flagship Mission (VFM) concept study. VFM is a large Flagship Mission with five platforms that would study the myriad processes that control how volatiles move through the Venus system: interior, surface, atmosphere, and ionosphere. Obviously, ADVENTS could not have the same scope as VFM—the anticipated New Frontiers cost cap is >\$2 billion less than the estimated cost of VFM. Despite a drastically reduced total cost, ADVENTS is still able to address many of the highest-priority, community-consensus science goals for Venus exploration (which connect to many cross-cutting themes in planetary science and astrobiology): Understanding the potential past and present habitability of the Venus surface and clouds, respectively, and how Venus is the key to understanding the formation of the inner Solar System and the evolution of rocky exoplanets.

At a practical level, the ADVENTS payload selection may seem like a descope and redesign of the VFM concept study. Relative to VFM, ADVENTS removes the lander and the SmallSats. The ADVENTS orbiter does not include most of the instruments from the VFM orbiter, including the radar, the sub-mm spectrometer, and the space physics instrumentation (*i.e.*, electrostatic analyzers and neutral mass spectrometers). However, our goal was to achieve a certain set of science goals—not simply to reduce the cost of the VFM concept. To maximize our science return at the New Frontiers (or small Flagship) level, we decided to add a few key elements to the orbiter and aerobot that were not included on those platforms in the VFM. Specifically, we added a second IR imager to the orbiter. We also added a small Tunable Laser Spectrometer (TLS) and a dropsonde to the aerobot. The VFM report describes the science value of the instruments that we carried over to ADVENTS. Our sub-sections below explain the scientific justification for our payload additions relative to VFM.

##### A.1.1.1 Scientific Rationale for the New IR Camera (NIR-C)

The ADVENTS Orbiter has a near-circular, near-surface orbit with a ~12-hour period (~20,000 km altitude) that enables frequent contacts with the Aerobot and the relay of all data back to Earth. The Orbiter has two scientific purposes. As for the VFM Orbiter, a NIR imager (NIR-S) will determine the rock types (*e.g.*, felsic vs. mafic) at different geologic regions such as tesserae (*e.g.*, Helbert *et al.* 2013) building on preliminary attempts by the VMC and VIRTIS instruments on the ESA VenusExpress spacecraft. Studying surface composition based on only a small number of spectral channels in a very narrow spectral range is very challenging. The task is further complicated by the fact that Venus has an average surface temperature of 460°C. Spectral signatures of minerals are affected by temperature and therefore a comparison with mineral spectra obtained at room temperature can be misleading. Recently, the first laboratory measurements of Venus analog materials were obtained at Venus surface temperatures. The spectral signatures show clear temperature dependence. Based on the experience gained from using the VIRTIS instrument to observe the surface of Venus combined with the high temperature laboratory experiments, the Venus Emissivity Mapper (VEM) concept was de-

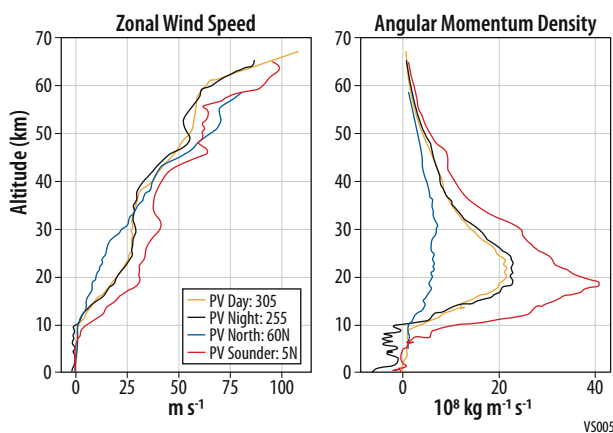


**Figure A-1:** ADVENTS will determine the extent of spatial and temporal variability in wind speeds and momentum transport at the cloud levels in the Venus atmosphere. Zonal winds and angular momentum density were measured by Doppler tracking of the Pioneer Venus (PV) entry probes—and observed to vary at different local times and locations.

veloped, which this report and the VFM study refer to as NIR-S. NIR-S is designed to use Venus's NIR atmospheric windows to map the surface emission and is outfitted with 4 channels for surface emissivity, 3 channels for near surface water, 4 channels for cloud decontamination, and 3 channels for characterizing the stray light within the instrument. NIR-S will primarily be operational during the nighttime, but a few channels will be implemented on the dayside to help with cloud characterization. Additionally, also as for the VFM Orbiter, the ADVENTS Orbiter will provide context about the magnetic fields in the solar wind (MAG-O) and the EUV flux from the Sun (EUV).

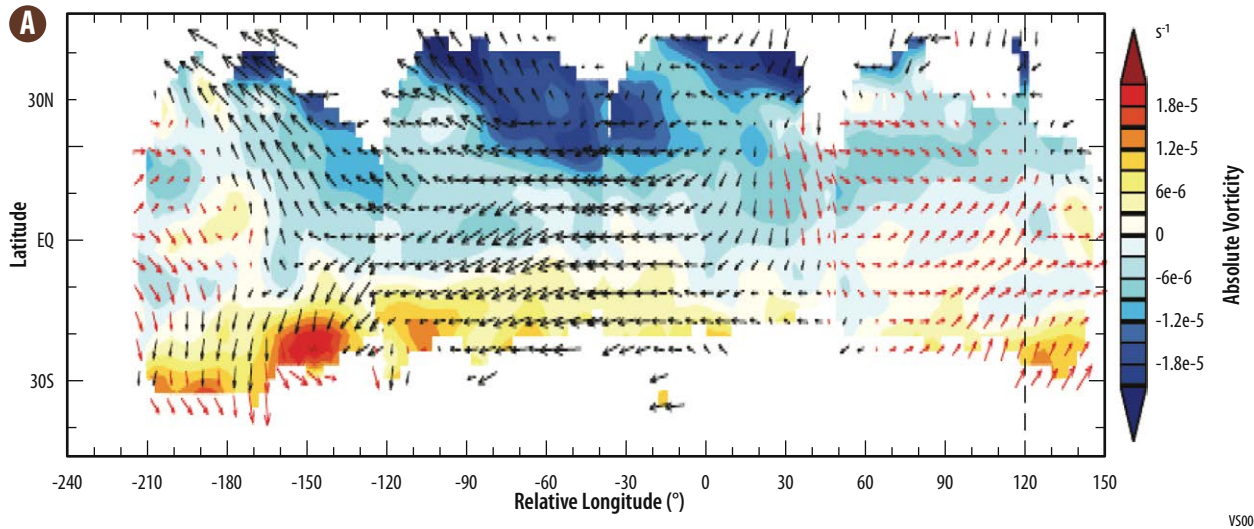
We decided to add a second IR imager (NIR-C) based on the Akatsuki IR2 instrument (*e.g.*, Satoh *et al.*, 2017) to the Orbiter payload to provide additional regional context for the atmospheric measurements taken by the Aerobot and Dropsonde. Specifically, NIR-C is nadir pointed and will provide contextual imaging of the altitudes encountered by the Aerobot by mapping the middle (45–55 km) cloud level zonal and meridional wind motion, aerosol opacity, and cloud morphology. NIR-C has 3 nighttime channels and 3 dayside channels.

One of the most distinct processes occurring at Venus is the atmospheric super-rotation which is defined as an excess of angular momentum relative to the surface. Indeed, while the solid body has a rotation period of 243 days, the atmosphere rotates with a period as low as 4 days at the top of the global cloud cover (70 km) (*e.g.*, Schubert *et al.*, 1980). Along with Titan, Venus is the only known planetary body with a super-rotating atmosphere, though it is thought that atmospheric super-rotation is common in the Universe, especially for tidally locked exoplanets (*e.g.*, Imamura *et al.*, 2020). The causes and origin of the super-rotation of Venus are still unknown to this day. The various explanations brought forward by theory and numerical climate models suggest a balance in the transport of momentum by the mean meridional circulation and waves. Understanding the mechanisms behind super-rotation is crucial for the characterization of the atmospheres of exoplanets (*e.g.*, Lee *et al.*, 2020). Indeed, at the beginning of the space exploration era, ground-based observations of Venus initially concluded to a fast-rotating planet, until refined observations revealed that the rotation only concerned the cloud deck while the planet was actually a slow rotator. Such misinterpretations may prove to be a challenge for making sense of future exoplanets measurements in the absence of a proven theory for superrotation.

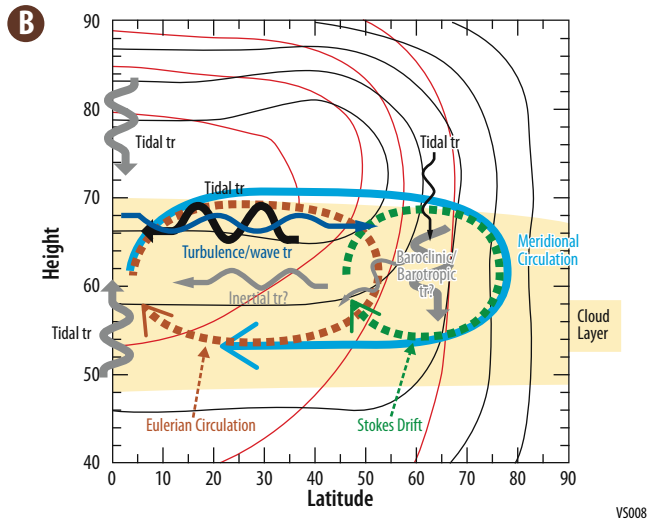
Recent advancements in our understanding of the superrotation mechanism on Venus were brought forward by a suite of IR and UV cameras on board Akatsuki (Nakamura *et al.*, 2011, 2016). The increased image resolution of the features of the cloud top by Akatsuki made possible the estimation of zonal and meridional winds at an unprecedented accuracy by tracking cloud features. The winds are a crucial derived product for elucidating the mechanism at work in the maintenance of the superrotation by identifying the physical processes responsible for the transport of angular momentum. This approach led to the discovery that thermal tides contributes to maintain superrotation at the cloud top, while large-scale turbulence acts against it (**Figure A-2**) (Horinouchi *et al.*, 2020). Nevertheless, the picture is missing for lower altitudes, as the existing dataset of lower cloud deck winds obtained by Akatsuki do not have the accuracy and completeness to conduct such a study. ADVENTS will fill this gap.

Another major recent discovery related to the origin of super-rotation is the presence of a large-scale meridional disruption in the lower cloud decks, found first in Akatsuki images (**Figure A-3**) and later in older dataset dating back from the 1980s. This disruption propagates with a 4-day period, faster than the 9-day period of the atmospheric layer in which it exists (Peralta *et al.*, 2020). Intriguingly, the disruption has the same 4-day period as the cloud top, suggesting a strong, direct connection of the superrotation mechanism across all cloud layers. The nature of this disruption is unknown, but it may be triggered by a Kelvin wave (Peralta *et al.*, 2020).

The combination of the ADVENTS Orbiter near-infrared imagers (NIR-C, NIR-S) and the meteorological suite included on the in-situ Aerobot (AMET) will ensure consistent monitoring of middle cloud level (45–65 km) wind and dynamics processes. The pushbroom imaging of the Orbiter cameras will deliver global maps of the cloud layers at a fast pace of 12h due to the ~20,000 km altitude of the Orbiter. The equatorial orbit will provide an increased resolution of the low latitudes, monitoring both the cloud disruption in the lower cloud deck and the planetary-scale wave, such as the Y-shape feature (Travis *et al.*, 1979) and thermal tides (Rossby, Kelvin wave thermal tide) in the upper cloud deck.

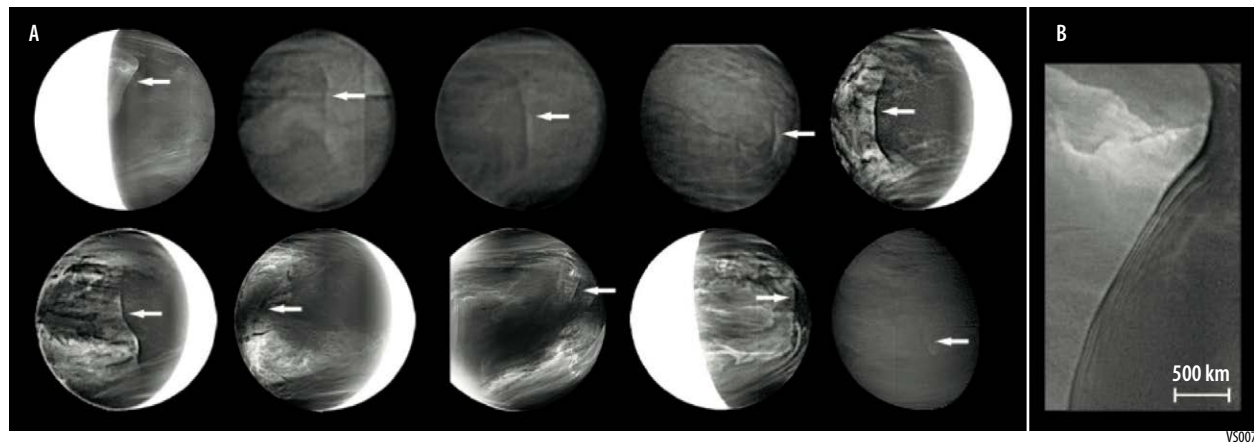


VS006



VS008

**Figure A-2:** ADVENTS will determine which of the proposed mechanisms maintain superrotation in the Venus atmosphere. (A) Cloud-top level winds derived by tracking cloud features seen by the Akatsuki UV camera that led to (B) an updated comprehension of the mechanisms maintaining superrotation. (Horinouchi *et al.*, 2020).



VS007

**Figure A-3:** Disruption of the Venus cloud layers seen by the Akatsuki 2  $\mu\text{m}$  IR camera (Peralta *et al.*, 2020). ADVENTS will correlate global observations of atmospheric dynamics from orbit with in situ chemical and dynamical measurements made by the Aerobot.

Additionally, a plethora of morphological patterns (the lower cloud disruption being one example) will be monitored and some possibly discovered, as was the case with Akatsuki Orbiter (Peralta, Sánchez-Lavega, *et al.*, 2019). For instance, repeated close-in views of the disruption may elucidate its nature by characterizing the downstream ripples seen in the Panel B of **Figure A-2**.

Moreover, both the NIR-S and NIR-C imagers will provide wind maps every 12 hours via cloud tracking. ADVENTS will thus assess the dynamics from the lower cloud deck to the cloud top, eventually closing the angular momentum budget in the whole cloud layer, addressing the missing processes in **Figure A-3** (bottom panel). This is a necessary step before elucidating the cause of superrotation, a feature that would probably require continuous wind mapping by a future mission in the deep atmosphere below the cloud deck, where 90% of the atmospheric angular momentum lies (**Figure A-1**) (Peralta, Iwagami, *et al.*, 2019; Schubert *et al.*, 1980).

Likewise, the in-situ meteorological measurements of the Aerobot will connect the morphological patterns seen in the lower cloud deck with the local pressure and temperature measurements, eventually identifying the physical nature of the morphological patterns seen by NIR-C. The motion of the Aerobot will give a validation point for the retrievals of winds by cloud tracking of orbital images, eventually giving more confidence in the accuracy of the wind vectors, which are a key parameter for constraining the circulation and the transport of angular momentum. The vertical profiles derived from the Dropsonde will further constrain the transfer of angular momentum over the altitude range extending from the surface to the cloud layers.

#### **A.1.1.2 Scientific Rationale for the Dropsonde**

The baseline ADVENTS mission architecture also includes a single Dropsonde that is carried by the Aerobot but deployed immediately during the entry, descent, and float sequence. The Dropsonde will be outfitted with temperature, pressure and chemical sensors that will obtain a vertical profile between the upper clouds (~62 km) and the surface. These measurements will provide the data needed to identify the altitudes at which Venus' atmospheric temperature, pressure, and species profiles transition between hydrostatic to super-critical at low altitude and will help characterize atmospheric conditions where Venus's mountain ranges seem to exhibit the existence of "snow" or at least the fall-out of some precipitated atmospheric constituent. Tracking the position of the Dropsonde as it descends will also provide information on the angular momentum profile between upper clouds and the surface.

#### **A.1.1.3 Scientific Rationale for the Miniature Tunable Laser Spectrometer (TLS)**

The ADVENTS science objectives require sensitive measurements of key isotopic ratios. Along with the aerosol mass spectrometer with nephelometer (AMS-N) from the VFM Aerobot, the ADVENTS Aerobot includes a TLS instrument that is a smaller version of the TLS on the VFM lander. Here we summarize the scientific importance of these measurements and why we believe that data from the TLS (or another mission such as NASA DAVINCI+) may be needed to interpret data from the AMS-N.

##### **A.1.1.3.1 Noble Gases**

Noble gases (He, Ne, Ar, Kr, Xe) are chemically inert, so their isotopes and abundances can vary only through physical processes such as phase changes and isotopic fractionation, and as a result of nuclear reactions. Some of their compositions are primordial and depend on their origins (*e.g.*, nucleosynthetic, solar, meteoritic); others result from nuclear reactions and have the potential to act as geochronometers, as well as monitors of irradiation. Notably, their isotope ratios fractionate during atmospheric escape processes, making them unique tracers of atmospheric evolution.

Because several of the noble gases have three or more isotopes, they offer the possibility to investigate the nature (*e.g.*, thermal, non-thermal) and strength of escape processes that cannot otherwise be addressed with chemically reactive species such as those hosting conventional stable isotopes.

Some of the noble gas isotopes are produced by extinct and extant radioactivities from parent isotopes having half-lives varying between 16 Myr and 14 Gyr. The produced isotopes ( $^{40}\text{Ar}$ ,  $^{129}\text{Xe}$ ,  $^{131-136}\text{Xe}$ ) were released in the Venusian atmosphere at different periods of time and for different outgassing durations. Hence, their relative abundances (normalized to stable isotopes) will help to answer the following questions: Was the bulk of the atmosphere of Venus degassed very early (within the first 100

Myr), as on Earth? How strong has subsequent Venusian degassing been, and how has its rate varied through time? Were subsequent injections of gas catastrophic (*e.g.*, during planetary resurfacing), or sporadic (like mantle plumes), or were they continuous, as might have resulted from plate tectonics or episodic-lid mantle convection?

In the terrestrial atmosphere, the isotope composition of helium,  $^3\text{He}/^4\text{He}$ , is transient as its value depends on different sources and sinks.  $^3\text{He}$  is primordial and was trapped during Earth's accretion, whereas  $^4\text{He}$  is radiogenic, produced by the decays of U and Th isotopes. Both isotopes escape to space at different rates, with a residence time on Earth of  $10^5$ – $10^6$  yr. Even if the residence time is somewhat longer on Venus, as a consequence of its cold upper atmosphere, the detection of  $^3\text{He}$  will signify active degassing and volcanism on the planet and will also help to place constraints on escape processes.

The isotopic composition of terrestrial atmospheric neon indicate that Earth's volatiles now present in the atmosphere were derived mainly from a carbonaceous chondrite-type of material, thought to originate at radial distances from the Sun larger than that of the present-day Earth. The origin of Venusian building material being unclear, measurements of the three isotopes of neon has the potential to identify the main contributing cosmochemical reservoir(s) – solar, meteoritic (and which kind of meteoritic material), and possibly cometary.

Xenon is both depleted and isotopically fractionated in the atmospheres of Earth and Mars compared to carbonaceous chondrites. From the analysis of ancient terrestrial atmospheric samples, it has been recognized that this peculiar Xe composition was caused by Xe loss to space, triggered by its preferential ionization relative to other noble gases, and, possibly, by the lift-off of Xe isotopes by escaping  $\text{H}^+$  ions from photodissociation of  $\text{H}_2\text{O}$ . On Earth, this process took place during the Hadean and Archean eons before the rise of atmospheric oxygen. On Mars, a similar process might have taken place during the Noachian eon when oceans were present. Xenon in the atmosphere of Venus also appears to be elementally depleted but its isotopic composition has not been accurately measured. Hence, the precise measurement of Venusian Xe (at the percent level) will shed exceptional light on escape processes under ionizing conditions and will constitute a strong constraint on the possible past existence of Venusian oceans. Furthermore, measurements of cometary Xe have established a genetic link between comets and the terrestrial atmosphere which can be tested with Venusian Xe isotope measurements.

### A.1.1.3.2 Oxygen Isotopes

Oxygen has three stable isotopes ( $^{16}\text{O}$ ,  $^{17}\text{O}$ ,  $^{18}\text{O}$ ), which in most cases are fractionated proportionally to their masses. In contrast, meteorites show variations that do not depend on isotopic masses and are

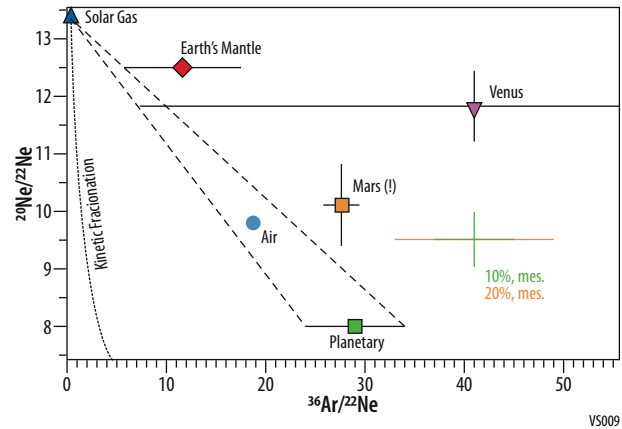


Figure A-4: From Parai and Avice (2021).

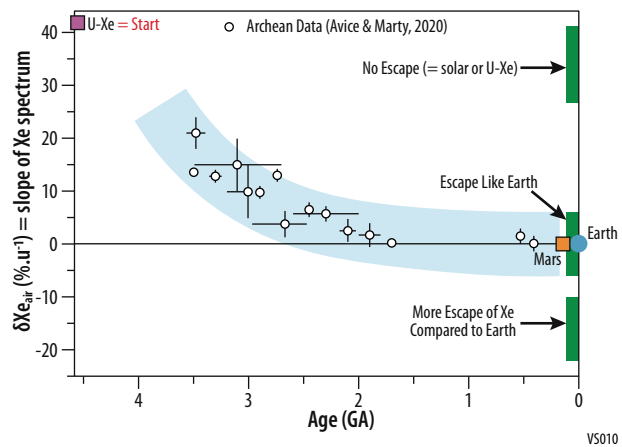


Figure A-5: From Avice and Parai (submitted). Xe isotopes exhibit a linear fractionation pattern. On Earth, the slope of the fractionation pattern declined with time prior to the Great Oxidation Event at  $\sim 2.4$  Ga, possibly as a result of preferential loss of lighter Xe isotopes during hydrodynamic escape of hydrogen. On Venus, the slope of the Xe isotope pattern is unknown.

attributed to specific isotope fractionation during photochemical reactions in the presolar nebula.  $\Delta^{17}\text{O}$  represents the mass-independent fractionation (MIF) of oxygen isotopes relative to the terrestrial composition, that is, the deviation of the sample composition relative to a purely mass-dependent isotope fractionation. This value constitutes a unique fingerprint for the origin of matter in the solar system. Inner planetary bodies (Earth and Moon, Mars, Vesta) and the different of meteorites differ markedly by their  $\Delta^{17}\text{O}$  values as shown in **Figure A-6**, which permits to establish genetic relationships between different bodies.

### A.1.1.3.3 Contextualizing the Claimed Detection of Phosphine

Certainly, the most provocative (and publicly scrutinized) Venus exploration result reported in the past year was the claimed detection of phosphine ( $\text{PH}_3$ ) in the Venusian atmosphere. Phosphine on Earth is exclusively biogenic, so this detection was billed as possible evidence for extraterrestrial life. The report was based on sub-millimeter wave observations from two different, ground-based telescopes (Greaves *et al.*, 2020). The detection itself has been challenged by other researchers; however, the question of whether living organisms might exist within the Venus cloud layer remains unresolved. Some theories for how Venus' climate evolved suggest that liquid water could have been present on Venus' surface for the first few billion years of its existence (Way & Del Genio, 2020) and that it could have migrated to the clouds when the surface itself became uninhabitable.

ADVENTS will test this hypothesis by looking directly for the presence of  $\text{PH}_3$  at different times and locations using the mass spectrometer on the Aerobot (AMS-N). But ADVENTS will also do more than a search for a single molecule.  $\text{PH}_3$  cannot be produced by Venusian cloud life unless other phosphorus-containing gases are present in Venus' atmosphere. Thermodynamic calculations suggest that the stable form of phosphorus in Venus' lower atmosphere is  $\text{P}_4\text{O}_6$ . Phosphorus in this compound would be in the +3 oxidation state, which is reduced compared with the common phosphate ion on Earth,  $\text{PO}_4^{-3}$ , in which P is in the +5 valence state.  $\text{P}_4\text{O}_6$  dissolves in water to yield phosphonic acid,  $\text{H}_3\text{PO}_3$ . In laboratories on Earth, phosphonic acid disproportionates above  $200^\circ\text{C}$  to form phosphoric acid and phosphine:  $4 \text{H}_3\text{PO}_3 \rightarrow 3 \text{H}_3\text{PO}_4 + \text{PH}_3$ . So, it could be that phosphine is present in Venus' atmosphere but its formation mechanism is abiotic rather than biotic. ADVENTS will measure the concentrations of  $\text{P}_4\text{O}_6$  and its associated acids to test whether this potential abiotic formation pathway for phosphine might operate within the Venusian atmosphere.

### A.1.1.3.4 Synergy between the TLS and AMS-N

Making the requested noble gas isotope measurements should be straightforward, provided one has an accurate mass spectrometer that can measure the least-abundant noble gas isotopes. By contrast, the measurement of oxygen isotope ratios, and the detection of phosphine, can be complicated by the presence of abundant deuterium on Venus. The D/H ratio in Earth's oceans is  $1.56 \times 10^{-4}$ . By contrast, D/H in Venus' atmosphere is  $\sim 120$  times higher (De Bergh *et al.*, 1991) where the atmosphere is sounded in the altitude range from 32 to 42 kilometers (8 to 3 bars, putting it at almost 2%). That is higher than the relative abundance of minor isotopes of carbon ( $^{13}\text{C}/^{12}\text{C} = 1.1\%$ ) or oxygen ( $^{18}\text{O}/^{16}\text{O} = 0.2\%$ ,  $^{17}\text{O}/^{16}\text{O} = 0.04\%$ ) on Earth. One minor sulfur isotope,  $^{34}\text{S}$ , is more abundant than this ( $\sim 4\%$ ) but the other minor isotopes of sulfur are again much less abundant in a relative sense.

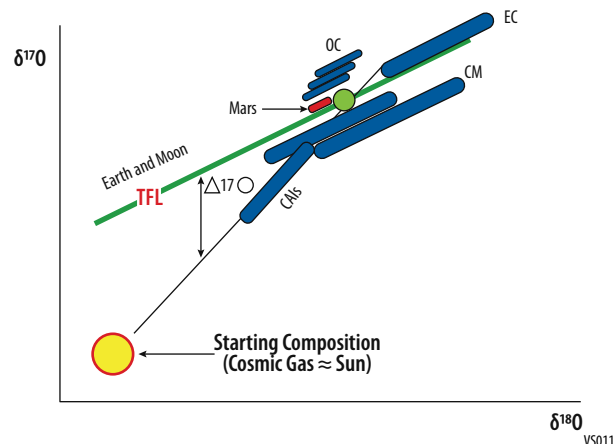


**Figure A-6:** Modified from Hashizume and Chaussidon 2005. TFL is the terrestrial fractionation line which includes also the Moon. The brown area is Mars and the blue areas represent different classes of meteorites. CAIs are calcium-aluminum-rich inclusions. Measuring the oxygen isotopic composition of Venusian atmosphere (*i.e.*, on  $\text{CO}_2$ ) will shed light on the linkage to different types of primitive material in the nascent solar system and on the location where the latter formed.

Consider what might happen if one was trying to interpret the measurement of a mass 19 species in Venus' atmosphere. This could be either  $\text{H}_2^{17}\text{O}$ , or it could be  $\text{HD}^{16}\text{O}$ . Similarly, and perhaps more likely if  $\text{H}_2\text{O}$  is fragmented upon ionization, mass 18 could be either  $\text{H}_2\text{O}$ ,  $\text{H}^{17}\text{O}$ , or  $\text{D}^{16}\text{O}$ . The abundance of the deuterated compounds should be higher than that of the species containing  $^{17}\text{O}$ , so measurement of the  $^{17}\text{O}$  species would be compromised by this overlap. The very accurate mass spectrometer listed as payload on this mission (AMS-N) is reportedly capable of resolving mass differences of as little as 0.001 AMU, so this ambiguity might be removed by observations that could resolve the mass difference between, say,  $\text{H}^{17}\text{O}$  and  $\text{D}^{16}\text{O}$ . But doing so requires a time-consuming, slow progression through the relevant mass range. Inclusion of a tunable laser spectrometer (TLS) that could independently measure the ratios of  $\text{HDO}/\text{H}_2\text{O}$  and of  $\text{CO}_2^{17}\text{O}/\text{CO}_2$  would solve this problem directly, thereby enhancing confidence in the determination of the mass spectrometry data. The 2-channel, mini-TLS instrument included in the strawman payload for the Aerobot would do just that.

A problem that is not directly addressed by the 2-channel mini-TLS is that of the detection of phosphine,  $\text{PH}_3$ . Phosphorus has atomic mass of  $\sim 31$  AMU, whereas sulfur has atomic mass of  $\sim 32$  AMU. Thus,  $\text{PH}_3$  has approximately the same molecular weight ( $\sim 34$  AMU) as  $\text{H}_2\text{S}$ . The latter species is expected to be present in the Venus' clouds as a consequence of sulfur photochemistry starting from dissociation of  $\text{SO}_2$ . The predicted abundance of  $\text{H}_2\text{S}$  is roughly equal to that of  $\text{PH}_3$  in the middle part of the cloud deck (Greaves *et al.*, 2020, Extended Data Fig. 9). Hence, any purported detection of phosphine by the mass spectrometer could instead be  $\text{H}_2\text{S}$ . An additional channel on the TLS that could measure  $\text{PH}_3$  directly would resolve this ambiguity. But keeping the overall number of channels at two to save mass and power on the Aerobot would require sacrificing the capability to measure D/H or the isotopes of carbon and oxygen. A more detailed analysis could reveal whether this problem is serious enough to merit inclusion of a more capable TLS with additional frequency channels.

### **A.1.2 Potential Enhancements to the ADVENTS Payload**

The baseline ADVENTS concept was selected to achieve our science goals and objectives. However, we recognize that proposal teams may choose to address different (but related) science goals and objectives using a modified selection of instruments. Adding (instead of substituting) instruments could transform ADVENTS into a small Flagship mission—and also provide Flagship-worthy science. Other elements could be separately funded as ride-along missions to Venus that enhance the overall science return. Here we briefly summarize the scientific and/or programmatic value of potential substitutions and/or augments to the ADVENTS payload that we discussed during the study process. The VFM report details several potentially desired options (*e.g.*, a lander, a SmallSat constellation, and radar on the Orbiter) that were not considered in any additional detail during the ADVENTS study.

#### **A.1.2.1 Visible Cameras**

Mars 2020 carried several engineering cameras that provided an amazing view of (so far) the entry, descent, and landing process and the first flight of the Ingenuity helicopter. These cameras (and one microphone) captivated the public and provided mission engineers valuable data about the performance of their hardware. The ADVENTS science goals and objectives do not require a visible camera. However, we would support adding one or more engineering cameras to the Aerobot to document the entry, descent, and float procedure, especially the inflation of the balloons. Such cameras could also monitor the effects of the atmosphere on the Aerobot hardware over time—and provide compelling views of the clouds. We suggest exploring different avenues to fund such a valuable tool for education and public outreach. For example, the VFM concept envisioned including a camera as a student contribution.

#### **A.1.2.2 Atmospheric Composition and Dynamics from Orbital Measurements**

At the start of the study process, we designed the Orbiter with a  $\sim 5$ – $7$  Earth-day period to acquire full-disk images of Venus while remaining synchronous with the circumnavigation of the Aerobot. However, we found that the large orbital altitude ( $> 100,000$  km above the Aerobot) led to a very slow data rate between the Aerobot and the Orbiter. To return the science data from the Aerobot to Earth (via the Orbiter), we needed to vastly increase that data rate. We could not augment the telecom sys-

tem without substantially increasing the mission cost above the New Frontiers level—so we decided to decrease the orbital altitude to the baseline  $\sim 0.5$  Earth-day period ( $\sim 20,000$  km above the surface). Along with the Aerobot-synchronous orbit, the original payload for ADVENTS featured capable UV instruments that were ultimately descope to reach our baseline.

Future teams may wish to revisit the science case for UV instruments on the Orbiter. In the past, UV imaging observations at 283 and 365 nm have been used to characterize Venus' zonal circulation patterns at  $\sim 68$  km altitude, which is  $\sim 1$ – $2$  atmospheric scale heights above the altitude where our Aerobot would operate. Acquiring these UV data in conjunction with the Aerobot measurements would provide valuable insights about the atmospheric dynamics occurring in Venus' middle and upper cloud layers. Likewise, UV spectra at  $\sim 200$ – $240$  nm would help characterize vertical mixing in the upper clouds. UV spectra at longer wavelengths ( $\sim 300$ – $640$  nm) would have several purposes. First, these spectra would constrain the overall radiative balance of the atmosphere. Second, joint analyses of these spectra and Aerobot measurements of aerosol and gas composition could reveal the vertical distribution and even composition of Venus' unknown UV absorber—which has been a high-priority scientific target for decades. Notably, each of the investigations enabled by possible UV instrumentation, as well as the acquisition of the UV data in conjunction with Aerobot data, are given a high priority in the VEXAG GOI document.

Adding a capable UV imager and/or spectrometer to the baseline ADVENTS Orbiter payload would push the concept into a small Flagship-class mission. However, a New Frontiers class mission concept could make a credible argument for flying UV instruments in lieu of one or more instruments presented in this study. Given their role in revealing the atmospheric dynamics and composition at Venus, UV instruments could enhance the science return of any Venus Orbiter.

#### **A.1.2.3 Sub-Cloud Imaging with a Towbody**

One of the most important ADVENTS objectives is to determine the rock types of different regions of the surface. In particular, ADVENTS would test the hypothesis that the tesserae are felsic, which would indicate that they formed in the presence of water oceans (*e.g.*, Gilmore *et al.* 2017; Gilmore *et al.* 2015). This objective would be accomplished with a NIR imager (NIR-S), which is based on the Venus Emissivity Mapper (VEM) that is part of both the proposed VERITAS and EnVision mission concepts (*e.g.*, Helbert *et al.* 2013). Unlike the previous IR mapping spectrometer that was sent to Venus (VIRTIS on Venus Express), NIR-S is designed to peer through the spectral “windows” in the atmosphere where surface emission can reach space. Unfortunately, atmospheric scattering of the emitted light limits the spatial resolution of emissivity maps made from orbit to  $\sim 50$  km or worse. Although NIR-S can spatially oversample the IR images (*e.g.*, at a spatial resolution  $< 25$  km), no orbital instrument can overcome this fundamental limitation. However, IR images collected from below the clouds (at  $< 47$  km altitude) can reach sub-km spatial resolution by avoiding most atmospheric scattering. As part of the ADVENTS study, we designed a towbody that would be deployed on a  $> 5$ -km tether below the Aerobot. The towbody would conduct a  $\sim 4$ -hour imaging traverse over selected regions on the nightside before being raised back up to the Aerobot to cool down. Overall, towbody-enabled imaging would provide surface emissivity maps that could be correlated with the radar maps from NASA Magellan, which have a spatial resolution of  $\sim 125$  m. Such detailed maps would aid efforts to determine rock types and stratigraphic relationships at key features such as tesserae and coronae. To keep the cost of ADVENTS close to the New Frontiers class, we did not include a towbody in our baseline concept. However, **Appendix A.3.1.5** describes the engineering of the towbody. Overall, we suggest that future teams consider the towbody if clever means are found to reduce costs overall or if ADVENTS were “up-scoped” to a small Flagship mission.

#### **A.1.2.4 Multiple Descent Probes**

ADVENTS mission architecture also includes a single trajectory dropsonde. Multiple traces of temperature, pressure, and chemical species would only increase the rigor and scientific value of the measurements. Likewise, a distribution of the measurements over ranges of latitudes and local times would allow a better understanding of the global atmospheric structure between the upper clouds and the



surface. Ideally, these measurements would not be limited to the cloud top regions but would be collected at Venus's mesosphere (~60–100 km) and troposphere (0–60 km) altitudes. High-altitude data are key because in the mesospheric region (~72–100 km) the zonal wind speeds change substantially in what seems to be a response to a transition in the mechanism (atmospheric pressure gradients) that dominantly control the zonal flow.

A more complete understanding of the links between Venus's mesosphere and the intervening deep atmosphere region extending from 75 km down to the surface would be best obtained with multiple distributed descent probes. Traditionally, this would require the release of several probes or dropsondes from the carrier spacecraft (e.g., Pioneer Venus). Because each probe is housed in its own aeroshell and the number and capability of probes included in a mission will tend to be cost limited. Currently, NASA is investing in the development of a number of novel, low-cost miniature entry probes and platforms. For example, LEAVES (Lofted Environmental and Atmospheric VEnus Sensors) is kite-like entry probe concept, which is in its 1<sup>st</sup> year of a NASA Innovative Advanced Concepts (NIAC) phase II funding cycle. A swarm (~10 to ~100) of probes could be deployed from orbit without individual aeroshells and gather *in situ* data over large regions of the atmosphere. If any of these technology development programs succeed, teams designing missions for launch in the 2030–2040s could exploit novel means of obtaining unprecedented data on the dynamical, chemical, and energy exchange process operating at Venus between the surface and upper atmosphere, which would be game-changing for the development of general circulation and atmospheric climate models.

### A.1.3 Traceability from ADVENTS to the 2019 NASA VEXAG GOI

The prime focus of the ADVENTS mission is to answer the fundamental questions about Venus's Evolution, Habitability and near-term climatic and geophysical conditions that have remained a mystery throughout the 60-year tenure of the NASA space exploration program. **Table A-1** shows how ADVENTS mission concept addresses 10 of the 12 investigations identified in the VEXAG GOI document as Essential (and two more described as Targeted) to advancing our understanding of Venus system science. **Foldout 1** shows the ADVENTS Science Traceability Matrix.

**Table A-1:** ADVENTS fully or partially addresses 10 of the 23 total high-priority investigations identified in the 2019 VEXAG GOI, which represents the community consensus about the scientific aims of Venus exploration. Eight of these 10 ADVENTS investigations are marked Essential in the 2019 VEXAG GOI, while the Magnetism and Outgassing Investigations are described as Targeted (but still high priority overall).

ADVENTS Science Investigation (see Foldout 1, Science Traceability Matrix)		
Goals	Objectives	Associated Investigation from VEXAG GOI
1. Understand how Venus formed and evolved for comparison to other rocky (exo)planets.	1A. Determine if Venus and Earth accreted volatiles from similar reservoirs.	I.B.IS. Isotopes
	1B. Determine if there is active tectonic and volcanic activity on Venus today.	III.A.GA. Geologic Activity
2. Understand the potential past habitability of the Venus surface.	2A. Determine if tesserae on Venus formed in the presence of water oceans.	I.A.HO. Hydrous Origins
	2B. Determine if the crust of Venus preserves a record of an early dynamo.	I.A.MA. Magnetism
3. Understand the composition, dynamics, and potential habitability of the present-day atmosphere of Venus.	3A. Assess the present-day habitability of the Venus cloud environment.	II.B.IN. Interactions II.B.AE. Aerosols II.B.UA. Unknown Absorber
	3B. Determine what mechanisms control the composition, transport, and production of volatiles in the Venus cloud environment.	II.A.DD. Deep Dynamics II.A.UD. Upper Dynamics II.B.OG. Outgassing III.B.CI. Chemical Interactions

## A.2 MISSION OVERVIEW

The ADVENTS flight system consists of an Orbiter and an Aerobot with a Dropsonde as shown in **Figure A-7**. The Orbiter functions as a carrier for the Aerobot, a communication relay for the Aerobot and Dropsonde, and a science platform. The Aerobot is contained within an entry system so that it

can survive entry and descent through the Venus atmosphere. The Orbiter spins up to 5 rpm and then releases the Aerobot in its entry system for the entry and descent phase 5.5 days prior to the Orbiter inserting into its Operational Orbit about Venus. The Aerobot carries a dropsonde that is released during entry that carries pressure, temperature and chemical sensors to measure the atmosphere down to the surface for upto an hour. During its nominal 60-day lifetime the Aerobot floats at a nominal altitude of 55 km allowing it to circumnavigate Venus every 7 days.

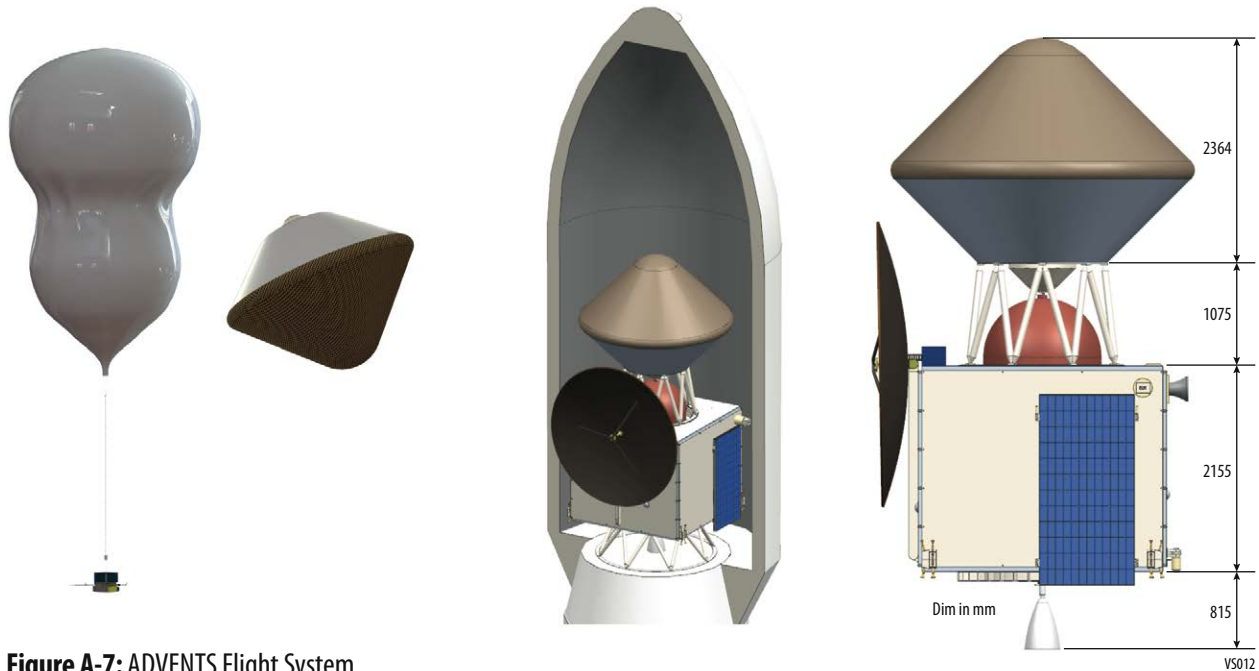


**Figure A-7:** ADVENTS Flight System.

ADVENTS is launched on a Falcon Heavy with a 5 m diameter fairing. The primary launch opportunity is June 4, 2039 with a backup launch opportunity of December 4, 2039. Both launch opportunities have a minimum of a 14-day launch window. The Orbiter releases the Aerobot 5.5 days prior to the Venus Orbit insertion (VOI) that places it in a low eccentricity, low-inclination, retrograde orbit with a ~12 hour period (~20,000 km altitude) that enables frequent contacts with the Aerobot and the relay of mission data back to Earth. **Table A-2** shows the ADVENTS mission summary.

**Table A-2:** ADVENTS Mission Summary.

Parameter	Value	Units
Orbit Parameters (apogee, perigee, inclination, etc.)	24,856.2 km circular 170° inclination	
Mission Lifetime	78	mos
Maximum Eclipse Period	58	min
Launch Site	Cape Canaveral	
Aerobot Mass <b>with</b> contingency (includes instruments)	1,878.6	kg
Orbiter Mass <b>with</b> contingency (includes instruments)	1,494.7	kg
Propellant Mass <b>without</b> contingency	2,273.1	kg
Propellant contingency	10	%
Propellant Mass <b>with</b> contingency	2,500.4	kg
Launch Adapter Mass <b>with</b> contingency	71.0	kg
Total Launch Mass	5,944.7	kg
Launch Vehicle	Falcon heavy Expendable	Type
Launch Vehicle Lift Capability	11,694.0	kg
Launch Vehicle Mass Margin	5,749.3	kg
Launch Vehicle Mass Margin (%)	96.7	%

The strawman payload on the ADVENTS Mission is distributed across three synergistic platforms: Orbiter, Aerobot, and a single Dropsonde. The Orbiter carries (2) near infrared imagers (NIR-C for cloud layer dynamics and NIR-S for surface emissivity) and an Extreme Ultraviolet (EUV) monitor. The NIR-C draws heritage from the JAXA Akatsuki IR2 instrument. The Orbiter and Aerobot platforms each carry the NASA GSFC standard fluxgate magnetometer (MAG) which is mounted on a deployable boom. The MAG draws heritage from MAVEN, Juno, and Parker Solar Probe and has been in Mars orbit since 2014.

The Aerobot instrument payload includes an aerosol mass spectrometer with nephelometer (AMS-N), mini tunable laser spectrometer (TLS), a suite of meteorological (MET) sensors to measure barometric pressure, temperature, and wind speed, and a radiation dosimeter.

The Dropsonde contains a pressure and temperature sensor and a chemical sensor array.

The mass and power of the instruments are summarized in **Table A-3**. The instrument characteristics are discussed in **Appendix A.3.1.1** and **Appendix A.3.2.1**. The Orbiter and Aerobot payload operations are discussed in **Appendix A.2.4**.

**Table A-3: ADVENTS Instrument Summary.**

Instrument Name	Flight Element(s)	Mass			Average Power		
		CBE (kg)	% Cont.	MEV (kg)	CBE (W)	% Cont.	MEV (W)
NIR-S	Orbiter	3.4	30	4.4	1.03	30	16.9
NIR-C	Orbiter	18.0	30	23.4	114.0	30	148.2
Magnetometer	Gondola Orbiter	1.5	30	2.0	1.0	30	1.3
EUV	Orbiter	7.0	30	9.1	14.0	30	18.2
AMS-N	Aerobot	10.5	30	13.7	7.0	30	9.1
Mini-TLS	Aerobot	3.3	30	4.3	24.0	30	31.2
Meteorological sensors	Aerobot	4.0	30	5.2	5.0	30	6.5
Chemical Sensor Array	Dropsonde	0.1	30	0.13	3.0	30	3.9
Pressure and temperature sensors	Dropsonde	2.3	30	3.0	10.7	30	13.9
Total Payload Mass		51.6	30	67.2			

### A.2.1 Key Architecture and Mission Trades

The primary mission trade was to determine the architecture elements for the mission. Options for a fixed balloon with a dropsonde vs variable-altitude balloon with dropsonde and a towbody were evaluated as shown in **Table A-6**.

A towbody that would deploy from the Aerobot to conduct surface imaging below the cloud deck was initially evaluated for inclusion on the fixed-altitude balloon, but the option was eliminated for further consideration on the fixed altitude balloon due to the large length and mass of tether needed to deploy it from the 55 km fixed-altitude. It was evaluated for inclusion on the variable-altitude balloon. Details of the towbody are shown in **Appendix A.3.1.5**.

The result of the trade was an architecture comprised of a variable altitude balloon and a single dropsonde attached to the Aerobot that releases just prior to backshell separation and no towbody (**Table A-6** highlighted column). The following paragraphs describe the trade in further detail. The dropsonde design concept is discussed in **Appendix A.3.1.4**. The towbody considered is discussed in **Appendix A.3.1.5**. Additional Aerobot (**Appendix A.3.1**) and Orbiter (**Appendix A.3.2**) subsystem and design trades are discussed in each of the subsystems.

#### A.2.1.1 Balloon Type

There are many different types of balloons possible for use at Venus and this study was asked to evaluate two of them:

- 1) **A spherical superpressure balloon.** This type of balloon consists of a spherical structure that is inflated with enough gas to always be pressurized compared to the local atmosphere and therefore maintain its spherical shape throughout the flight. This constant volume feature provides passive

altitude stability such that the balloon will always seek to fly at a constant density level in the atmosphere and will return to that point if displaced vertically by wind gusts. The 1985 Soviet VeGa balloons were of this type (**Figure A-8**), though much smaller than the size considered for this study.

- 2) **A variable-altitude balloon.** This type of long-duration balloon relies on gas pumping between chambers in a two-part balloon to change the net buoyancy and thereby effect altitude changes. This allows for exploration over a potentially wide altitude range, in contrast to the constant altitude superpressure balloon. Many different options exist for implementing such a variable altitude balloon (see for example Hall *et al.*, “Altitude-Controlled Light Gas Balloons for Venus and Titan Exploration”, AIAA Paper 2019-3194) but this study adopted the same option as the 2020 Venus Flagship Study that consisted of a balloon-within-a-balloon architecture with helium gas pumping between the outer not-pressurized balloon (also known as a “zero pressure balloon”) and the inner pressurized balloon (a superpressure balloon itself). A recent Venus sub-scale prototype balloon of this type is shown in **Figure A-9** with a diagram showing how this type of balloon works in **Figure A-10**.

The team conducted a trade study between these two options that quantified the mass penalty associated with using the more complicated, but more capable, variable-altitude balloon compared to the simpler constant altitude superpressure balloon. The results are summarized in **Table A-5** for the scenario where the superpressure balloon is designed for a 55 km altitude and the variable altitude balloon range is 52 to 62 km. The balloon materials used in these designs are shown in **Table A-4**.

For both the inner and outer balloon, the Teflon provides sulfuric acid resistance to the aerosols in the Venus clouds, the metallization reflects most sunlight and limits solar heating, and the Vectran provides high strength to contain the pressurization loads. The aluminum coating on the outer balloon also reduces loss of helium by diffusion. This is particularly important at the higher temperatures when the balloon is at the lower end of its altitude range.



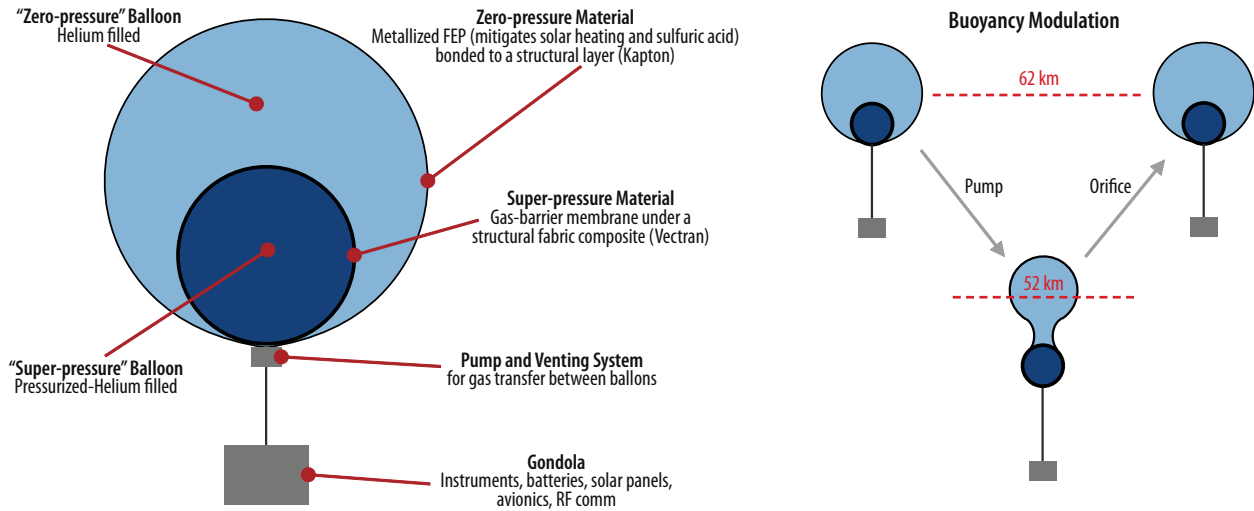
VS013

**Figure A-8:** Soviet VeGa balloon (1985).



VS014

**Figure A-9:** JPL/Near Space Corporation 4 m sub-scale variable altitude balloon (2020), illustrating the volume expansion required for changing altitude. [Izraelevitz, J., Pauken, M., Elder, T., Carlson, K., Lachenmeier, T.I.M., Baines, K., Cutts, J.A. and Hall, J.L. “Pumped-Helium Aerobots for Venus: Technology Progress and Mission Concepts. 2020, December”. In AGU Fall Meeting 2020. AGU.]



VS015

**Figure A-10:** Diagram summarizing the structure and operation of a balloon-in-a-balloon variable altitude concept.

**Table A-4:** Inner and Outer Balloon Materials for the Variable Altitude Balloon.

Outer Balloon Material	Inner Balloon Material
1mil FEP – High Epsilon & Acid Barrier	Vectran Fabric – Superpressure Strength
150nm VD Silver/Inconel Layer - Low Alpha & Diffusion Barrier	
Thermoset Adhesive	
100nm VD Aluminum Layer - Diffusion Barrier	Urethane Bladder – Gas Barrier
1mil Kapton - Gas Barrier & Structure	

\*Adapted from Hall et al., "Prototype design and testing of a Venus long duration, high altitude balloon", *Advances in Space Research*, Vol. 42, pp 1648-1655, 2008).

**Table A-5:** Mass Comparison Between Constant and Variable Altitude Balloon Options.

Gondola Mass (kg)	Fixed Altitude (55 km)			Variable Altitude (52-6 km)			Floating Mass Increase (%)
	Balloon Mass (kg)	Floating Mass (kg)	Gondola (% of Floating)	Balloon Mass (kg)	Floating Mass (kg)	Gondola (% of Floating)	Var. Alt. vs Fixed Alt.
140	78	218	64	126	266	53	22
180	98	276	65	149	329	55	19
200	105	305	66	156	356	56	17
230	117	347	66	170	400	58	15

The data in **Table A-5** shows that the constant-altitude balloon provides a small mass advantage across a wide range of gondola masses. The team concluded that the significant science benefit provided by the variable-altitude capability was worth the additional mass required and therefore adopted it as the baseline.

### A.2.1.2 Dropsonde Mounting

**Figure A-11** shows the four options that were considered for accommodating the dropsonde. To minimize float mass all options were required to release the dropsonde prior to Aerobot float.

The first option was to mount the dropsonde to the Aerobot and release it prior to the backshell separation. Due to packaging constraints only 1 dropsonde could be accommodated.

The second option allowed for mounting of multiple dropsondes to the back of the heat shield. **Figure A-12** shows that the dropsondes would separate from the backshell after the backshell is jettisoned by the use of small parachutes.

The third option considered was to mount the dropsonde to the backshell as an integrated pressure vessel that would float away with the backshell as shown in **Figure A-13**.

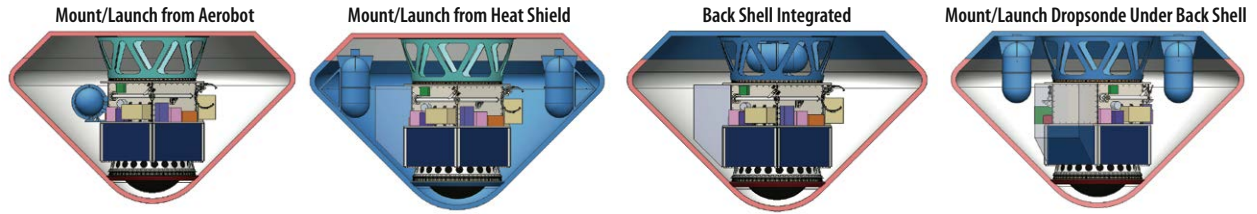


**Figure A-11:** Dropsonde Accommodation Options.

The four options were evaluated, and the team concluded that the significant entry mass required for options 2-4 would drive the size and cost of the entry system significantly more than option 1. Option 1 was selected as the baseline mounting design concept.

The final option considered was to mount dropsondes to the backshell and deploy them via lightband separation systems as shown in **Figure A-14**.

Mounting the dropsonde to the Aerobot and releasing it prior to backshell separation was selected as the baseline concept since it minimized the mass of the entry system and allowed for the center of gravity to be lower during entry than the other options. A concern with this mounting is the c.g. offset that needs to be minimized due to the 5 rpm spin rate that the entry system has after release from the Orbiter and during entry and descent. Adjusting the mounting locations of electronic boxes and battery units was used to provide this offset.

### A.2.1.3 Towbody

The evaluation of including a Towbody showed that in all cases a significant increase in cost and float mass occurred. For this reason, the Towbody was not selected for inclusion in the baseline concept.

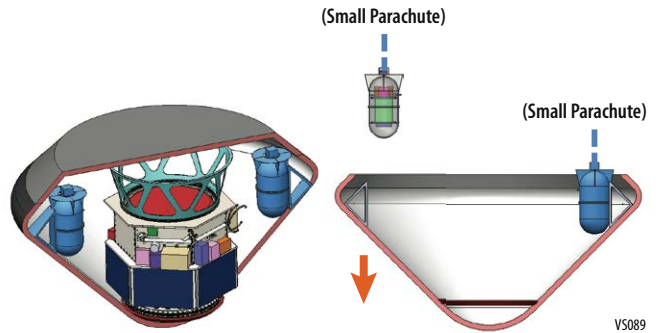


**Figure A-12:** Dropsonde mounted to back of heat shield.

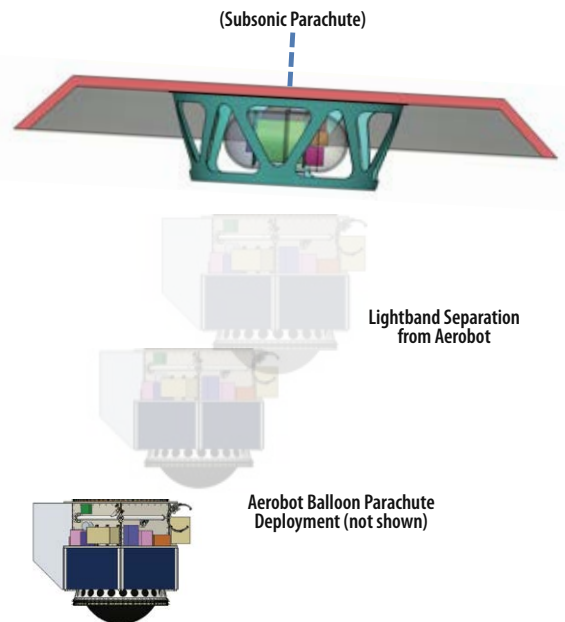


**Figure A-13:** Backshell Integrated pressure vessel.

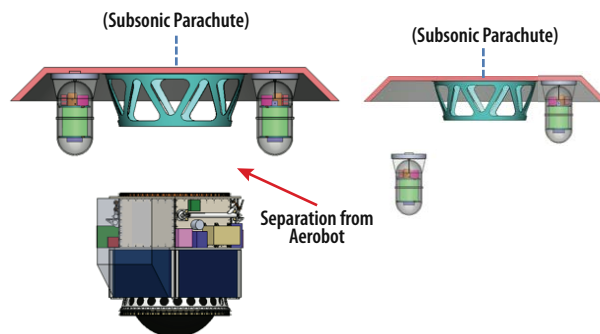


**Figure A-14:** Backshell mounted dropsonde deployment.

**Table A-6: ADVENTS Configuration Trade.**

	Fixed Altitude Balloon					Variable Altitude Balloon			
	Dropsonde Mounting Option 1	Dropsonde Mounting Option 2	Dropsonde Mounting Option 3	Dropsonde Mounting Option 4	Dropsonde Mounting Option 1	Towbody + Dropsonde Mounting Option 1	Towbody + Dropsonde Mounting Option 2	Towbody + Dropsonde Mounting Option 3	Towbody + Dropsonde Mounting Option 4
Cost	\$	\$\$	\$\$	\$\$	\$\$	\$\$\$	\$\$\$\$	\$\$\$\$	\$\$\$\$
Float Altitude Range (km)	55	55	55	55	52-62	52-62	52-62	52-62	52-62
Maintain Float Altitude	No	No	No	No	Yes	Yes	Yes	Yes	Yes
Adjust circumnavigation period	No	No	No	No	Yes	Yes	Yes	Yes	Yes
Number of Dropsondes	1	1+	1	1+	1	1	1+	1	1+
Dropsonde Support Mass on Gondola	Yes	No	No	No	Yes	Yes	No	No	No
Dropsonde Drop Time	1 hour	1-3 hours	1-3 hours	1-3 hours	1 hour	1 hour	1-3 hours	1-3 hours	1-3 hours
Dropsonde Parachute(s)	No	Yes	No	Yes	No	No	No	No	No
Dropsonde Release mechanism(s)	Yes	Yes	No	Yes	Yes	Yes	Yes	No	Yes
Dropsonde Parachute Required	No	Yes	No	No	No	No	Yes	No	No
1 Dropsonde mass (kg)	116.9	116.9	116.9	116.9	116.9	116.9	116.9	116.9	116.9
Dropsonde Accommodation on Gondola mass (kg)	6.5	0	0	0	6.5	6.5	0	0	0
Dropsonde accommodation Mass on Entry System (kg)	0.0	10	5	10	0.0	0.0	10	5	10
Towbody System mass (kg)	N/A	N/A	N/A	N/A	0.0	22.8	22.8	22.8	22.8
Towbody Accommodation on Gondola: Battery and SA Delta, Mounting Mass (kg)	0	0	0	0	0.0	12.0	12.0	12.0	12.0
Balloon Mass (kg)	136.5	130.7	130.7	130.7	214.3	233.1	234.7	232.4	234.7
He (kg)	38.8	37.2	37.2	37.2	38.8	44.8	45.3	44.5	45.3
He Tank (kg)	471.1	468.2	468.2	468.2	471.1	481.5	482.4	481.1	482.4
Entry System Mass (kg)	841.9	841.9	841.9	841.9	878.2	878.2	888.2	883.2	888.2
Entry Mass (kg)	1,800.8	1,800.5	1,795.5	1,800.5	1,878.6	1,913.8	1,930.2	1,916.0	1,930.2
Gondola Mass (kg)	198.0	191.5	191.5	191.5	198.0	239.3	242.8	237.8	242.8

### A.2.2 Mission Requirements

The mission requirements shown in **Table A-7** are derived from the Science Traceability Matrix (**Fold-out 1**) and the architecture and mission trades. Key requirements that drive the mission are limiting entry peak g loads on the Aerobot to less than 50 g, and providing continuous coverage of the entry, descent, and initial float of the Aerobot. As discussed in the architecture trade section above, the mission had a goal of accommodating a towbody. The architecture trade showed that it was not possible to accommodate the towbody without significant mass and cost growth.

**Table A-7: Mission Traceability Matrix.**

Mission Req. (Top Level)	Mission Design Requirements	Orbiter	Aerobot and Entry System	Ground System Requirements	Operations Req.
Mission Lifetime 6.5 years Orbiter 6.5 years Aerobot 60 days	Launch mass (kg): 4,221.6 Launch date: 2036 – 2040	Reliability Category 2, Class B Perform Venus Orbit Insertion Ka-Band $\geq$ 1.0 Mbps to Earth	Reliability Category 2, Class B Max Entry G-Load of $\leq$ 50 g Deploy balloon with a dynamic pressure of $<$ 25 Pa	34m DSN Antenna, Ka-Band at maximum of 100 Mbps Receive housekeeping & science data telemetry	Manage time correlations Maneuvers Support DSN passes
Provide communication with Earth during all critical events	Launch Window of at least 14 consecutive days	X-Band $\geq$ 263 kbps to Earth with two-way tracking S-Band $\geq$ 4 kbps from Aerobot	Data Storage 1 Gbit Conduct Science Operations as defined in the operations concept	Provide commanding	Monitor Landers state of health
Mission Reliability Category 2, Class B	Falcon Heavy Expendable with 5m fairing	S-Band $\geq$ 0.8 kbps from Dropsonde	Return all science data to Orbiter	Record/Store science data	Implement contingency procedures
Conduct Science Operations as defined in the operations concept	Orbiter orbit that provides minimum of 10 minutes per Earth day of contact with Aerobot Obtain 92% coverage of Venus with NIR-S Monitor the sun with EUV Provide $>$ 4 hours contact with Aerobot when it is floating in the Venus daylight Minimum 4 hours daily Orbiter contact with Earth	1 ms timing accuracy with 1e-15 stability relative to ground station Data Storage 1 Tbits Conduct Science Operations as defined in the operations concept Accommodate instrument interfaces 3-Axis Stabilized Spin Aerobot Entry Vehicle to 5 rpm and sperate it on Entry trajectory Provide Aerobot $>$ 1 m/s separation velocity from Orbiter Nadir pointing	Provide beacon for tracking by Orbiter from Separation thru backshell deployment Provide s-band communication from initial float thru end of mission Control operational altitude between 52 km and 62 km Maintain commanded altitude within $\pm$ 1 km Survive altitudes down to 50 km Provide interfaces for instruments Deploy Dropsonde at $>$ 52 km (70 km goal) altitude for P/T and chemical sensor measurements with $<$ 0.5 km vertical spacing down to the surface. Deploy towed platform (Goal) to $<$ 47 km for $>$ 1 hours of NIR Imaging on the nightside during each circumnavigation	DDOR Tracking of Orbiter during transfer Orbit and VOI, Tracking of Aerobot from release through end of mission, Tracking of Lander from release through landing Provide critical event telecom coverage: Launch, Separation from Launch Vehicle, DSM, Aerobot entry Targeting, Aerobot separation, Orbit insertion targeting, Instrument Deployments, Descent of Aerobot, Descent of Dropsonde	Implement science sequences Inventory data & re- transmit if needed Perform ops sim testing

### A.2.3 Mission Design

The mission study began with an analysis to determine the heliocentric transfer trajectory and Venus orbit insertion. The results showed a variety of launch and arrival dates that have a required delta-V that meet mission requirements. The Falcon Heavy is selected as the primary launch vehicle for this study as it outperforms all other current commercial launch vehicles except for the SLS, which is not considered for the study. Solutions include a capture maneuver into a circular orbit around Venus. Direct captures into a circular orbit are not assumed to be the most efficient capture sequence and as a result additional trajectory design could be done to decrease the capture delta-V if needed. The primary trajectory was selected from the trade results and a comprehensive capture analysis was performed to reduce the delta-V. **Table A-8**, shows key bounding requirements set for the interplanetary trajectory design.

**Table A-8: Requirements for the ADVENTS interplanetary trajectory.**

Requirements	Value
First launch date	January 1, 2036
Maximum time of flight	4 years
Minimum time of flight	2 years
Propulsion type	Chemical

The flyby combination was the primary trajectory trade conducted. Earth and Venus combinations of up to two flybys were considered. Results show that the most delta-V efficient trajectory requires



one Venus flyby. The total delta-V for this trajectory was 1.321 km/s. **Table A-9** presents the results of all flyby combinations with case 3 as the lowest delta-V solution, one Venus flyby.

**Table A-9:** Flyby Delta-V Results.

Case number	Trajectory	Delta-v [km/s]
1	Direct Earth to Venus	1.72
2	Earth Gravity Assist	1.323
3	Venus Gravity Assist	1.321
4	Earth-Earth Gravity Assist	2.426
5	Venus-Venus Gravity Assist	1.327
6	Earth-Venus Gravity Assist	1.414
7	Venus-Earth Gravity Assist	2.174

### A.2.3.1 ADVENTS Launch Vehicle Analysis

With the transfer trajectory flyby sequence selected, an exhaustive launch date search was conducted. The launch period for this study was defined by the requirement to launch within the next Planetary Decadal timeline window of 2036–2040 for New Frontiers 6 (**Figure A-15**). At the end of the study, the release of the New Frontiers 5 request for proposal was delayed. This delay provides an opportunity for ADVENTS to be part of New Frontiers 5 with launch dates as early as 2030. **Figure A-16** shows the full range of launch opportunities from 2030–2040. Launch dates with delta-V equivalent to the primary and backup launch dates are found on December 9, 2030 and June 5, 2031 respectively. The launch trajectories for 2030 and 2031 are expected to have similar eclipses and communication links allowing science operations for the earlier launch opportunity to be identical to the launch dates in 2039. The primary and backup launch dates discussed in the rest of the study report are for 2039.

The mission design requires a primary and backup launch opportunities that have a launch window of at least 14 days. With the objective of reducing the required propellant as much as possible the range between May to December, 2039 was selected. **Figure A-17** outlines the aforementioned period with a cap for solutions that require more than 2.2 km/s. Two groups of solutions results from this selection, mid 2039 and late 2039. **Table A-10** presents the details of the same range.

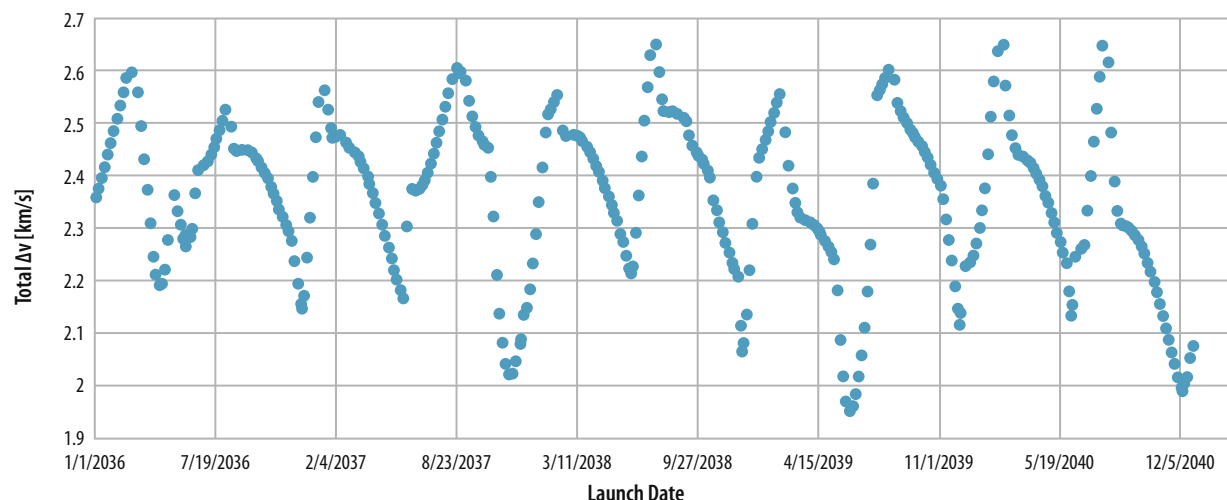


**Figure A-15:** ADVENTS launch opportunities 2036-2040.

VS016

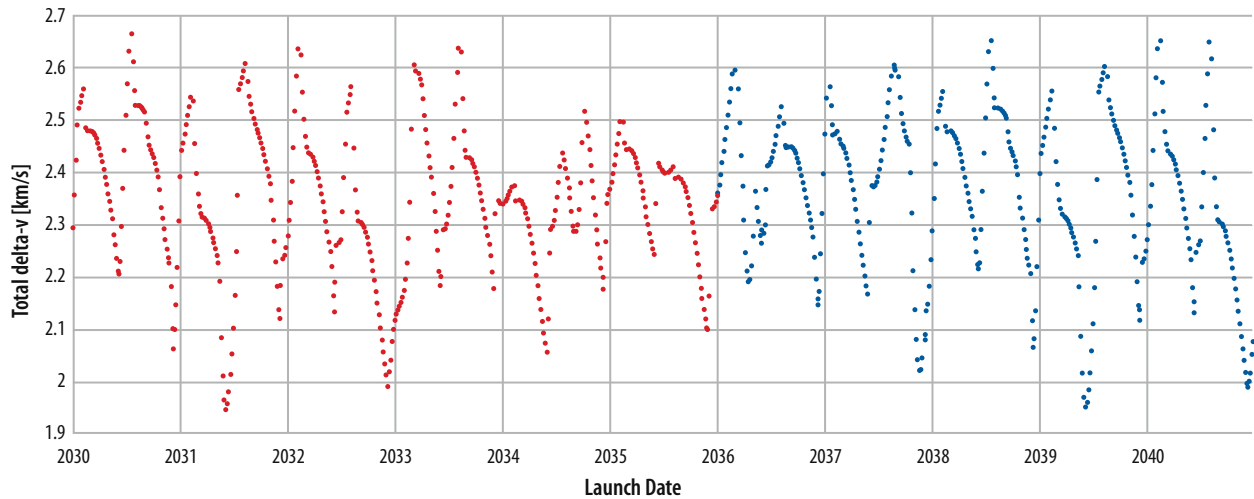


Figure A-16: ADVENTS launch opportunities 2030-2040.

VS017

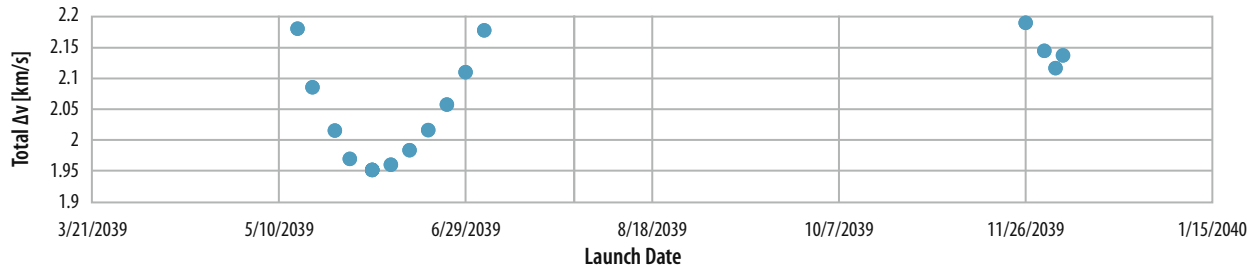


Figure A-17: ADVENTS 2039 Delta-v solutions.

VS018

Table A-10: ADVENTS 2039 Delta-v solutions.

Launch Date	C3 [km <sup>2</sup> /s <sup>2</sup> ]	Launch Declination [deg]	Flyby Date	Flyby Velocity [km/s]	Total Delta-v [km/s]	Flight Time [years]	SOI Interface Velocity [km/s]	Orbit Insertion Date
5/15/2039	15.48	-28.50	9/24/2039	3.91	2.18	3.97	2.02	5/3/2043
5/19/2039	14.61	-25.35	9/27/2039	3.54	2.09	3.97	1.96	5/9/2043
5/25/2039	13.97	-21.39	10/1/2039	3.23	2.02	3.98	1.96	5/17/2043
6/29/2039	30.98	9.93	10/4/2039	3.65	2.11	3.88	1.96	5/15/2043
7/4/2039	39.05	11.39	10/4/2039	3.92	2.18	3.86	1.96	5/12/2043
5/29/2039	13.52	-16.35	10/5/2039	3.01	1.97	3.98	1.96	5/23/2043
6/24/2039	24.88	8.01	10/5/2039	3.42	2.06	3.90	1.96	5/18/2043
6/19/2039	20.24	5.44	10/6/2039	3.24	2.02	3.92	1.95	5/21/2043
6/4/2039	13.43	-9.96	10/7/2039	2.92	1.95	3.98	1.95	5/27/2043
6/4/2039	13.48	-9.10	10/7/2039	2.92	1.95	3.98	1.95	5/27/2043
6/14/2039	16.77	1.87	10/7/2039	3.08	1.98	3.94	1.95	5/23/2043
6/9/2039	14.43	-3.22	10/8/2039	2.97	1.96	3.96	1.95	5/26/2043
11/6/2039	12.15576	28.50	12/25/2041	2.82	2.14	2.90	2.00	10/28/2042
11/26/2039	12.41943	20.08	12/27/2041	2.97	2.19	2.92	1.90	10/28/2042
12/1/2039	12.23027	24.76	12/28/2041	2.84	2.14	2.92	1.98	10/31/2042
12/4/2039	12.26637	28.50	12/28/2041	2.77	2.12	2.91	2.03	11/1/2042

The variation of total Delta-v in the entire selected period is ~10%, which will be carried as margin. The primary launch date is selected for the lowest Delta-v solution in the first group June 4, 2039.

The backup launch date is selected for the lowest Delta-v solution in the second group December 4, 2039. Both launch dates are separated by 6 months, which is also desired from a mission development point of view. The cases shown in **Table A-9** were simulated without the aerobot deployment. When we included the aerobot deployment in the final analysis, the Venus Orbit Insertion (VOI) dates shown in **Table A-10** changed a bit because of the targeting maneuver. For example, the 12/4/2039 launch dates VOI date moved from 11/1/2042 as shown in the table to 11/15/2042.

### A.2.3.2 Primary Launch Opportunity

The primary launch opportunity of June 4, 2039 and its associated trajectory are shown in **Figure A-18**. **Table A-11** shows the key dates for the primary launch opportunity.

**Table A-11:** ADVENTS Primary Launch trajectory key dates.

Event	Epoch
Launch date open	June 4, 2039
Venus flyby	October 7, 2039
Venus arrival	May 20, 2043
VOI	May 27, 2043

### A.2.3.3 ADVENTS Design Point

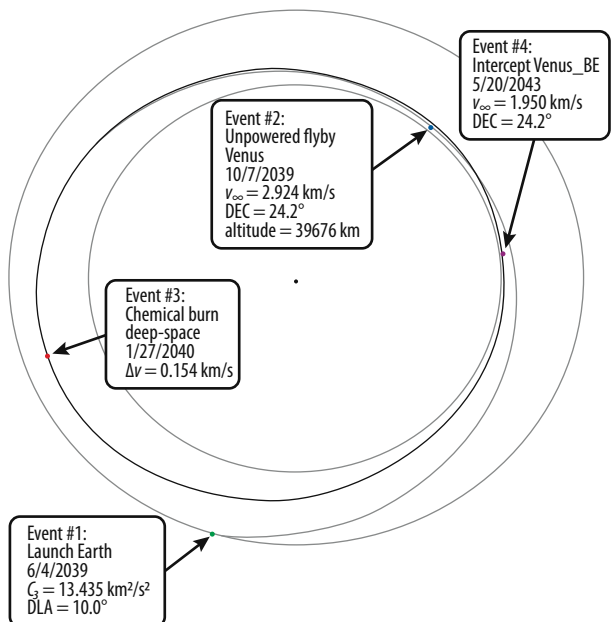
The Orbiter and propellant budget are designed to be compatible with both launch opportunities. In order to ensure such compatibility, the ADVENTS design point is selected based on the more stringent case, which in this case is the backup launch opportunity, December 4 2039, since it has the highest total Delta-v. Furthermore, a 10% propellant margin is added. **Figure A-19** shows the December 4 trajectory solution, now selected as the ADVENTS design point. Trajectory key dates are outlined in **Table A-12**.

**Table A-12:** ADVENTS design point trajectory key dates.

Event	Epoch
Launch date open	December 4, 2039
Venus flyby	December 28, 2041
Venus arrival	November 7, 2042
VOI	November 15, 2042

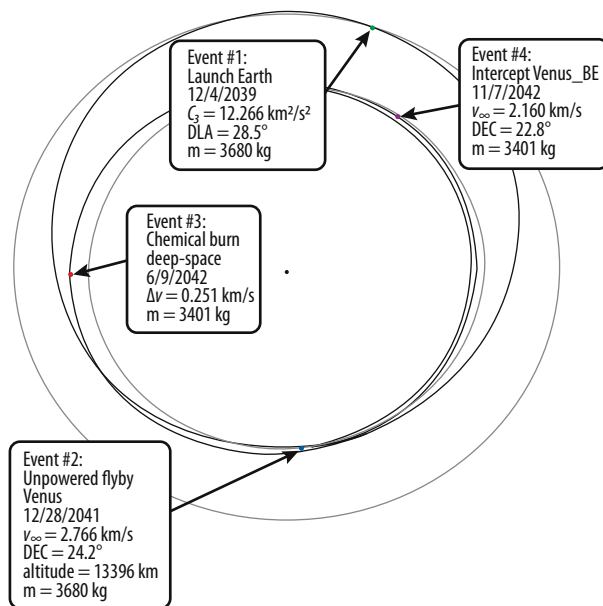
The launch mass with its corresponding launch  $C_3$  is presented in **Figure A-19**. **Figure A-20** shows the various launchers that can provide the required mass  $C_3$  launch characteristic. As previously indicated, the Falcon Heavy was selected as the primary launch vehicle.

ADVENTS Delta-v budget is then sized as shown in **Table A-13**. The mission propulsion budget adds an additional 10% margin over the sub-total Delta-v for each configuration.



VS019

**Figure A-18:** ADVENTS Primary Launch Opportunity Trajectory.



VS020

**Figure A-19:** ADVENTS design point trajectory.

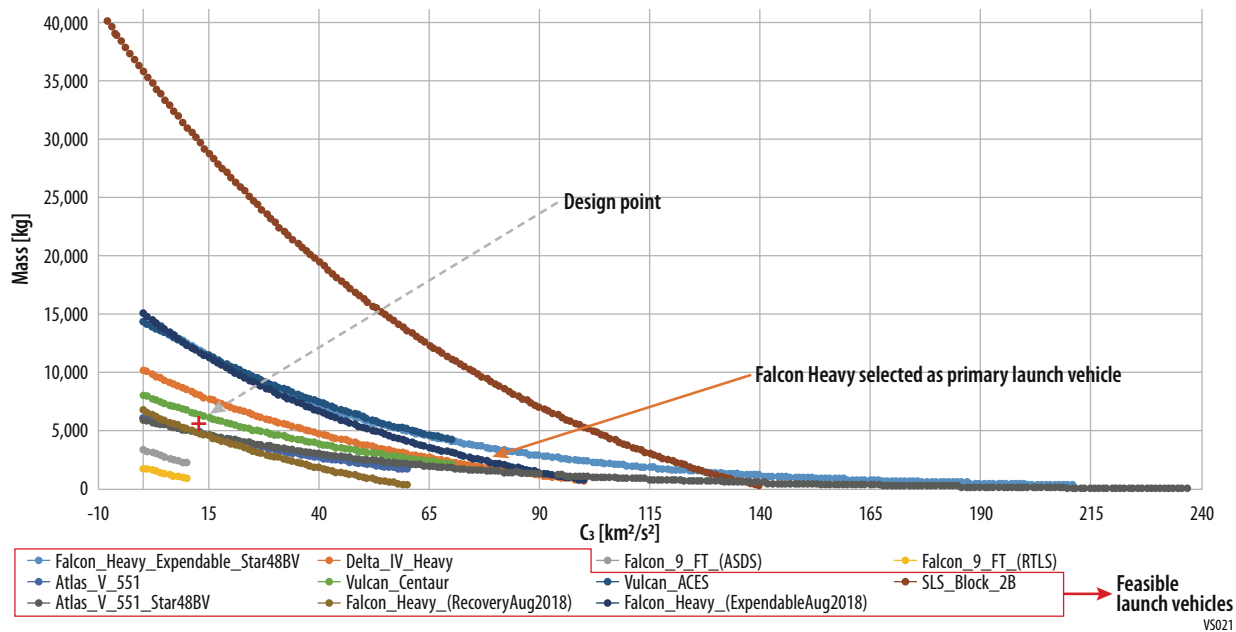


Figure A-20: VEMC launch vehicle selection.

Table A-13: Design point Delta-v budget.

Configuration	Maneuver	Delta-V [m/s]
Orbiter + Aerobot	DSM	251.0
	TCM1	10.0
	TCM2	2.0
	Station Keeping/Mom Dumps/Dispersion	--
	<b>Sub Total:</b>	<b>263.0</b>
Orbiter	TCM3	20.0
	TCM4	5.0
	Direct Capture	1876.0
	Station Keeping/Mom Dumps/Dispersion	--
	<b>Sub Total:</b>	<b>1901.0</b>
	<b>Grand Total:</b>	<b>2164.0</b>

For the same solution, the minimum Venus altitude at the flyby is 6,000 km (above the surface). Orbiter distance during flyby is illustrated in Figure A-21. In the figure, elapsed time is measured from and to the Venus sphere of influence.

Finally, the Venus Orbit Insertion (VOI), as a mission critical event, is required to be observable from Earth. Figure A-22 shows that the Orbiter is fully visible from SOI to VOI from the NASA Deep Space Network (DSN) stations, Robledo, Tidbindilla, and Goldstone respectively. The total duration inside the Venusian SOI is about 7 hours with capture occurring at 15:37:08.754 Venus local time, as indicated in Figure A-22.

For insertion into the science orbit after the interplanetary transfer, a direct insertion solution was compared to a 2-ellipse transfer solution. In the general 2-ellipse transfer solution, the Orbiter enters the sphere of influence of Venus in a hyperbolic orbit with the prescribed velocity. At the periapse of the hyperbola, a 1<sup>st</sup> Delta-v maneuver is performed to insert into a capture ellipse of variable apoapse altitude. At the apoapsis of the capture ellipse, a 2<sup>nd</sup> Delta-v maneuver is performed to raise the periapse to match the altitude of the desired science orbit. At the periapse, a 3<sup>rd</sup> Delta-v maneuver is performed to circularize the orbit and achieve the final desired science orbit. The cost of the full insertion is then the sum of the 1<sup>st</sup>, 2<sup>nd</sup>, and 3<sup>rd</sup> maneuvers, with the altitude of the capture ellipse being the primary free variable. Upon inspection, the minimum solution occurs for a capture periapse equal to

the desired science orbit altitude, as this negates the need for a 2<sup>nd</sup> maneuver for apoapse raising. Given the prescribed hyperbolic velocity at the sphere of influence and the desired science orbit altitude, the minimum possible Delta-v required for the 2-ellipse transfer was greater than the Delta-v required for the direct insertion—thus, the direct insertion is the chosen method.

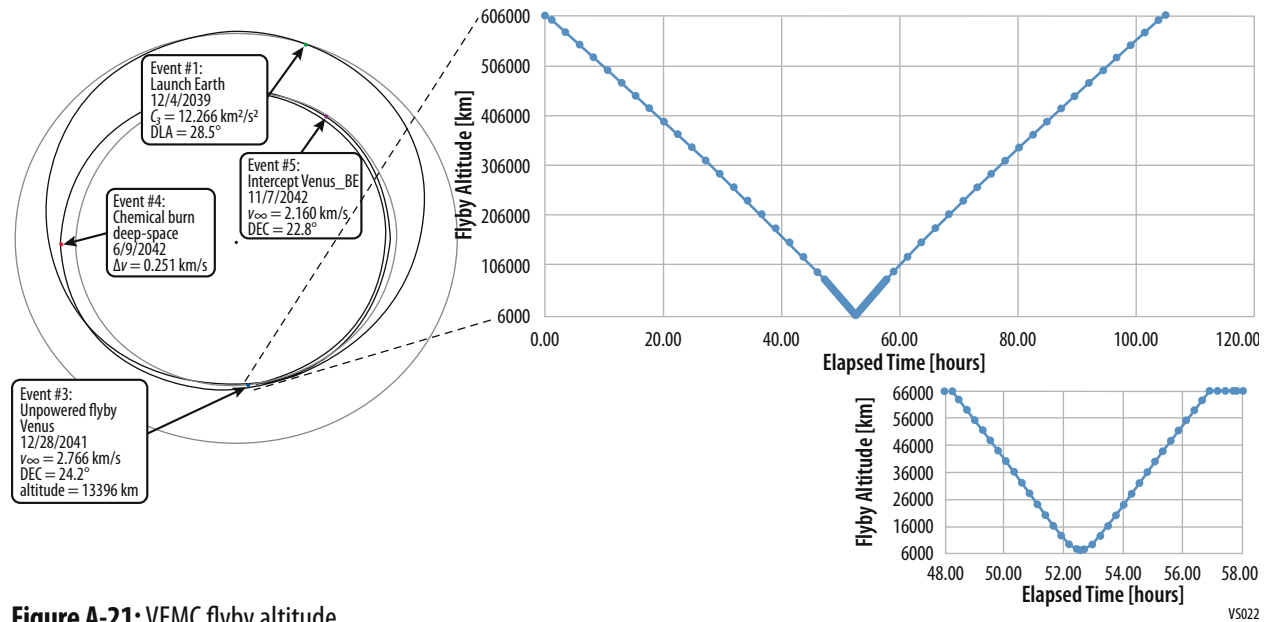


Figure A-21: VEMC flyby altitude.

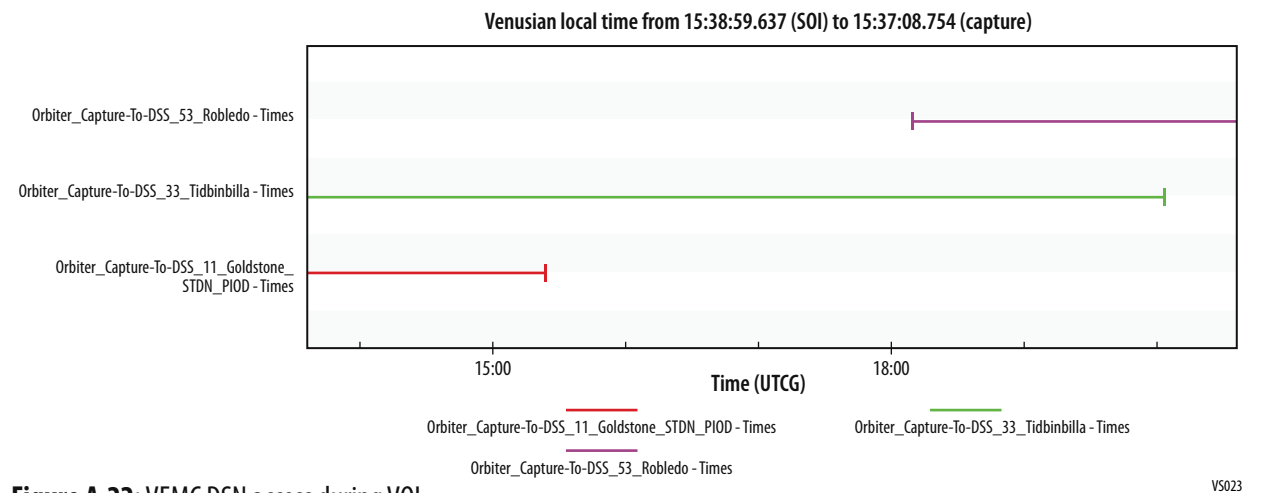


Figure A-22: VEMC DSN access during VOI.

### A.2.3.4 Aerobot Entry Analysis

The deep space maneuver (DSM) during the heliocentric phase targets the Orbiter to the Aerobot entry (AE) defined as 175 km above the Venus surface also referred to Venus atmospheric entry interface. The events timeline post-DSM is outlined in **Table A-14**, with the sequence starting at 30 days prior to AE until AE. In this sequence, the Orbiter-Aerobot separation takes place AE-5.5 days.

Table A-14: Aerobot deployment timeline.

OD for at least 20 days after the DSM	AE-30 days
Aerobot entry targeting TCM1 (~10 m/s)	AE-10 days
4 days to update OD, plan, command TCM2	

Aerobot entry targeting TCM2 (~2 m/s)	AE-6 days
Aerobot spin up and separation (~1 m/s)	AE-5.5 days
Orbiter VOI targeting maneuver TCM3 (~20 m/s)	AE-5 days
3 days to update OD, plan, command TCM4	
Orbiter VOI targeting TCM4 (~5 m/s)	AE-2 days
<b>Aerobot entry (AE)</b>	<b>AE+0 days</b>

The Aerobot's entry conditions are summarized in **Table A-15**. Entry begins at an altitude of 175 km with a downward flight-path angle of 8°. The entry latitude was set to 0° to maximize the contact time with the Orbiter during science operations. The Aerobot entry occurs within minutes from the Orbiter insertion maneuver. The Aerobot like the Orbiter is in view of Earth during its entry and descent. Due to the power of the Aerobot transmitter it is not expected that the 34m DSN antennas will be able to obtain a communication link with the Aerobot. The Aerobot communicates directly with the Orbiter during its entry and descent and has 4 (1 hour entry and descent plus 3 initial float) hours of contact during the first Earth day after its entry while in the Venusian sunlight (**Figure A-29**). Additional contacts are available with the Orbiter every 12 Earth hours.

**Table A-15:** Aerobot's entry conditions at ED. (Venus-centered ICRF).

Epoch [TDB Gregorian]	Entry velocity [km/s]	Flight-path angle [deg]	Azimuth [deg]	Latitude [deg]	Longitude [deg]	Local Time [UTC]
15 Nov 2042 09:20:02.294	10.45	-8.85	-70	0	113	03:24:25.994

The Aerobot-Orbiter relative distance from deployment to EDL is given in **Figure A-23**. The maximum relative distance is approximately 30,000 kilometers. The actual separation occurs 5.5 days before EDL. The Aerobot and Orbiter trajectories are depicted in **Figure A-24**.

### A.2.3.5 Science Orbit Operations Analysis

The parameters used for the Science Orbit analysis are presented in **Table A-16**. The dry mass value was chosen for the solar radiation pressure (SRP) model as it is conservative for the key area/mass ratio. Additionally, the value of effective SRP area was selected as a conservatively high estimate for the area/mass ratio.

**Table A-16:** Orbital and dynamical parameters considered for the analysis of Science Orbit operations.

Orbit	
Semi-major axis	24,856.2 km (0.5-day period)
Inclination	170°
Eccentricity	0 (circular)
Gravity model	
Bodies considered	Venus (10x10), Sun (point mass)
SRP model (cannon ball)	
Mass	1,507.8 kg
Area	10 m <sup>2</sup>

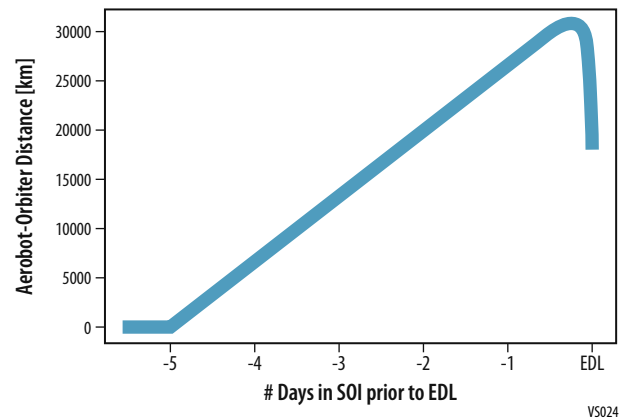


**Figure A-23:** Aerobot-Orbiter relative distance from deployment to EDL.

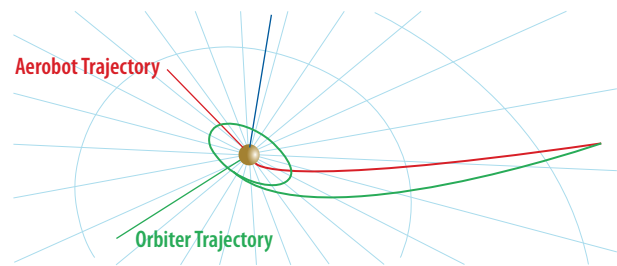
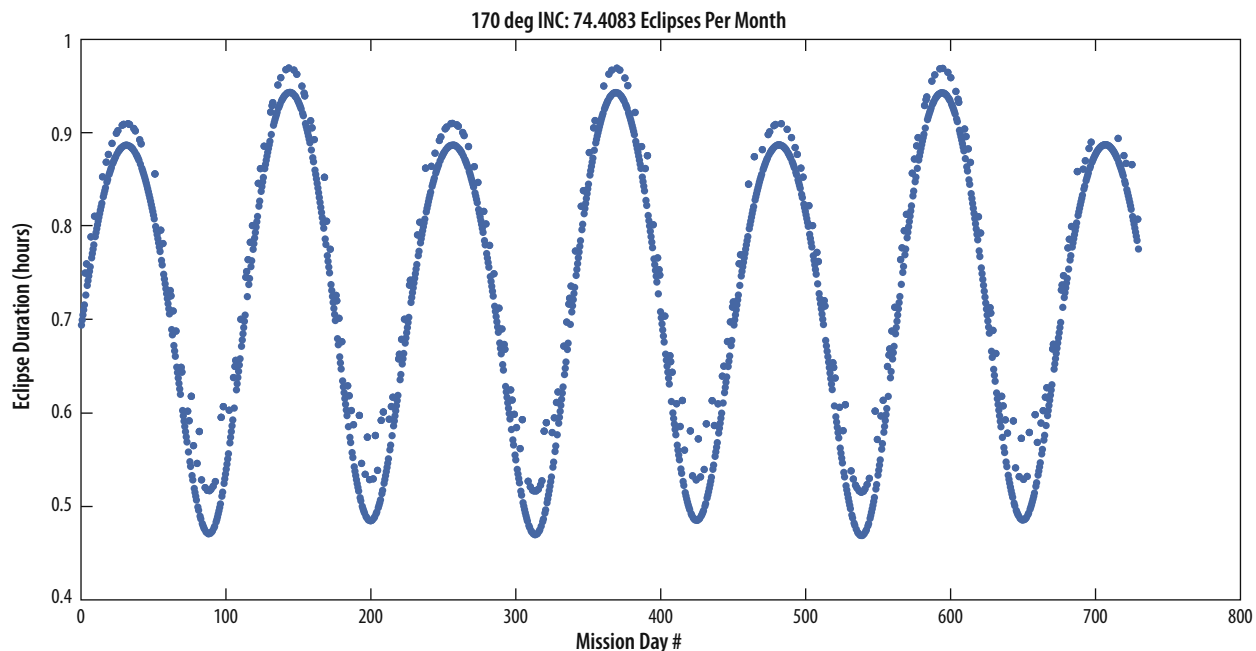


**Figure A-24:** Aerobot and Orbiter, trajectories from separation to EDL (Venus-centered ICRF).

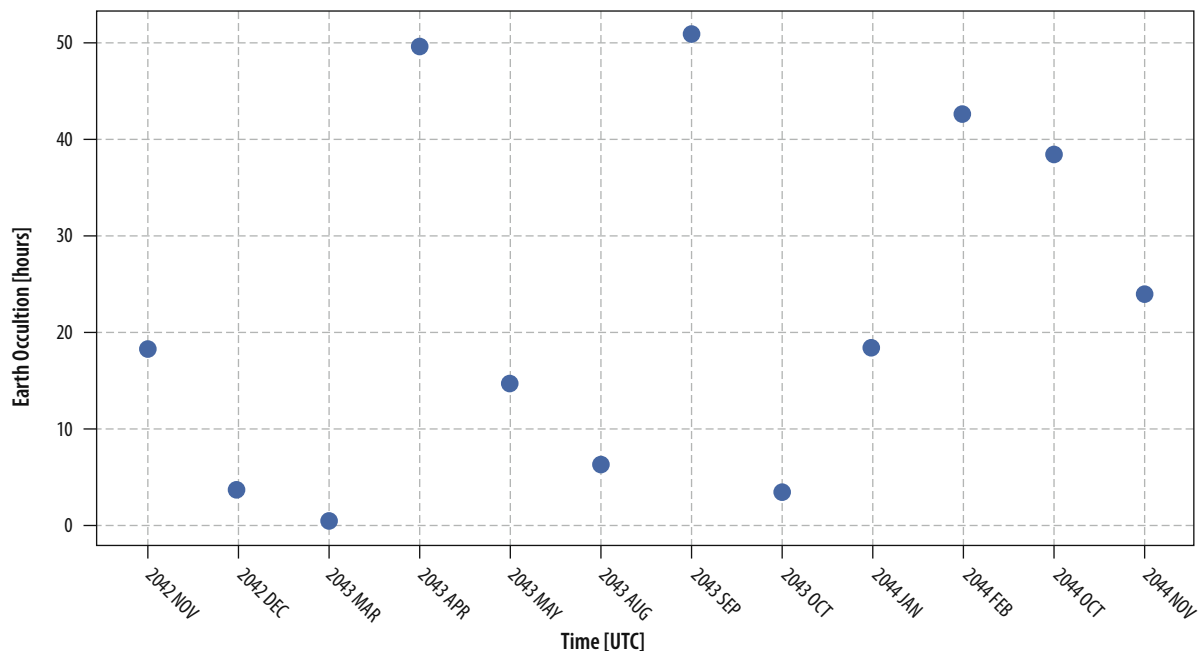
The durations of solar eclipses with respect to the Aerobot over the course of the 2-year mission are shown in **Figure A-25**. The average time between two eclipses is 11.3 hours, with eclipse durations ranging between 28 minutes and 58 minutes. Eclipses occur on average 51.9 times per Earth month, or on average 1.9 times per Earth day, due to the half-day period of the orbit.



VS026

**Figure A-25:** Science Orbit's solar eclipse durations over the course of a 2 year mission.

The cumulative times per month with no visibility between the Earth and Orbiter during the Science Orbit are given in **Figure A-26**. Periods with no visibility are sparse due to the inclination of the orbit. The longest cumulative period is 51 hours in a single month.



VS027

**Figure A-26:** Earth-Orbiter cumulative occultation time per month for the Science Orbit.

The Earth-Science Orbit distance over the course of several years is provided in **Figure A-27**. The distance from the Earth ranges from 0.25 AU to 1.75 AU over a 2-year period.

The communication link concept between the Orbiter and the Aerobot is outlined in **Figure A-28**. The inter-visibility constraints are given as the angle range from 120° to 150° as measured from the nadir vector. The region in 120° to 90° is considered poor for communications due to atmospheric

losses. The region from 150° to 180° is assumed to be obscured by the body of the Aerobot. This leaves a narrow 30° toroid around the Aerobot in which the Orbiter considered “visible” to the Aerobot for communications.

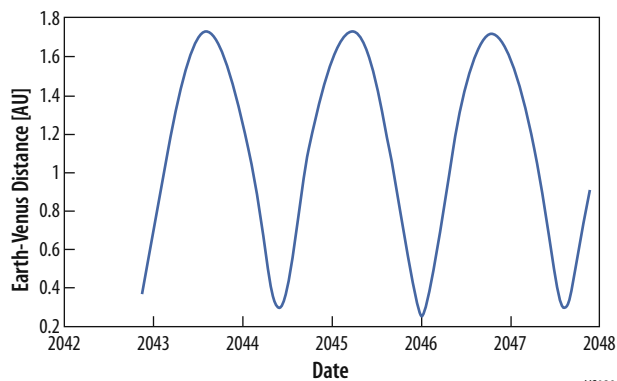


**Figure A-27:** Earth communication distance during science orbit.

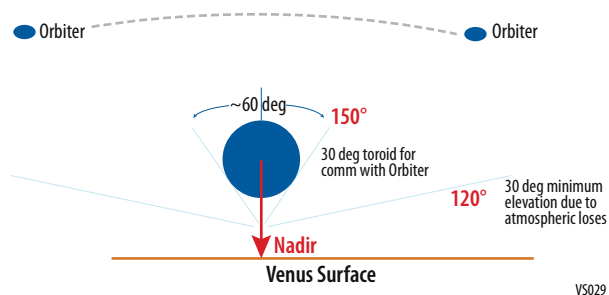


**Figure A-28:** Visualization of the Orbiter-Aerobot communication link and regions of possible communication.

The implemented strategy to extend possible communication periods consists of choosing an Orbiter’s initial orbital elements, primarily true anomaly, such that the phasing between Orbiter visibility and “daylight” periods results in sufficient communication periods specifically during daylight periods.

Several latitude values for the Aerobot entry were studied to determine the worst case number of hours per day with communication available over the possible ranges of latitude that the Aerobot may drift over during the course of a circumnavigation. Such values were 0, ±15, and ±45°, assuming a 7-day circumnavigation period for the Aerobot. **Figure A-29** through **Figure A-33** show the results of these case; yellow regions indicate the daylight periods of each Venusian day.

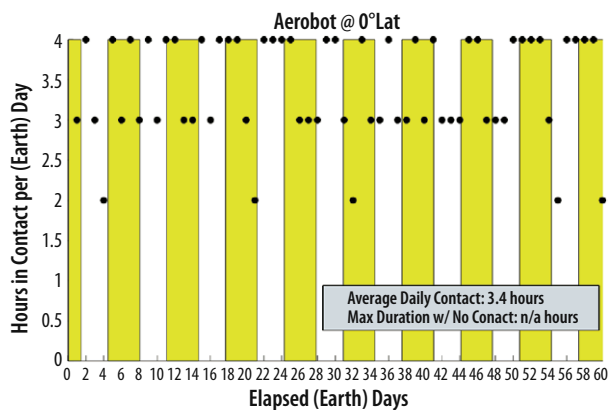


**Figure A-29:** Hours of possible communications contact between the Orbiter and Aerobot per (Earth) day for an Aerobot at 0° latitude. Yellow bars indicate daylight periods.

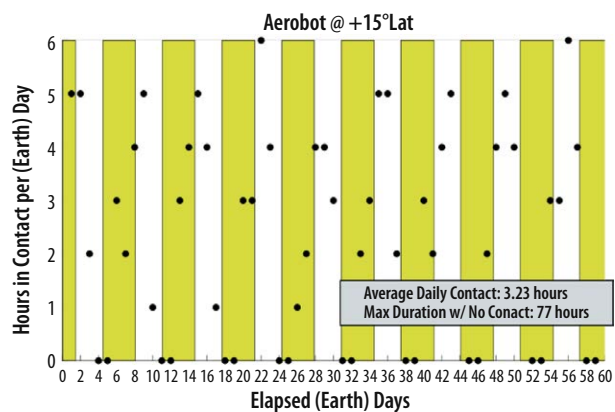


**Figure A-30:** Hours of possible communications contact between the Orbiter and Aerobot per (Earth) day for an Aerobot at 15° latitude. Yellow bars indicate daylight periods.

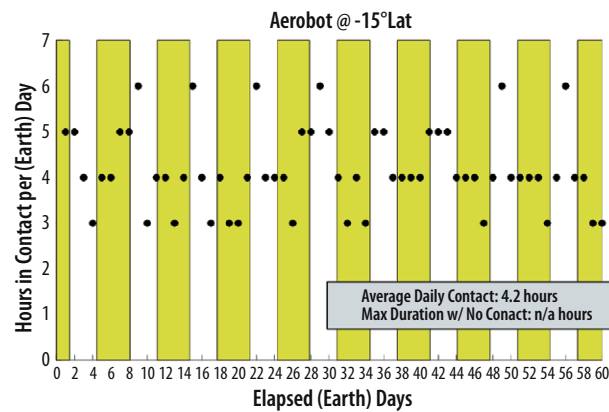
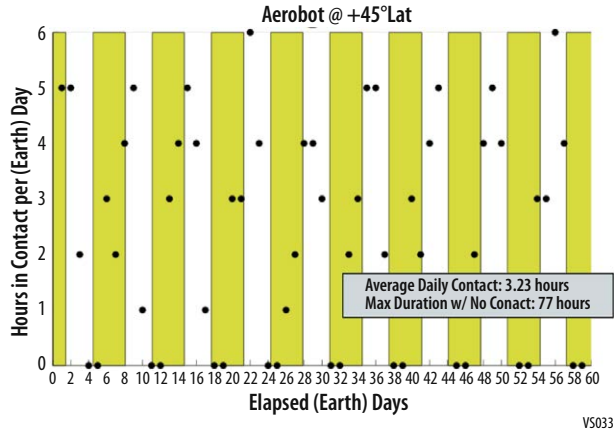
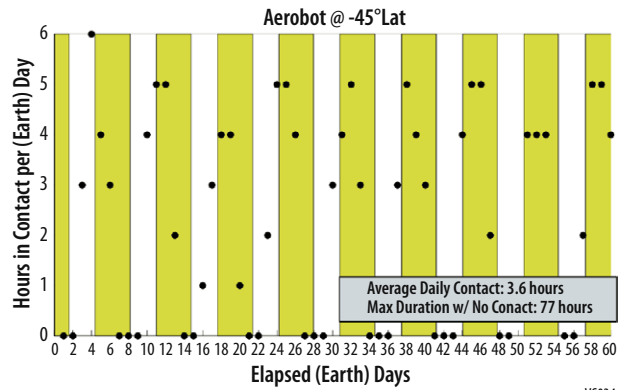


**Figure A-31:** Hours of possible communications contact between the Orbiter and Aerobot per (Earth) day for an Aerobot at -15° latitude. Yellow bars indicate daylight periods.





VS033



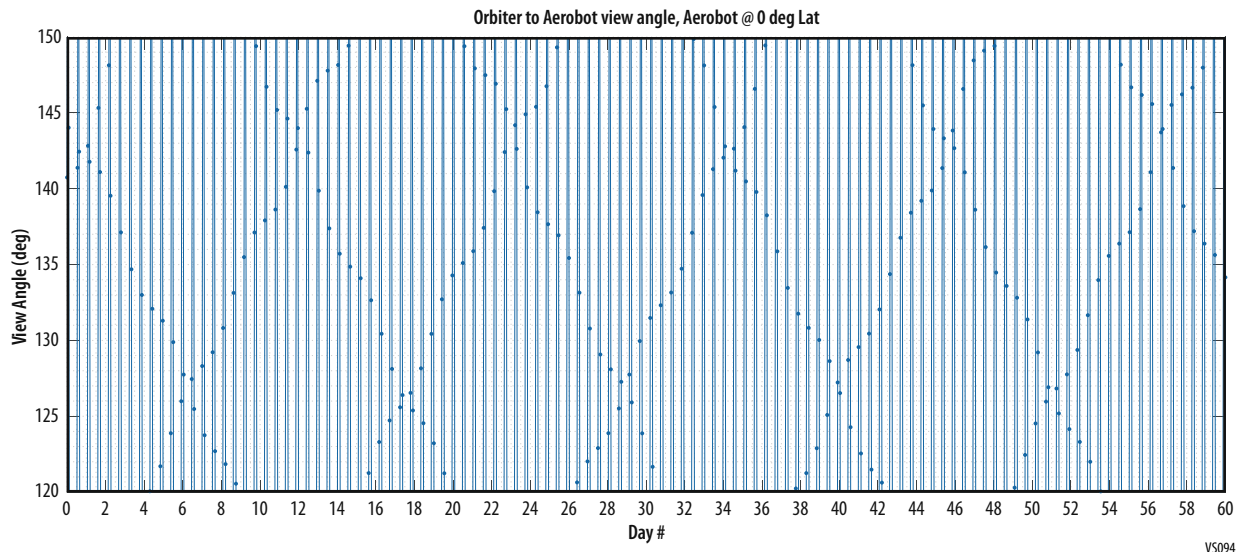
VS034

**Figure A-32:** Hours of possible communications contact between the Orbiter and Aerobot per (Earth) day for an Aerobot at 45° latitude. Yellow bars indicate daylight periods.

**Figure A-33:** Hours of possible communications contact between the Orbiter and Aerobot per (Earth) day for an Aerobot at -45° latitude. Yellow bars indicate daylight periods.

For each latitude case representing the full range of Aerobot drift, daily contact of more than 4 hours during the daylight is achieved. For each latitude analyzed it is assumed that the Aerobot remains at that latitude for the full mission duration. This results in the worst case maximum duration without a contact of 77 hours for latitudes of +15°, +45° and -45° due to the geometry of the Orbiter's orbit and the Aerobots view angle restrictions. The view angles for each latitude case are shown in **Figure A-34** through **Figure A-38**. In reality, the Aerobot will change latitude due to winds. It is expected, that there will be at least one contact each day at any given latitude.

The Venus ground coverage seen by the Orbiter as a function of latitude is shown in **Figure A-39**. This figure assumes a single-conic sensor with a 22.5° aperture (half angle), viewing from the nominal half-day period inclined orbit described in **Table A-16**.



VS094

**Figure A-34:** Orbiter to Aerobot view angle, Aerobot @ 0° Lat.

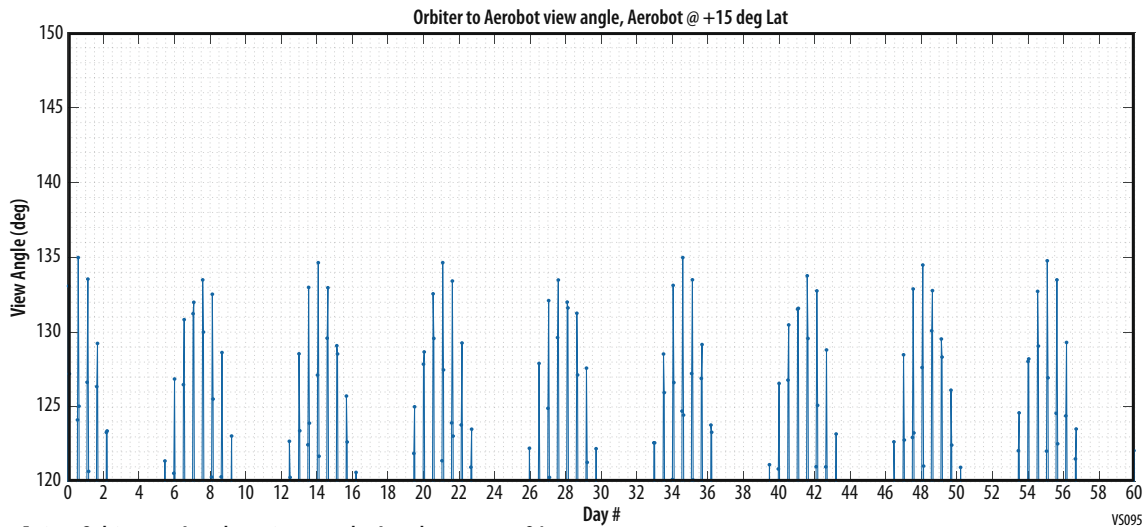


Figure A-35: Orbiter to Aerobot view angle, Aerobot @ +15° Lat

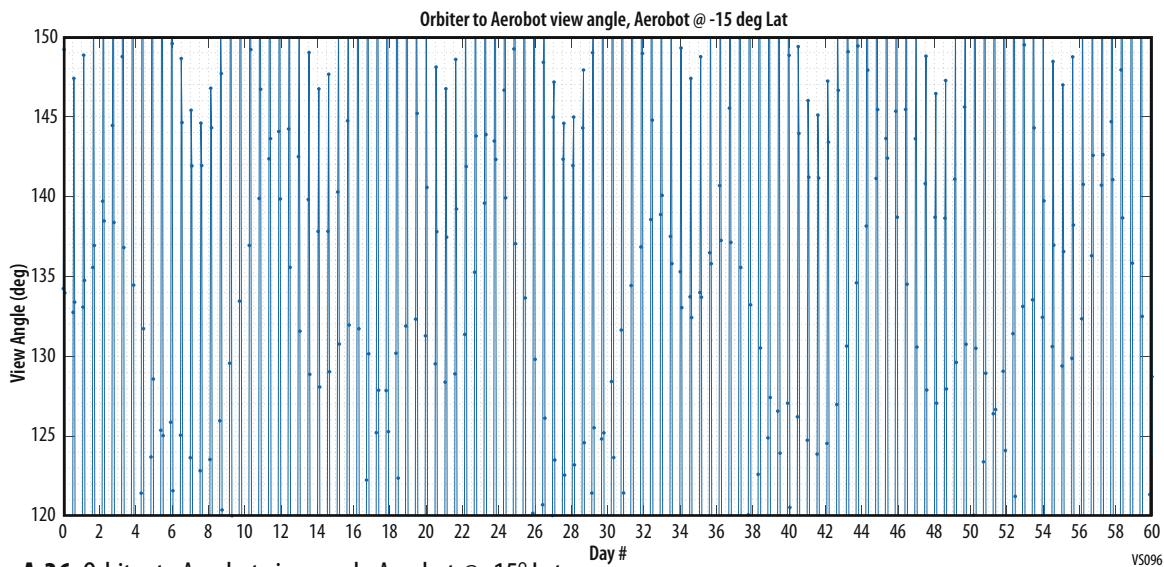


Figure A-36: Orbiter to Aerobot view angle, Aerobot @ -15° Lat.

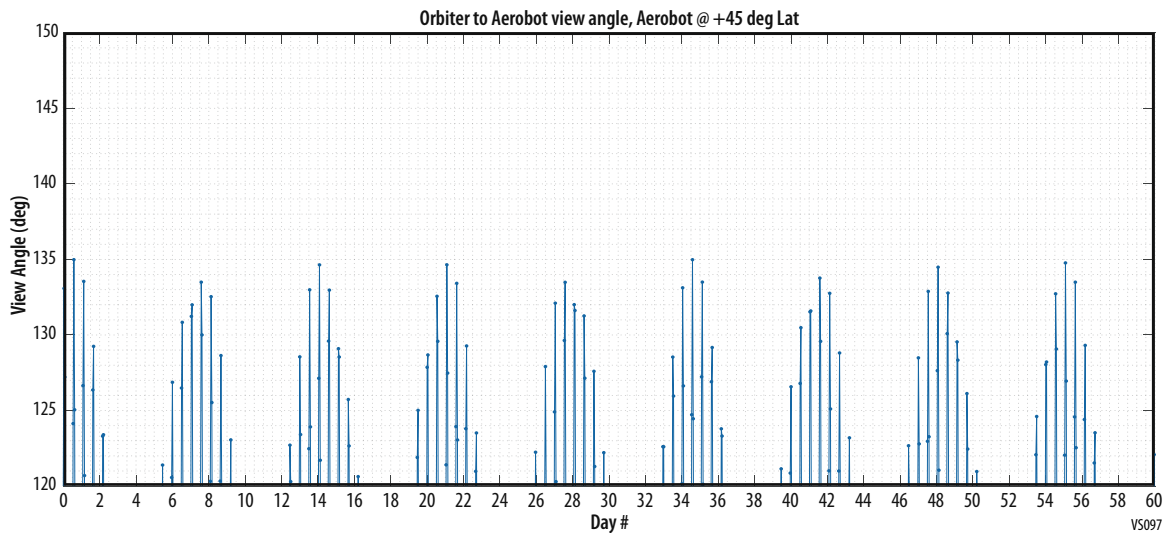


Figure A-37: Orbiter to Aerobot view angle, Aerobot @ +45° Lat.

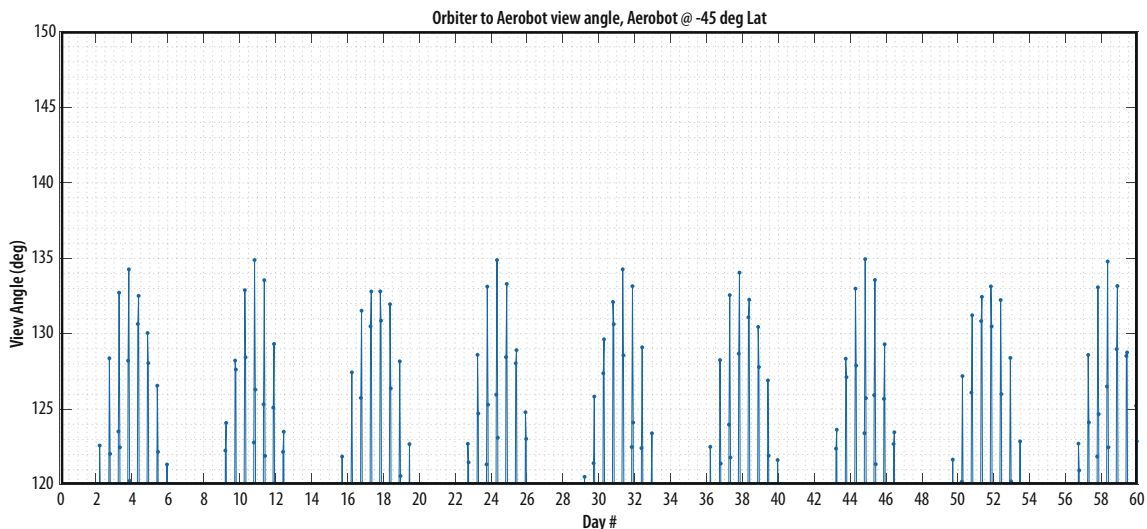


Figure A-38: Orbiter to Aerobot view angle, Aerobot @ -45° Lat.

VS098

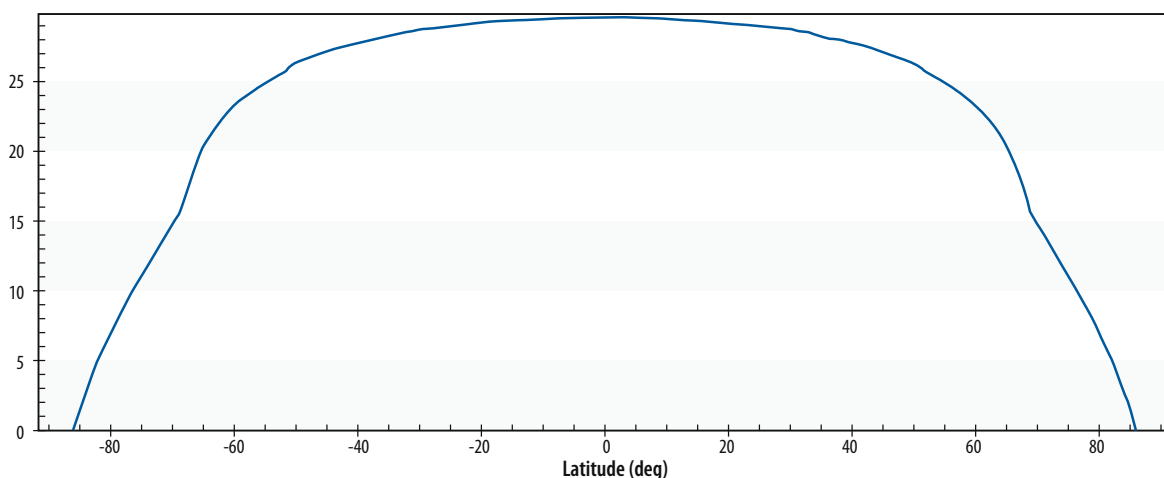


Figure A-39: Venus ground coverage provided by the Orbiter, as a function of latitude.

VS035

## A.2.4 Concept of Operations

ADVENTS operations are broken up into four phases (**Table A-17**). The first is Launch and Cruise to Venus followed by Entry and Descent, Aerobot operations and Orbiter science operation.

**Table A-17:** Mission Operations and Ground Data Systems.

Down link Information	Launch and Cruise to Earth	Entry and Descent Drogsonde to Orbiter	Aerobot to Orbiter	Venus Orbiter to Earth
Number of Contacts per Week	1	1	7	7
Number of Weeks for Mission Phase, weeks	191	1 hour	8	113
Downlink Frequency Band, GHz	HGA 32 MGA LGA 2.1	2.1	2.1	HGA 32 LGA 2.1
Orbiter Antenna Telemetry Data Rate(s), kbps	HGA min 1,030 HGA max 42,700 MGA min 1.2 LGA min 0.04	MGA 0.01 HGA 2.23	LGA min 0.01 MGA min 0.033 HGA 8.9	HGA min 1,030 HGA max 42,700 MGA min 1.2 LGA min 0.04
Transmitting Antenna Type(s) and Gain(s), DBi	HGA 47.05 MGA 22.0 LGAs 7.4	MGA 5.0	Toroid 0 gain	HGA min 1,030 HGA max 42,700 MGA min 1.2 LGA min 0.04

Down link Information	Launch and Cruise to Earth	Entry and Descent Dropsonde to Orbiter	Aerobot to Orbiter	Venus Orbiter to Earth
Transmitter peak power, Watts	200	20	20	200
Downlink Receiving Antenna Gain, DBi	79.0	35.0	35.0	79.0
Transmitting Power Amplifier Output, Watts	100	10	10	100
Total Daily Data Volume, (MB/day)	1	24	128	14,400
Uplink Information				
Number of Uplinks per Week	1	1	7	7
Uplink Frequency Band, GHz	34.3	N/A	2.1	
Telecommand Data Rate, kbps	>2,000	N/A	14.5	>2,000
Receiving Antenna Type(s) and Gain(s), DBi	HGA 58.7	N/A	HGA 58.7	HGA 58.7

#### A.2.4.1 Launch and Cruise to Venus

ADVENTS launches from Cape Canaveral, Florida on a single Falcon Heavy vehicle with 5m fairing. The primary launch opportunity is June 4, 2039 with a backup launch opportunity of December 4, 2039. Both launch opportunities have a minimum of a 14-day launch window. The launch and cruise timeline is shown in **Table A-18**. During cruise, the Orbiter will primarily be in a low power mode with only essential systems on. The communication subsystem will be in receive mode, except for once a day to transmit health and status, perform ranging with DSN and receive any necessary updates from the ground. Just prior to the Venus flyby, the Orbiter will enter a science mode for calibration of its instruments and to take measurements during the flyby. Ten days prior to Aerobot entry, the Orbiter will perform the first Aerobot entry targeting trajectory correction maneuver (TCM1) to orient the Aerobot for its entry trajectory. Additional Aerobot entry targeting TCM's are planned as shown in **Table A-18**. The Orbiter will spin up and release the Aerobot 5.5 days prior to the desired Aerobot entry. After Aerobot separation, the Orbiter will maintain daily contact with the Aerobot communication beacon to monitor its trajectory.

**Table A-18:** Mission Launch and Cruise timeline.

Date	Event
06/4/2039	Launch
10/7/2039	Venus Flyby
05/17/2043	Aerobot Entry Targeting TCM1
05/21/2043	Aerobot Entry Targeting TCM2
05/21/2043	Aerobot Separation
05/22/2043	Orbiter VOI Targeting TCM3
05/25/2043	Orbiter VOI Targeting TCM4
05/27/2043	Aerobot Entry
05/27/2043	VOI

#### A.2.4.2 Aerobot Operations

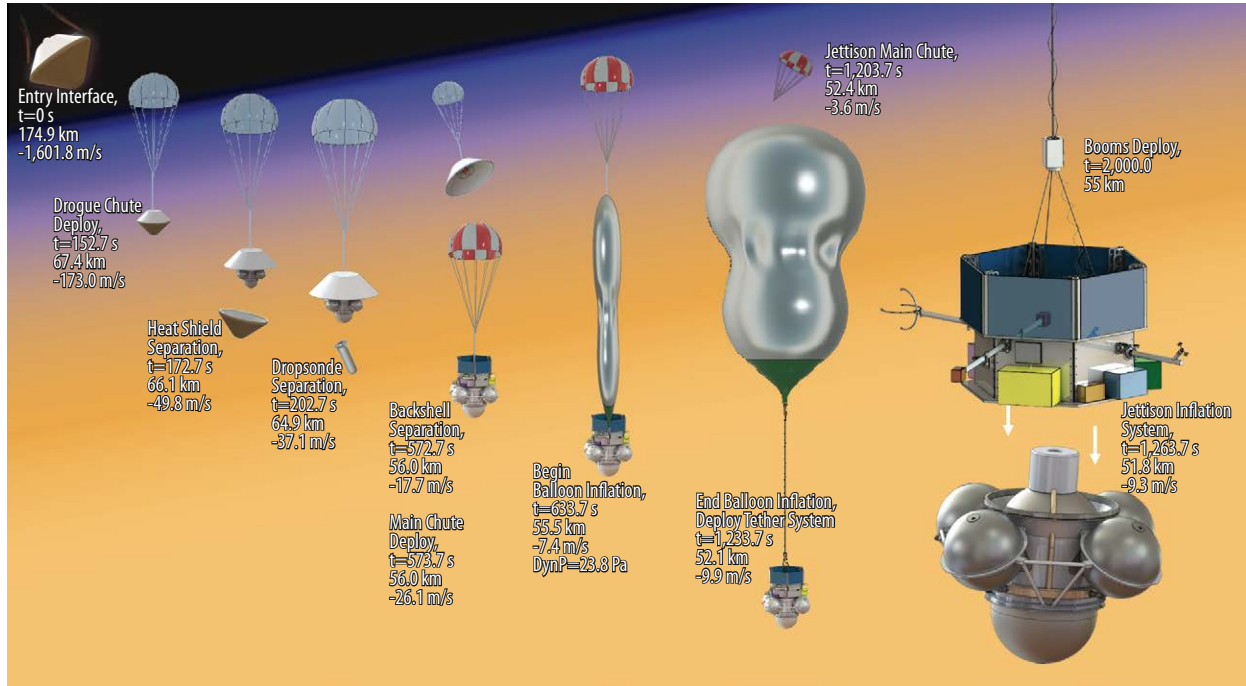
Aerobot operations are divided into three phases. The first is the 5.5 day cruise while inside the entry vehicle after separation from the Orbiter to the entry point in the Venus atmosphere. The second is the Entry and descent phase. The final phase is the 60-day float.

##### A.2.4.2.1 Five and a Half Day Cruise

After separation from the Orbiter the Aerobot turns on its communication beacon system that is attached to the backshell of the entry vehicle. All other subsystems on the Aerobot remain off until the entry point is reached.

##### A.2.4.2.2 Entry and Descent

Five and a half days after release by the Orbiter, the Aerobot enters the Venusian atmosphere on November 15, 2042 at 3:24pm Venus local time and begins the Entry, Descent and Float (EDF) sequence shown in **Figure A-40**.



VS036

**Figure A-40:** Aerobot Entry and Descent timeline.

The communication beacon remains active through backshell separation at entry plus 232.7 seconds. There is an expected gap in communication from backshell separation until the antennas are deployed at entry plus 2,000 seconds at the nominal float altitude of 55 km.

The Aerobot like the Orbiter is in view of Earth during its entry and descent. Both the Orbiter and Aerobot are in view of Earth during VOI and entry and descent respectively. Due to the power of the Aerobot transmitter, it is not expected that the 34m DSN antennas will be able to obtain a communication link with the Aerobot. Using the 70m DSN the Aerobot is able to downlink 260 bps (at Entry the Earth is at the minimum range of 39,671,122 see **Table A-34** for maximum range capability). For nominal operations the Aerobot communicates directly with the Orbiter during its entry and descent and has 4 hours of contact during the first Earth day after its entry while in the Venusian sunlight (**Figure A-30**). Additional contacts are available with the Orbiter every 12 Earth hours with one planned 10-minute opportunity (up to 4 hours are available as shown in **Figure A-30**) occurring 12 hours after initial float prior to the Venusian night.

The dropsonde is released at 202.7 seconds and begins transmitting to the Orbiter. The dropsonde will take no longer than 1 hour to reach the surface.

Balloon inflation begins at 55.5 km and ends at 52.1 km as shown in **Figure A-40**. The 7.4 m/s descent speed at this altitude provides a 23.8 Pa dynamic pressure on the balloon which meets the requirement to limit dynamic pressure at the start of balloon inflation to less than 25 Pa.

Once the Aerobot is fully deployed after atmospheric descent, the Aerobot altitude will be set to a nominal 55 km altitude, where the temperature is about 20 °C. Carried by ambient winds, the Aerobot will circumnavigate Venus every 7 days, on average. The instruments will begin their checkout procedures as shown by the red bars in **Figure A-41** and enter a standby state beginning at entry plus 2,000 seconds. Two instruments (blue bars in the figure), the magnetometer and the pressure sensors in the meteorological suite, will begin taking their continuous data. The Aerobot will have approximately 1 Earth day after entry to complete checkout before it enters the Venus night. During the Venus night the avionics will be in low power receive only mode with short 10-minute contacts (green bars in the figure) each Earth day.

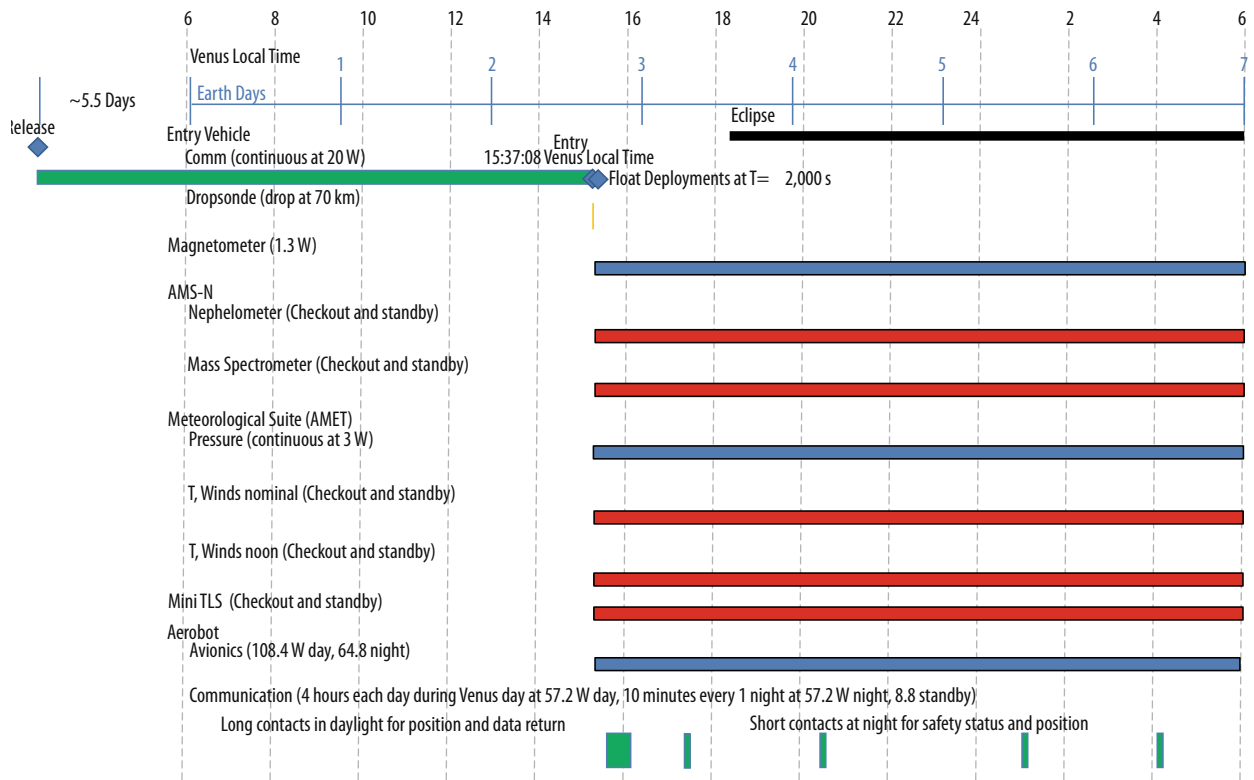


Figure A-41: Aerobot Entry and initial float timeline.

VS037

### A.2.4.2.3 Nominal 60-day Mission

Once the Aerobot exists the first Venusian night, all of the instruments will begin normal operations as shown in **Figure A-42**. During the nominal mission, the Aerobot will communicate with the Orbiter daily during 1 of two planned communication opportunities during the Venusian daylight. During the Venusian night, one 10-minute communication opportunity is planned for every Earth day. Additional night communication periods are available for mission operations within the limits of the battery. Should the Aerobot experience an anomaly, it will enter safe mode and broadcast an alert message to the Orbiter.

The data budget for a typical 7-day circumnavigation is shown in **Table A-19**.

Table A-19: 7-day circumnavigation data budget.

Payload	Data Rate (kbps)	Number of Samples in 24 hours	Duration (seconds)	Operations	Data Volume for 7 day orbit								
					Day 1 (kb)	Day 2 (kb)	Day 3 (kb)	Day 3.5 (kb)	Night 4 (kb)	Night 5 (kb)	Night 6 (kb)	Night 7 (kb)	Total (Mb)
Fluxgate Magnetometer	0.06	86,400.0	1	Continuous	5,400	5,400	5,400	2,700	2,700	5,400	5,400	5,400	37.8
Aerosol Mass Spectrometer (AMS-N)	31.07			See Breakout below	8,621.80	8,621.80	8,621.80	4,310.90	4,310.90	8,621.80	8,621.80	8,621.80	60.4
Nephelometer	2.40	13.7	420	7 minutes out of 105, 3x compression	4,608.00	4,608.00	4,608.00	2,304.00	2,304.00	4,608.00	4,608.00	4,608.00	32.3
Mass Spectrometer Measurements	28.67	1.0	420	7 minutes out of 28 hours, 3x compression	4,013.80	4,013.80	4,013.80	2,006.90	2,006.90	4,013.80	4,013.80	4,013.80	28.1

Payload	Data Rate (kbps)	Number of Samples in 24 hours	Duration (seconds)	Operations	Data Volume for 7 day orbit									
					Day 1 (kb)	Day 2 (kb)	Day 3 (kb)	Day 3.5 (kb)	Night 4 (kb)	Night 5 (kb)	Night 6 (kb)	Night 7 (kb)	Total (Mb)	
Mini TLS	37.63	1.0	300	Take 4 sets of data for 5 minutes synced with Isotopic measurements 28 hours apart at 24 W Worst case assume 1 bakeout on Day 2 for 2 hours at 34 W  One observation at night at 24 W is desired	11,290	11,290	11,290	11,290	11,290					56.4
Atmospheric Meteorological Temperature (AMET)	0.44				12,668	12,676	12,668	6,335	6,335	12,668	12,668	12,668	12,668	88.7
Pressure and dosimeter	0.15	86400.0	1	Continuous	12,666	12,666	12,666	6,333	6,333	12,666	12,666	12,666	12,666	88.7
Temp and Winds nominal	0.15	13.7	1	1 every 105 minutes	2	2	2	2	2	2	2	2	2	0.0
Temp and Winds noon	0.15	56.0	1	1 every 30 minutes for 28 hours at local noon. Assume all data collected in day 2		8								0.0
Gondola Subsystems	0.30	1.0	Continuous	25920	25920	25920	25920	25920	25920	25920	25920	207.4		
				Totals	72,521	72,530	72,521	54,867	54,867	61,232	61,232	61,232	61,232	511.0
				Daily transmit Time (hrs)	4	4	4	4.00	0.17	0.17	0.17	0.17	16.7	
				Daily Volume Capability	128,304	128,304	128,304	128,304	5,346	5,346	5,346	5,346	5,346	534.6
				Night Stored Science Data for day transmit	0	0	0	0	49,521	55,886	55,886	55,886	217.2	
				Total Daily Volume Req	144,914	144,922	144,914	54,867	5,346	5,346	5,346	5,346	511.0	
				Transmit Volume Margin	-16,610	-16,618	-16,610	73,437					23.6	

During the first circumnavigation, the balloon is passively altitude stable. The He pump can be used as the mission progresses to maintain a near-constant altitude by raising or lowering the balloon, and thus a near-constant temperature, for sensitive characterizations of atmospheric composition including isotopic ratio of noble gases if altitude dispersions are observed. In later circumnavigations, the Aero-bot's altitude control will also be used to descend or ascend as needed to counter expected variations in the wind speed (**Figure A-43**) to maintain the 7-day circumnavigation period. For resource planning purposes, the variation in altitude is assumed to be done once each circumnavigation in the Venusian daylight and Venusian night over the course of 20 hours as shown in **Figure A-42**. Descents require the use of the He pump while Ascents do not require the use of the pump. This allows operational flexibility to plan descents just prior to Venusian night with ascents done at night.

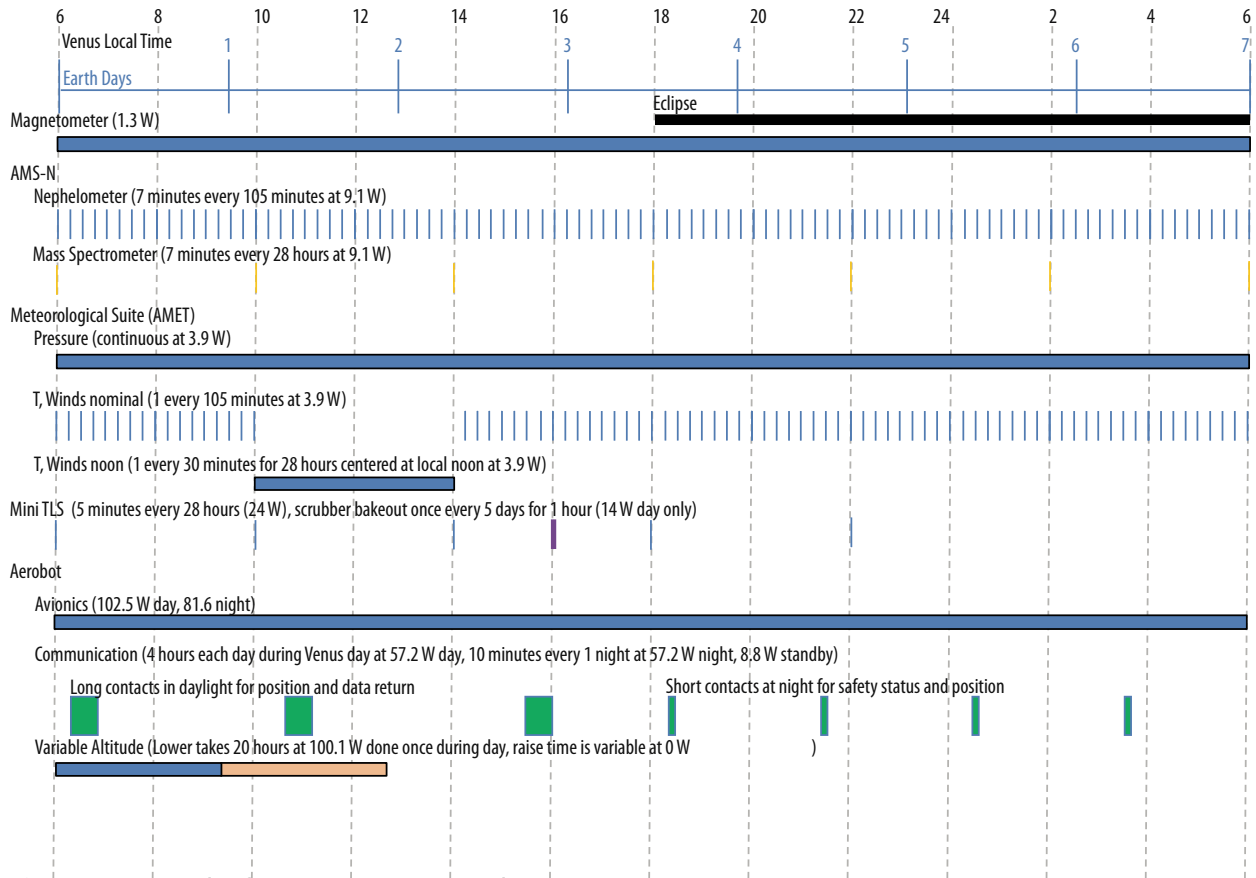


Figure A-42: Typical 7-day circumnavigation timeline.

VS038

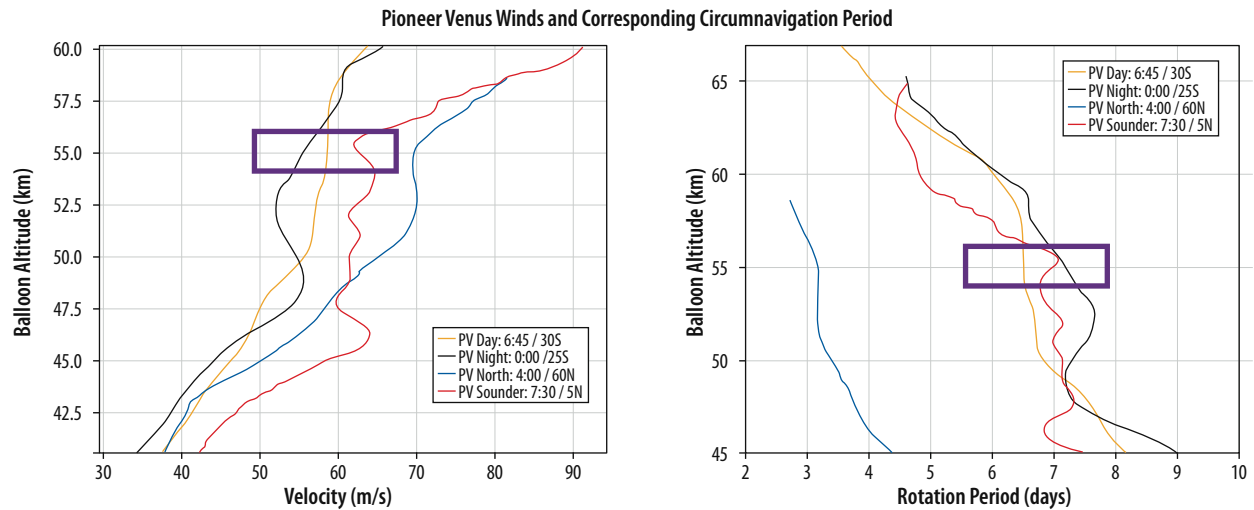


Figure A-43: Winds variation from Pioneer Venus.

VS035

The balloon's AMET pressure sensor will be powered on at all times, measuring continuously. Temperature will be taken every 1-5 minutes except around local noon when it will be taken every 30 minutes for 28 hours. Magnetometer data is taken continuously and down sampled to 0.5 Hz, which is sufficient for measurement of remnant magnetism, and occasional high-rate data is collected for investigations such as Schumann resonances characterization and search for lightning.

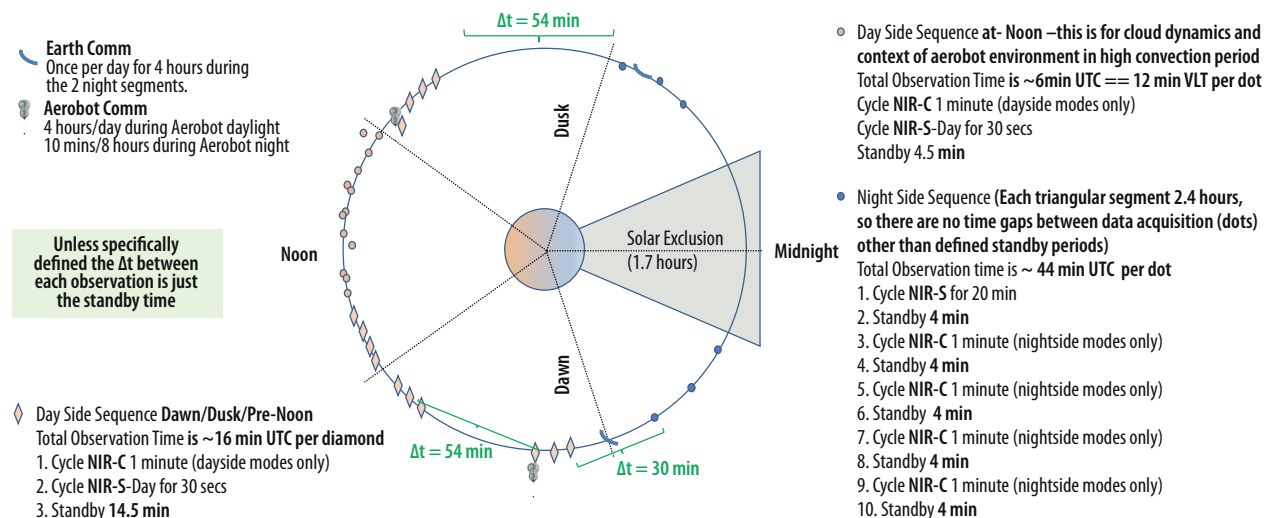


The AMS-N is powered on for seven minutes, once every 105 minutes. At each time, after a 2-minute warm up period, the mass spectrometer will measure composition of the atmosphere for five minutes, and then of cloud/aerosol particles which are separated from atmospheric gas using an aerodynamic aerosol separator. The incoming atmosphere passes through a nephelometer that optically interrogates cloud and aerosol particles entering the mass spectrometer to constrain their size, shape, composition. The mass spectrometer data are integrated over 10-second periods in order to reduce data rate. After each operational period, the instrument will remain in standby power until it is ready to ingest the next sample.

The mini-TLS operates for 5 minutes every 28 hours with a scrubber bakeout once every 5 days for one hour.

### A.2.4.3 Venus Orbit Operations

The Orbiter is in a 12-hour orbit as shown in **Figure A-44**. The Orbiter nominally communicates with the Aerobot once per day for 4 hours when the Aerobot is in the Venusian sunlight and for 10 mins/Earth day when the Aerobot is in the Venusian night throughout the Aerobots 60 day nominal lifetime. There are two planned opportunities per day to communicate with the Aerobot. The primary opportunity is planned for the early dawn portion of the Orbiter orbit with backup opportunity in the late afternoon. The Orbiter is in listen mode on its low gain antennas at all times should the Aerobot enter safe mode and broadcast an alert. Communication with the Aerobot are constrained by the communications viewing angle constraints (as discussed in **Appendix A.2.3** and as shown in **Figure A-28**). Communication is not possible when the Orbiter is within 30° of zenith with respect to the Aerobot or within 30° of the horizon. As the Aerobot mission progresses the latitude of the Aerobot will change. To account for this the mission design analyzed four representative cases for daily maximum contact times as shown in **Figure A-29** through **Figure A-33** for representative latitudes of 0, 15, -15, 45 and -45°. For each latitude analyzed, it is assumed that the Aerobot remains at that latitude for the full mission duration. This results in the worst case maximum duration without a contact of 77 hours for latitudes of +15°, +45° and -45° due to the geometry of the Orbiter's orbit and the Aerobots view angle restrictions. The view angles for each latitude case are shown in **Figure A-29** through **Figure A-33**. In reality, the Aerobot will change latitude due to winds. It is expected that there will be at least one contact each day at any given latitude.



VS040

**Figure A-44:** Orbiter Operations.

Each of the 5 segments defined by the dashed lines in the figure is 2.4 hours. The Orbiter communicates 4 hours a day with Earth during the post dusk to early dawn segments. The Orbiter data

budget is shown in **Table A-20**. All EUV observations are sun pointed and continuous. All Orbiter NIR observations are nadir pointed looking at full Venus disk. The NIR observations shown in **Figure A-44** are divided into three sequences: Day side sequence for Dawn/Dusk/Pre-noon, Day side sequence at noon, and the night sequence. The orbiter makes no NIR observations during the solar exclusion zone of 1.7 hours.

**Table A-20:** Orbiter Data budget.

	Data Rate (kbps)	Operations	Observation Time (sec)	Number of Observations per Orbit	Total Data Volume for 1 12 hour Orbit (kbits)	Total Data Volume for 1 Earth Day (kbits)	Total Data Volume for 1 Earth Day (Mbits)
NIRI	150.46	Day side sequence Dawn/Dusk/Pre-Noon	30	14	63,193	126,386	126
NIRI	150.46	Day side sequence at Noon	30	13	58,679	117,359	117
NIRI	150.46	Night Side Sequence	1,200	1	180,552	361,104	361
IRCAM	1800	Day side sequence Dawn/Dusk/Pre-Noon	60	13	1,404,000	2,808,000	2,808
IRCAM	1800	Day side sequence at Noon	60	14	1,512,000	3,024,000	3,024
IRCAM	1800	Night Side Sequence	240	6	2,592,000	5,184,000	5,184
EUV	2.08	Continuous	43,200	1	89,856	179,712	180
Magnetometer	6.02	Continuous	43,200	1	260,064	520,128	520
Spacecraft Subsystems	1	Continuous	43,200	1	43,200	86,400	86
Orbiter Sub Total					6,203,545	12,407,089	12,407
Aerobot Daily Volume Req't						128,304	128
Total Daily Data Volume						12,535,393	12,535
Daily transmit Time (hrs)			4				
Daily Capability						14,400,000	14,400
Daily Volume Margin						1,864,607	1,865

### A.3 FLIGHT SYSTEM

The ADVENTS flight system consists of an Orbiter and an Aerobot with a Dropsonde as shown in **Figure A-7**. The Orbiter functions as a carrier for the Aerobot, a communication relay for the Aerobot and Dropsonde, and a science platform. The Aerobot is contained within an entry system so that it can survive entry and descent through the Venus atmosphere. The Aerobot carries a dropsonde that is released during entry carrying pressure, temperature, and chemical sensors that measure the atmosphere down to the surface for up to an hour. **Table A-21** provides a summary of the Aerobot and Orbiter characteristics. The following sections provide design concept details for the Aerobot and Orbiter.

**Table A-21:** ADVENTS Flight System Characteristics.

Flight System Element Parameters (as appropriate)	Aerobot	Orbiter
<b>General</b>		
Design Life, months	2	78
Structure		
Structures material (aluminum, exotic, composite, etc.)	Aluminum, honeycomb panels	Aluminum, honeycomb panels
Number of articulated structures	0	3 Solar Arrays, HGA, EUV spin table
Number of deployed structures	3 Mag Boom, Antenna boom, Wind sensor/Antenna boom	2 HGA and Mag boom
Aeroshell diameter, m	3.2	N/A

Flight System Element Parameters (as appropriate)	Aerobot	Orbiter
<b>Thermal Control</b>		
Type of thermal control used	Passive – convection and radiation off of white painted surfaces	MLI, radiator patches, heaters
<b>Propulsion</b>		
Estimated delta-V budget, m/s	N/A	2,380 m/s
Propulsion type(s) and associated propellant(s)/oxidizer(s)	N/A	Pressure Regulated, Bi-Propellant (MMH & MON-3)
Number of thrusters and tanks	N/A	1 Main Engine 20 ACS Thrusters (Pri+Red) 2 Propellant Tanks 4 COPV Helium Tanks
Specific impulse of each propulsion mode, seconds	N/A	Primary, ME Mode: 315s (299.7s at -3σ) Secondary, ACS Mode: 300s (285s at -3σ)
<b>Attitude Control</b>		
Control method (3-axis, spinner, grav-gradient, etc.)	N/A	3-axis, spinner
Control reference (solar, inertial, Earth-nadir, Earth-limb, etc.)	N/A	Inertial, Venus-Nadir, Solar
Attitude control capability, degrees	N/A	< 0.1°
Attitude knowledge limit, degrees	N/A	< 30 arcsec
Agility requirements (maneuvers, scanning, etc.)	N/A	Spin S/C to 5 RPM. Slew rate during calibration not specified
Articulation/#–axes (solar arrays, antennas, gimbals, etc.)	N/A	Solar Array, HGA
Sensor and actuator information (precision/errors, torque, momentum storage capabilities, etc.)	N/A	CSS: stradian ST: 30 arcsec boresight IMU: ARW = 0.07 deg/root-hour, Bias: 1 deg/hr RCS: 5 lb Wheel: 0.2 Nm, 250 NMS
<b>Avionics</b>		
Flight Element housekeeping data rate, kbps	0.3	1
Data storage capacity, Mbits	600	20,000
Maximum storage record rate, kbps	20,000	20,000
Maximum storage playback rate, kbps	75,000	75,000
<b>Power</b>		
Type of array structure (rigid, flexible, body mounted, deployed, articulated)	Rigid, Body Mounted	Rigid, Deployed
Array size, meters x meters	2.1	8.3
Solar cell type (Si, GaAs, Multi-junction GaAs, concentrators)	TJGAS	TJGAS
Expected power generation at Beginning of Life (BOL) and End of Life (EOL), watts	510/432	3,658/2,989
On-orbit average power consumption, watts	Day 163.8 Night 100	1,442.4
Battery type (NiCd, NiH, Li-ion)	Li - Ion	Li-Ion
Battery storage capacity, amp-hours	260	210

### A.3.1 Aerobot

**Figure A-45** shows the ADVENTS Aerobot (robotic balloon vehicle) that is a variable-altitude, floating platform for a broad range of scientific instruments. It is comprised of a helium-filled balloon attached by a tether to the gondola (**Figure A-46**). The balloon generates the buoyancy lift force needed to float the gondola. The gondola contains the science instruments and all supporting subsystems such as avionics, power, communications, structure, and thermal management.

The ADVENTS Aerobot uses a helium balloon system which enables the Aerobot to be flown at variable altitudes high above the Venusian surface. Throughout the (60) sixty-day mission, the balloon system allows changes in the flight altitude by transferring helium between Zero Pressure balloon and the Superpressure balloon. The Aerobot's science instruments will be able to gather data from different levels of the planet's atmosphere during one balloon mission. The operational range of the Aerobot is from 52 to 62 km above the surface of Venus. Variations in temperature and pressure throughout this

operational range will be a driving factor in the final package design of all instruments and systems on board Aerobot. The Aerobot is designed to survive down to 50 km and up to 64 km.

A detailed Master Equipment List (MEL) was created for the Aerobot with mass contingency applied based on heritage with 10% for components with high heritage, 20% for components needing additional qualification testing and 30% for TRL 6 with no flight heritage. The total mass of the Aerobot entry system is shown in **Table A-22**. Aerobot Gondola Mass is shown in **Table A-23**. Aerobot float power modes are discussed in **Appendix A.3.1.3.4**.

**Table A-22: Aerobot Entry System Element Mass and Power.**

	Mass			Average Power		
	CBE (kg)	% Cont.	MEV (kg)	CBE (W)	% Cont.	MEV (W)
Payload	19.3	30.0	25.1	48.5	30.0	63.1
Gondola	147.6	17.2	173.0	86.1	11.6	96.1
Balloon System	173.8	23.3	214.3	77.0	30.0	100.1
<b>Subtotal Float Mass</b>	<b>321.4</b>	<b>21.0</b>	<b>412.3</b>			
Inflation System	370.4	27.2	471.1	N/A	N/A	N/A
Entry System	676.0	29.9	878.2	1.2	30.0	1.6
Dropsonde	89.9	30.0	116.9	21.2	30.0	27.6
<b>Total Entry Mass</b>	<b>1,477.0</b>	<b>27.2</b>	<b>1,878.6</b>			

**Table A-23: Aerobot Gondola Mass.**

	Mass		
	CBE (kg)	% Cont.	MEV (kg)
Structures & Mechanisms	50.4	30	65.4
Thermal Control	3.3	10	3.6
Attitude Control	0.1	10	0.1
Avionics	27.7	10	30.5
Communications	5.8	18.7	6.8
Power	60.5	10	66.5
<b>Aerobot Gondola Mass</b>	<b>147.6</b>	<b>17.2%</b>	<b>173.0</b>



**Figure A-45: ADVENTS Aerobot.**

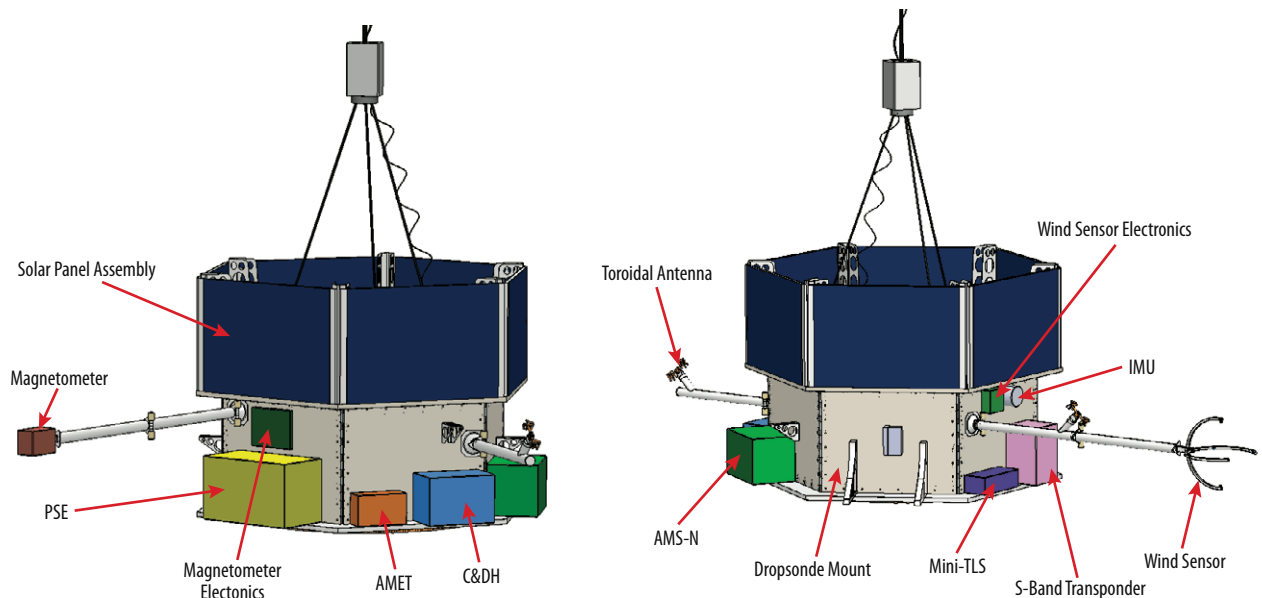


**Figure A-46: Aerobot Gondola.**

### A.3.1.1 Instruments

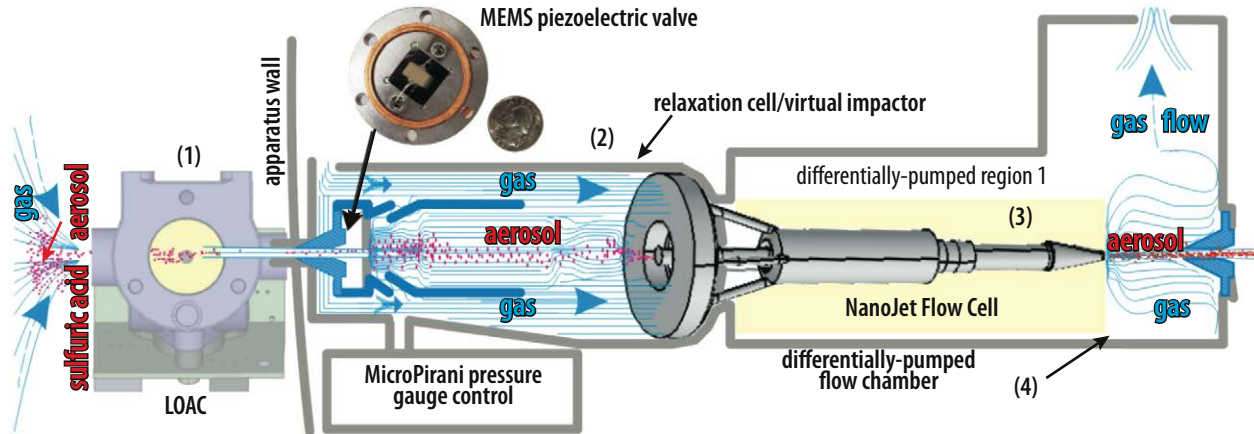
All the instruments (**Table A-24**) on the Aerobot were also studied in VFM concept study. This study selected a smaller version TLS from the VFM lander. Also, the Aerobot carries a Dropsonde that contains the pressure, temperature sensor, and chemical sensor array instrument. The technology development plans for the AMS-N and chemical sensor array are discussed in **Table A-25** and **Table A-26**, respectively.

**Table A-24:** Aerobot Instruments.

Item	Aerosol Mass Spectrometer with Nephelometer (AMS-N)	Mini Tunable Laser Spectrometer (TLS)	Meteorological Suite (MET)	Fluxgate Magnetometer Gondola (MAG-G)	Dropsonde Pressure and Temperature Sensors	Dropsonde Chemical Sensor Array
	Aerosol spectrometer	Laser Spectrometer	P, T, wind, radiation sensors, infrasound	Magnetometer	P, T sensors	Chemical sensors
Number of channels	6	2	3	1	2	8
Size/dimensions (m x m x m)	0.30 x 0.20 x 0.20	0.25 x 0.11 x 0.07	0.20 x 0.12 x 0.08	0.08 x 0.10 x 0.12	0.2 x 0.12 x 0.08	0.05 x 0.05 x 0.03
Instrument mass <b>without</b> contingency (Kg, CBE*)	10.5	3.3	4.0	1.5	2.3	0.1
Instrument mass contingency (%)	10.5	30.0	30.0	30.0	30.0	30.0
Instrument mass <b>with</b> contingency (Kg, CBE+Reserve)	13.7	4.3	5.2	1.9	2.9	0.13
Instrument average payload power <b>without</b> contingency (W)	7.0	24.0	5.0	1.0	10.7	3.0
Instrument average payload power contingency (%)	30.0	30.0	30.0	30.0	30.0	30.0
Instrument average payload power <b>with</b> contingency (W)	9.1	31.2	6.5	1.3	13.9	3.9
Instrument average science data rate <b>without</b> contingency (kbps)	0.4	37.6	0.9	2	0.4	0.4
Instrument average science data rate <b>with</b> contingency (kbps)	0.52	48.9	1.2	2.6	0.36	0.36

#### A.3.1.1.1 Aerosol Mass Spectrometer with Nephelometer (AMS-N)

The AMS-N measures separately the composition of atmospheric gases and aerosol particles in the Venus clouds and characterizes the size distribution and optical properties of the aerosol particles (nephelometer mode). The instrument has an aerosol separator (**Figure A-47**), which focuses aerosol particles on to a hot filament where they are volatilized and directed to a mass spectrometer. In the gas analysis mode, only the gas is directed to the mass spectrometer. The resolution of the mass spectrometer must be tunable in order to discriminate species such as CO and N<sub>2</sub> which both have mass near 28 Daltons (Da). The long duration of the mission will enable tuning of the instruments to optimize discrimination of many different species and to allow long integration times for improving detection limits. Species that can be measured include noble gases and their isotopes, SO<sub>2</sub>, SO<sub>3</sub>, HCl, CO, OCS, H<sub>2</sub>O, HDO, H<sub>2</sub>S, PH<sub>3</sub> to a sensitivity of 1 ppb. The instrument must be capable of measuring components of the aerosol including H<sub>2</sub>SO<sub>4</sub>, H<sub>2</sub>O, FeCl<sub>3</sub>, and sulfur (S<sub>3</sub>, S<sub>4</sub>, S<sub>X</sub>) and phosphorus compounds to a sensitivity of better than 1%. The AMS-N will characterize diurnal variation of composition and altitude variation of gas and aerosol within the clouds. The LOAC instrument will also measure particle size and identify non-volatile particulates by their refractory scattering properties.



V504

**Figure A-47:** Aerosol separator in the AMS-N. Gas containing the Venus cloud particles is admitted through nephelometer (1) from the left side of the figure and through the relaxation cell (2) directed to the NanoJet flow cell (3) which strips away gas inside the differentially pumped chamber (4). The aerosol particles pass through the orifice on the right side and impinge on a vaporizer in the mass spectrometer.

**Table A-25:** AMS-N Technology Development Plan.

AMS-N Component	Current TRL	Rationale for TRL assessment	Development Program	Development Start Date	TRL Development Description	Cost and Schedule of TRL Development	TRL at completion of Development Program
QIT-MS Mass Spectrometer	5	Prototype Electronics Compact QIT-MS, S.A.M. instrument onboard ISS as technology demonstration	DAL119	April, 2020	Thermal vacuum tests of compact QIT-MS	Reach TRL 6 before 2023	6
Aerosol Separator	2	Simulations performed at low pressures with pumping model developed (TRL2); NanoJet Flow Cell tested in industrial conditions for 8hrs of continuous operation 1 atm without clogging (TRL2); MEMS piezo valve (TRL4); basic operation of differential pumping system established but not designed (TRL1);	SBIR20, PICASSO20	CIF20 PICASSO20 May 2021, if awarded	NanoJet Flow Cell needs redesign and testing for long operations in low pressure corrosive acidic environment, Design and Fabrication of Differential pumping system with pressure control electronics; pumps need testing in acidic vapor environments for lifetime degradation; aerosol vaporizer needs to be designed, fabricated, and tested in high vacuum; mechanical vibration certification	\$1.2M for maturation of technology plus parts and labor reach TRL 4 before 2022	6
Nephelometer LONSCAPE	2	Stratospheric balloon flight heritage (LOAC, 2 laser channels); vacuum compatibility not tested, 4 laser channel prototype tested in laboratory, 6 laser channel under design including software and electronics	CNRS, CNES French Space Agency	April, 2020	Laser light scattering chamber with 6 channels and optical detectors, vacuum compatible electronics, testing in acidic environments and test balloon flights, mechanical vibration tests	\$6M to deliver flight Reach TRL 6 before 2023	6

### A.3.1.1.2 Tunable Laser Spectrometer (TLS)

The TLS measures selected gas abundances and isotopic ratios. Whereas AMS-N may fragment molecular species during ionization, TLS probes absorptions in the intact molecules using a laser that is tuned to scan through the diagnostic spectral lines. TLS will not detect noble gases and their isotopes and will not analyze aerosols but it has greater sensitivity for many species including phosphine (1 ppbv) and is not vulnerable to ambiguities resulting from identical mass numbers. The baseline TLS has 4 channels (lasers) that typically measure abundances to ~1% and isotope ratios to  $\pm 1$  or 2 per mil in delta values: Channel 1: CO<sub>2</sub> and H<sub>2</sub>O with isotopic ratios of <sup>18</sup>O/<sup>17</sup>O/<sup>16</sup>O in CO<sub>2</sub> and H<sub>2</sub>O, D/H in H<sub>2</sub>O, and <sup>13</sup>C/<sup>12</sup>C in CO<sub>2</sub>. Channel 2: CO and OCS with <sup>34</sup>S/<sup>33</sup>S/<sup>32</sup>S in OCS, <sup>13</sup>C/<sup>12</sup>C in CO and OCS Channel 3: SO<sub>2</sub> abundance and <sup>34</sup>S/<sup>33</sup>S/<sup>32</sup>S isotope ratios. Channel 4: HCl and H<sub>2</sub>O abundance and <sup>37</sup>Cl/<sup>35</sup>Cl. The instrument used as the baseline is the TLS in SAM on Curiosity. Cell pumping and filling is achieved using passive molecular sieve as flown on Curiosity.

The mini-TLS instrument was selected to meet the science requirements for this study. This high-resolution IR laser spectrometer has been developed and equipped with two channels. It is made up of 3 system-level parts: a spectrometer; a passive gas ingests and pump system for in-situ analysis, and an electronics board. The mini-TLS instrument is currently TRL 6, with many MSL Curiosity components at TRL 7 or 8.

### A.3.1.1.3 Meteorological Suite and Infrasonic Measurements (MET)

The MET is a suite of meteorological sensors that will continuously measure local pressure, air temperature, turbulence and windspeed. Also, the Aerobot includes a radiation dosimeter to quantify ionizing radiation levels in the Venus cloud environment. In addition to slowly varying pressure changes as the balloon changes altitude, the instrument measures the rapid pressure variations known as infrasonic including signal originating from Venusquakes and volcanic events.

The airborne measurement of seismic activity using its infrasonic signature is a relatively new area of research, but rapid progress has been made with artificial seismic sources such as seismic hammers and subsurface chemical explosions. Experiments using weak artificial seismic sources and Earth's atmosphere as a Venus analog have shown that seismic activity is detectable in the air from infrasonic signatures (Krishnamoorthy *et al.*, 2018). Moreover, the frequency content of ground motion is imprinted into its atmospheric signature, meaning that the measurement of pressure in the air may be equivalent to measuring ground motion to within a multiplicative factor in the infrasonic frequency regime (Krishnamoorthy *et al.*, 2019). A magnitude 4.2 earthquake was detected from a balloon at an altitude of 4.8 km was detected recently using this technique (Brissaud *et al.*, 2021). The recorded signal was also used for a first-order characterization of crustal layering. Quakes may also be localized on the ground by deploying multiple barometers on a tether and measuring the time of flight of the signal between the barometers. Time-of-flight measurements can also be used to distinguish direct infrasonic arrivals from the quake's epicenter from infrasonic generated by traveling seismic waves as they pass under the balloon (Figure A-48). With reliable motion tracking using Earth-based and orbital tracking assets and stable inertial measurement units (IMUs) on board the balloons, pressure variations induced by altitude change in a convective atmosphere can be removed.

Because of the higher atmospheric density of Venus, seismic energy is coupled into the atmosphere 60× more effectively on Venus than on Earth. Preliminary computations with one-dimensional geometric attenuation profiles suggest that infrasonic from quakes with surface magnitudes as low as 3.0

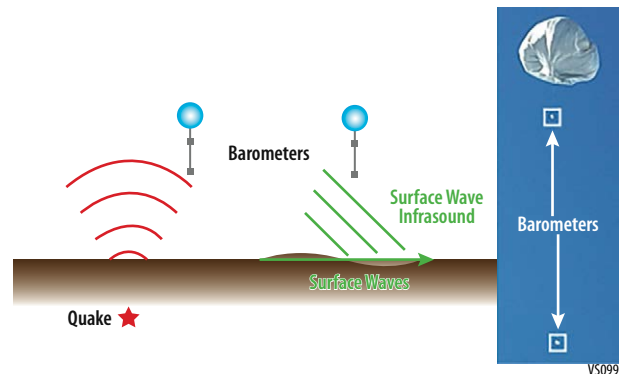


**Figure A-48:** (Left) A schematic showing the detection of seismic activity from balloon-borne infrasonic barometers on a tether. (Right) Picture of a stratospheric balloon on Earth with two barometers on a tether.

may be detected over 100 km away from the epicenter of a quake on Venus, if pressure fluctuations as low as  $10^{-3}$  Pa can be accurately measured. Further refinement of detection limits is being pursued through a coordinated campaign of data collection in Earth's atmosphere over regions of high seismic activity, and mapping the results to Venus. Once detected, the infrasound signature may be used to study several outstanding questions about Venus seismicity. The direction of first motion inferred from the waveform, when compared with existing radar images of the surface from Magellan or any future spacecraft, can help understand the types of faulting mechanisms present on Venus, in turn informing models of Venus' interior. If large quakes with multiple detectable seismic phases occur, the time difference of arrival between these phases can place bounds on estimates of crustal rigidity and density. In particular, the dispersion of low-frequency seismic modes such as Rayleigh waves from large quakes can help in studying the crustal structure of Venus.

The constant monitoring of atmospheric pressure using the meteorological suite will be combined with information on prevailing winds and balloon motion from the IMU to autonomously identify of snippets of scientific interest for transmission to the orbiter and further analysis on Earth.

### A.3.1.1.4 Dropsonde (Dropsonde)

The single Dropsonde will include temperature, pressure and chemical sensors that will obtain a vertical profile between the upper clouds (64.6 km) and the surface. Pressure and temperature sensors as well as a chemical sensor array are mounted on the outside of Dropsonde with connections to electronics in the Dropsonde. There is an approximately 1-hour operational period where the Dropsonde is released from the Aerobot to the surface.

The chemical sensor array is made up of small, compact high-temperature micro sensors (see **Table A-26** for sensor array characteristics). It requires no cooling when combined with SiC electronics. The sensor array will be mounted on the outside of the Dropsonde and exposed to the Venus environment (See **Figure A-49**). The sensor array in this study will measure six different species:  $H_2$ ,  $O_2$ ,  $CO$ ,  $H_2O$ ,  $HCl$ , and  $NO$ . The Si-based control electronics will be mounted in thermally protected interior operational to  $125\text{ }^\circ\text{C}$ . The cable and harnessing from control electronics to sensor array is through the chamber wall. Power, communications, and temperature control are provided by the Dropsonde. The sensors are powered continuously, and the data rate is defined by the sampling rate of electronics.

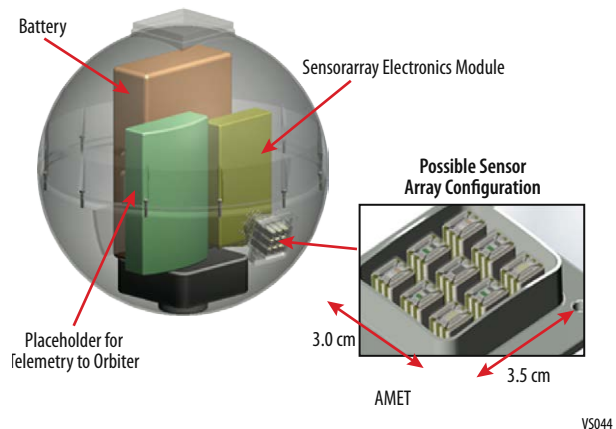


**Figure A-49:** Chemical Sensor Array mounted on Dropsonde.

The notional view of the chemical sensor array carried by the Dropsonde is shown in **Figure A-49**.

**Table A-26:** Chemical Sensor Array Characteristics.

Instrument Name	Venus In-situ Atmospheric Measurement Instrument Package (VIAMIP)
General Description	Chemical sensors for $CO$ , $SO_x$ , $OCS$ , $O_2$ , $HF$ , $HCl$ , $H_2O$ , $NO$
Science Objectives	Vertical profiles $\sim 72$ km and lower
Mounting Location	Sensor mounted near exterior with access to atmospheric gas, electronics mounted in thermally protected interior
Mass	under 0.1 kg - could be on order of 0.04 kg
Dimensions	5 cm x 5 cm x 3 cm
Power	1 W assuming powered with under 10 VDC; Peak 0.5 W per sensor at ambient temp $20\text{ }^\circ\text{C}$ at 55 km
Data Rate	20 Hz; sensors are powered continuously, and the data rate is defined by sampling rate of electronics
Unique Hardware	Use of high reliability electronics or extended temperature electronics using suitable substrate and hybrid packaging



The current technology readiness levels for each chemical species are contained in **Table A-27**. The technology maturity plan is described **Table A-28**.

**Table A-27:** Chemical Sensor Array TRL.

Chemical Sensor Species	TRL	TRL Demonstration
SOx	6	Multiple tests in GEER in addition to lab tests
CO	6	Multiple tests in GEER in addition to lab tests
OCS	6	Multiple tests in GEER in addition to lab tests
NO	6	Multiple tests in GEER in addition to lab tests
HF	6	Multiple tests in GEER in addition to lab tests
O <sub>2</sub>	5 to 6	Single GEER Test
H <sub>2</sub> O	5 to 6	Single GEER Test
HCl	5	GEER Test - design improvement in processes
Electronics	TRL	TRL Demonstration
Silicon Electronics	6 to 7	Operated external to GEER with sensors inside GEER
		Based on flight qualified electronics

\*GEER - NASA Glenn Extreme Environments Rig (GEER) facility designed to simulate extreme environments

### A.3.1.1.5 Chemical Sensor Array Technology Maturity

The sensor testing has been performed in simulated Venus surface conditions at NASA GRC GEER and electronics are adapted from MEMS sensor systems flown on ISS and commercial launch vehicles for propellant leak detection. Presently, the technology is at TRL 5-6 with extended surface conditions and limited upper atmosphere environment testing. Further laboratory testing for TRL 6 system development is planned at 3 different static levels: upper, mid, and surface.

**Table A-28:** Chemical Sensors Array Technology Development Plan.

	Test Description	Development Schedule	TRL at completion
Qualification Testing: Vibration, EMI and Thermal	Dropsonde system level testing only. Testing is for Dropsonde material compatibility. 3 tests in descent simulation conditions; 3-4 hour descent testing starting at 70 km	2 year plan; FY25 Start FY26 End	TRL 6 or greater

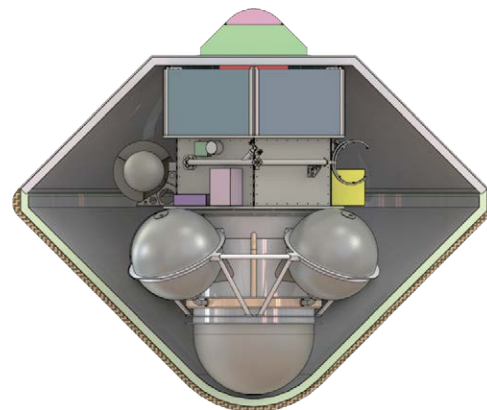
### A.3.1.2 Entry Vehicle

The Entry vehicle includes the forebody and afterbody aeroshells with Thermal Protection System (TPS) and the parachute(s). **Figure A-50** shows the Aerobot stowed within the entry vehicle. The Aerobot structure is discussed in **Appendix A.3.1.3.6**.

The entry system protects the Aerobot from entry heating and deceleration forces during the entry into Venus' atmosphere. The Entry system was designed to meet the following requirements:

- 1) Temperatures at the bondline not to exceed 260 °C. This is driven by the temperature limits on the adhesive that bonds the TPS to the aeroshell structure.
- 2) Peak deceleration not to exceed 50 Earth-g. This requirement stems from the science instrumentation. This lower value (compared to prior missions) enables a wider array of science instrumentation to be used as part of this mission.
- 3) Achieve flight conditions acceptable for balloon extraction and inflation at desired altitudes between 62 and 50 km.

The Entry system must meet these requirements subject to entry conditions consistent with the interplanetary approach trajectory. **Table A-29** shows the resulting Aerobot Entry sys-



Notional view of Aerobot payload stowed in Entry Shell

VS045

**Figure A-50:** Aerobot stowed inside the entry system.

tem design parameters. The Requirement on peak deceleration (for the nominal entry velocity of 10.56 km/s) yields an Entry Flight Path Angle of near  $-8.85^\circ$ , significantly shallower than prior missions (such as Pioneer Venus Large Probe,  $-32.4^\circ$ ) and mission concepts (such as VITAL,  $-23.5^\circ$ ). The entry mass of 1,900 kg used for the analysis and design results in a ballistic coefficient of  $225.0 \text{ kg/m}^2$  (compared to the value of  $188 \text{ kg/m}^2$  for Pioneer Venus Large Probe).

**Table A-29:** Aerobot Entry System Design Parameters.

	Item	Units	Values
Aeroshell	Aeroshell Geometry	deg (sphere cone)	45
	Aeroshell max diameter	m	3.2
	Entry Mass design value	kg	1,900
Entry Vector	Entry Interface	km	175
	Entry Velocity	km/s	10.45
	Peak Deceleration	Earth-g	<50
	Entry Flight Path Angle	deg	-8.85
	Heading	Deg (relative to North)	-70
	Entry Latitude	deg (relative to equator)	0
	Entry Longitude	deg	113
	Entry time	UTC	03:24:25.994

The aeroshell is a  $45^\circ$  sphere cone geometry with a max diameter of 3.2 m. This geometry was chosen for its good stability and packaging characteristics as well as significant flight heritage at Venus. The aeroshell structure is titanium-composite sandwich with a mass of 300 kg (not including the TPS), based on preliminary analysis. This estimate is conservative and detailed design could provide avenues of optimization and a reduction in mass.

The Thermal Protection System (TPS) is a Tiled Single Layer System of HEEET (Heatshield for Extreme Entry Environment Technology) with a mass of 373 kg and a uniform thickness of 1.26 inches. HEEET is a 3-dimensional woven TPS system developed for extreme entry environments, and the single-layer HEEET (as proposed here) only utilizes the insulation layer (versus the standard dual layer HEEET). This single-layer (insulation layer only) HEEET is the baseline material for the Mars Sample Return Earth Entry Vehicle, that will bring the samples back from Mars and land them safely on Earth. PICA (Phenolic Impregnated Carbon Ablator) is proposed for use as the backshell TPS. The tiles are expected to be bonded to the structure using HT-424 and with RTV-560 filled gaps, using the same techniques as Mars Science Lab and Mars2020. The backshell TPS mass is estimated to be 30 kg.

The concept of operations for the Aerobot calls for two parachutes, one extracting the backshell and the other extracting the balloon. For the purposes of this early design, the two parachute are assumed to be identical, weighing 27.4 kg each.

### A.3.1.2.1 Summary of Performance Capability

The Aeroshell structure is designed to withstand the deceleration loads of 50 g during entry. The Thermal Protection system is designed to keep the temperature at the bondline between the TPS and the structure, below  $260^\circ\text{C}$  during the entry pulse. The expected peak heating during the entry is about  $3,000 \text{ W/cm}^2$  (convective+radiative, rough wall, margined, at the shoulder) with an integrated heat load of over  $52,000 \text{ J/cm}^2$  (margined). The aerothermal environment at the shoulder is (turbulent) convective heating dominated, with the peak radiative heating being only around  $25 \text{ W/cm}^2$ . Heatshield thermal protection characteristics are shown in **Table A-30** and **Table A-31** for the forebody and the backshell respectively.

**Table A-30:** Heatshield Forebody Thermal Protection System Characteristics.

TPS Material	TPS Thickness (inch)	Recession Layer Thickness (inch)	Insulative Layer Thickness (inch)	Aerial Density ( $\text{kg/m}^2$ )	Area ( $\text{m}^2$ )	Mass (kg)
T/SL HEEET	1.26	-	1.26	26.26	14.2	373

**Table A-31:** Heatshield Backshell Thermal Protection System Characteristics.

TPS Material	TPS Thickness (inch)	Aerial Density (kg/m <sup>2</sup> )	Area (m <sup>2</sup> m)	Mass (kg)
PICA	0.40	2.74	10.77	30.0

**Table A-32:** Entry Event Sequence.

Event	Time from Entry (sec)	Altitude(km)	Altitude Rate (m/s)	Mass (kg)	Dynamic Pressure (Pa)
Entry Interface	0.0	174.9	-1,601.8	1,835.1	0.0
DrogueChute Deploy	152.7	67.4	-173.0	1,835.1	2205.1
DrogueChute Full	153.2	67.3	-160.4	1,835.1	1916.2
Heatshield Sep	172.7	66.1	-49.8	1,265.4	211.6
Dropsonde Sep	202.7	64.9	-37.1	1,138.4	143.7
Backshell Sep	572.7	56.0	-17.7	955.1	127.6
MainChute Deploy	573.7	56.0	-26.1	955.1	278.7
Begin Balloon Inf	633.7	55.5	-7.4	955.1	23.8
Jettison MainChute	1,203.7	52.4	-3.6	940.1	7.8
End Balloon Inf	1,233.7	52.1	-9.9	940.1	62.0
Jettison Inf Sys	1,263.7	51.8	-9.3	492.6	56.6
End Sim	2,000.0	55.0	-0.1	492.6	0.0

**Table A-32** provides a summary of main events from entry interface to the descent of the Aerobot to the desired altitude.

The entry vehicle enters the atmosphere, at a relative velocity of 10.4 km/s 5.5 days after release. The steepest, dispersed Entry Flight Path Angle (EFPA) cannot be steeper than  $-8.85^\circ$  to limit the peak deceleration to 50 times earth-g (the nominal EFPA for the current design is  $-8^\circ$ ). The heat/drag pulse (**Figure A-51** and **Figure A-52**) lasts for about 2 min, slowing down the capsule. The drogue parachute deploys at Mach 0.75 and an altitude of 67.4 km. The capsule descends under the parachute for a few seconds, followed by heatshield separation at 66.1 km altitude. This is followed by the Dropsonde deploy (30 seconds after heatshield separation) and backshell separation (60 seconds after heatshield separation). Note that there might be some potential to change these time interval between events to tailor the altitudes of interest, while ensuring sufficient separation and reduce probability of re-contact. Inflation of the balloon begins 60 seconds after the main chute deployment, at about 55.5 km altitude when the dynamic pressure is 23.8 Pa which is below the required 25 Pa. 570 seconds later, while the balloon is partly inflated, the main chute is jettisoned. The balloon is assumed to be fully inflated in 10 min, whereafter the inflation system is jettisoned, leaving the balloon at an altitude of 51.8 km. The balloon then quickly rises to the nominal float altitude of 55 km over approximately 12 minutes.

In order to achieve a descent time of at least 1

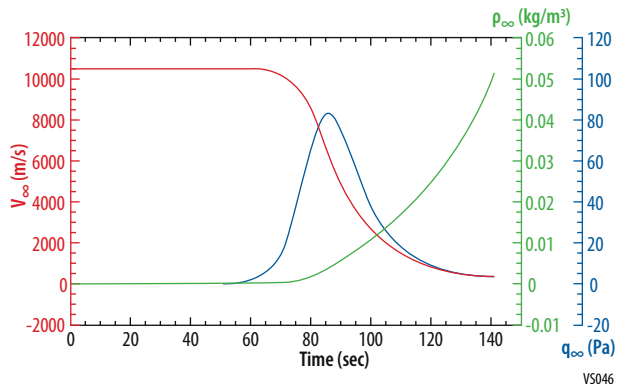


**Figure A-51:** Trajectory of the capsule from Entry Interface through the end of the heat pulse. Curves show temporal variation of velocity, atmospheric density and the resulting freestream dynamic pressure. The EDL design is driven by the requirement on peak deceleration.

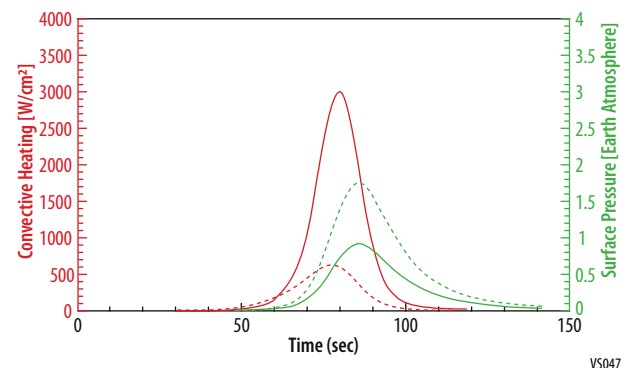


**Figure A-52:** Aerothermal environment on the capsule are shown using time-traces of margined convective heating, and margined pressure. Environments are shown for stagnation point (dashed) and the shoulder (solid). While the stagnation pressure is higher, the shoulder heating drives the TPS design.

hour, the Dropsonde will have to have a drag\*area of at least 0.59 m<sup>2</sup>. For the diameter of 0.324 m (12.75") this implies a drag coefficient of 7.2. With this drag\*area, the Dropsonde reaches a peak descent rate of 110 m/s shortly after separation from the gondola, slowing to 8 m/s at the surface.

### **A.3.1.2.2 Challenges**

**EFPA:** Previous missions to Venus (as well as studies) were designed with a requirement on peak deceleration much higher than the current value of 50 earth-g. This requirement imposes a significantly different entry flight path angle; -8.85°, as opposed to Pioneer-Venus' value of -32.4°. Lofting (the vehicle flying "up" relative to Venus' surface) was used as a conservative upper limit on EFPA. This upper limit precludes skip-out and limits the size of the "footprint" when the balloon is released. The lofting limit angle for the nominal entry velocity at entry interface is about -6.4°. This implies a flyable corridor of just over 2° in EFPA. This ±1° in flight path must be met at the end of a long, uncontrolled flight phase after the Aerobot separates from the launch vehicle/Orbiter.

### **A.3.1.2.3 Technology Maturity**

#### **A.3.1.2.3.1 Thermal Protection System**

Entry into Venus atmosphere is challenging due to the high atmospheric density and resulting heating. Typical entry trajectories result in heat fluxes in excess of 2000 W/cm<sup>2</sup> and pressures in excess of 100 kPa. To withstand these challenging entry environments, previous missions/studies to Venus have used Carbon Phenolic (tape-wrapped, or chop-molded) as the heatshield material (*e.g.* Pioneer Venus, ViTAL). However, heritage Carbon-Phenolic is no longer available due to unavailability of raw material and atrophy of manufacturing capabilities. The Heatshield for Extreme Entry Environment Technology (HEEET) system was developed as an alternative to Heritage Carbon Phenolic for missions with extreme entry environments (*e.g.* to Venus, Saturn, Ice Giants, high speed Earth re-entry). It is a novel, three-dimensional, woven TPS technology consisting of layers of carbon (and/or phenolic) mechanically woven together. HEEET TPS can be either single-piece or tiled, and either dual-layer or single-layer. A dual layer TPS has a high-density all-carbon weave (recession layer) on the outside and a low-density (blended carbon and phenolic) weave (insulation layer) underneath. The single-layer HEEET TPS, featured in the current design, is composed of the insulation layer only. HEEET TPS technology has demonstrated exemplary performance when subject to arc jet conditions of ~3,600 W/cm<sup>2</sup> and 5 atmospheres of pressure in both the single and dual layer configurations. The tiled dual-layer TPS has been matured to TRL 6 (Braun *et al.*, 2020) and is ready for flight infusion. Single-layer HEEET is currently the baseline TPS for the Mars Sample Return (MSR) Earth Entry Vehicle (EEV), resulting in ongoing improvements in loom and weaving capabilities. The geometry proposed here (at a max diameter of 3.2m) is likely beyond the capability of existing looms to weave a single piece heatshield. Therefore the baseline design assumes a tiled insulation layer configuration. As a result, the TPS design requires some early engineering work in terms of demonstration, build and testing of seams with gap-fillers for single-layer HEEET tiled design. It is expected that this activity will be less challenging and complex than the gap/seam design that has already been demonstrated for the dual-layer HEEET TPS. Finally, the TPS thickness for the current design is 1.26 inches, well within the demonstrated capability of current weaving vendors.

#### **A.3.1.2.3.2 Parachute**

The proposed parachute is a standard design used in many previous planetary missions. Material selection will take into consideration the caustic nature of the Venus atmosphere. To ensure proper inflation, the drogue parachute is deployed via a small mortar. The second parachute is deployed by the backshell and first parachute separating from the aerostat 60 seconds after the heatshield is released.

#### **A.3.1.2.3.3 EDL ConOPS Trigger(s)**

The drogue parachute deployment event is triggered on a navigated velocity of 180 m/s, corresponding to roughly Mach 0.75. All other EDL events are triggered on times from drogue deploy. The EDL sequence is not expected to be sensitive to reasonable errors in the navigated state.

#### A.3.1.2.4 Key Trades

##### A.3.1.2.4.1 EFPA

Early in the design process (of the precursor 2.8 m capsule), trades involved entry flight path angle and the resulting heating and the peak deceleration. Steeper entries resulted in higher peak deceleration and higher heating while reducing the entry pulse width. At an entry velocity of 10.5 km/s, an EFPA of  $-8.85^\circ$  provided 50 g of peak deceleration, with a narrow entry corridor (between the designed EFPA and lofting, at  $-6.4^\circ$ ). Particularly since the Aerobot is released so long before entry, the narrow entry corridor is a concern (*i.e.*, EFPA accuracy needs to be within  $\pm 1^\circ$ ).

##### A.3.1.2.4.2 Dropsonde descent time

The requirement of 1 hour “hang time” on the Dropsonde may require uncomfortably large drag devices. A constant drag shape will lead to relatively high velocities in some portions of the descent and low velocities in other. Future design work should attempt to balance time needed to take and transmit measurement data, against the aerodynamic properties of the Dropsonde.

##### A.3.1.2.4.3 Aeroshell cg and mass properties

Mass properties of the aeroshell (heatshield + backshell + aeroshell structure + payload) need to be evaluated to ensure that it has the desirable attributes (location of the center of gravity) to ensure a stable hypersonic and supersonic flight. In particular, with only 1 dropsonde, balancing the aeroshell for the required 5 rpm spin after separation from the Orbit until jettison of the forebody heatshield is a challenge.

##### A.3.1.2.4.4 Narrow Entry Corridor

Due to the requirement on peak deceleration, the design entry flight path angle for this trajectory is  $-8.85^\circ$ , pretty close to the skip out angle of  $-6.4^\circ$ . The Aerobot separates days prior to entry, raising the risk of missing the narrow entry corridor.

#### A.3.1.3 Aerobot Subsystems

##### A.3.1.3.1 Avionics

**Figure A-53** shows the Aerobot block diagram. The Aerobot avionics consists of a Power System Electronics unit (PSE) and a Command and Data Handling unit (C&DH). The PSE and C&DH are implemented with Goddard's Mustang Avionics. The Mustang Avionics will fly on the PACE mission in 2023.

The PSE and C&DH, are block redundant. The PSE and C&DH backup units fly as cold backups.

The PSE consists of 6 types of cards. Its PSE Monitor Card provides PSE control and telemetry acquisition functions. The Solar Array Module handles 16 Amps of solar array current, and performs battery charging and distribution functions. A Segment Modules each handle 40 Amps of solar array current. Altogether, the Solar Array Module and Segment Modules can handle 56 Amps of solar array power. The requirement is 34 Amps, leaving a margin of 40%. Two Low Current Power Output Modules have sixteen 3 Amp outputs each. Those outputs provide a total of thirty two 3 Amp outputs. Nineteen 3 Amp outputs are required on the Aerobot, leaving a margin of 68%. Two Deployment Modules provide 16 actuation outputs. Thirteen deployment outputs are required: Four for the Dropsonde release, four for the Tank ejection, one for the Magnetometer Boom deployment, one for the Helium Tubing cutter, two for the Aeroshell parachute release mechanisms, and one for the antenna boom deployment. Lastly, a Low Voltage Power Converter provides the secondary voltage power required by the PSE cards.

The C&DH consists of 4 types of cards. Its Processor Card is based on a GR712RC Dual-Core LEON3FT SPARC V8 Processor ASIC (200 MIPS). It has 32 MB SRAM and 128 Gits of Flash memory. The Aerobot only requires 600 Mbits of data storage. A Housekeeping Card provides 68 temperature sensor inputs. A Communication Card provides the RF Communication system interfaces. Lastly, a Low Voltage Power Converter provides the secondary.

The total ionizing dose requirement is 3.2 krad (with 2.5 mm shielding). The Mustang Avionics is survivable to 60 krad.

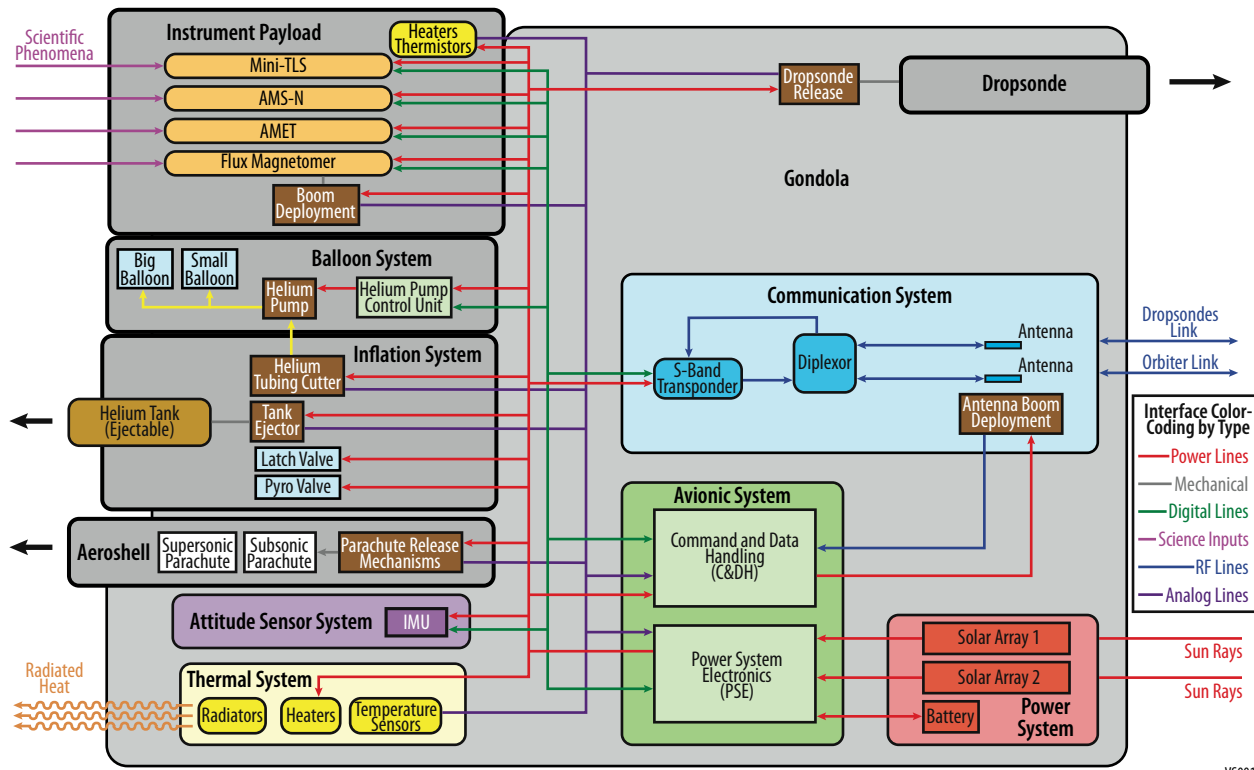


Figure A-53: Aerobot Block Diagram.

V5001

### A.3.1.3.2 Balloon

The Balloon portion of the architecture design trade was discussed in **Appendix A.2.1**. The key design parameters for the variable-altitude balloon required to float a mass design value of 200 kg gondola in the baseline design are summarized in **Table A-33**. The methodology used in this preliminary design is based on an equilibrium approach where the buoyancy at each altitude balances the total floating weight. The key design margins and assumptions include:

- A 2x structural safety factor on the superpressure balloon material after accounting for standard strength knockdown factors for Vectran fabric operating at up to 80 °C.
- The balloon is already sized for a 240 kg gondola mass providing a further 20% mass margin on the current baseline design.
- The balloon is designed to tolerate ±3 m/s sustained vertical winds that temporarily will displace the Aerobot outside of its nominal 52 to 62 km operating altitude range.
- A pump of 70% efficiency for transferring helium against the balloon's internal pressure gradient.
- Venus atmosphere properties are from the standard VIRA model supplemented with optical and IR flux values from: Robinson, Tyler D. and Crisp, D., Linearized Flux Evolution (LiFE): A technique for rapidly adapting fluxes from full-physics radiative transfer models, J. Quant. Spect. Radiat, 2018.

Table A-33: Variable Altitude Balloon Design parameters for a 200 kg gondola mass.

Zero Pressure balloon diameter	14 m
Superpressure balloon diameter	8.2 m
Zero Pressure balloon mass	91 kg
Superpressure balloon mass	60 kg
Total balloon mass	151 kg

Mass allocation for helium pump and valve system	5 kg
Helium mass (both balloons combined)	38.8 kg
Total floating mass (balloon+gondola+pump system, not counting helium)	356 kg
Pumping energy to descend 62 to 52 km (in daylight)	2,000 W-hr
Pumping energy to descend 62 to 52 km (in darkness)	1,080 W-hr

An important update from the VFM Aerobot design for ADVENTS was using an inflation system design that operated at 6,000 psi vs. the 10,000 psi operation of VFM. This update allows lower cost off the shelf tanks, pump, and lines reducing the overall cost of the system. However, the lower pressure resulted in the need for additional He tanks which increased the volume and mass that had to be accommodated in the Entry Vehicle. This drove an increase in size of the Entry Vehicle.

### A.3.1.3.3 Communication

The Aerobot communications system operations (**Appendix A.2.3**) and the required data budgets (**Table A-19**) were discussed previously.

The Aerobot has a Thales S-Band Transponder and toroidal S-Band low gain antennas. **Table A-34** shows the communication link between the Aerobot and the Orbiter. As mentioned in **Appendix A.2.3** communication between the Orbiter and Aerobot is restricted to elevation angles 30° to 60°. The lower bound of 30° is due to S-Band attenuation in the Venus atmosphere. The upper bound of 60° is due to the balloon material not being RF transparent and acting as an attenuator above 60° of elevation. All Aerobot to Orbiter links have a 2db loss applied to account for atmospheric attenuation in the allowed elevation angles. The Aerobot and Dropsonde communication diagram are shown in **Appendix A.3.2.3**, Orbiter communication.

**Table A-34:** Aerobot to Orbiter Downlink and Uplink.

From	To	Operational Frequency (GHz)	Tx Antenna	Tx Antenna Gain (dBi)	Rx Antenna	Range (km)	Information Rate (kbps)
Aerobot	Earth	2.1	Toroid	0.0	DSN 70m	2.5 x 10 <sup>8</sup>	0.006
Earth	Aerobot	2.295	DSN 70m	65	Toroid	2.5 x 10 <sup>8</sup>	0.5
Aerobot	Orbiter	2.1	Toroid	0.0	LGA	24,856.2	0.01
Aerobot	Orbiter	2.1	Toroid	0.0	MGA	24,856.2	0.033
Aerobot	Orbiter	2.1	Toroid	0.0	3 m HGA	24,856.2	8.91
Orbiter	Aerobot	2.1	LGA	0.0	Toroid	24,856.2	0.16
Orbiter	Aerobot	2.1	MGA	0.0	Toroid	24,856.2	0.55
Orbiter	Aerobot	2.1	3 m HGA	35.01	Toroid	24,856.2	14.5

The Dropsondes and entry vehicle backshell each have low power L3 Harris S-Band Transponders and titanium S-Band antennas. The Dropsonde data rate is 2.23 kbps with the Orbiter during its one hour fall to the surface. The entry system communication link with the Orbiter has a minimum link data rate of 100 bps.

All of the communication subsystem components have flight heritage or are under development for future flight systems.

### A.3.1.3.4 Power

The Aerobot power system consists of solar arrays, a secondary battery, and supporting power electronics. The Aerobot mission requirement is 60 days in the Venusian atmosphere at various altitudes and positions around the planet. To conserve power the instruments are used per the operations concept (**Appendix A.2.4.2**). The instrument power usage for the different modes: Day, Night and Standby are shown in **Table A-35**. The Aerobot

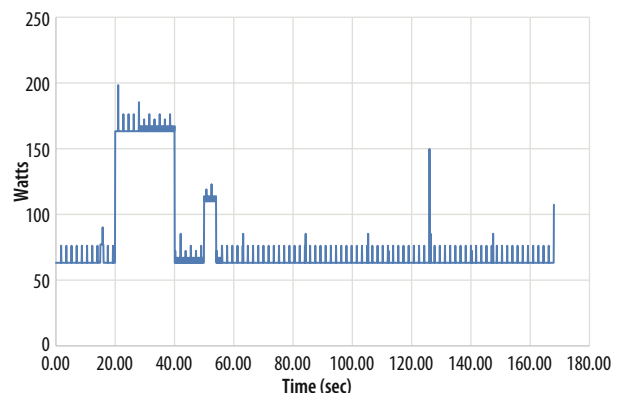


**Figure A-54:** Aerobot Power Profile.

VS048

avionics and He pump power by mode are shown in **Table A-36**. The instrument power and Aerobot avionics and He pump power were used to create the 7 day Aerobot power profile shown in **Figure A-54**.

**Table A-35:** Aerobot Instrument Power by mode.

	Day Ops Power [W]			Night Ops Power [W]			Standby Power			Operations
	CBE	Contingency	MEV	CBE	Contingency	MEV	CBE	Contingency	MEV	
Instrument	[W]		[W]	[W]		[W]	[W]		[W]	Frequency
Aerosol Mass Spectrometer										
- Nephelometer	7	30.0%	9.1	7	0.3	9.1	0	0.3	0	On 7 minutes every 105 minutes at 9.1 W
- Isotopic Measurements	7	30.0%	9.1	7	0.3	9.1	0	0.3	0	On 7 minutes every 28 hours at 9.1 W
Fluxgate Magnetometer	1.0	30.0%	1.3	1.0	0.3	1.3	1.0	0.3	1.3	Continuous
Atmospheric Meteorological Temperature (AMET)										
- Pressure	3	30.0%	3.9	3	30.0%	3.9	3	30.0%	3.9	Continuous
- Temperature, Winds Nominal	3.5	30.0%	4.6	3	30.0%	3.9	0	30.0%	0	On 1 minute every 105 minutes for 3.9 W Increased sampling rate around Venus Local Noon as shown below.
- Temperature, Winds around Noon	3.5	30.0%	4.6	3	30.0%	3.9	0	30.0%	0	On 1 minute every 30 minutes for 28 hours centered around Venus local noon. Power here is total for measurements – don't double book previous line during the 28 hour period.
Mini TLS	24.0	30.0%	31.2	24.0	0.3	31.2	7.0	0.3	9.1	5 minutes every 28 hours (24 W) for total of 4 times in Venus day and only 1 at Venus night. No second measurement at night. Scrubber bakeout once every 5 days for 1 hour (14 W day only)

**Table A-36:** Aerobot avionics and He pump power by mode.

Unit	Day Ops Power [W]			Night Ops Power [W]			Standby Power			Operations
	CBE [W]	Contingency	MEV [W]	CBE [W]	Contingency	MEV [W]	CBE [W]	Contingency	MEV [W]	
S-band Transponder	52	10%	57.2	52	10%	57.2	8	10%	8.8	4 hours each day during Venus day at 67.6W day, 10 minutes every 1 Venus night at 75.4 W, 8.8 W standby
IMU	2.0	10.0%	2.2	2.0	10.0%	2.2	2.0	10.0%	2.2	Continuous
LVPC	3.3	10.0%	3.6	3.3	10.0%	3.6	3.3	10.0%	3.6	Continuous
Solar Array Module	2.0	10.0%	2.2	2.0	10.0%	2.2	2.0	10.0%	2.2	Continuous
Segment Module	2.0	10.0%	2.2	2.0	10.0%	2.2	2.0	10.0%	2.2	Continuous
Low Current Output Module	3.2	10.0%	3.5	3.2	10.0%	3.5	3.2	10.0%	3.5	Continuous
PSE Monitor Card	2.2	10.0%	2.4	2.2	10.0%	2.4	2.2	10.0%	2.4	Continuous
LVPC	3.6	10.0%	4.0	3.6	10.0%	4.0	3.6	10.0%	4.0	Continuous



Unit	Day Ops Power [W]			Night Ops Power [W]			Standby Power			Operations Frequency
	CBE [W]	Contingency	MEV [W]	CBE [W]	Contingency	MEV [W]	CBE [W]	Contingency	MEV [W]	
Processor Card	3.5	10.0%	3.9	3.5	10.0%	3.9	3.5	10.0%	3.9	Continuous
Communication Card	3.0	10.0%	3.3	3.0	10.0%	3.3	3.0	10.0%	3.3	Continuous
Housekeeping Card	2.3	10.0%	2.5	2.3	10.0%	2.5	2.3	10.0%	2.5	Continuous
Harness Losses	7.0	30.0%	9.1	7.0	30.0%	9.1	7.0	30.0%	9.1	Continuous
Helium pump, 70% efficiency	77.0	30.0%	100.1	N/A	N/A	N/A	0.0	30.0%	0.0	20 hours at 100.1 W done once during day

TJGaAs solar cells with bare cell efficiency of 29.5%, a panel output of 206 w/m<sup>2</sup> within the Venusian atmosphere, and an array operating temp at 120 °C were modelled. **Figure A-54** shows the solar flux input varies from 200 W/m<sup>2</sup> at 50 km to 450 W/m<sup>2</sup> at 60 km. Not evaluated in this study is the impact due to latitudinal variations. The 206 w/m<sup>2</sup> used in the sizing of the solar array was assumed to cover the losses due to latitudinal variations at 55 km. A fixed panel with 2.1m<sup>2</sup> active area will provide 432 W EOL and 510 W BOL of power to support loads and battery recharge. A high energy density 260 AH Li Ion battery is used to support night loads. The Power System Electronics (PSE) will be a heritage 28VDC battery dominated bus included as cards in the avionics package. The PSE will control battery charging and power distribution.

The entry system power subsystem is located on the backshell and consists of a primary (non-rechargeable) battery and supporting power electronics. The power system configuration is driven by a requirement to support a load of 20W for 120 hours after release from the Orbiter plus the 4 minutes of descent time prior to backshell separation as shown in **Table A-32**. LS26500 7700 mAh 3.6V LithiumThionyl Chloride cells are used in a 9 series 16 parallel (9s14p) to provide 123.2 AH of energy at 32V. The Power System Electronics (PSE) will be a heritage 28VDC battery dominated bus included as cards in the avionics package. The PSE will control switching and power distribution.

The battery, harness, and PSE are all current state of practice and have a TRL of 7.

### A.3.1.3.4.1 Dropsonde Battery Sizing

The ADVENTS Dropsonde power system consists of a primary (non-rechargeable) battery and supporting power electronics. The power system configuration is driven by a requirement to support a load of 60W for 1 hour after release from the Aerobot. LS26500 7700 mAh 3.6V LithiumThionyl Chloride cells are used in a 9 series 1 parallel (9s1p) to provide 2.45AH of energy at 32V. The Power System Electronics (PSE) will be a heritage 28VDC battery dominated bus included as cards in the avionics package. The PSE will control switching and power distribution.

The battery, harness and PSE are all current state of practice and have a TRL of 7.

### A.3.1.3.5 Radiation

The radiation environment at Venus was analyzed. The Total Ionizing Dose (TID) and Displacement Damage Dose (DDD) is dominated by solar protons and was modeled statistically with data covering 3 solar cycles. The contribution of one transit through Van Allen belts is small and the TID and DDD environments are moderate as shown in **Figure A-55**.

The GSFC ESP model was used for this analysis. Cumulative solar proton energy spectra were calculated for 7 year requirement at 95% confidence level. Radiation transport code was used to obtain TID and DDD requirements and dose-

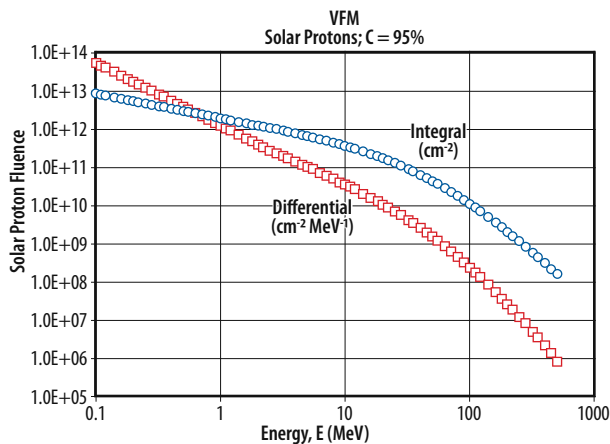


**Figure A-55:** Solar Proton Fluence.

depth curves (**Figure A-56**) were calculated with the NOVICE radiation transport code.

TID requirement for EEE parts having 7mm titanium shield is 9.4 krad (Si).

With 7 mm shielding, Aerobot lifetime is 1.04 years.

With 2.5 mm shielding, Aerobot lifetime is 81 days with TID requirement of 3.2 grad (Si). These levels are benign, and conservative given that the Aerobot is protected in the space environment by the entry system and by the substantial attenuation the Venus atmosphere provides. The Aerobot does not require any extra shielding.

With 7 mm shielding, Aerobot lifetime is 1.04 years.

With 2.5 mm shielding, Aerobot lifetime is 81 days with TID requirement of 3.2 grad (Si).

The Venus Single Event Effects (SEE) environment is generally more severe than for Earth-orbiting spacecraft but can be dealt with in part selection/testing program. Single event rates for ambient (quiet time) environment are due to galactic cosmic rays. The Moscow State University model was used. Rates are similar to lunar missions and those at L1 and L2.

Worst case single event rates (**Figure A-57**) occur during solar particle events (coronal mass ejections and solar flares). The well-known October 1989 event is used as a worst case situation (**Figure A-58**). Single event rates will be about a factor of 1.9 greater than those seen for lunar missions and at L1 and L2.

Class B mission requirements are:

- Single-event latchup
  - LETth > 75 MeV·cm<sup>2</sup>/mg at maximum temperature of 78 C for Aerobot, OR
  - LETth > 37 MeV·cm<sup>2</sup>/mg and radiation test and failure analysis per NASA Alert NA-GSFC-2005-05
- Destructive single events (single-event burn-out, gate rupture) LETth > 37 MeV·cm<sup>2</sup>/mg with proper derating applied
- Non-destructive events must be evaluated for rate and criticality of effect
  - There is no minimum LETth but it is recommended not to use circuits with LETth < 20 MeV·cm<sup>2</sup>/mg to reduce system risks
  - Mitigation techniques are often used to reduce rates to acceptable levels
    - EDAC for single event upsets in memory
    - Filtering for transients

Worst case charging environment will be encountered when passing through outer Van Allen Belt

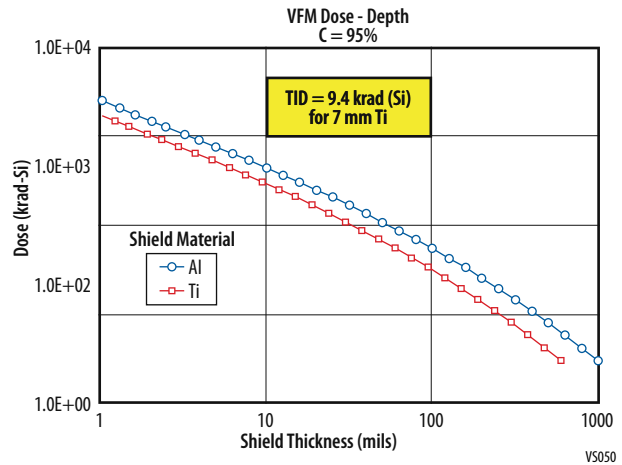


**Figure A-56:** Dose Depth.

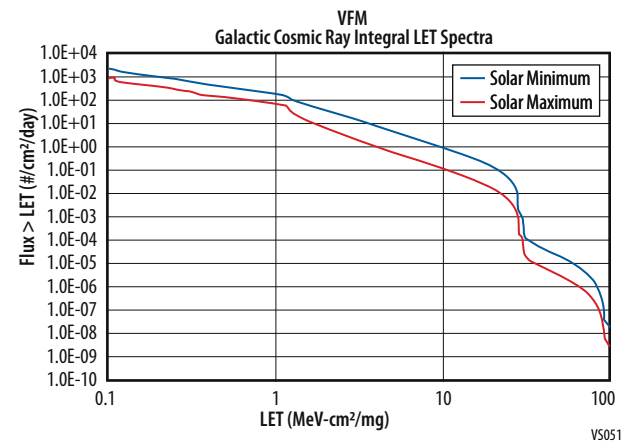


**Figure A-57:** Galactic Cosmic Ray Integral LET Spectra.

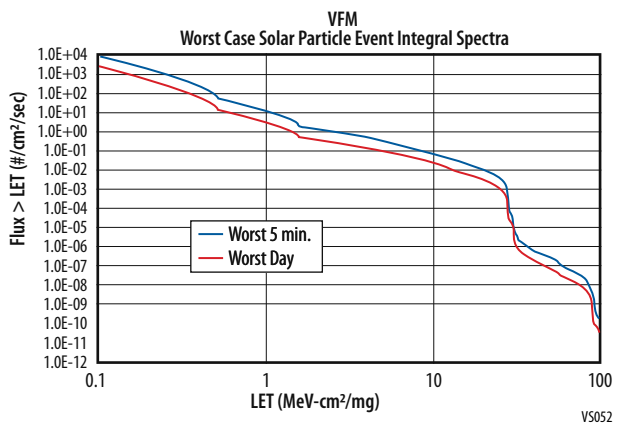


**Figure A-58:** Worst case solar particle event integral spectra.

- Calculated for Geostationary orbit at 95% confidence level using AE9 model
- Charging environment (**Figure A-59**) at Venus is due to solar wind
- Should not be significant for Aerobot due to atmospheric attenuation

The Aerobot is well protected in its Entry system during the short passage through the outer Van Allen Belt and protected by the Venus atmosphere during its operation. No single event latchups are expected.

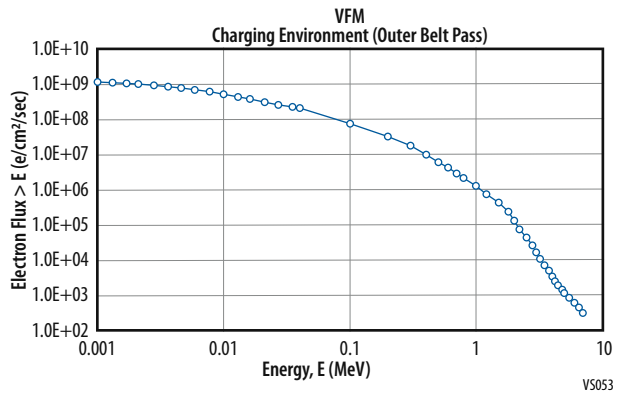


**Figure A-59:** Charging Environment.

### A.3.1.3.6 Structure

The structure design for Aerobot provides for various configurations needed for launch, flight, entry, deployment, and mission operations. Aluminum is the baseline material used for Aerobot's primary and secondary structures. All environmentally exposed materials used in Aerobot and its subsystems will require optimized coatings to mitigate corrosive, atmospheric elements which may be encountered during the mission. The Aerobot's stowed configuration (**Figure A-60**) packages the main parachute, balloon system, and main helium storage tank inside and along the centerline of Aerobot's interior structure. Four smaller helium tanks are mounted radially around the main, center tank. Aerobot's hexagonal framework and tank support structure provide for the primary load path for both launch and entry. The separation interface between Aerobot and the aeroshell is accomplished using commercial-off the-shelf [COTS] such as Lightband or RUAG separation rings. These separation rings are the current baseline for this design. All Aerobot instruments and systems are mounted both about the external faces of the main structure's honeycomb panels, as well as the inside surfaces. Signal and power harnesses will be mounted and routed on both external and internal panel surfaces. A Lightband is used to securely connect the Tank Assembly to the Aerobot and upon activation will release the entire tank assembly

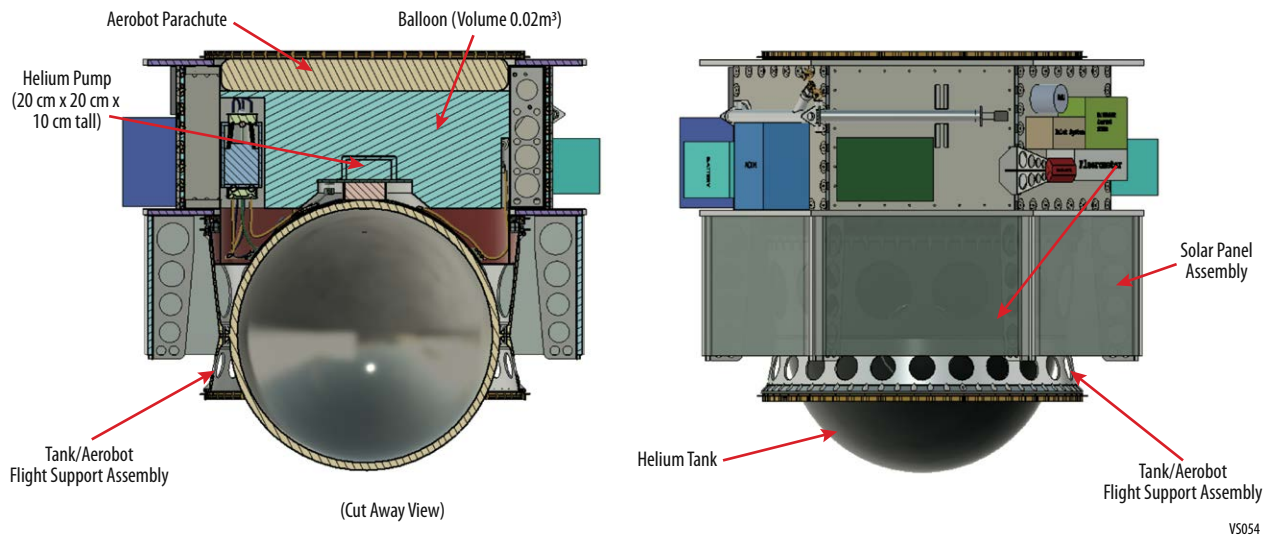


**Figure A-60:** Aerobot Structure.

#### A.3.1.3.6.1 Parachute, Balloon, Tether System Stowage

During flight and entry, Aerobot's parachute, balloon, and tether system are stowed inside the Aerobot's structure (**Figure A-61**). The folded balloon is stowed inside a canister so that the trapped helium

gas does not cause the balloon to expand once exposed to low pressure / vacuum. The canister is jettisoned during the balloon deployment. The main parachute is stowed in its packaging above the balloon canister. The drogue parachute is stowed on the exterior of the entry system back-shell as shown in **Figure A-50**.

The current design meets volume requirements for all elements described in this section. The tether system will be stowed beneath the balloon in the canister, using layered blankets and hook and loop fastener strips. These blankets and fasteners organize and manage the tether system during flight; and provide an orderly, tangle-proof, release during the balloon and tether deployment sequence.

### A.3.1.3.6.2 Tether System

The tether system is comprised of (3) three mechanical sections. Section 1 is a three-point mount from the Balloon to a union buckle. Section 2 is a single main cable that is 8m long which spans between Section 1 and Section 3. Section 3 of the tether system incorporates an inertia braking system for the deployment of the main cable in Section 2. This includes a three-point mount tether configuration between the gondola and the union buckle that is integral with inertia braking assembly.

The entire tether system is stowed inside the balloon canister, beneath the balloon, during flight. There are three swivel mounts connecting the termination of the tether system to the gondola. Additional work is needed to mitigate individual, component, sudden deceleration events and/or backlash activity during individual sequences of tether system deployment.

### A.3.1.3.6.3 Balloon Fill & Tank Assembly Separation

During entry vehicle back shell separation from Aerobot a parachute is deployed which pulls the stored Balloon from inside the Aerobot. At this time, Helium transfer will begin the balloon fill operation. Once the transfer of helium to Balloon is complete, a non-explosive actuator (NEA) will separate the balloon assembly from the helium transfer and control assembly. As the balloon lifts upward and away from Aerobot's gondola, the Aerobot tether system is deployed. Following the complete deployment of the tether system, the separation ring between Tank Assembly and Aerobot is activated. The Tank Assembly jettisons underneath and away from Aerobot (**Figure A-62**).

### A.3.1.3.6.4 Solar Panel Array

The 6-panel dual sided solar array (**Figure A-63**) provides an active surface area of 3.18 m<sup>2</sup>. The requirement is 2.1 m<sup>2</sup>. The outward facing surface of the array provides

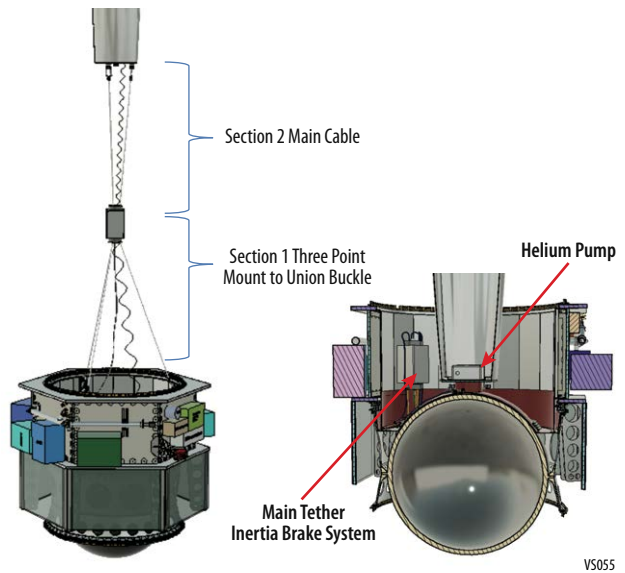


**Figure A-61:** Aerobot Tether System.

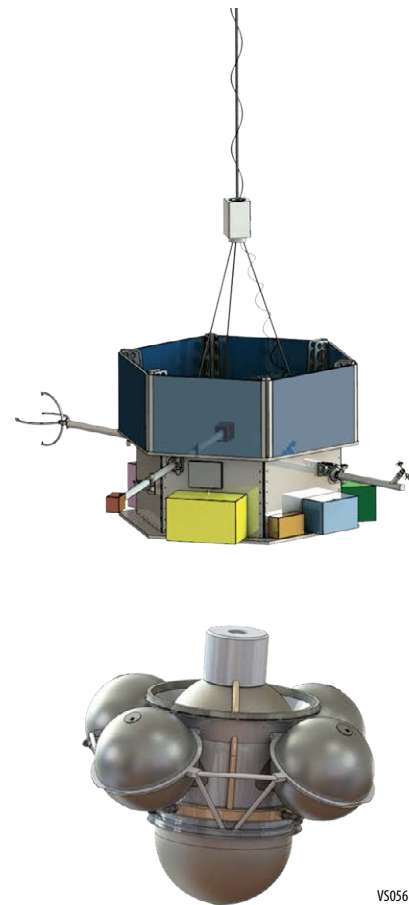


**Figure A-62:** He Tank separated from the Gondola.

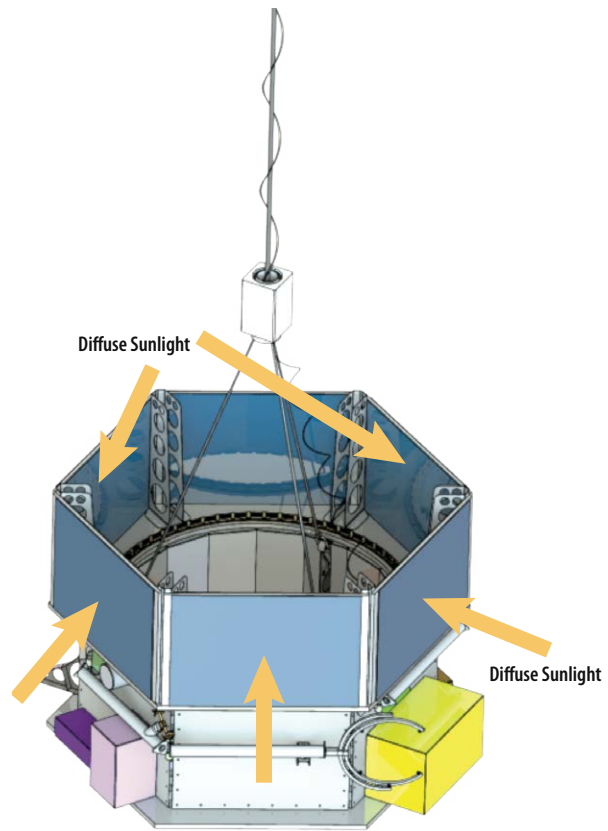
a physical area of 1.614 m<sup>2</sup>. The obverse side provides an additional surface area of 1.566 m<sup>2</sup>. The solar array is fixed and does not require deployment. This structure is also isolated from flight and entry load paths. The Solar Array Assembly brackets are designed to protect the arrays and serve as passive guide rails for the back-shell mount ring during back-shell separation.

### A.3.1.3.6.5 Deployable Structures

There are three simple hinge/drive/latch deployable booms which extend away from Aerobot (**Figure A-43**). The wind sensor and Antenna are on a shared boom. Antenna two is on a separate boom. The third boom deploys the Magnetometer. The current design for the three deployable booms and their respective release mechanisms are notional. Detailed design of these would be future work, but all are well within the state-of-the-art.

#### Key Trades and Design Efforts

- Gondola
  - Configuration of instruments
  - Instrument packaging trades
  - Parachute and Balloon packaging
  - Exterior Canister design (load path difficulties, mass)
  - Interior Canister design (utilizes existing structure, simplifies load path)
- Tether Systems for Scientific Instruments
  - Research existing space flight and airborne Earth deployment systems
  - Single Tether with mechanism and electronic controls
- Aeroshell
  - Design study to increasing the size and profile of the Venus Entry Vehicle [VEV]
- Deployable Systems
  - Iterative design study for mass and deployment
- Dropsonde
  - Iterative design study for mass, pressure and deployment of scientific payload to measure chemicals, temperature and pressure
  - Various mount and deployment from Aerobot options were explored
- Solar Array Assembly
  - Design study for relocation of the assembly from earlier design
  - Maintained simplified mounting to gondola, no mechanisms or deployment
- Antenna
  - Design study to accommodate short term communications antenna, integrated into back-shell
- Tow Body System
  - Concept development and integration/mount locations within existing gondola design
- Helium Tank System
  - Design iteration to accommodate increase in helium mass and decrease in tank pressure
  - Additional tank assembly structure design iteration and optimization of design for mass.



VS057

**Figure A-63:** Diffuse sunlight reaches the inside panels of the solar array.

### A.3.1.3.7 Thermal

The Aerobot operates in the atmosphere of Venus at altitudes ranging from 52 km to 62 km above the surface. Ambient conditions vary greatly over this altitude range. As altitude decreases, the temperature and pressure of the atmosphere increase, while the solar flux decreases due to attenuation by the clouds. The solar flux is roughly omnidirectional, due to high light scattering by the clouds. **Figure A-64** and **Figure A-65** show the ranges of ambient temperatures and solar fluxes.

Primary operations take place at 55 km altitude and above. Lower altitudes (52-50 km) may be used for short term operations and are assessed here for survival limits.

The Aerobot consists of a six-sided gondola suspended from a balloon. Instruments and equipment are mounted in boxes on the sides of the gondola. The thermal control system for the Aerobot must maintain all components within their temperature limits. **Table A-37** lists available temperature limits for the Aerobot instruments. For other components, a temperature range of 20 °C to +50 °C for operations and 30 °C to +60 °C for survival was assumed for assessments.

**Table A-37:** Temperature limits for Aerobot instruments.

Instrument	Temperature Limits
AMS-N	Op: -40 °C to +80 °C
Flux Mag	Op: -180 °C to +80 °C
AMET	Op: -40 °C to +80 °C

To keep the components within temperature limits, the thermal control system must dissipate heat generated by the equipment and mitigate solar heating. The design uses an approach similar to what was developed for the Venus Flagship Mission (VFM). It employs passive approaches to thermal control in order to minimize mass, volume, and power requirements. Exterior surfaces of the Aerobot are painted with Z93C55 white paint to reflect sunlight and radiate heat to the environment. Thermistors on the instruments and electronics boxes provide temperature monitoring. No heaters are required. **Figure A-66** shows the thermal model of the Aerobot.

The thermal control system operates passively. White Z93C55 paint on exterior surfaces reflects sunlight while promoting radiative heat transfer to the environment. Instruments and electrical boxes are externally mounted on the sides of the Aerobot, which promotes convective cooling. Thermistors provide temperature monitoring.

While the thermal control system is designed around passive techniques, additional thermal control is possible through adjustment of operations. Temperature decreases at higher altitudes, and the

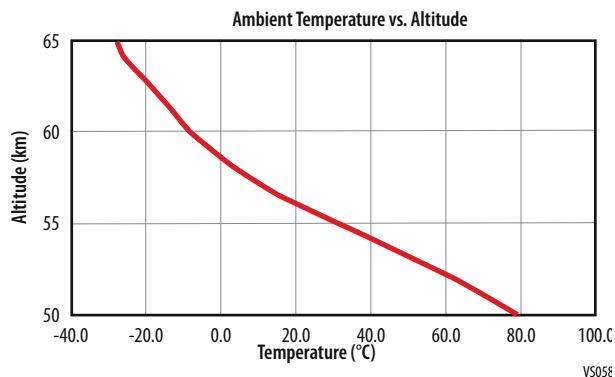


**Figure A-64:** Atmospheric temperature of Venus across Aerobot altitude range.

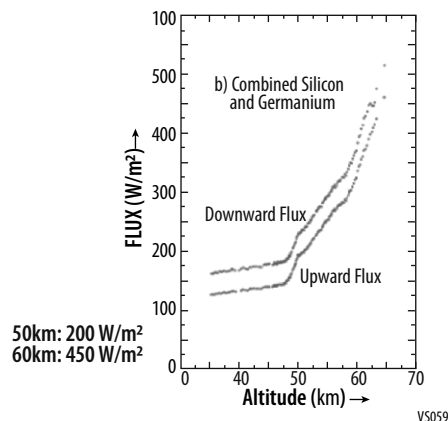


**Figure A-65:** Variation of solar flux with altitude in the Venus atmosphere.

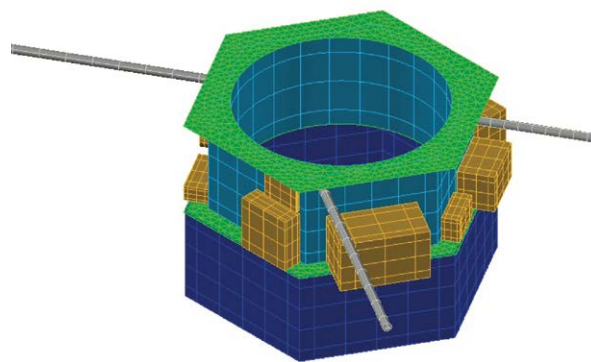


**Figure A-66:** Thermal model of the Aerobot.

Aerobot can ascend passively, so if conditions are too hot the Aerobot can ascend to a cooler altitude without requiring energy input. If a particular electrical box overheats during operation, it can be turned off until it cools.

The thermal model was used to run analysis cases for the worst case hot and cold conditions. These include daytime operations at 55 km at the equator (high ambient temperature, low solar flux), daytime operations at 62 km at the equator (low ambient temperature, high solar flux), daytime survival at 52 km, and nighttime survival at 62 km. In the analysis cases, the relative wind speed is assumed to be 1.5 m/s for purposes of convective heat transfer. Operational cases assume all components run continuously at MEV operational power levels, which is highly conservative. **Figure A-67** to **Figure A-70** show the steady state temperature distributions for these analyses.

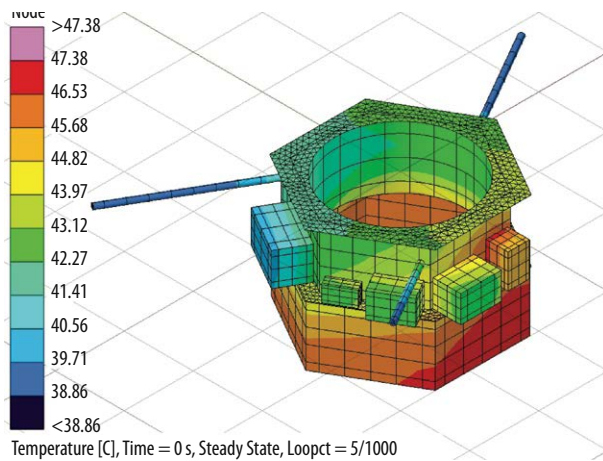


**Figure A-67:** 55 km altitude (29.2 °C ambient T, 200 W/m<sup>2</sup> solar flux).

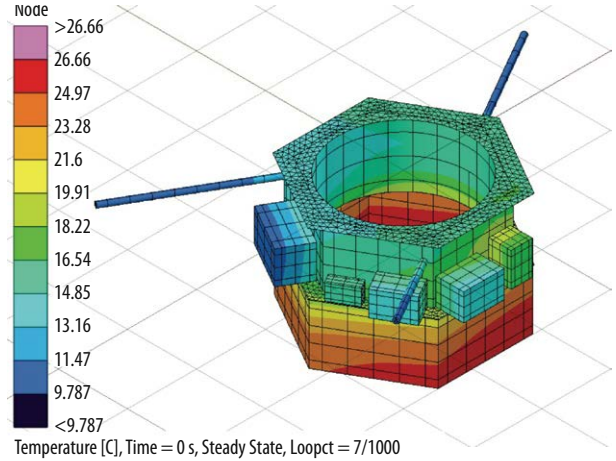


**Figure A-68:** 62 km altitude (-18.7 °C ambient T, 450 W/m<sup>2</sup> solar flux).

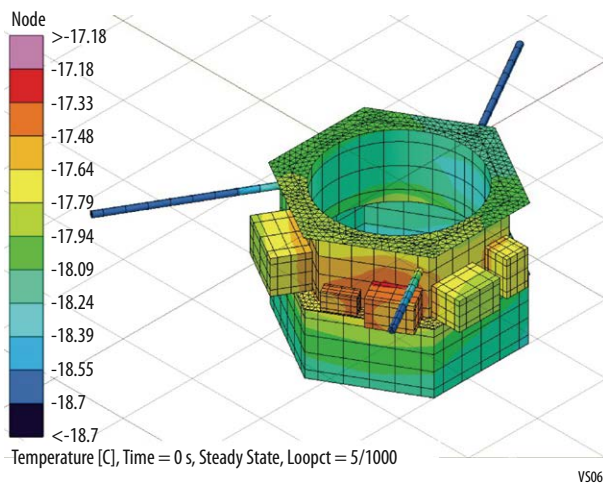


**Figure A-69:** Cold survival case: 62 km altitude (-18.7 °C ambient T, night – no solar flux).

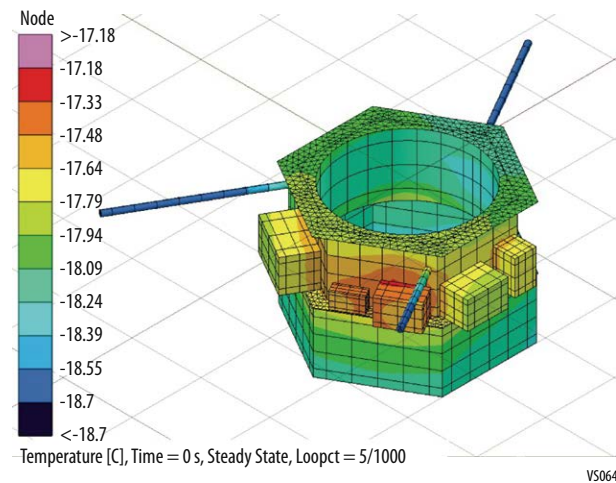


**Figure A-70:** Hot survival case: 52 km altitude (60.2 °C ambient T, 200 W/m<sup>2</sup> solar flux).

Both operational cases fall within acceptable temperature limits, even with the added conservatism of continuous MEV power levels. The cold survival case at 62 km also stays above minimum temperature limits—temperatures are high enough that full operation would also be possible at these conditions. The hot survival case at 52 km has temperatures that are likely above acceptable limits. Components would need to be qualified up to approximately 72 °C for these conditions, or the Aerobot should remain above this altitude.

All thermal hardware used on the Aerobot is TRL 9. The thermal coating (Z93C55 white paint) is standard thermal coating used at Goddard for many missions. Thermistors are all TRL 9.

No major thermal trades were done for the Aerobot. Based on the analysis results, 55 km operation is acceptable, but the lower elevation limit should be higher than 52 km unless components can be qualified to the necessary temperatures. Limiting operations at lower elevations to nighttime would remove solar flux, allowing somewhat lower altitudes to be accessible while remaining within temperature limits.

Convection coefficients, based on relative wind speed between the Venus atmosphere to the Aerobot electronics, are highly variable. The convection coefficient scales with the square root of the relative wind velocity or atmospheric density, *i.e.*, a fourfold increase in wind velocity will double the convection coefficient. For our mission cases, higher convection coefficients are beneficial as they promote convection cooling of the Aerobot. At our intended operating altitudes, absolute wind velocities range from 40-110m/s. The relative wind velocity will be determined by the aerodynamics of the balloon and gondola, with higher drag producing larger relative wind velocities and therefore better convective cooling. For conservatism, our analysis assumed a fairly low convection coefficient based on a relative wind velocity of 1.5m/s.

### A.3.1.4 Dropsonde

During the study, a series of design concept iterations were produced for Dropsonde. A sample of some of these can be seen in **Figure A-71**. Throughout the trade study, instrument and equipment requirement changes were incorporated and/or descoped from each iteration. Several pressure vessel design concepts were examined, as well as, various methods of internal and external insulation to mitigate effects of pressure and temperature. While additional work is required to refine the current baseline design concept, the current design falls within the state of the art and applied rules of thumb are sufficient to meet requirements and to estimate mass and cost.

The baseline Dropsonde (**Figure A-72**) is a scientific instrument package housed in a sealed pressure vessel. While the entry vehicle back-shell is still connected to the Gondola, the Dropsonde will be released from the Aerobot Gondola. During Dropsonde descent to the surface of Venus, various instruments will measure atmospheric chemicals, temperature, and pressure. Simple, passive fins rotate a bearing mounted plate which opens and closes a pass through to refresh the flow of atmosphere across chemical sensor. This rotating plate provides a surge of different atmosphere at timed intervals during the Dropsonde's descent to the surface.

Dropsonde uses a combination of pressure vessel, insulation, and phase change material to mitigate the effects of outside temperature and pressure. The driving design factors were *in situ* high temperatures (900 ° F) and pressure (92 Bar) and duration of exposure to the harsh environ-



**Figure A-71:** Dropsonde design iterations.

VS087

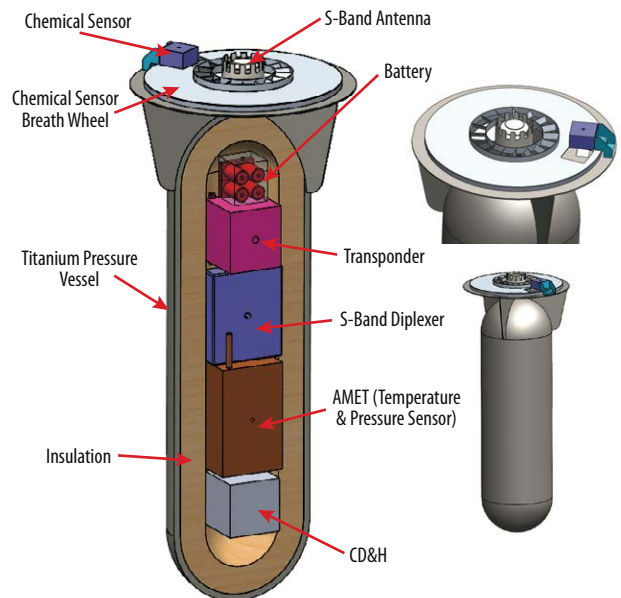


**Figure A-72:** ADVENTS Dropsonde.

VS065



ment. Additional work is required to refine the overall concept and design.

Traditional pressure vessel design rules of thumb were utilized, and the overall design concept is within the state of the art. The design concept was compared to work done by Izraelvitz and Hall on “Minimum-Mass Limits for Streamlined Venus Atmospheric Probes” and found to be mass conservative. Additional design iterations using the principles from Izraelvitz and Hall should provide substantial improvement in the design concept. A simple mount and release mechanism in the design is notional and will require additional work. Preliminary analysis of Dropsonde ballistic characteristics, estimate a descent time of approximately 30 minutes. Further work is required to modify the Dropsonde to extend this descent time to 60 minutes.

The Dropsonde free falls through the Venus atmosphere from an altitude of 64.6 km to the ground over a period of less than one hour, and conducts scientific operations during descent. As it falls, it encounters progressively higher temperatures and pressures at lower altitudes, as shown in **Figure A-73**. Over most of the altitude range, ambient temperatures are expected to exceed survival temperatures for electronics.

The thermal control system for the Dropsonde must protect sensitive components from the excessive temperatures of the environment, keeping components within temperature limits long enough for the Dropsonde to reach the ground and complete its mission. The thermal control system is designed to do this passively. The equipment decks include supplies of phase change material to maintain a stable temperature for the equipment. The equipment decks are mounted on the pressure vessel shell with thermal isolators, in order to limit heat leak via conduction. The interior of the shell is lined with a silica insulation to slow the flow of heat from the environment. The interior of the pressure vessel is under vacuum, which optimizes the insulation performance and reduces convective heat transfer.

Analysis of the Dropsonde thermal performance used n-icosane for the phase change material (melting point = 37 °C), and LI-900 for the insulation material, though aerogel is another viable option. The Dropsonde was assumed to fall at terminal velocity, which gives the altitude and temperature timeline shown in **Figure A-74**.

While the interior of the Dropsonde is nominally covered with insulation, a small uninsulated area of 3 in<sup>2</sup> was also included in the analysis to account for instrument ports, gaps in the insulation, and other sources of heat leak. Analysis showed that an insulation thickness of 12.5 mm and 6.6 kg of phase change material kept the Dropsonde interior at a stable temperature for the entire descent, while occupying the minimum amount of volume.

The thermal control system operates passively. Insulation on the interior of the pressure vessel slows the transfer of heat from the hot environment to the pressure vessel interior. Thermal isolators are used to mount the equipment decks to the shell to limit conduction of heat in. The interior of the pressure vessel is under vacuum to optimize the insulation performance and limit convection. Phase change material in the equipment decks absorbs heat generated by the electronics and flowing in from the environment, and keeps the equipment at a stable temperature.

All thermal hardware has a generally high TRL level. Phase change material has been used in the

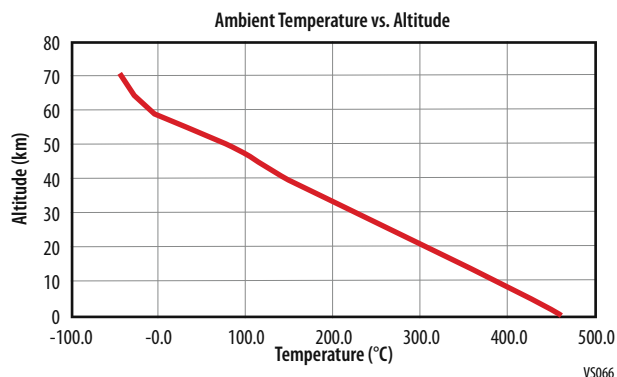


**Figure A-73:** Temperature variation with altitude in the Venus atmosphere, over the range traversed by the Dropsonde.

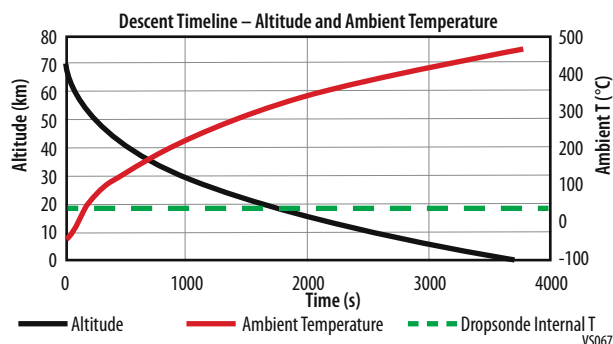


**Figure A-74:** Analysis timeline of altitudes and temperatures during Dropsonde descent.

space industry, but this exact PCM has not been used at Goddard (but has been used elsewhere). Silica and aerogel insulations have long histories in space applications.

Analysis was performed to determine the insulation thickness that would result in a minimum total volume for the thermal control system. Increasing the insulation thickness can reduce the amount of phase change material required, or add margin. Increasing the quantity of phase change material can likewise add margin, or allow additional time for operations.

While descending to the Venus surface is inherently risky, there are thermal risks worth mentioning:

- 1) If the Dropsonde develops a leak, vacuum will be lost and convection inside the sphere will heat up the electronics faster than expected. Silica insulation is less effective at higher pressures but will still provide benefit.
- 2) Thermal testing of the flight article is difficult to perform under the GOLD rule “test as you fly”, as the article is expected to overheat and fail shortly after reaching the hottest temperatures on the ground. A partial test can be performed.

### **A.3.1.5 Towbody**

#### **A.3.1.5.1 Background**

The tethered towbody is a payload concept that can extend imaging capabilities below the cloud layer on Venus for direct observation of the surface. The Venus Aerial Platform Study (Cutts *et al.*, 2018) first made the scientific case for subcloud imaging. More recently, the VeCaTeX decadal white paper (2020) proposed a variable altitude balloon that could descend below the clouds and is now being pursued by Paragon and Thin Red Line through a NASA SBIR. The towbody concept has also been presented as a reduced complexity and risk alternative to a balloon descent during the 2020 VEXAG meeting. The towbody was evaluated as part of the architecture trade for this study and the design shown below developed. As discussed in the trade section, the towbody was not included as part of the ADVENTS baseline.

#### **A.3.1.5.2 Motivation**

Extending our knowledge of the nature and evolution of Venus below the cloud layer, including active and past volcanism and other geologic processes at the surface as well as any potential to harbor life in the clouds, is limited due to the lack of in-situ, long-duration exploration technologies. While a balloon observatory can be deployed within the cloud layer (Hall, J.L. *et al.*, 2009), it would need to maintain a mid-range altitude of 52-62 km to avoid exposure to extreme temperatures ( $> 100\text{ }^{\circ}\text{C}$ ) and maintain access to viable solar for power (Hall, J.L. *et al.*, 2019). Yet, due to cloud scattering and atmospheric attenuation through the lower, turbulent cloud layer, in-cloud imaging of the surface is limited to tens of km in resolution. More than a thousand-fold improvement, down to 10-m-resolution for IR imaging of the nighttime surface, appears favorable (Davis, A. *et al.*, 2020), but requires deploying a camera to  $\sim 47$  km. Several concepts for reaching these altitudes from a balloon include dropped payloads (Klaasen, K.P., and Greeley, R., 2003), rotorcraft (Husseyin, S., and Warmbrodt, W.G., 2016), and tethered towbodies (Horzempa, P., 2020). The towbody approach is advantageous because it extends the reach of a balloon mission to sub-cloud regions using a supportive tether, which repeatedly lowers and retracts a suite of instruments to i) obtain measurements at a range of altitudes over a large spatial area (versus a single location observed by a dropped probe), ii) maintain altitude-based temperature control for sensitive electronics, iii) preserve the balloon's capability for solar power and keeping standard instrumentation at a safe altitude and temperature ( $< 80\text{ }^{\circ}\text{C}$ ), and iv) provide reliable, real-time optical communication through the cloud layer.

#### **A.3.1.5.3 Concept**

Based on recent design and analysis work conducted at JPL, we have created a conceptual towbody and tether design for the ADVENTS mission. The towbody is a 4-kg, low-drag, aerodynamic vehicle that self stabilizes using a gimbal system and is deployed from a balloon gondola on a high-strength, sub-mm-diameter tether with an internal optical communication link. A gondola-side spool is used

for a controlled descent of towbody to the target altitude of 47 km, where an IR camera can directly image the night-time side of Venus. At 47 km the ambient temperature is 100 °C. Accordingly, the towbody is constructed with a vacuum-sealed, thermal-insulation shell that limits heat flow. Phase Change Materials (PCM) and Multi-Layer Insulation (MLI) are used to keep the internal temperature of the towbody < 35 °C for ~2 hours at 47 km altitude to allow for periodic IR imaging along a swath of terrain. Once an internal target temperature is reached, the towbody is reeled in over the course of several hours while it cools. Finally, the towbody is retracted into the gondola for stowage and charging of internal batteries. While docked, the insulated shell prevents residual heat from flowing back into the gondola while the towbody slowly and continually cools to refreeze PCM materials at a temperature < 27 °C. The process is repeated every ~5 days corresponding to Venus' day/night cycle, with the towbody deploying during the night for optimal imaging.

### Validation

Models for different tether types are shown in **Figure A-75** for different altitudes at 52 km (left) and 55 km (right) down to 47 km. Wind shears are calculated from the VIRA model (Seiff, Alvin, *et al.*, 1985) ignoring potential turbulence. The parameters shown for each plot are tether diameter (D), deployed length (L), mass (M), tension (FT), and factor of safety (FoS). The tethers modeled are commercial, off-the-shelf optical cables for underwater usage. The red tether is preferred and would need to be 10-30 km in length depending on the deployment altitude. We expect that a customized version of this tether would yield a higher strength-to-weight ratio and provide > 4 factor of safety in order to account for turbulence-based tension.

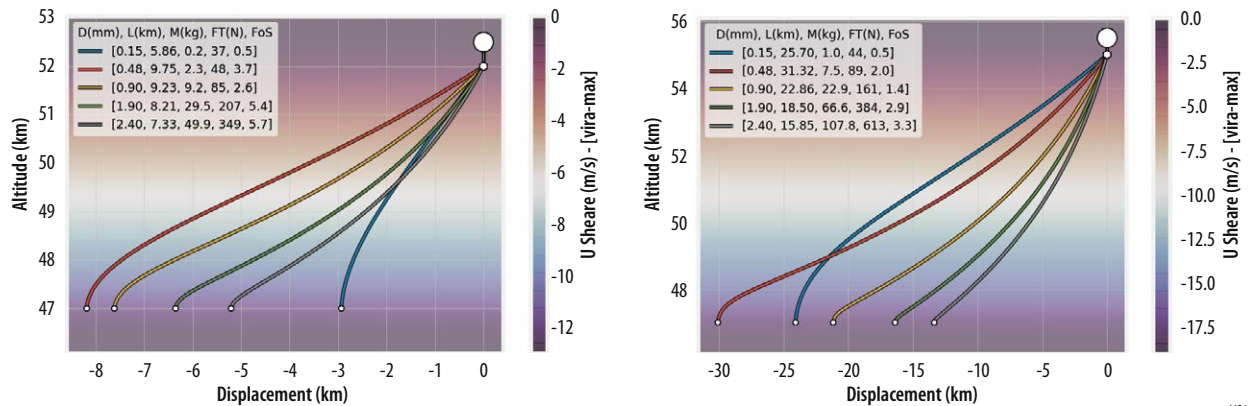


**Figure A-75:** Tether modeling in the Venus atmosphere.

### A.3.1.5.4 Design and Accommodation

A notional design for a towbody and its accommodation to the ADVENTS gondola are shown in **Figure A-76**. The towbody houses a down-ward pointing IR camera that is of similar form factor and mass to the EE cameras currently in use on NASA's Perseverance Rover. Image processing and data handling require an on-board computer on both the towbody and the gondola side. Optical communication allows for data rates up to 1 Gb/s the length of the tether and will be routed through an optical slip ring on the gondola side. The accommodation volume for the gondola is illustrated in **Figure A-76** by a red body for which the towbody fits with sufficient margin. Preliminary mass and power numbers are provided in **Table A-38**, which support the 4 kg, low-power payload. Note that these numbers are a first cut and should be considered notional.

**Maturity:** The towbody concept consists of elements that are mid-to-high TRL but little testing has been done in a Venus relevant environment. The payload as a system is early TRL 2-3 but we have identified the key technical challenges that are in need of development prior accommodation of this payload:

- IR Camera: TRL-9 EE Camera needs modification to work for IR spectrum with potential changes to packaging and operation.

- **Towbody Stability:** Passive stability for the towbody's IR camera is desired but rotational requirements (100 urad / 100 ms in pitch/roll, 3800 urad / 100 ms in yaw) may require an active controlled approach. Further effort will be required to develop and test such a system beyond our notional 'torpedo' design that guarantees the required stability.
- **Towbody Thermal Management:** We have shown a passive approach to maintain safe temperatures for the camera while imaging, but more development is required to specify exactly how long we can maintain the 47-km deployment altitude and by what means.
- **Tether Management:** Robustness to fouling over many reeling cycles and tensions during deployment are key risks that need to be addressed in design, test, and operation.

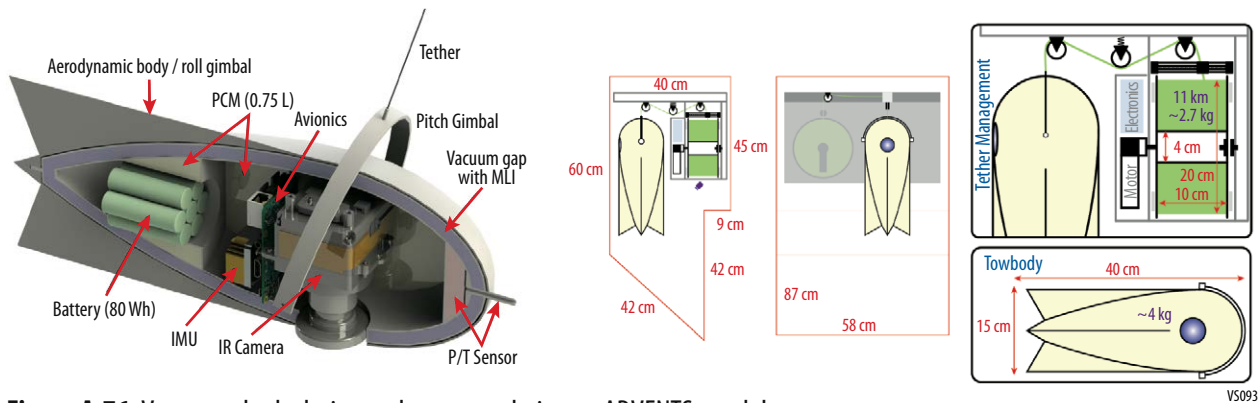


**Figure A-76:** Venus towbody design and accommodation on ADVENTS gondola.

**Table A-38:** Payload Master Equipment List (MEL) and Powered Equipment List (PEL).

Venus Towbody MEL & PEL				
	Equipment	Mass (kg)	Power (W cont.)	Power (W peak)
Towbody	Battery	0.4	-	-
	Camera	0.6	1.0	3.0
	Computation (includes comms)	0.4	0.5	1.0
	IMU	0.1	0.1	0.5
	Structure	1.5	-	-
	Thermal (MLI+PCM)	0.8	-	-
	<b>Towbody Total</b>	<b>3.8</b>	<b>1.6</b>	<b>4.5</b>
Tether System	Computation (includes comms)	0.4	1.0	3.0
	Encoder(s)	0.1	0.1	0.2
	Level Winder	2.0	-	-
	Motor + Gearing + Clutch + Controller	3.0	15.0	30.0
	Optical Slip Ring	0.02	-	-
	Structure	5.0	-	-
	Tether (11 km)	2.7	-	-
	Tether Harnessing	1.0	-	-
	Thermal (MLI)	0.5	-	-
	<b>Tether System Subtotal</b>	<b>13.72</b>	<b>16.10</b>	<b>33.20</b>
<b>Totals</b>	<b>17.47</b>	<b>17.70</b>	<b>37.70</b>	

### A.3.2 Orbiter

The ADVENTS Orbiter (**Figure A-77**) functions as a carrier for the Aerobot, a communication relay for the Aerobot and Dropsonde as well as a science platform. **Table A-39** shows the Orbiter subsystems masses and power as well as the total Orbiter mass. The instruments on the Orbiter are listed in **Appendix A.3.1.1** along with their mass, power and mission data rates.

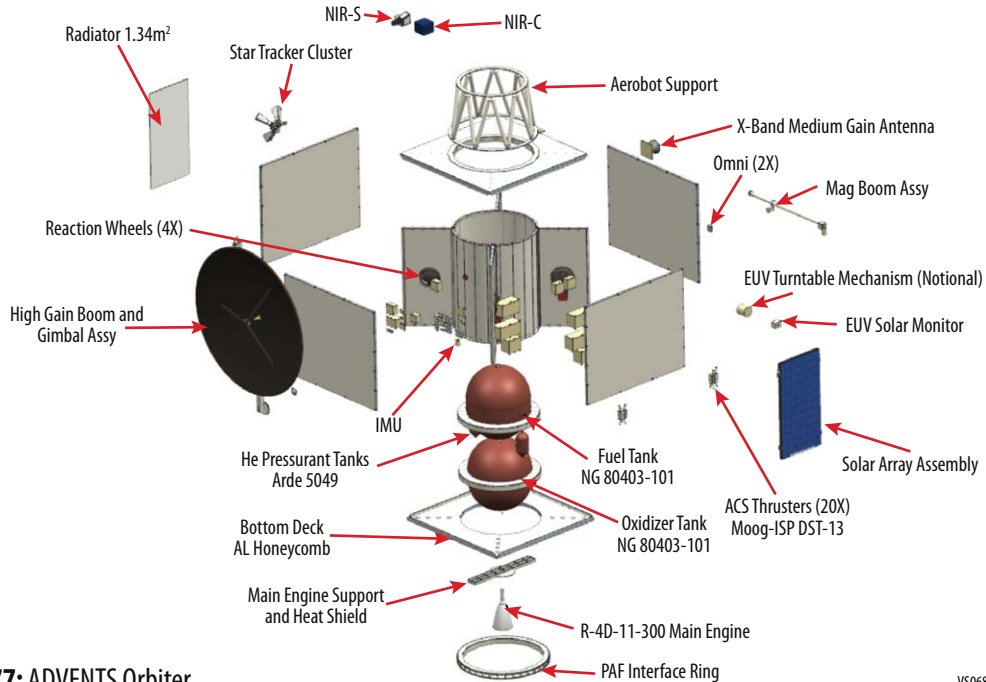


**Figure A-77:** ADVENTS Orbiter.

VS068

**Table A-39:** Orbiter Mass and Power.

	Mass			Average Power		
	CBE (kg)	% Cont.	MEV (kg)	CBE (W)	% Cont.	MEV (W)
Structures & Mechanisms	568.7	30	739.3	N/A	N/A	N/A
Thermal Control	23.1	10	25.4	N/A	N/A	N/A
Propulsion (Dry Mass)	243.4	7.5*	261.6	N/A	N/A	N/A
Attitude Control	85.9	10	94.5	104.3	30	135.6
Avionics	59.6	10	65.6	166.5	30	216.5
Telecommunications	46.8	11.3	52.0	671.0	30	872.3
Power (includes harness)	197.6	10	217.4	0.3	30	0.4
<b>Total Spacecraft Bus</b>	<b>1,225.1</b>	<b>18.8</b>	<b>1,455.8</b>	<b>942.1</b>	<b>30</b>	<b>1,224.73</b>

\*Propulsion mass includes pressurant and residual propellant that have no contingency applied. Excluding these items results in the Propulsion subsystem having 10% contingency

The Orbiter structural design was driven by carrying the launch load of the Aerobot to the launch vehicle. The Aerobot is mounted on top of the Orbiter using the Aerobot support structure. The Orbiter structural radials are the transition load path from the 3.1 m interface to the launch vehicle and the central cylinder, which carries the launch loads for both the Orbiter and the Aerobot. The basic structure of a central cylinder, upper and lower deck, radials and equipment panels is very common and well understood. A Master Equipment List (MEL) was developed and contingency was assigned at the component level based on TRL. Those items that have flown before and required no modification with a high TRL were assigned a contingency of 10%. Items that had to be modified were assigned 20% and new items or those that required significant modifications were assigned 30%. All structural items were assigned 30%. The total system has 13% Launch mass margin on the Wet Mass. A conservative approach was taken with Power and 30% contingency was used on all loads.

The Orbiter power system consists of solar arrays, a secondary battery, and supporting power electronics. TJGaAs solar cells with bare-cell efficiency of 29.5% are used. The solar constant at Venus is 2263 w/m<sup>2</sup>, and the arrays operate at 140 °C. Space Environmental Effects and Education System (SPENVIS) solar array degradation factors were used to derive the array area. A single two axis tracking

panel with 5.4 m<sup>2</sup> active area (5.9 m<sup>2</sup> total substrate area) will provide 1,845 W EOL and 2181W BOL of power to support loads and battery recharge. A high energy density 38AH Li Ion battery is used to support night loads. The Power System Electronics (PSE) will be a battery dominated bus included as cards in the avionics package. All Orbiter power components are greater than TRL 7.

The avionics for the Orbiter are a block redundant system to meet the reliability for a Class A Flagship Mission. The avionics consists of the following functions: Command and Data Handling (C&DH), attitude control sensors and thrusters, power conditioning and distribution, mechanisms for launch locks, deployments and motors, and control of main engine propulsion. The avionics implementation consists of three enclosures, C&DH Unit, the Power System Electronics (PSE) and the Mechanism, and Propulsion Unit (MPU) and is detailed in **Appendix A.3.2**. All avionics components are TRL 7 or greater with significant heritage.

The Orbiter, for most of the mission, functions as a communication relay between Earth and the Lander, and the Aerobot. The Orbiter utilizes a store and forward protocol called Delayed Tolerant Network (DTN), which has the ability to store packets from the Dropsonde and Aerobot and then forward them to Earth or receive commands from Earth and forward them to the Aerobot.

The Orbiter is three-axis stabilized with significant momentum and torque capabilities to account for the large inertia associated with the stacked configuration. The Orbiter ACS design is discussed in **Appendix A.3.2.2**. All of the ACS components have significant flight heritage and meet the life mission requirement.

The VFM Orbiter thermal design has radiators on the Orbiter -z surface, bottom deck, to dissipate electronics heat while keeping the radiators out of the Sun (and view of the hot Venus surface). During cruise phase, the attached aeroshell will somewhat cover the radiators' view to space, but no enhancements to the thermal system are needed; the radiators can still dissipate the requisite cruise phase heat. A 'toasty' cavity approach eliminates Propulsion system heaters on the Prop tanks and lines while orbiting Venus.

### A.3.2.1 Instruments

The Orbiter carries four science instruments (**Table A-40**). The first is a NIR-S to determine rock types at different geologic regions such as the tesserae. NIR-S is designed to use Venus's NIR atmospheric windows to map the surface emission and is outfitted with 4 channels for surface emissivity, 3 channels for near surface water, 4 channels for cloud decontamination, and 3 channels for characterizing the stray light within the instrument. NIR-S will primarily be operational during the nighttime, but a few channels will be implemented on the dayside to help with cloud characterization.

The second instrument is the NIR-C which is nadir pointed and provides contextual imaging of the altitudes encountered by the Aerobot by mapping the middle (45–55 km) cloud level zonal and meridional wind motion, aerosol opacity and cloud morphology. NIR-C has 3 nighttime channels and 3 dayside channels.

The third instrument is the magnetometer to provide context about the magnetic fields in the solar wind. In addition, radio occultations between the orbiter and Earth through the atmospheric limb will be assessed for information on atmospheric dynamics and the Venus ionosphere.

The fourth instrument is the EUV which is pointed towards the sun and provides context for the solar flux.

**Table A-40:** Orbiter Instruments.

Item	Near IR Imager, NIR-S	Near IR Imager, NIR-C	Extreme Ultraviolet Monitor, EUV	Magnetometer Orbiter, MAG-O
Type of instrument	Spectral imager	Spectral imager	EUV	Magnetometer
Number of channels	14	6	3	1
Size/dimensions (m x m x m)	0.6 x 0.22 x 0.21	0.25 x 0.25 x 0.20	0.97 x 1.5 x 1.1	0.08 x 0.10 x 0.12
Instrument mass <b>without</b> contingency (Kg, CBE*)	3.4	18	7	1.5
Instrument mass contingency (%)	30	30	30	30

Item	Near IR Imager, NIR-S	Near IR Imager, NIR-C	Extreme Ultraviolet Monitor, EUV	Magnetometer Orbiter, MAG-O
Instrument mass <b>with</b> contingency (Kg, CBE+Reserve)	4.4	23.4	9.1	1.9
Instrument average payload power <b>without</b> contingency (W)	13	114	14	1
Instrument average payload power contingency (%)	30	30	30	30
Instrument average payload power <b>with</b> contingency (W)	16.9	148.2	18.2	1.3
Instrument average science data rate <sup>^</sup> <b>without</b> contingency (kbps)	115.8	1,384.6	1.6	2
Instrument average science data <sup>^</sup> rate contingency (%)	30	30	30	30
Instrument average science data <sup>^</sup> rate <b>with</b> contingency (kbps)	150.5	1,800	2.1	2.6

### A.3.2.2 Attitude Control

The Orbiter is three-axis stabilized with significant momentum and torque capabilities to account for the large inertia associated with the stacked configuration (Aerobot in its Entry Vehicle attached to the Orbiter). The Attitude Control System (ACS) maintains control of the Orbiter during the cruise, during Aerobot separation, during VOI, and during the final circular 12-hour elliptical orbit. The Orbit points the large 3m antenna at Earth for communication, at the Aerobot, and at the Dropsonde for communication. Key mission requirements and derived requirements are:

Provide 3-axis control of the Orbiter during all phases of the mission post separation from the launch vehicle.

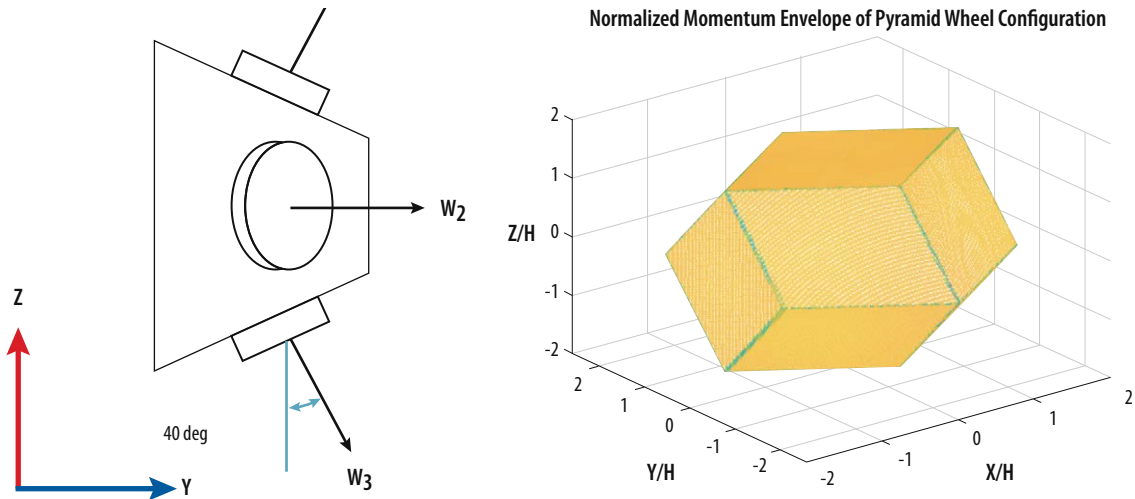
- 1) Spin up the Aerobot Entry vehicle to 5 RPM before release.
- 2) Orient the antennae to receive the beacon signal from the Aerobot from separation to atmospheric entry.
- 3) Orient the antennae for communication with Earth 4 hours a day.
- 4) Orient the antennae for communication with the Aerobot 4 for hours each day when the Aerobot is in in the Venusian day and for 10 minutes each day when the Aerobot is in the Venusian night.
- 5) Orient the antennae at all times, when not communicating with the dropsonde or Earth during the first 60 days at the Aerobot in case of an Aerobot anomaly.
- 6) Orient the antenna to communicate with the dropsonde during its 1 hour descent to the surface.
- 7) Maintain Nadir pointing for Science.

The following set of sensors were selected to provide knowledge estimation

- 1) Coarse Sun Sensor Assembly (×16)
  - Provides estimate of direction of the sun. Each coarse sensor comes as in grouping of four which provides 2pi steradian angle. Each of these assemblies are mounted on each side of Orbiter to get full 360° of coverage.
- 2) Northrop Grumman LN200s Fiber Optic Gyro + Accelerometer
  - LN200 is Inertial Measurement Unit which provides low noise estimate of angular velocity.
- 3) DTU Micro Advanced Stellar Compass
  - Since, no knowledge or pointing requirement is explicitly specified, in addition to digital processing unit, 3 camera heads are selected to provide attitude knowledge on the order of few arcseconds. Each of the camera heads include baffle and a MEMS gyro that provides rate estimates.

The following set of ACS actuators are utilized on ADVENTS. Selection of these ACS actuators were derived ability to perform fine pointing, momentum management and delta-v capability.

- 4) Honeywell HR16-250
  - 4 wheels each with 250 Nms. of momentum capacity was selected primary based on transfer phase of mission. 4-wheel pyramid configuration provide redundancy. Each provide 0.2 Nm around their spin axis. **Figure A-78** shows the wheel mounting configuration.



VS069

**Figure A-78:** 4-Wheel 40-degree wheel Pyramid configuration (Left), Effective Momentum Capacity on Each axis (Right).

- 5) Moog DST-13 ACS thrusters
  - Net total of 20 5-lb thrusters were selected. 8 thrusters provide primary attitude control, 8 of them provide secondary ACS control capability and 4 additional thrusters are used as contingency for main engine failure. Primary thrusters are canted at 45° to evenly maximize torque authority on each axis. Secondary ACS thrusters are canted at 20° to provide balance between axial thrust capability and ACS control authority. **Table A-41** shows the ACS control authority from both primary and secondary configuration.

**Table A-41:** ACS Thruster Capability.

Primary ACS Thruster Configuration (Nm)			Secondary ACS Thruster Configuration (Nm)		
X	Y	Z	X	Y	Z
71	86	71	95	114	42

The ACS mode diagram is shown in **Figure A-79**. There are total of 7 Orbiter control modes:

- 1) Launch
  - ACS is inhibited in this mode until ADVENTS observatory has separated from Launch Vehicle and required amount of time has passed to avoid potential collision.
- 2) Rate Null
  - This mode utilizes RCS thrusters on board to null rates. This mode is used once ACS becomes active after separation and removes the tip-off rates.
- 3) Sun Acquisition
  - Orbiter uses Coarse Sun sensors and reaction wheel to point the solar array in the direction of the sun to ensure Orbiter is sufficiently charged.

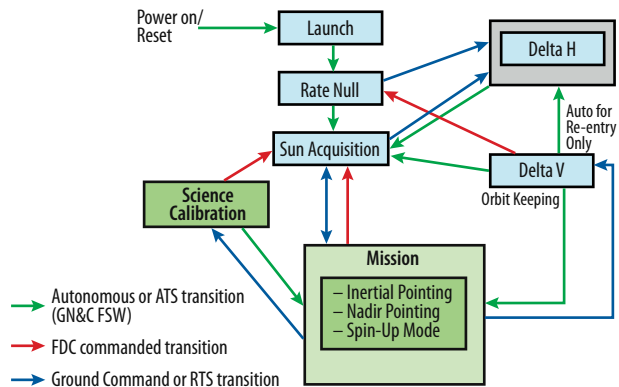


**Figure A-79:** ACS Mode Diagram.



- 4) Mission
  - Inertial Pointing Mode
    - This mode is used most of the time during transfer trajectory. Orbiter is held either in direction such that the solar arrays are pointed at sun or comm antennas are pointed toward the earth. Reaction wheels are used as primary actuation device, while Star Tracker and IMU's are used as primary attitude sensors.
  - NADIR Pointing
    - This mode is used when orbiting Venus and continues to maintain its sensor pointed toward the planet. Reaction wheels are used as primary actuation device, while Star Tracker and IMU's are used as primary attitude sensors.
  - Spin-Up Mode
    - This mode is used to spin up Aerobot before separation and entering into Venus cloud system. For this mode, RCS are used to aid in providing spin.
- 5) Delta H
  - This mode is used to dump momentum from the wheels. RCS are fired occasionally to desaturate the wheels.
- 6) Delta V
  - This mode is used main transfer burn and TCMs.
- 7) Calibration
  - Although this mode is not finalized, combination of RCS and Wheels can be used to achieve this depending on slew rate requirement. These are typically 360-degree spin around any of the axis.

Several analyses were performed to ensure that ACS hardware provided adequate control authority. The first looked at ACS detumble due to high tip off rates during separation from the Falcon Heavy launch vehicle assuming a conservative tip-off rate. Analysis used the "42", in-House 6-DOF simulation tool. Ideal torque was assumed and evaluation of the maximum torque required based on ADVENTS mass properties was performed. **Figure A-80** shows required torque on each axis as function of time. All required torques are below the minimum ACS torque authority. Impulse from ideal torque was used to assess the firing duration shown in **Table A-42**.

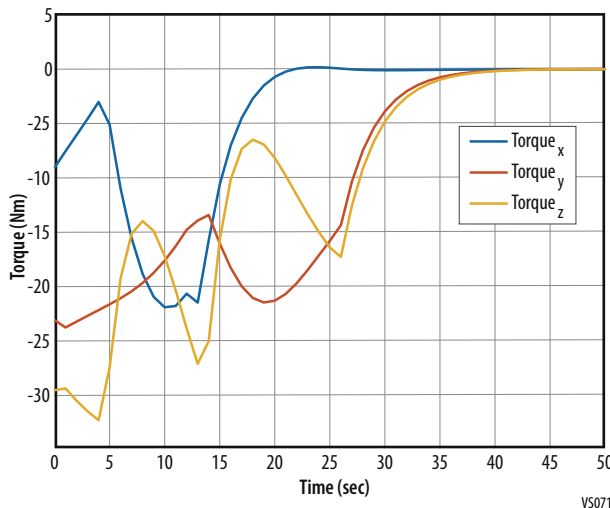


**Figure A-80:** Ideal Torque Required for  $\pm 12^\circ/s$  tip-off rates.

**Table A-42:** Thruster Firing Duration.

	Minimum Torque (Nm)	Cant Angles (deg)	Firing Duration (sec)	Firing Frequency
Primary ACS (x4)	71.6	45	9	1
Secondary ACS (x4)	41.7	20	16	1

- 8) ACS during transfer to Venus
  - Analysis assumed that it was required to ensure solar arrays are always pointing toward the sun. In this orientation, maximum solar disturbance torque was estimated to be. **Table A-43** shows number of thrusters firing, and duration of each firing based in Primary or ACS thruster firing to perform momentum dump in order to desaturate reactions wheels.

**Table A-43:** Number of Firings and Duration for Momentum Management.

	Minimum Torque (Nm)	Cant Angles (deg)	Number of Firings	Firing Duration (sec)
Primary ACS (x4)	71.6	45	395	3.5
Secondary ACS (x4)	41.7	20	395	5.98

9) Aerobot Separation Phase

- Prior to Aerobot is separation, Orbiter spins up to 5 RPM to provide spin stabilization. This analysis assumed Maximum Inertia and minimum torque to assess how long RCS thruster needs to be fired in order to achieve 5 RPM. **Table A-44** shows Minimum Torque, Maximum Inertia and corresponding firing duration to achieve desired spin rate.

**Table A-44:** Thruster Firing duration required to achieve 5 RPM.

	Minimum Torque (Nm)	Inertia	Number of Firings	Firing Duration (sec)
Primary ACS (x4)	71.6	2177	1	32
Secondary ACS (x4)	41.7	2177	1	55

10) Orbiter ACS during Venus Orbit

- Orbital analysis was performed using in-House simulation to ensure that the selected actuators provide adequate margin. During the orbit, disturbance torques are periodic as shown in **Figure A-81**. Net momentum over a periodic orbit and over 5 years duration was translated into Number of RCS firing and firing duration as shown in **Table A-45**.

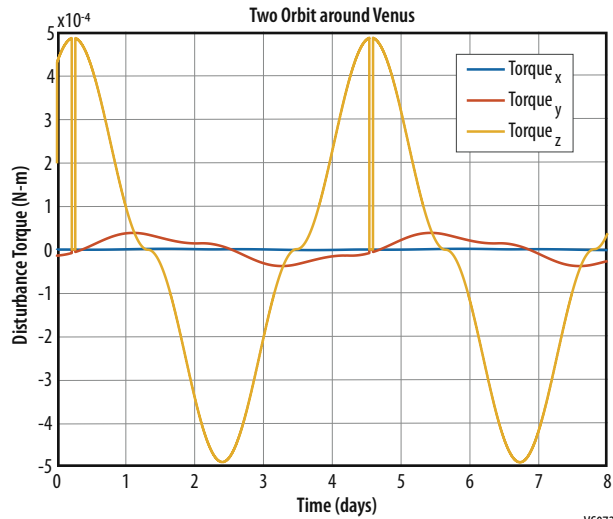


**Figure A-81:** Periodic Disturbance Torque.

**Table A-45:** RCS number and duration of firing.

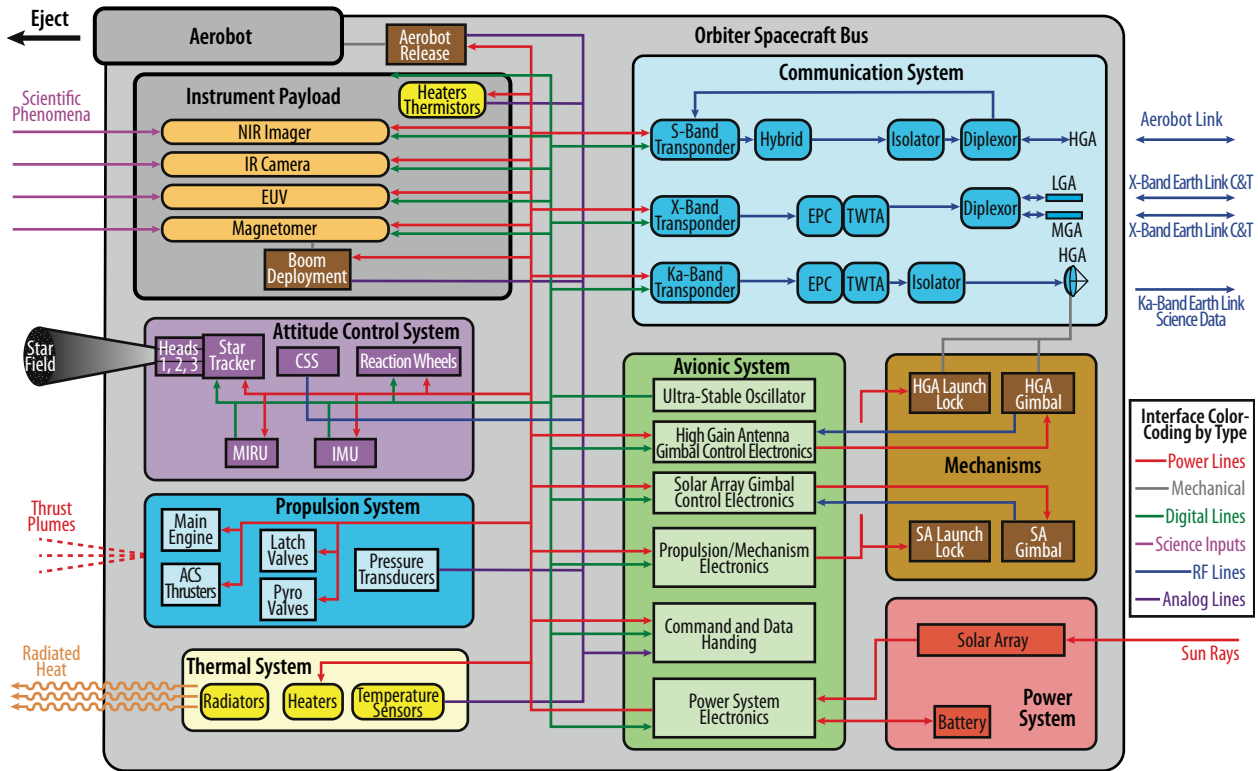
	Minimum Torque (Nm)	Cant Angles (deg)	Number of Firings	Firing Duration (sec)
Primary ACS (x4)	71.6	45	30	3.5
Secondary ACS (x4)	41.7	20	30	5.98

### A.3.2.3 Avionics

**Figure A-82** shows the Orbiter block diagram. The Orbiter avionics consists of a Power System Electronics unit (PSE), Command and Data Handling unit (C&DH), Propulsion/Mechanism Electronics unit (PME), Solar Array Gimbal Control Electronics unit (SA GCE), High Gain Antenna Gimbal Control Electronics unit (HGA GCE), and an Ultra-Stable Oscillator (USO). The PSE, C&DH, and PME are implemented with Goddard's Mustang Avionics. The Mustang Avionics will fly on the PACE mission in 2023. The SA GCE and HGA GCE are implemented with Moog Gimbal Control Electronics. The Moog Gimbal Control Electronics flew on the NICER Mission. The USO is implemented with a Microsemi 9700 USO that has flown on numerous missions.

The PSE, C&DH, and PME are block redundant. The PSE and C&DH backup units fly as warm backups, and the PME backup flies as a cold backup. The SA GCE and HGA GCE are internally redundant. Their backup cards fly as cold backups.

The PSE consists of 6 types of cards. Its PSE Monitor Card provides PSE control and telemetry acquisition functions. The Solar Array Module handles 16 Amps of solar array current, and performs



VS002

**Figure A-82:** Orbiter Block Diagram.

battery charging and distribution functions. Three Segment Modules each handle 40 Amps of solar array current. Altogether, the Solar Array Module and Segment Modules can handle 136 Amps of solar array power. The requirement is 99 Amps, leaving a margin of 27%. A High Current Power Output Module with 7.5 Amp outputs accommodates the power input requirement of the X-Band TWTA and Ka-Band TWTA. Three Low Current Power Output Modules have sixteen 3 Amp outputs each. Those outputs along with four 3 Amp outputs on the High Current Power Output Module provide a total of fifty two 3 Amp outputs. Forty one 3 Amp outputs are required on the Orbiter, leaving a margin of 27%. Lastly, a Low Voltage Power Converter provides the secondary voltage power required by the PSE cards.

The C&DH consists of 4 types of cards. Its Processor Card is based on a GR712RC Dual-Core LEON3FT SPARC V8 Processor ASIC (200 MIPS). It has 32 MB SRAM and 128 Gits of Flash memory. The Orbiter only requires 20 Gbits of data storage. Three Housekeeping Cards provide a total of 30 course sun sensor inputs (15 are required), 12 pressure sensor inputs (12 are required), and over 200 temperature sensor inputs. A Communication Card provides the RF Communication system interfaces. Lastly, a Low Voltage Power Converter provides the secondary voltage power required by the C&DH cards.

The PME consists of 4 types of cards. A Main Engine Valve Drive Card provides the actuation outputs for the Main Engine. Three ACS Valve Drive Cards provide a total of twenty four thruster outputs (20 are required), and 12 latch valve outputs (8 are required). A Deployment Module provides 8 actuation outputs. Six deployment outputs are required: Two for the Aerobot release, two for the solar array launch locks, one for the high gain antenna launch lock, and one for the Magnetometer boom deployment. Lastly, a Low Voltage Power Converter provides the secondary voltage power required by the PME cards.

The SA GCE and HGA GCE are identical. They consist of 3 types of cards: Two Controller Cards, two Gimbal Drive Cards, and two Low Voltage Power Converters. The solar array has two gimbals and the high gain antenna has two gimbals. Each Gimbal Drive Card controls the dual coil of one gimbal.

The total ionizing dose requirement is 9.4 krad. The Mustang Avionics is survivable to 60 krad, and the Moog GCE and Microsemi 9700 USO are survivable to 100 krad.

### A.3.2.4 Communication

The communication subsystem performed two key design concept trades. The first was what combination of communication frequencies to use. The decision was made to continue with the Venus Flagship Mission (VFM) design that used all three Ka-, X-, and S-Band after thoroughly exploring the different options and configurations. The only major change was that the HGA would remove the X-Band component, therefore simplifying the design to only be a dual-band HGA. Other minor changes were made to the communications path layouts to optimize for less loss as opposed to redundancy as the data rate requirements pushed the need for higher gain.

The second trade was the HGA size (**Table A-46**) as there are multiple heritage examples of differing parabolic dish sizes. Dishes with 2- and 3-meter diameters have been successfully used on other deep space missions so those were the main choices with flight heritage, but larger antennas were also considered as they provide significant gain increases. It was decided that keeping within heritage examples provided a known quantity that outweighed the benefit of a larger, more costly dish and allowed the Orbiter to fit comfortably in the launch fairing without introducing a complex, high cost, deployable antenna. The decision to go with the 3-meter antenna was obvious as it more than doubles the gain of the system without a large increase in cost or complexity as compared with a 2-meter dish.

**Table A-46:** HGA Size trade options.

From	To	Operational Frequency (GHz)	Tx Antenna	Tx Antenna Gain (dBi)	Rx Antenna	Range (km)	Information Rate (kbps)
Aerobot	Orbiter	2.1	Toroid	0	4 m HGA	113829	0.75
Aerobot	Orbiter	2.1	Toroid	0	4 m HGA	140000	0.5
Aerobot	Orbiter	2.1	Toroid	0	5 m HGA	113829	1.18
Aerobot	Orbiter	2.1	Toroid	0	5 m HGA	140000	0.78
Aerobot	Orbiter	2.1	Toroid	0	3 m HGA	18804	15.57
Aerobot	Orbiter	2.1	Toroid	0	3 m HGA	33404	4.92
Aerobot	Orbiter	2.1	Toroid	0	2 m HGA	18804	6.91
Aerobot	Orbiter	2.1	Toroid	0	2 m HGA	33404	2.19
Aerobot	Orbiter	2.1	Toroid	0	4 m HGA	24856.2	15.83
Aerobot	Orbiter	2.1	Toroid	0	4 m HGA	39456.7	6.28
Aerobot	Orbiter	2.1	Toroid	0	3 m HGA	24856.2	8.91
Aerobot	Orbiter	2.1	Toroid	0	3 m HGA	39456.7	3.53
Aerobot	Orbiter	2.1	Toroid	0	2 m HGA	24856.2	3.96
Aerobot	Orbiter	2.1	Toroid	0	2 m HGA	39456.7	1.57

The communications subsystem must maintain uplink and downlink with the Deep Space Network (DSN) with high enough data rates to ensure timely delivery of the mission science, telemetry, and command data volumes. For this mission a three frequency system was determined to meet the needs and constraints. This system can be separated into specific craft/vehicle sections. The orbiter communications system consists of a General Dynamics (GD) Small Deep Space Transponder (SDST), a Thales S-Band Transponder, Traveling Wave Tube (TWT) with electronic power conditioner (EPC), high power isolators, a 3m parabolic high gain antenna (HGA) similar to the one used on MRO, a x-band and a s-band medium gain antennas (MGA), and two x-band low gain antennas (LGAs) and two s-band LGAs.

The Aerobot communications system has a Thales S-Band Transponder and toroidal S-Band low gain antennas. The dropsondes and entry vehicle backshell each have low power L3 Harris S-Band Transponders and titanium S-Band antennas. These components have redundancy where necessary and are connected with RF cabling, waveguides, switches, and duplexers to allow for options in the communications path. These systems are designed to use Ka-, X-, and S-Band for different use cases as they provide the best option for high data rates within the mission constraints. **Figure A-83** to **Figure A-87** show the communication block diagrams for the various links.

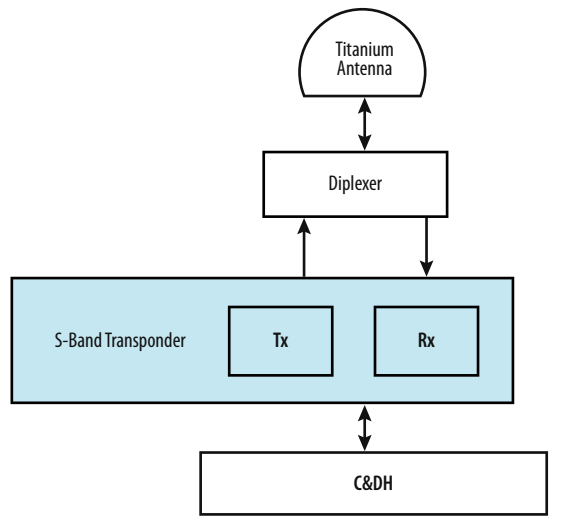


Figure A-83: Dropsonde Comm System Block Diagram.

VS073

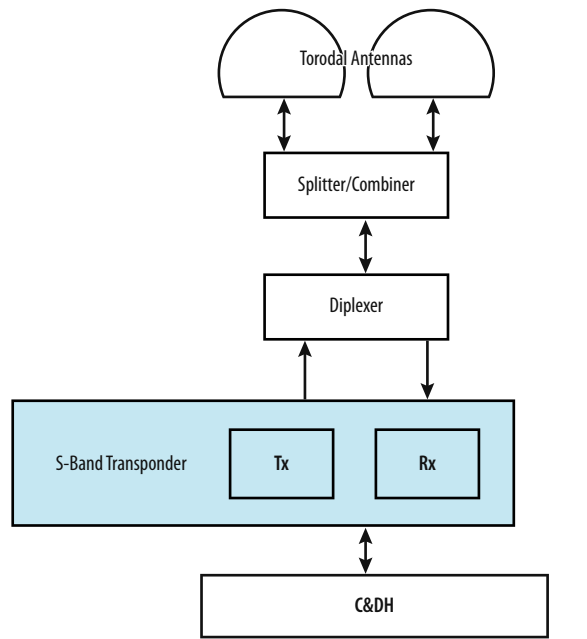
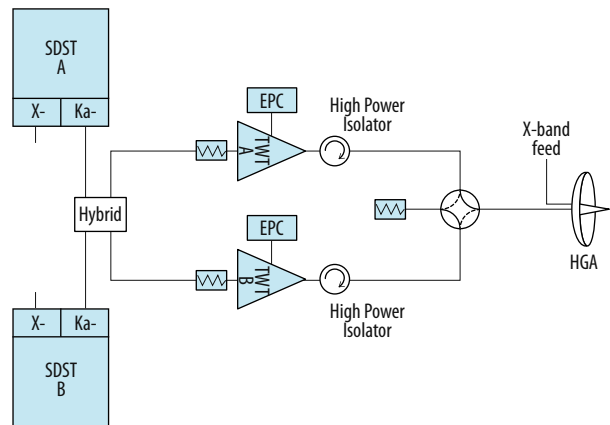


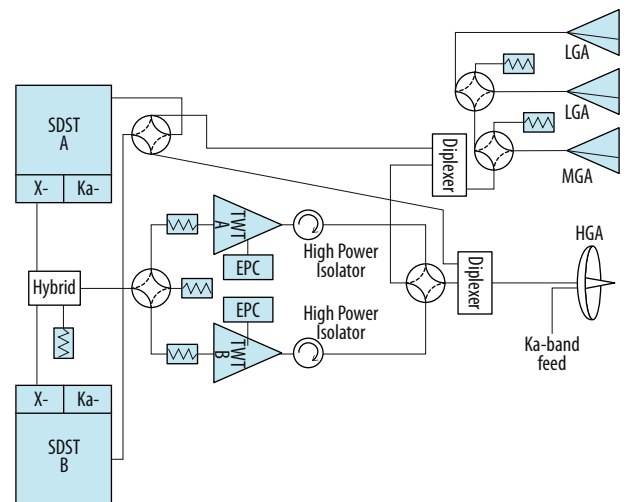
Figure A-84: Aerobot Comm System Block Diagram.

VS074



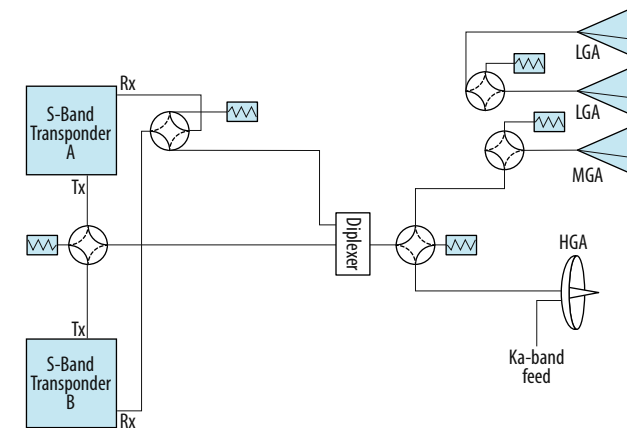
VS075

Figure A-85: Direct-to-Earth (DTE) Ka-band link for high data rate science data block diagram.



VS076

Figure A-86: DTE link at X-band for command and housekeeping telemetry block diagram.



VS077

Figure A-87: S-band link to communicate with Aerobot and DSN Telemetry block diagram.

When the HGA is in contact with the Aerobot the link between Earth and the Orbiter is the best link from the LGA or MGA.

When the HGA is pointed at Earth then the best link with the Aerobot is through the LGA or MGA..

Uplink and downlinks between Earth and the Orbiter are shown in **Table A-47** and **Table A-48** respectively. Links between the Orbiter and the Aerobot and Dropsonde are shown in **Table A-34** above and also discussed in **Appendix A.2.3**.

**Table A-47:** Earth to Orbiter Uplink Links.

From	To	Operational Frequency (GHz)	Tx Antenna	Tx Antenna Gain (dBi)	Rx Antenna	Range Au	Information Rate (kbps)
Earth	Orbiter	34.45	DSN-34m	79	3 m HGA	0.264	14000
Earth	Orbiter	34.45	DSN-34m	79	3 m HGA	1.701	340
Earth	Orbiter	34.45	DSN-34m	79	3 m HGA	1.727	330
Earth	Orbiter	34.45	DSN-34m	79	3 m HGA	0.264	56000
Earth	Orbiter	34.45	DSN-34m	79	3 m HGA	1.701	1360
Earth	Orbiter	34.45	DSN-34m	79	3 m HGA	1.727	1320
Earth	Orbiter	2.295	DSN-34m	56.7	3 m HGA	0.264	91
Earth	Orbiter	2.295	DSN-34m	56.7	3 m HGA	1.701	2.2
Earth	Orbiter	2.295	DSN-34m	56.7	3 m HGA	1.727	2.15
Earth	Orbiter	2.295	DSN-34m	56.7	3 m HGA	0.264	9100
Earth	Orbiter	2.295	DSN-34m	56.7	3 m HGA	1.701	220
Earth	Orbiter	2.295	DSN-34m	56.7	3 m HGA	1.727	215

**Table A-48:** Earth to Orbiter Downlink Links.

From	To	Operational Frequency (GHz)	Tx Antenna	Tx Antenna Gain (dBi)	Rx Antenna	Range Au	Information Rate (kbps)
Orbiter	Earth	32	3 m HGA	58.67	DSN-34m	0.264	42700
Orbiter	Earth	32	3 m HGA	58.67	DSN-34m	1.701	1030
Orbiter	Earth	32	3 m HGA	58.67	DSN-34m	1.727	1000
Orbiter	Earth	2.1	3 m HGA	35.01	DSN-34m	0.264	155
Orbiter	Earth	2.1	3 m HGA	35.01	DSN-34m	1.701	3.75
Orbiter	Earth	2.1	3 m HGA	35.01	DSN-34m	1.727	3.63

**Table A-49:** Orbiter to Aerobot and Dropsonde Links.

From	To	Operational Frequency (GHz)	Tx Antenna	Tx Antenna Gain (dBi)	Rx Antenna	Range (km)	Information Rate (kbps)
Aerobot	Orbiter	2.1	Toroid	0.0	LGA	24,856.2	0.01
Aerobot	Orbiter	2.1	Toroid	0.0	MGA	24,856.2	0.033
Aerobot	Orbiter	2.1	Toroid	0	3 m HGA	24,856.2	8,910
Orbiter	Aerobot	2.1	LGA	0.0	Toroid	24,856.2	0.16
Orbiter	Aerobot	2.1	MGA	0.0	Toroid	24,856.2	0.55
Orbiter	Aerobot	2.1	3 m HGA	35.01	Toroid	24,856.2	77.5
Dropsonde	Orbiter	2.1	Titanium	5	3 m HGA	24,856.2	2.23
Entry	Orbiter	2.1	Toroid	0	3 m HGA	140000	0.354

All communication hardware has flown previously and are high TRL (< 6) for the Venus application. The scaling adjustment to the LGA will take some engineering development. The titanium antennas will need to undergo environmental testing for the harsh Venusian atmosphere.

### A.3.2.5 Power

The Orbiter power system consists of solar arrays, a secondary battery, and supporting power electronics. The ADVENTS orbital period is 12 hrs. with 2.5 hrs. of night. TJGaAs solar cells with bare cell efficiency of 29.5%, a solar constant of 2622 w/m<sup>2</sup>, array operating temp at 140 °C, and Space Environmental Effects and Education System (SPENVIS) solar array degradation factors were used to

derive the array area requirement. A single two-axis tracking panel with 8.3 m<sup>2</sup> active area will provide 2,988.8 W EOL and 3,658.2 W BOL of power to support loads and battery recharge. A high energy density 210 AH Li Ion battery is used to support night loads. The Power System Electronics (PSE) will be a heritage 28VDC battery dominated bus included as cards in the avionics package. The PSE will control battery charging and power distribution.

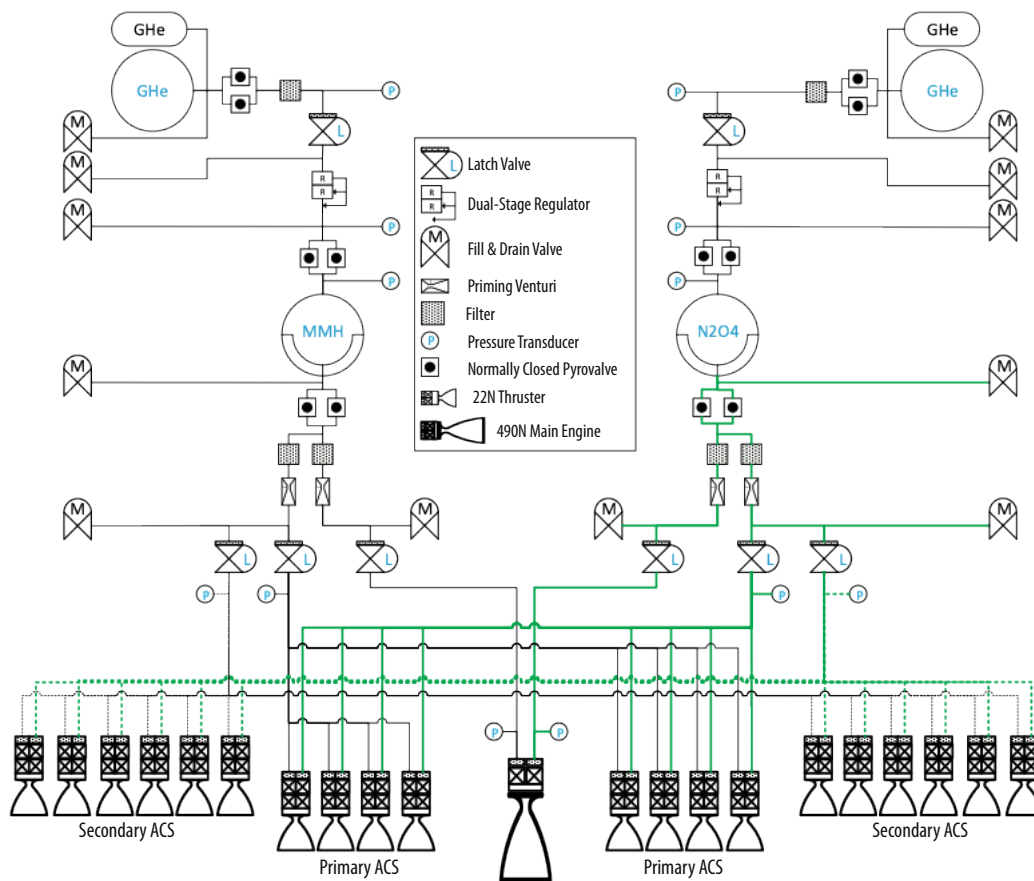
The Orbiter power subsystem was sized for a nominal orbit average power of 1,109.5 W with 30% contingency applied for a total of 1,442.4 W.

The Orbiter solar array, battery, PSE, and harness are all state of practice with a TRL of 7.

### A.3.2.6 Propulsion

The propulsion system (Figure A-83 through Figure A-88) for the ADVENTS Orbiter is a pressure regulated, bi-propellant system utilizing a 490N-class main engine with ACS control provided by 20N-class thrusters. The propulsion system is contained within the Orbiter and provides all required delta-V to maneuver the both the Orbiter and Orbiter + Aerobot configurations from Earth the Venus, enable Venus orbit capture, and provide all station keeping and ACS control while the while in orbit around Venus.

The propulsion subsystem was designed to meet the total delta-V requirement of 2380 m/s. Table A-50 shows the breakdown of the required delta-V for both Orbiter and Aerobot configurations and Table A-51 summarizes the flight system element characteristics.



VS078

Figure A-88: ADVENTS Propulsion System Schematic.

**Table A-50:** Required Delta-V.

S/C Configuration	Delta-V (m/s)
Orbiter + Aerobot	263
Orbiter	1901
Contingency	216
Total:	2,380

**Table A-51:** Flight System Element Characteristics.

Flight System Element Parameters	Value/ Summary, units
<b>Propulsion</b>	
Estimated delta-V budget, m/s	2380 m/s
Propulsion type(s) and associated propellant(s)/oxidizer(s)	Pressure Regulated, Bi-Propellant (MMH & MON-3)
Number of thrusters and tanks	1 Main Engine 20 ACS Thrusters (Pri+Red) 2 Propellant Tanks 4 COPV Helium Tanks
Specific impulse of each propulsion mode, seconds	Primary, ME Mode: 315s (299.7s at $-3\sigma$ ) Secondary, ACS Mode: 300s (285s at $-3\sigma$ )

The propulsion system employs features and lessons learned from GSFC’s Solar Dynamics Observatory and JPL’s Europa Clipper propulsion systems. The design is operationally robust by utilizing a redundant set of ACS thrusters to impart all delta-V changes of the mission, thus being single-fault tolerant to a main engine loss. Separate helium pressurant systems for the propellant tanks remove operational risks associated with propellant vapor migration (see **Figure A-88**). The propulsion system meets range safety requirements by using at least three mechanical seals to prevent propellant leakage during ground operations. Propellant tanks are pyro-isolated from both pressurant and propellant feed manifolds, allowing for streamlined integration and test operations and propellant loading, reducing cost and schedule.

Two identical propellant tanks contain a total propellant load of 2500.5 kg. Four COPV tanks store 11.3 kg of helium pressurant. **Table A-52** summarizes propellant mass breakdowns and margins for each tank. Delta-V is primarily achieved by utilizing a single, 490N-class main engine with a nominal specific impulse of 315s (299.7s at  $-3\sigma$ ). Attitude control and redundant delta-V operations are provided by 20 ACS, 22N-class thrusters with a nominal specific impulse of 300s (285s at  $-3\sigma$ ). Both main engine and ACS thrusters utilize a nominal mixture ration of 1.63. The total propulsion system dry mass, including helium pressurant and unusable propellant residuals, is 243.4 kg.

**Table A-52:** Propellant & Pressurant Quantities & Margins.

Propellant/Pressurant	Mass (kg)	Mass Margin	Propellant Residuals
MMH	950.7	8%	2%
MON-3	1,549.7	8%	2%
Gaseous Helium (Pressurant)	11.31	9%	N/A

The ADVENTS propulsion system primarily operates using a single main engine for all delta-V, with eight (8) ACS thrusters providing 3-axis control and momentum management.

A dual, main engine trade was evaluated early in the VEMC design process. This configuration would use a redundant pair of 490N-class engines to accomplish all delta-V, with ACS thrusters providing 3-axis control and momentum management. While this trade resulted in less propellant mass required, it required significant additional complexity in the ACS control design to account for an off-center mounting of the two main engines. To address this, a gimbal controlled main engine concept—similar to that used on Cassini—was explored. The redundant main engine configuration was ultimately abandoned due to the added complexity and risk associated with the gimbal and ACS control schemes, and increased mass required for the gimbal.

Nominal operations involve activating the system by opening pyro-isolating and mechanical valves to pressurize both propellant tanks via a mechanical regulator, and by opening liquid isolation valves



to prime the main engine and ACS thruster manifolds. In the event of a main engine failure, a secondary mode utilizing only twelve (12) ACS thrusters can be employed to accomplish all delta-V, control and momentum management. Robustness to main engine failure does require additional propellant to be stored. **Table A-53** through **Table A-55** summarize the propellant budget for each operating mode. All propellant budgets utilize  $-3\sigma$  thruster specific impulse, account for a 10% uncertainty in total delta-V, and unusable propellant trapped in the system (2% of total propellant load).

**Table A-53: Propellant Mass Summary.**

Mode	Wet Mass (kg)	Dry Mass (kg)	Propellant Mass (kg)	Pressurant Mass (kg)	Contingency Propellant (kg)	EOL Spacecraft Mass (kg)
Primary: Main Engine	5,816.2	3,315.8	2,315.8	11.31	184.4	3,500.2
Secondary: ACS Thrusters	5,816.2	3,315.8	2,500.4	11.31	0.0	3,315.8

**Table A-54: ACS Secondary Mode Propellant Budget for 1,827.3 kg Aerobot and 1,488.5 kg Orbiter.**

Configuration	Maneuver	dV (m/s)	Wet Mass (kg)	Isp (s)	Mass of Propellant (kg)	Spacecraft Mass Post Maneuver (kg)
Orbiter and Aerobot	DSM	251	5,816.2	285.0	530.1	5,286.1
	TCM1	10	5,286.1	285.0	20.1	5,266.0
	TCM2	2	5,266.0	285.0	4.0	5,262.0
	Corrections/dV uncertainty	26.3	5,262.0	285.0	52.4	5,209.6
	Momentum Unloading	-	5,209.6	285.0	69.9	5,139.7
	Nulling, Tip-off Rates	-	5,139.7	285.0	0.5	3,311.9
	Subtotal		289.3		677.0	
Orbiter	TCM3	20	3,311.9	285.0	25.1	3,286.8
	TCM4	5	3,286.8	285.0	6.3	3,280.6
	Direct Capture	1,876	3,280.6	285.0	1,674.6	1,605.9
	Corrections/dV Uncertainty	190.1	1,605.9	285.0	112.1	1,493.8
	Momentum Unloading	-	1,493.8	285.0	5.3	1,488.5
	Subtotal		2,091.1		1,823.4	
Grand Total		2,380		2,500.0		

**Table A-55: Main Engine Primary Mode Propellant Budget.**

Configuration	Maneuver	dV (m/s)	Wet Mass (kg)	Isp (s)	Mass of Propellant (kg)	Contingency Propellant (kg)	Spacecraft Mass Post Maneuver (kg)
Orbiter and Aerobot	DSM	251	5,816.2	299.7	476.1	54.1	5,340.2
	TCM1	10	5,340.2	299.7	18.1	2.0	5,322.0
	TCM2	2	5,322.0	299.7	3.6	.4	5,318.4
	Corrections/dV uncertainty	26.3	5,318.4	299.7	47.4	5.1	5,271.0
	Momentum Unloading	-	5,271.0	285.0	30.8	39.1	5,240.3
	Nulling, Tip-off Rates	-	5,240.3	285.0	0.2	0.3	3,412.8
	Subtotal		289.3		576.2	100.6	

Configuration	Maneuver	dV (m/s)	Wet Mass (kg)	Isp (s)	Mass of Propellant (kg)	Contingency Propellant (kg)	Spacecraft Mass Post Maneuver (kg)
Orbiter	TCM3	20	3,412.8	299.7	23.1	2.0	3,389.6
	TCM4	5	3,389.6	299.7	5.8	0.5	3,383.9
	Direct Capture	1,876	3,383.9	299.7	1,596.5	78.2	1,787.4
	Corrections/dV Uncertainty	190.1	1,787.4	299.7	111.9	0.2	1,675.5
	Momentum Unloading	-	1,675.5	285.0	2.3	3.0	1,673.1
	Subtotal	2,091.1			1,729.6	83.8	
	Grand Total	2,380			2,316	184.4	

All components of the propulsion system are TRL9 (**Table A-56**), except for the propellant tanks, which employ a modified design of flight-proven models. The propellant tank TRL was conservatively estimated to be at TLR 7+ since a delta-qualification of previously flown design would be required to increase the maximum tank operating pressure from 250 psia to 300 psia. This pressure increase is required to ensure the performance of the main engine and ACS thrusters falls within the performance envelop of the hardware, as well as reduce required propellant mass.

A delta-Qualification test of the ACS thrusters will be needed to ensure they can meet the single-burn impulse and propellant throughput required in the Secondary ACS mode for the Direct Capture burn.

**Table A-56:** Propulsion System Components & TRL.

Item	Make	Model	QTY	TRL
Pressurant Tanks	Arde	5049	2	9
	Arde	4307	2	9
Fuel Tank	Northrop Grumman	80403-101	1	7+
Oxidizer Tank	Northrop Grumman	80403-101	1	7+
Main Engine	Aerojet-Rocketdyne	R-4D-11-300	1	9
ACS Thrusters	Moog-ISP	DST-13	20	9

### A.3.2.7 Structure

The ADVENTS Orbiter serves many functions including a science platform, communication relay, and carrier for the Aerobot. The instruments on the Orbiter include the NIR-S, NIR-C, Magnetometer, and EUV Solar Monitor. The Orbiter also acts as a communication antenna relay with a 3-meter diameter gimbaled High Gain Antenna system and two Omni antennas. All the instruments are small and easy to package with the Orbiter primary structure driven by the propellant/oxidizer tanks size and the requirement to act as a load path from the Aerobot system to the launch vehicle. All structural elements have been sized using hand-calculations or rules-of-thumb (which is typically conservative) as time did not permit a full structural analysis. The design of the structure is a typical “cylinder-in-a-box” with machined aluminum bracketry and aluminum honeycomb panels. Since the mission was not mass constrained, the aluminum structural design was considered more cost effective than composite alternatives despite a small mass penalty. The load path for both the tanks and the Aerobot assembly is directly through the central cylinder providing an efficient, low mass, and commonly used design. The central cylinder was based on the diameter of the standard 1575 payload attach fitting. The central cylinder is stiffened by structural radials which support equipment panels for mounting boxes and other elements. The mechanisms include the solar array assembly which is notionally a folded four panel drive/hinge/latch deployment with a single axis tracking drive. The EUV Solar Monitor is mounted on a notional single axis turntable. The High Gain Antenna has a deployable boom with a two axis gimbal. The Magnetometer is mounted to a single deploy boom with a simple drive/hinge/latch mechanism. Release mechanisms between the Orbiter and the launch vehicle and the Orbiter and the Aerobot are expected to be commercial-off-the-shelf (COTS) separation systems such as a Lightband or RUAG system.

Below is a list of operations that directly affect the structural and mechanism design:

- 1) Launch – launch loads and packaging
- 2) Separation from 2<sup>nd</sup> stage – shock loads
- 3) Orbiter Solar Arrays deployment – release and deployment mechanism shock
- 4) Orbiter High Gain Antenna deployment – release and deployment mechanism shock and reaction loads
- 5) Propulsion burns – reaction loads and center of mass (CM) shift.
- 6) Solar Array rotation – rotary drive mechanism reaction loads
- 7) Orbiter Magnetometer deployment – release and deployment mechanism shock and reaction loads
- 8) EUV Solar Monitor rotation – rotary drive mechanism vibration and reaction loads
- 9) High Gain Gimbal motion – drive reaction loads
- 10) Separation of Aerobot – shock loads. This also abruptly shifts the center of mass (CM).

#### **A.3.2.7.1 Load Path and Mechanisms**

The Orbiter structural design was driven by carrying the launch loads of the mission elements in a simple load path to the launch vehicle. The cylinder-in-a-box design provides more than adequate mounting surfaces for boxes and instruments. The basic structure of a central cylinder, upper and lower deck, radials and equipment panels is very common and well understood. The dry mass efficiency (Primary Structure Mass/Dry Mass) of the structure is approximately 16% which is reasonable and reflects an efficient concept. The mechanisms and launch locks are notional but are all expected to be COTS or modified COTS, well understood, and with extensive flight heritage.

The design of the structural elements and assemblies is well within the current state of the art and has extensive heritage. All primary structural elements are expected to be TRL6

Considered using composite to reduce mass but it was decided that the additional cost of composite was not justified since there was not a mass constraint and the less expensive aluminum structure was adequate.

#### **A.3.2.8 Thermal**

The Orbiter travels from Earth through deep space to Venus, where it is inserted into an orbit approximately 100,000 km above the planet. Primary operations take place in Venus orbit. The Orbiter has an almost continuous view of the sun during its mission, with occasional eclipses during the Venus orbit of up to 2.5 hours in duration. The Venus orbit is high enough that heat input from the planet is negligible.

The thermal control system for the Orbiter must maintain all components within their temperature limits. The approach uses passive thermal control techniques augmented with heaters. Exterior Orbiter surfaces are covered with MLI, and radiator patches are placed on an exterior side which is oriented to be kept out of the sun and given a continuous view of space. Equipment is primarily packaged within the Orbiter cavity, which the thermal control system has been designed to keep at a moderate temperature. The interior of the cavity is painted black to promote distribution of heat through radiation. Heat pipes and spreaders are used as needed to distribute heat generated by electronics. Patch heaters are located on electronics boxes and other temperature-sensitive components to provide heat as needed during the cold cruise to Venus. Exterior propulsion tanks and lines are equipped with heaters, as well as external instruments. Thermistors are placed on components and within the Orbiter cavity for temperatures monitoring and heater control.

The thermal control system requires approximately 1.72 m<sup>2</sup> of radiator area to dissipate sufficient heat while in Venus orbit. Approximately 400W of heater power is required to maintain components above survival temperatures during the cold cruise to Venus. These values are within the available surface area and power budget.

The thermal control system operates mostly passively. The Orbiter is blanketed with MLI, with the

exception of radiator patches on one side. The Orbiter is oriented so that the radiator is kept out of the sun with a continuous view of space. Heater patches are placed on electrical boxes, instruments, and propulsion tanks and lines. Thermistors are used for temperature monitoring of components and control of heaters as required to maintain temperatures above minimum limits. A minimum amount of heater power is required to maintain temperatures above survival limits during the cruise to Venus, or this power can be supplied by additional operation of electronics.

All thermal hardware has a high TRL level, and nothing needs time or money for development.

**APPENDIX B - ADVENTS COST BASIS OF ESTIMATE**

The majority of the instrument costs were generated through the GSFC RAO office and carried over from the Venus Flagship Mission study conducted at GSFC in 2020 or generated from grass roots estimates by instrument designers. Costs for the IR Camera and Mini-TLS were generate through the GSFC RAO office. Detailed MELS were used by the CEMA office to generate costs for the Orbiter Bus (**Appendix B.1**), Aerobot Bus (**Appendix B.2**) and Dropsonde (**Appendix B.3**). CEMA costs at the 70% confidence level on the costing S-Curve level are assumed equivalent to a point cost estimate with 50% reserve added as summarized in **Table B-1**. For example the orbiter bus cost at the 70% confidence level is \$384.4M (\$FY25) which corresponds to a \$256 baseline point cost estimate.

**Table B-1: CEMA Cost Estimates (M\$FY25).**

	CEMA Cost at 70% Confidence Level (S curve)	Cost with 50% reserve added	Baseline Cost
Orbiter Bus	384.4	384.4	256.3
Aerobot Bus	143.4	143.4	95.6
Dropsonde*	27.1	27.1	18.1

\* Cost included in higher level Dropsonde assembly

B.1 CEMA Cost Estimate for ADVENTS Orbiter BUS. . . . . B-2  
 B.2 CEMA Cost Estimate ADVENTS Aerobot BUS . . . . . B-3  
 B.3 CEMA Cost Estimate for ADVENTS Dropsonde (Not including instrumentation). . . . . B-4

### B.1 CEMA Cost Estimate for ADVENTS Orbiter Bus

ADVENTS Orbiter CEMA Ground Rules & Assumptions	
<ul style="list-style-type: none"> <li>• Estimate in FY25\$</li> <li>• Mission Risk Class B</li> <li>• Contractor Build</li> <li>• Estimate covers cost from development through delivery to higher level I&amp;T.</li> <li>• FPGA development cost - 4 FPGA, assumed &gt;65% reuse from heritage designs</li> <li>• FSW development + testbed - ROM estimate</li> <li>• ETU, Flight Spares not specified in MEL - ROM estimate</li> <li>• Ground Support Equipment - ROM estimate</li> <li>• Environmental Testing - ROM estimate (includes testing prior to mission level environmental testing)</li> </ul>	

ADVENTS Orbiter Spacecraft Bus CEMA Parametric Cost Estimate (Development and Production Costs)	50% CL FY25\$M	
<b>Cost Model Summary</b>		
29-Mar-21		
<b>ADVENTS Orbiter</b>	<b>\$260.8</b>	
Attitude Control		\$21.7
Avionics		\$29.6
Communication		\$49.5
Electrical Power		\$18.8
Structure		\$54.1
Mechanisms		\$5.1
Propulsion		\$31.2
Thermal		\$1.2
Management, Systems Engineering, Assembly, Integration & Test		\$49.6
<b>Additional Costs</b>	<b>\$82.4</b>	
FPGA Development		\$3.5
FSW Development		\$25.8
FSW Testbed		\$1.3
ETUs + Flight Spares		\$25.8
Ground Support Equipment		\$12.9
Environmental Test		\$12.9
<b>ADVENTS Orbiter Spacecraft Bus TOTAL</b>	<b>\$343.2</b>	

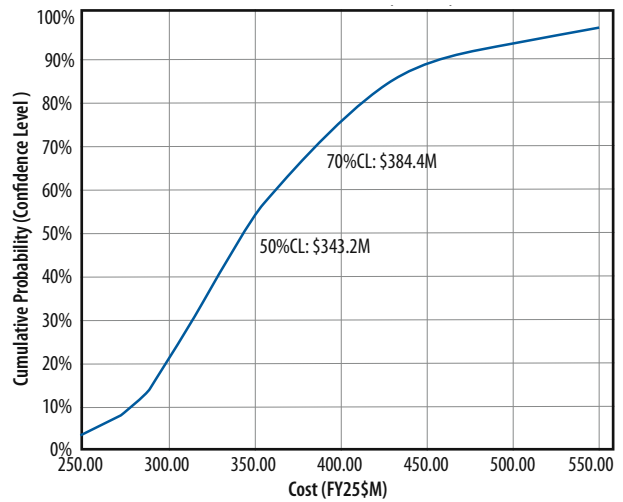


Figure B-1: ADVENTS Orbiter S-Curve (FY25\$M).

## B.2 CEMA Cost Estimate for ADVENTS Aerobot Bus

ADVENTS Aerobot Ground Rules & Assumptions	
<ul style="list-style-type: none"> <li>• Estimate in FY25\$</li> <li>• Mission Risk Class B</li> <li>• Contractor build</li> <li>• Estimate covers cost from development through delivery to higher level I&amp;T</li> <li>• FPGA development cost - 3 FPGA, assumed &gt;65% reuse from heritage designs</li> <li>• FSW development + testbed - ROM estimate</li> <li>• ETU, Flight Spares not specified in MEL - ROM estimate</li> <li>• Ground Support Equipment - ROM estimate</li> <li>• Environmental Testing - ROM estimate (includes testing prior to mission level environmental testing)</li> <li>• Using updated prices provided for main and auxiliary COPV pressurant tanks</li> <li>• Hardware not included in estimate:               <ul style="list-style-type: none"> <li>– Balloon system</li> <li>– Payloads</li> <li>– Helium pump</li> <li>– Inflation system plumbing HW</li> <li>– Parachutes</li> <li>– TPS</li> <li>– Aeroshell</li> <li>– Radome</li> </ul> </li> <li>• Per customer request: CEMA estimate for Aerobot does not include costs in PM, SE, AI&amp;T related to the hardware not included. The estimate assumes that hardware does not exist. ROM Additional costs do not reflect the hardware not included either. These costs should be accounted for when incorporating the hardware listed above.</li> </ul>	

ADVENTS Aerobot Spacecraft Bus CEMA Parametric Cost Estimate (Development and Production Costs)	50% CL FY25\$M	
<b>Cost Model Summary</b> 21-Apr-21		
<b>ADVENTS Aerobot</b>	<b>\$93.5</b>	
Attitude Control		\$0.6
Avionics		\$16.9
Communication		\$8.4
Electrical Power		\$5.7
Structure		\$5.6
Mechanisms		\$2.1
Inflation System		\$31.4
Thermal		\$0.1
Entry System (former Aeroshell)		\$3.0
Entry System Avionics		\$1.7
Entry System Communication		\$6.0
Management, Systems Engineering, Assembly, Integration & Test		\$17.8
<b>Additional Costs</b>	<b>\$30.7</b>	
FPGA Development		\$2.6
Flight Software		\$9.2
FSW Test Bed		\$0.5
Flight Spares & Engineering Test Units		\$9.2
Environmental Test		\$4.6
Ground Support Equipment		\$4.6
<b>ADVENTS Aerobot Spacecraft Bus TOTAL</b>	<b>\$124.3</b>	

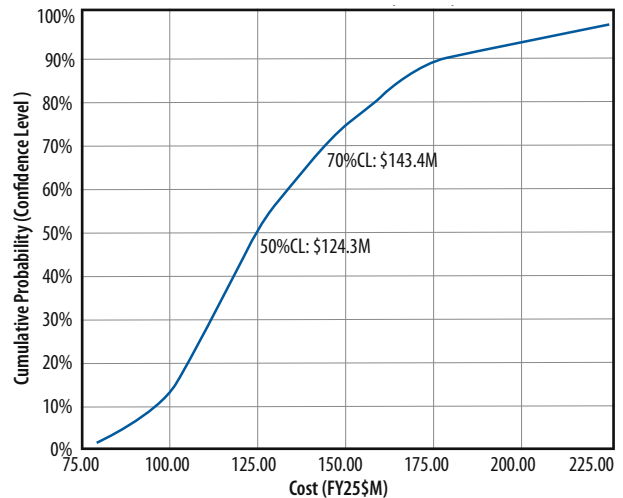


Figure B-2: ADVENTS Aerobot S-Curve (FY25\$M).

### B.3 CEMA Cost Estimate for ADVENTS Dropsonde (Not including instrumentation)

ADVENTS Dropsonde Ground Rules & Assumptions	
<ul style="list-style-type: none"> <li>• Costs in FY25\$</li> <li>• Mission Risk Class B</li> <li>• Contractor Build</li> <li>• Estimate covers cost from development through delivery to higher level I&amp;T.</li> <li>• FPGA development cost - assumed &gt;65% reuse from heritage designs</li> <li>• FSW development + testbed - ROM estimate</li> <li>• ETU, Flight Spares not specified in MEL - ROM estimate</li> <li>• Ground Support Equipment - ROM estimate</li> <li>• Environmental Testing - ROM estimate (includes testing prior to mission level environmental testing)</li> </ul>	

ADVENTS Dropsonde Spacecraft Bus CEMA Parametric Cost Estimate (Development and Production Costs)	50% CL FY25\$M	
<b>Cost Model Summary</b>		
21-Apr-21		
<b>ADVENTS Dropsonde</b>	<b>\$17.92</b>	
Avionics		\$1.76
Communication		\$6.10
Electrical Power		\$0.04
Mechanical		\$6.07
Thermal		\$0.24
Management, Systems Engineering, Assembly, Integration & Test		\$3.71
<b>Additional Costs</b>	<b>\$6.29</b>	
FPGA Development		\$0.88
Flight Software		\$1.77
FSW Test Bed		\$0.09
Flight Spares & Engineering Test Units		\$1.77
Environmental Test		\$0.89
Ground Support Equipment		\$0.89
<b>ADVENTS Dropsonde Spacecraft Bus TOTAL</b>	<b>\$24.21</b>	

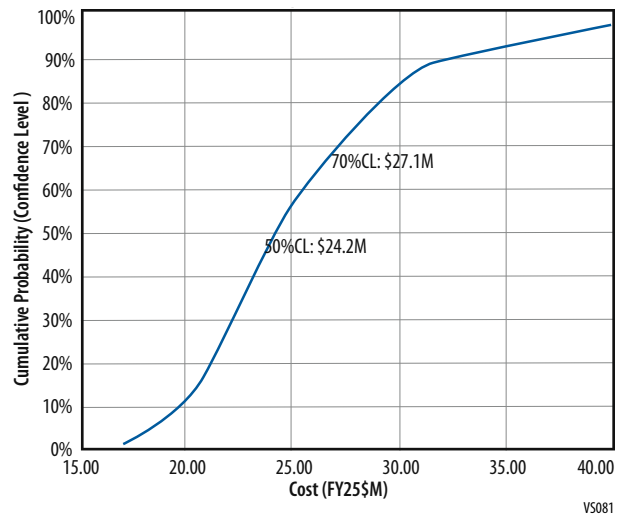


Figure B-3: ADVENTS Dropsonde S-Curve (FY25\$M).



## APPENDIX C - REFERENCES

- Baines, K. H., Nikolic, D., Cutts, J. A., Delitsky, M. L., Renard, J.-P., Madzunkov, S. M., Barge, L. M., Mousis, O., Wilson, C., Limaye, S. S., and Verdier, N. (2021). Investigation of Venus cloud and aerosol composition including potential biogenic materials via an Aerosol-Sampling Instrument Package. *Astrobiology* 21, 8, DOI:10.1089/ast.2021.0001
- Braun B., Independent Review Board Final Assessment and Determination of HEEET at TRL 6, private communication.
- Brissaud, Q., Krishnamoorthy, S., Jackson, J. M., Bowman, D. C., Komjathy, A., Cutts, J. A., *et al.* (2021). The first detection of an earthquake from a balloon using its acoustic signature. *Geophysical Research Letters*, 48, e2021GL093013. <https://doi.org/10.1029/2021GL093013>
- De Bergh, C., Bézard, B., Owen, T., Crisp, D., Maillard, J. P., & Lutz, B. L. (1991). Deuterium on Venus: Observations from Earth. *Science*, 251(4993), 547–549. <https://doi.org/10.1126/science.251.4993.547>
- Campbell, I. H., & Taylor, S. R. (1983). No water, no granites - No oceans, no continents. *Geophysical Research Letters*, 10(11), 1061–1064. <https://doi.org/10.1029/GL010i011p01061>
- Chassefière, E., Wieler, R., Marty, B., & Leblanc, F. (2012). The evolution of Venus: Present state of knowledge and future exploration. *Planetary and Space Science*, 63–64, 15–23. <https://doi.org/10.1016/j.pss.2011.04.007>
- Davis, A. *et al.* “Near-IR Imaging of Venus’ Surface Features from Below its Clouds” In AAS/Division for Planetary Sciences Meeting Abstracts, (2020).
- Cutts *et al.* “Aerial platforms for the scientific exploration of Venus.” Pasadena, CA (2018).
- Gilmore, M. S., Mueller, N., & Helbert, J. (2015). VIRTIS emissivity of Alpha Regio, Venus, with implications for tessera composition. *Icarus*, 254, 350–361. <https://doi.org/10.1016/j.icarus.2015.04.008>
- Gilmore, M. S., Treiman, A., Helbert, J., & Smrekar, S. (2017). Venus Surface Composition Constrained by Observation and Experiment. *Space Science Reviews*, 212(3–4), 1511–1540. <https://doi.org/10.1007/s11214-017-0370-8>
- Glaze, L. S., Wilson, C. F., Zasova, L. V., Nakamura, M., & Limaye, S. (2018). Future of Venus Research and Exploration. *Space Science Reviews*, 214(5). <https://doi.org/10.1007/s11214-018-0528-z>
- Greaves, J. S., Richards, A. M. S., Bains, W., Rimmer, P. B., Sagawa, H., Clements, D. L., *et al.* (2020). Phosphine gas in the cloud decks of Venus. *Nature Astronomy*. <https://doi.org/10.1038/s41550-020-1174-4>
- Hall, J.L. *et al.* “Second generation prototype design and testing for a high altitude Venus balloon.” *Advances in Space Research* 44, no. 1 (2009).
- Hall, J.L. *et al.* “Altitude-Controlled Light Gas Balloons for Venus and Titan Exploration.” In AIAA Aviation 2019 Forum, p. 3194. 2019.
- Hamano, K., Abe, Y., & Genda, H. (2013). Emergence of two types of terrestrial planet on solidification of magma ocean. *Nature*, 497(7451), 607–10. <https://doi.org/10.1038/nature12163>
- Hashizume, K., & Chaussidon, M. (2005). A non-terrestrial 16O-rich isotopic composition for the protosolar nebula. *Nature*, 434(7033), 619–622. <https://doi.org/10.1038/nature03432>
- Helbert, J., Müller, N., Maturilli, A., Nadalini, R., Smrekar, S., D’Incecco, P., & D’Amore, M. (2013). Observing the surface of Venus after VIRTIS on VEX: New concepts and laboratory work. *Infrared Remote Sensing and Instrumentation*, 8867, 88670C–88670C–8. <https://doi.org/10.1117/12.2025582>
- Horinouchi, T., Hayashi, Y., Watanabe, S., Yamada, M., Yamazaki, A., Kouyama, T., *et al.* (2020). How waves and turbulence maintain the super-rotation of Venus’ atmosphere. *Science*, 368(6489), 405–409. <https://doi.org/10.1126/science.aaz4439>

- Horzempa, P. "Calypso Venus Scout." arXiv preprint arXiv:2008.08620 (2020).
- Husseyin, S., and Warmbrodt, W.G. "Design considerations for a stopped-rotor cyclocopter for Venus exploration." (2016).
- Imamura, T., Mitchell, J., Lebonnois, S., Kaspi, Y., Showman, A. P., & Korablev, O. (2020). Super-rotation in Planetary Atmospheres. *Space Science Reviews*, 216(5). <https://doi.org/10.1007/s11214-020-00703-9>
- Izraelvitz and Hall. Minimum-Mass Limits for Streamlined Venus Atmospheric Probes. May 2020. *Journal of Spacecraft and Rockets* 57(4):1–9 DOI:10.2514/1.A34437
- Kane, S. R., Arney, G., Crisp, D., Domagal-Goldman, S., Glaze, L. S., Goldblatt, C., *et al.* (2019). Venus as a Laboratory for Exoplanetary Science. *Journal of Geophysical Research: Planets*, 124(8), 2015–2028. <https://doi.org/10.1029/2019JE005939>
- Kasting, J. F., & Catling, D. (2003). Evolution of a Habitable Planet. *Annual Review of Astronomy and Astrophysics*, 41(1), 429–463. <https://doi.org/10.1146/annurev.astro.41.071601.170049>
- Klaasen, K.P., and Greeley, R. "VEVA Discovery mission to Venus: exploration of volcanoes and atmosphere." *Acta Astronautica* 52, no. 2–6 (2003).
- Krishnamoorthy, S., Komjathy, A., Pauken, M. T., Cutts, J. A., Garcia, R. F., Mimoun, D., *et al.* (2018). Detection of Artificially Generated Seismic Signals Using Balloon-Borne Infrasound Sensors. *Geophysical Research Letters*, 45, 3393–3403. <https://doi.org/10.1002/2018GL077481>
- Krishnamoorthy, S. *et al.* (2019), "Aerial Seismology Using Balloon-Based Barometers," in *IEEE Transactions on Geoscience and Remote Sensing*, vol. 57, no. 12, pp. 10191-10201, doi: 10.1109/TGRS.2019.2931831.
- Lee, Y. J., García Muñoz, A., Imamura, T., Yamada, M., Satoh, T., Yamazaki, A., & Watanabe, S. (2020). Brightness modulations of our nearest terrestrial planet Venus reveal atmospheric super-rotation rather than surface features. *Nature Communications*, 11(1), 1–8. <https://doi.org/10.1038/s41467-020-19385-6>
- Limaye, S. S., Mogul, R., Smith, D. J., Ansari, A. H., Słowik, G. P., & Vaishampayan, P. (2018). Venus' Spectral Signatures and the Potential for Life in the Clouds. *Astrobiology*, 18(10), ast.2017.1783. <https://doi.org/10.1089/ast.2017.1783>
- Nakamura, M., Imamura, T., Ishii, N., Abe, T., Satoh, T., Suzuki, M., *et al.* (2011). Overview of Venus Orbiter, Akatsuki. *Earth, Planets and Space*, 63(5), 443–457. <https://doi.org/10.5047/eps.2011.02.009>
- Nakamura, M., Imamura, T., Ishii, N., Abe, T., Kawakatsu, Y., Hirose, C., *et al.* (2016). AKATSUKI returns to Venus. *Earth, Planets and Space*, 68(1). <https://doi.org/10.1186/s40623-016-0457-6>
- Peralta, J., Iwagami, N., Sánchez-Lavega, A., Lee, Y. J., Hueso, R., Narita, M., *et al.* (2019). Morphology and Dynamics of Venus's Middle Clouds With Akatsuki/IR1. *Geophysical Research Letters*, 46(5), 2399–2407. <https://doi.org/10.1029/2018GL081670>
- Peralta, J., Sánchez-Lavega, A., Horinouchi, T., McGouldrick, K., Garate-Lopez, I., Young, E. F., *et al.* (2019). New cloud morphologies discovered on the Venus's night during Akatsuki. *Icarus*, 333(April), 177–182. <https://doi.org/10.1016/j.icarus.2019.05.026>
- Peralta, J., Navarro, T., Vun, C. W., Sánchez-Lavega, A., McGouldrick, K., Horinouchi, T., *et al.* (2020). A Long-Lived Sharp Disruption on the Lower Clouds of Venus. *Geophysical Research Letters*, 47(11), 1–10. <https://doi.org/10.1029/2020GL087221>
- Satoh, T., Sato, T. M., Nakamura, M., Kasaba, Y., Ueno, M., Suzuki, M., *et al.* (2017). Performance of Akatsuki/IR2 in Venus orbit: The first year 7. *Planetary science Akatsuki at Venus: The First Year of Scientific Operation Masato Nakamura, Dmitri Titov, Kevin McGouldrick, Pierre Drossart, Jean-Loup Bertaux and Huixin Liu.* *Earth, Planets and Space*, 69(1). <https://doi.org/10.1186/s40623-017-0736-x>

- Schubert, G., Covey, C., Genio, A. Del, Elson, L. S., Keating, G., Seiff, A., *et al.* (1980). Structure and circulation of the Venus atmosphere. *Journal of Geophysical Research*, 85(A13), 8007. <https://doi.org/10.1029/JA085iA13p08007>
- Seiff, Alvin, *et al.* “Models of the structure of the atmosphere of Venus from the surface to 100 kilometers altitude.” *Advances in Space Research* 5.11 (1985): 3–58.
- Travis, L. D., Coffeen, D. L., Del Genio, A. D., Hansen, J. E., Kawabata, K., Lacy, A. A., *et al.* (1979). Cloud Images from the Pioneer Venus Orbiter. *Science*, 205(4401), 74–76. <https://doi.org/10.1126/science.205.4401.74>
- Venkatapathy, E., Ellerby, D., Gage, P., Prabhu, D., Gasch, M., Kazemba, C., Kellerman, C., Langston, S., Libben, B., Mahzari, M. and Milos, F., 2020. Entry system technology readiness for ice-giant probe missions. *Space Science Reviews*, 216(2), pp.1–21.
- Way, M. J., & Del Genio, A. D. (2020). Venusian Habitable Climate Scenarios: Modeling Venus through time and applications to slowly rotating Venus-Like Exoplanets. *Journal of Geophysical Research: Planets*, e2019JE006276. <https://doi.org/10.1029/2019je006276>
- Way, M. J., Del Genio, A. D., Kiang, N. Y., Sohl, L. E., Grinspoon, D. H., Aleinov, I., *et al.* (2016). Was Venus the first habitable world of our solar system? *Geophysical Research Letters*, 43(16), 8376–8383. <https://doi.org/10.1002/2016GL069790>

**APPENDIX D - ACRONYMS & ABBREVIATIONS**

9s9p .....	9 series 9 parallel
ACDH .....	Aerobot Command and Data Handling
ACS .....	Attitude Control System
ADC .....	Analog Digital Converter
ADVENTS .....	Assessment and Discovery of Venus' past Evolution and Near-Term climatic and geophysical State
AH .....	Amp Hour
ALHAT .....	Autonomous Landing Hazard Avoidance Technology
AMS .....	Aerosol mass spectrometer
AMS-N .....	Aerosol Mass Spectrometer with Nephelometer
AO .....	Announcement of Opportunity
AOS .....	Acquisition of Signal
APE .....	Attitude and Position Estimate
ARC .....	Ames Research Center
ARM .....	Advanced RISC (reduced instruction set computer)
ARTEMIS .....	Acceleration, Reconnection, Turbulence and Electrodynamic of the Moon's Interaction with the Sun
AS .....	Atmospheric Structure Suite
ASPIRE .....	Advanced Supersonic Parachute Inflation Research Experiment
ASRG .....	Advanced Stirling Radioisotope Generator
ATC .....	Analog Telemetry Card
ATLO .....	Assembly, Test, and Launch Operations
ATP .....	Authority To Proceed
B .....	Billion
BCM .....	Battery Charge Module
BECA .....	Bulk Elemental Composition Analyzer
BLDT .....	Balloon Launched Decelerator Test
BM .....	Breaking Maneuver
BOL .....	Beginning of Life
BPSK .....	Binary Phase Shift Keying
C .....	Celsius
C3 .....	launch energy
CBE .....	Current Best Estimate
CAD .....	Computer Aided Design
CADRe .....	Cost Analysis Data Requirement
CBE .....	Current Best Estimate
CCD .....	Charge Coupled Device
CCSDS .....	Consultative Committee for Space Data Systems
Cd .....	Coefficient of Drag
CDF .....	Cumulative Distribution Function
C&DH .....	Command and Data Handling
CDR .....	Critical Design Review
CEMA .....	Cost Estimating, Modeling & Analysis
CFD .....	Computational Fluid Dynamics

cg.....	center-of-gravity
CheMin-V.....	Chemistry and Mineralogy - Venus
CLPS.....	Commercial Lunar Payload Services
cm.....	centimeter
CM.....	Configuration Management
CMCP.....	Chopped Molded Carbon Phenolic
CMD.....	Command
CML.....	Concept Maturity Level
CMOS.....	Complementary metal–oxide–semiconductor
COEL.....	Committee on Origin and Evolution of Life
CoM.....	Center of Mass
ConOPS.....	Concept of Operations
COSPAR.....	Committee on Space Research
COTS.....	Commercial off the Shelf
CP.....	Carbon Phenolic
cPCI.....	Compact Peripheral Component Interface
CSR.....	Concept Study Report
CSS.....	Coarse Sun Sensors
CTE.....	Controlled Thermal Expansion, Coefficient of Thermal Expansion
DAVINCI+.....	Deep Atmosphere of Venus Investigation of Noble gases, Chemistry, & Imaging, Plus
dB.....	Decibel
DDOR.....	Delta Differential One-way Ranging
DEA.....	Digital Electronics Assembly
Dec.....	Declination
$\Delta V$ .....	Delta Velocity
DEM.....	Digital Elevation Model
DGB.....	Disk-Gap-Band
D/H.....	Deuterium/Hydrogen
DI.....	Descent NIR Imager
DIMES.....	Descent Image Motion Estimation System
DInSAR.....	Differential Interferometric SAR
DLA.....	Declination of Launch Asymptote
DOD.....	Depth Of Discharge
DOF.....	Degrees of Freedom
DPDT.....	Double Pull Double Throw
DPU.....	Data Processing Unit
DSM.....	Deep Space Maneuver
DSN.....	Deep Space Network
DTE.....	Direct to Earth
DTN.....	Delayed Tolerant Network
EDE.....	Entry and Descent Element
EDF.....	Entry, Descent and Float
EDL.....	Entry, Descent and Landing
EEV.....	Earth Entry Vehicle
E-FCM.....	Evolutionary Fuzzy Cognitive Map

E-FD.....	Electric Fields Detector
EFPA.....	Entry Flight Path Angle
EM .....	Engineering Model
EMTG.....	Evolutionary Mission Trajectory Generator
EOL.....	End of Life
ESA.....	European Space Agency
ESA.....	Electrostatic Analyzer
ESA-e.....	Electrostatic Analyzer - electrons
ESA-i .....	Electrostatic Analyzer - ions
ESCAPEDE.....	Escape and Plasma Acceleration and Dynamics Explorers
ESPA.....	Evolved Secondary Payload Adapter
EUV .....	Extreme Ultraviolet
EUV-D .....	Extreme Ultraviolet detector
FDIR .....	Fault detection, isolation, and recovery
FEC .....	Forward Error Correction
FEP .....	Fluorinated Ethylene Propylene
FETS .....	Field Effect Transistors
FM.....	Fluorimetric Microscope
FOV.....	Field of View
FPA.....	Flight Path Angle
FSW.....	Flight Software
FTE .....	Full Time Equivalent
FWHM .....	Full Width at Half Maximum
FY .....	Fiscal Year
g.....	Earth gravitational acceleration (9.81 m/s <sup>2</sup> )
Ga.....	Giga annum (billion years)
GaAs.....	Gallium Arsenide
Gbits .....	Gigabits
Gbps .....	Gigabits per second
GFIC .....	Goddard Fellow Innovation Challenge
GMSL.....	Gaussian Minimum Shift Keying
GN&C .....	Guidance Navigation and Control
GOI.....	Goals, Objectives, and Investigations
GPR.....	Goddard Procedural Requirements
GRS.....	Gamma Ray Spectroscopy/Spectrometer
GSDR.....	Global Slope Data Record
GSFC.....	Goddard Space Flight Center
GSM .....	Generic Switch Module
GTDR .....	Global Topographic Data Record
HA.....	Hazard Avoidance
HD&A .....	Hazard Detection and Avoidance
HEEET.....	Heat-shield for Extreme Entry Environment Technology
HiPAT .....	High Performance Apogee Thruster
HGA.....	High Gain Antenna
HK.....	Housekeeping
HOTLINE .....	Hot Operating Temperature Lithium combustion IN situ Energy

---

HOTTech.....	High Operating Temperature Technology
HPSC .....	High Performance Spacecraft Computing
HZ.....	Habitable Zone
Hz.....	Hertz
I2C .....	Inter-Integrated Circuit
I&T .....	Integration and Test
IAU.....	International Astronomical Union
ICDR.....	Instrument Critical Design Review
ICRF.....	Inertial Centered Reference Frame
IFOV .....	Instantaneous Field of View
IMU .....	Inertial Measurement Unit
InSAR.....	Interferometric SAR
InSight.....	Interior Exploration using Seismic Investigations, Geodesy and Heat Transport
IPDR .....	Instrument Preliminary Design Review
IR.....	Infrared
JAXA.....	Japan Aerospace Exploration Agency
JPL.....	Jet Propulsion Laboratory
JUICE.....	Jupiter Icy Moons Explorer
K.....	Kelvin
Ka-band .....	Ka-band Communication frequencies of 26.5-40GHz
KE .....	Kinetic Energy
kg.....	kilogram
KISS .....	Keck Institute for Space Studies
km/s.....	kilometers per second
kN .....	KiloNewtons
kPa.....	KiloPascals
kpbs .....	kilobits per second
KSC.....	Kennedy Space Center
kW .....	kilowatt
LaRC .....	Langley Research Center
LCDH .....	Lander Command and Data Handling
LDPC .....	Low Density Parity Check
LGN .....	Low Gain Antenna
LHA .....	Landing Hazard Avoidance
LHD&A.....	Landing Hazard Detection and Avoidance
LIBS.....	Laser Induced Breakdown Spectroscopy
LiDAR.....	Light Detection And Ranging
LLISSE .....	Long-Lived In Situ Solar System Explorer
LOS .....	Line Of Sight
LNT .....	lithium nitrate trihydrate
LP .....	Langmuir Probe
LRD .....	Launch Readiness Date
LRO.....	Lunar Reconnaissance Orbiter
LTRNHA.....	Landing Terrain Relative Navigation and Hazard Avoidance
LV .....	Launch Vehicle

LVDS.....	Low Voltage Differential Signaling
LVLH .....	Local Vertical, Local Horizontal
LVPS.....	Low Voltage Power Supply
LVS .....	Lander Vision System
m .....	meter
M.....	million
Ma .....	Mega annum (millions of years)
MAG .....	Magnetometer
MAG-G .....	MAG, Gondola
MAG-O.....	MAG, Orbiter
MatISSE .....	Maturation of Instruments for Solar System Exploration
MAVEN .....	Mars Atmosphere and Volatile Evolution
m/s.....	meters per second
Mbits .....	Megabits
Mbps.....	Megabits per second
MCC .....	Motor Controller Card
MCDR.....	Mission Critical Design Review
MCU .....	Mechanism Control Unit
MDL.....	Goddard Space Flight Center's Mission Design Lab
MEL .....	Master Equipment List
MER.....	Mars Exploration Rover Mission
MET .....	Meteorological Suite/Mission Elapsed Timer
MEV.....	Maximum Expected Value
MGA .....	Medium Gain Antenna
MGS.....	Mars Global Surveyor
MIC.....	Multi-Interface Cards
mJ .....	millijoules
MLI .....	Multi-Layer Insulation
mm .....	millimeter
MMH .....	Monomethylhydrazine
MMS .....	Magnetospheric Multiscale Mission
MOC.....	Mission Operations Center
MOCET .....	Mission Operations Cost Estimating Tool
MOSFETS.....	Metal–Oxide–Semiconductor Field-Effect Transistor
MPDR.....	Mission Preliminary Design Review
MPU.....	Mechanism and Propulsion Unit
MPR .....	Mean Planetary Radius; 6051.84 km for Venus
MRC.....	Mechanism Release Card
MSC/NASTRAN.....	MacNeal-Schwendler Corp (mechanical analysis software)
MSL.....	Mars Science Laboratory
MSPS.....	Million Symbols Per Second
MSR .....	Mars Sample Return
Mw .....	Moment Magnitude Scale
NASA .....	National Aeronautics and Space Administration
NASEM.....	National Academies of Sciences and Engineering
NEA .....	Non-Explosive Actuator



Neph.....	Nephelometer
NESZ .....	noise-equivalent-sigma-nought
NF .....	New Frontiers
NFR.....	Net Flux Radiometer
NFT.....	Natural Feature Tracker
NiCd.....	Nickel Cadmium
NICER .....	Neutron star Interior Composition Explorer
NICM.....	NASA Instrument Cost Model
NIMS .....	Near Infrared Mapping Spectrometer aboard Galileo
NIR .....	Near Infrared
NIR-C .....	NIR, Clouds
NIR-S .....	NIR, Surface
NIR-I.....	Near Infrared Imager/Imaging
nm .....	nanometer
NMS.....	Neutral Mass Spectrometer
NRC .....	National Research Council
ns .....	nanosecond
NTO.....	Dinitrogen tetroxide
OD .....	Orbit Determination
OSIRIS-REx.....	Origins, Spectral Interpretation, Resource Identification, Security, Regolith Explorer
OSAM-1 .....	On-orbit Servicing, Assembly, and Manufacturing Mission 1
OSR.....	Optical Solar Reflectors
Pa.....	Pascals
PAF.....	Payload Attach Fitting
PC.....	Panoramic Camera
PCM.....	Phase Change Material
PDC.....	Propulsion Drive Card
PDR.....	Preliminary Design Review
PEPP .....	Entry Parachute Program
PI .....	Principal Investigator
PICA.....	Phenolic Impregnated Carbon Ablator
PIPS.....	Pulsed Injection Position Sensor
PM.....	Project Management
PMCS .....	Planetary Mission Concept Studies
PPS .....	Pulse Per Second
PSE .....	Power System Electronics
PV.....	Pioneer Venus
PVLP.....	Pioneer Venus Large Probe
PVO.....	Pioneer Venus Orbiter
RAAN .....	Right Ascension of the Ascending Node
RADAR.....	Radio Azimuth Direction and Ranging
RADARSAT.....	Radar Satellite; Canadian Space Agency
RAM .....	Random Access Memory
RAO .....	Resource Analysis Office
REE.....	Rare Earth Elements

RF.....	Radio Frequency
R-LIBS.....	Raman-Laser Induced Breakdown Spectroscopy
RMS.....	Root Mean Square
ROCC.....	Radio Occultation
ROM.....	Rough Order of Magnitude
rpm.....	rotations per minute
RWA.....	Reaction Wheel Assembly
SA, S/A.....	Solar Array
SARM.....	Solar Array Regulation Module
S-band.....	2 to 4 GHz (15 to 7.5 cm wavelength) Communications Band
SBC.....	Single Board Computer
S/C.....	spacecraft
S/W.....	Software
S:N.....	Signal-to-Noise
SAR.....	Synthetic Aperture Radar
SBC.....	Single Board Computer
SEP.....	Solar Electric Propulsion
SEPD.....	Solar Energetic Particle Detector
SEU.....	Single Event Upset
SiAPD.....	Silicon avalanche photodiodes
SiC.....	Silicon Carbide
SIFT.....	Scale Invariant Feature Transform
SIMPLEx.....	Small Innovative Missions for Planetary Exploration
SINDA.....	Systems Improved Numerical Differencing Analyzer
SLS.....	Space Launch System
SmallSat.....	Small Satellite
SMAP.....	Soil Moisture Active Passive
S-mm.....	Sub-mm Spectrometer
SNR.....	Signal to Noise Ratio
SOC.....	Science Operations Center
SOI.....	Silicon on Insulator
SPED.....	Supersonic Planetary Entry Decelerator
SPENVIS.....	Space Environmental Effects and Education System
SPICAV.....	Spectroscopy for Investigation of Characteristics of the Atmosphere of Venus
SPENVIS.....	Space Environmental Effects and Education System
SPLICE.....	Safe and Precise Landing-Integrated Capabilities Evolution project
SQPSK.....	Staggered Quadrature Phase-Shift Keying
SRR.....	System Requirements Review
SSN.....	Sunspot Number
SSPA.....	Solid State Power Amplifier
SSR.....	Solid-State Recorder
STEREO.....	Solar Terrestrial Relations Observatory
STM.....	Science Traceability Matrix
SWaP.....	Size, Weight and Power
SWI.....	Submillimeter Wave Instrument

T.....	Tesla; e.g. mT - microTesla, nT - nanoTesla.
TCM.....	Trajectory Correction Maneuver
TESS.....	Transiting Exoplanets Survey Satellite
THEMIS.....	Thermal Emission Imaging System
TJGaAs.....	Triple Junction Gallium Arsenide
TLM.....	Telemetry
TLS.....	Tunable Laser Spectrometer
TMR.....	Triple Modular Redundant
TOF.....	Time of Flight
TPS.....	Thermal Protection System
TRL.....	Technology Readiness Level
TRN.....	Terrain Relative Navigation
TRN-LHA.....	Terrain Relative Navigation and Landing Hazard Avoidance
TWCP.....	Tape Wrapped Carbon Phenolic
TWTA.....	Traveling Wave Tube Amplifier
UART.....	Universal Asynchronous Receiver/Transmitter
UHF.....	Ultra High Frequency
ULA.....	United Launch Alliance
ULDB.....	Ultra Long Duration Balloon
USN.....	Universal Space Network
UTC.....	Coordinated Universal Time
UTCG.....	Coordinated Universal Time Greenwich
UV.....	ultraviolet
V.....	Volt
VEM.....	Venus Emissivity Mapper
VEMCam.....	Venus Elemental and Mineralogical Camera
VERITAS.....	Venus Emissivity, Radio Science, InSAR, Topography, And Spectroscopy
VEx.....	Venus Express
VEXAG.....	Venus Exploration Analysis Group
VFM.....	Venus Flagship Mission
VGA.....	Venus Gravity Assist
VI.....	Visible Imager
VICI.....	Venus In Situ Composition Investigations
VIRA.....	Venus International Reference Atmosphere
VIRTIS.....	Visible and Infrared Thermal Imaging Spectrometer on VEx
VISAGE.....	Venus In Situ Atmospheric and Geochemical Explorer
VITaL.....	Venus Intrepid Tessera Lander
VIXL.....	Venus Instrument for X-ray Lithochemistry
VME.....	Venus Mobile Explorer
VMTF.....	Venus Materials Test Facility (JPL)
VOI.....	Venus Orbit Insertion
VS.....	Vision System
VTF.....	Venus Thrust Fan
W.....	Watt
WBS.....	Work Breakdown Structure

X-band .....	2.5–3.5 cm; 7.0 to 11.2 GHz communications band
XFS.....	X-Ray Fluorescence Spectrometer
XRD.....	X-Ray Diffractometer
XFS.....	X-Ray Fluorescence
µm .....	micrometer